SCHOOL OF
CIVIL ENGINEERING

INDIANA
DEPARTMENT OF TRANSPORTATION

JOINT HIGHWAY RESEARCH PROJECT

FHWA/IN/JHRP-94/13
Final Report

FATIGUE STRENGTH OF GIRDERS WITH TAPERED COVER PLATES

Ahmed F. Hassan and
Mark D. Bowman

PURDUE UNIVERSITY

JOINT HIGHWAY RESEARCH PROJECT

FHWA/IN/JHRP-94/13
Final Report

FATIGUE STRENGTH OF GIRDERS WITH TAPERED COVER PLATES

Ahmed F. Hassan and
Mark D. Bowman

TECHNICAL REPORT STANDARD TITLE PAGE

1. Report No.	2. Government Accession No.	3. Recipient's Catalog No.
FHWA/IN/JHRP-94/13		

4. Title and Subtitle	5. Report Date
Fatigue Strength of Girders with Tapered Cover Plates	August 7, 1995
	6. Performing Organization Code
7. Author(s) Ahmed F. Hassan and Mark D. Bowman	8. Performing Organization Report No. JHRP-94/13
9. Performing Organization Name and Address Joint Highway Research Project Civil Engineering Building Purdue University West Lafayette, Indiana 47907-1284	10. Work Unit No. 11. Contract or Grant No. Indiana HPR-2047
12. Sponsoring Agency Name and Address Indiana Department of Transportation State Office Building 1000 North Senate Avenue Indianapolis, IN 46204	13. Type of Report and Period Covered Final Report 14. Sponsoring Agency Code

15. Supplementary Notes

Prepared in cooperation with the Indiana Department of Highways and Federal Highway Administration on HPR Part II Study "Fatigue Strength of Girders with Tapered Cover Plateo."

16. Abstract

This report represents results from a study to determine the fatigue strength of steel beams with welded partial-length cover plates. Results of an experimental investigation that examined the fatigue strength of various cracked cover plate end details that were subsequently repaired are presented. The repair methods investigated included a slip-critical bolted splice plate connection, air-hammer peening, and a combination of the previous two called a partial bolted splice connection. Also, an analytical model was developed to predict the fatigue behavior of a cover plate end detail that is repaired using one of the three repair methods investigated and which contains a fatigue crack of a known size.

The results of both the experimental and analytical studies indicate that a tapered cover plate detail can be effectively repaired with a corresponding improvement in the fatigue resistance.

17. Key Words	18. Distribution Statement
Welded Cover Plates, Repair, Retrofit, Fatigue, Experiments, Steel, Finite Element	No restrictions. This document is available to the public through the National Technical Information Service, Virginia, 22161

19. Security Classif. (of this report)	20. Security Classif. (of this page)	21. No. of Pages	22. Price
Unclassified	Unclassified	391	

Form DOT F 1700.7 (8-69)

FINAL REPORT

FATIGUE STRENGTH OF GIRDERS WITH TAPERED COVER PLATES

by

Ahmed F. Hassan

and

Mark D. Bowman
Purdue University
Department of Civil Engineering

Joint Highway Research Project

Project No: C-36-56DD
File No: 7-4-30

In cooperation with the
Indiana Department of Transportation

and

Federal Highway Administration

Purdue University
West Lafayette, IN 47907
August 7, 1995

FINAL REPORT

FATIGUE STRENGTH OF [illegible]
WITH TA[illegible] PLATES

by

[illegible]

and

[illegible]

[illegible]

[illegible]

[illegible]

in cooperation with the
Indiana Department of Transportation

and

Federal Highway Administration

The contents of this report reflect the views of the author who is responsible for the facts and the accuracy of the data presented herein. The contents do not necessarily reflect the official views or policies of the Federal Highway Administration and the Indiana Department of Transportation. This report does not constitute a standard, specification or regulation.

Purdue University
West Lafayette, IN 47907
August 7, 1995

ACKNOWLEDGEMENTS

The experimental phase of the research described herein was conducted in the Kettelhut Structural Engineering Laboratory at Purdue University. The authors would like to thank Russ Maurey, Charlie Crow, and Eric Romine for their help during the experimental phase of the study.

The support of the Joint Highway Research Project of Purdue University, the Indiana Department of Transportation, and the Federal Highway Administration is gratefully acknowledged for the research described.

The authors would also like to thank the study advisory committee members for their valuable input during this study. The advisory committee included James Karr, Joseph Torkos, William Dittrich, and Wesley Billups from Indiana Department of Transportation, and Thomas Saad from Federal Highway Administration.

TABLE OF CONTENTS

Page

Page

Page

Page

Page

Page

Page

Page

LIST OF TABLES

LIST OF FIGURES

Figure Page

Figure Page

Figure Page

Figure Page

Figure Page

Figure Page

IMPLEMENTATION REPORT

The main objective of the research was to investigate the fatigue strength of steel bridge beam members that contain welded partial-length, tapered cover plates which have been repaired. It is well known that welded cover plate details have a low fatigue resistance and are susceptible to the development of fatigue cracks at the toe of the end welds. The performance of three repair methods was evaluated experimentally: a friction type bolted splice plate connection, air-hammer peening, and a hybrid of the previous two called a partial bolted splice connection. Also, an analytical model was developed to predict the fatigue life of cracked cover plate ends which have been subsequently repaired. Based upon the experimental and analytical results it has been shown that cover plate details that develop fatigue cracks can be successfully repaired such that the fatigue resistance of the repair detail will be better than that of the original detail.

The primary benefit in using the repair procedures examined in the report involves avoiding expensive removal and replacement of damaged structural members and, instead, the continued use of highway bridge members already in place. Moreover, the use of preventative retrofit procedures were demonstrated to be highly successful in avoiding or significantly delaying the initiation of fatigue cracks. The exact benefit can be assessed by comparing the cost associated with removal and replacement of a bridge member versus the cost associated with the implementation of one of the fatigue repair details. Although data were not collected to compare the cost of member replacement with the cost of the repair schemes, it is believed that the cost of the repair procedures are significantly less than the cost of member replacement. Moreover, since the tapered cover plate was widely used in highway bridges throughout Indiana, and it is likely that most of these details will eventually need to be repaired, then the benefit of repair details will be multiplied many times over and will provide a significant long-term cost savings.

The following suggestions are made as possible ways to implement the results of the report to improve the performance of highway bridge members with tapered, partial-length cover plates.

The ends of welded cover plate details should be regularly inspected for any evidence of fatigue cracking. If no fatigue cracks are detected, then the use of air-hammer peening should be considered. Experimental results demonstrated that very significant improvements in the fatigue resistance were achieved when air-hammer peening was used prior to crack initiation. Peening

the weld toe region at the end of the cover plate detail induces compressive residual stresses that will offset the tensile stresses at the weld toe that cause fatigue damage.

Upon detection of cracks at welded cover plate ends, the size and location of the cracks should be determined. The fatigue propagation program should then be used to assess the structural integrity and estimate the remaining life of the critical detail as it exists under present field conditions. If the remaining life is not satisfactory, then one of the repair methods should be implemented as a long-term solution. The fatigue life of the beam after implementation of the repair detail can be estimated using the propagation program. It should be noted that the estimated fatigue life depends on crack length and depth, beam dimensions, applied stress, and type of repair. The repair type should be chosen depending on the desired target fatigue life with consideration of the detected crack sizes.

The slip-critical bolted splice plate connection was the most effective method of repairing cracked cover plate ends. (Experimental results indicated that the beam will typically be able to sustain an additional number of loading cycles equivalent to a Category B design life.) The splice plates can be designed by assuming that the maximum bending moment at the cover plate end is resisted by both the splice plates and the bare beam cross section, excluding the beam tension flange, without overstressing either the beam or the splice plates. High-strength bolts used to connect the splice plates to the beam flange should be designed to carry the splice plate force in a slip-critical type connection. The propagation program should then be used to evaluate the fatigue resistance of the detail once the splice plate size has been determined. Increasing the splice plate thickness will provide a corresponding improvement in the fatigue resistance of the bolted splice detail.

The partial bolted splice connection can also be used to repair the end of a welded cover plate detail. However, because the partial bolted splice connection was found to be less effective than the bolted splice connection, the partial bolted splice connection should not be used unless clearance is one of the governing factors at the bridge site.

The use of air-hammer peening on cover plate end-weld details was found to be not nearly as effective as the use of a bolted splice or partial bolted splice connection in improving the fatigue strength when fatigue cracks longer than 1/4-in. to 3/8-in. are present. Air-hammer peening, however, represents a good short-term solution until the repair can be scheduled and/or when funds become available for the needed repairs.

CHAPTER 1
INTRODUCTION

Cover Plates are widely used to increase the flexural strength of steel bridge members. A variety of cover plates, including full length and partial-length at high moment locations, are common in bridge construction. Although cover plates often have different end geometries, the most frequently used details are square-ended and tapered. While cover plates could be riveted, bolted, or welded to a beam member, welding has been widely used recently due to fabrication simplicity and ease.

1.1. Problem Statement

A comprehensive fatigue study of beams with welded cover plates (Fisher et al., 1970) suggested that the fatigue strength is influenced mainly by the stress range to which the beams are subjected. Cracks were found to develop primarily at the end of the welded cover plates.

A particular detail that has been utilized in many of the highway bridges in Indiana is different than the square-ended cover plate studied by Fisher et al. (1970). The detail utilized in Indiana involves a partial-length cover plate, with a tapered end, that is welded to the beam flanges; this detail is shown in Fig. 1.1.

Only a few tests have been conducted on welded, tapered cover plate details of the type used in Indiana (Munse and Stallmeyer, 1962; Grundy and Teh, 1985; and Yongii and Yanman, 1987). The main finding of these tests was that the fatigue strength of welded cover plates with tapered ends does not differ much from that of cover plates with square ends.

1.2. Objectives and Scope

The present study can be divided into two phases: an experimental phase and an analytical phase. The main objectives of the experimental phase of the study are as follows:

1- Evaluate the number of loading cycles required to develop detectable cracks in steel beams with welded, partial-length cover plates with tapered ends.
2- Evaluate the performance of several methods to repair steel beams with welded, partial-length cover plates that developed cracks at the tapered cover plate ends.

The investigated repair methods in this study are:

1- A friction type bolted splice plate connection (bolted splice repair).

2- Air-hammer peening of the weld toe at the cover plate ends (peening repair).

3- A combination of the previous two methods: a friction type bolted splice plate connection without the lower splice plate and air-hammer peening of the weld toe (partial bolted splice repair).

During the experimental phase of the study, 33 steel beams with welded, partial-length cover plates with tapered ends were tested. All the test beams were fabricated from ASTM A36 steel. Testing was limited to constant amplitude cyclic loading of the beam member at a loading rate of 2.0 - 2.5 Hz.

The main objective of the analytical phase of the study is to develop a method of predicting the fatigue life of steel beams with tapered, partial-length cover plates repaired with one of the studied methods. To achieve this objective, a computer program was developed to compute the fatigue propagation life of pre-cracked steel members. Finite element analyses were conducted to compute the stresses in different components of the studied details.

A review of previous experimental research on the fatigue of steel beams with welded cover plates is presented in Chapter 2. Chapter 3 presents the findings of a survey on steel bridges conducted during the early stages of this study. The experimental program is then discussed in Chapter 4. Chapter 5 discusses the crack detection results, while Chapters 6, 7, and 8 discuss the fatigue strength of beams with the bolted splice repair, peening repair, and partial bolted splice repair, respectively. In Chapter 9, an analytical model to predict the fatigue life of steel bridge girders with tapered, partial-length cover plates which have been repaired is presented. Finally, the conclusions and recommendations for the study are discussed in Chapter 10.

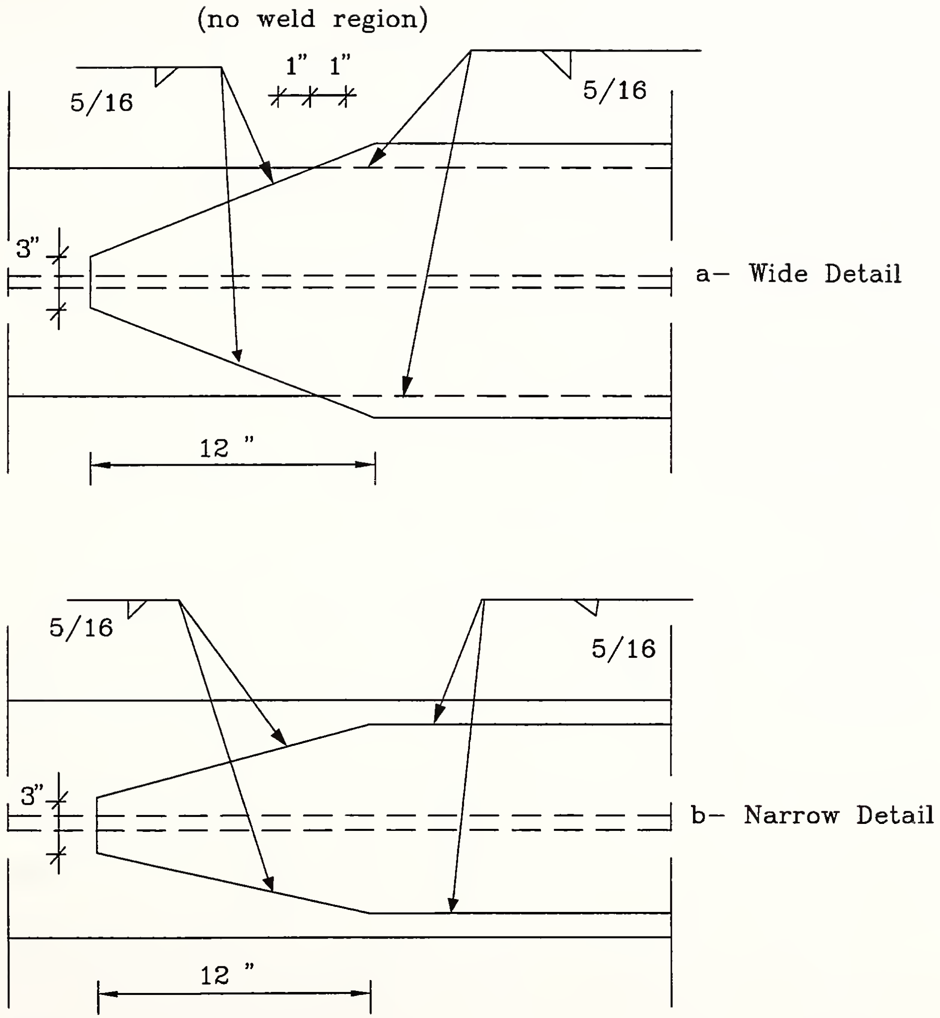

Fig. 1.1. Tapered Cover Plate Detail Used on Indiana Highway Bridges.

CHAPTER 2
LITERATURE REVIEW

2.1. General

As early as 1949, the fatigue strength of various details used for the repair of bridge members were investigated by Wilson and Munse at the University of Illinois, Urbana. The test specimens included riveted and riveted-welded joints, butt weld reinforced beams with strap plates, and spliced beams. The spliced beams tests included beams with full length cover plates of various thicknesses attached with continuous fillet welds. In 1962 Munse and Stallmeyer summarized the results of tests conducted at the University of Illinois to demonstrate the effect of details on the fatigue behavior of welded flexural members. The tests included plain rolled I-beams, plain welded beams, beams with welded splices, beams with welded stiffeners, and beams with welded partial-length cover plates. In 1967 the Task Committee on flexural members summarized the existing static and fatigue studies of steel sections with cover plates. In 1970 Fisher, Frank, Hirt, and McNamee examined the fatigue strength of steel beams with welded cover plate attachments. The specimens used in these tests were plain hot-rolled beams, welded beams, beams with square-ended cover plates, and beams with straight and curved flange width transitions. As a result of this work, AASHTO adopted the allowable Category E fatigue strength for the design of members with partial-length, welded cover plate attachments.

In 1975 Schilling, Klippstein, Barsom, and Blake conducted tests to determine the fatigue strength of cover plates under variable amplitude loading. In 1985 Grundy and Teh studied the fatigue strength of the welded termination of cover plates. In 1987 Yongii and Yanman conducted tests on plate girders with tapered and square end welded cover plates.

Studies have also been conducted to examine the improvement of the fatigue strength of steel members, including beams with welded cover plates. In 1974 Fisher, Sullivan, and Pense studied fatigue damage repair of welded attachments using grinding, air-hammer peening, and remelting techniques at the weld toe. In 1983 Hausammann, Fisher, and Yen studied the effect of peening on the fatigue strength of welded steel beams with square cover plates. In 1984 Sahli, Albrecht, and Vannoy studied the fatigue strength of retrofitted cover plates.

As reported by Fisher and Yen (1977), numerous fatigue test data, including various welded beam details, are available. From these data, it was observed that the plain welded beams represent an upper bound for the fatigue strength of welded beams. On the other hand, beams with partial-length cover plates welded to the flanges represent a lower bound for the fatigue strength of welded beams. From the available test data AASHTO classified the details used in bridge construction into five general categories, as shown in Fig. 2.1. Category E in this classification was intended to represent the most severe details with respect to fatigue strength, including beams with welded partial length cover plates. Afterwards, it was observed that the fatigue strength is reduced further when the flanges of beams are thick. To account for this observation, a lower category E' was added. For each category the straight line was found to be a good estimate of the relation log S_r - log N, where S_r is the stress range during a loading cycle and N is the number of such cycles to failure. Using statistical methods, a mean S_r - N line was found to represent each of the categories. For design purposes, where safety is a major concern, the mean line is not suitable. Rather AASHTO utilizes a much lower line corresponding to 95% confidence limit for 95% survival, as shown in Fig. 2.2. This line is parallel to the mean line but shifted by approximately two standard deviations.

The following sections discuss the previous work which has been conducted to assess the fatigue strength of steel beams with welded cover plates and to evaluate several methods of improving the fatigue strength of that detail.

2.2. Fatigue Strength of Steel Beams with Welded Cover Plates

2.2.1. Munse and Stallmeyer (1962)

The results of a number of tests conducted at the University of Illinois to study the effect of detail geometry and type on the fatigue behavior of welded flexural members were reported by Munse and Stallmeyer. The tests included details such as splices, stiffeners, cover plates, and attachments. The fatigue strength of these details was related also to that of the basic material.

Most of the test specimens were fabricated from ASTM A373 carbon structural steel. Manual shielded metal arc welding with E7016 electrodes was used in the fabrication of the specimens. The beams were tested in the 200,000 lb University of Illinois fatigue testing machine shown in Fig. 2.3. This machine is capable of applying a maximum mid-span load of 112,000

lb at a rate of 180 applications per minute. Most of the tests were conducted such that the stresses in the extreme fibers of the bottom flange of the member ranged from zero to full tension. However, selected members were subjected to a full reversal or partial tension to full tension cycles.

Various end details of the cover plate were used in the tests. These details are shown in Fig. 2.4. In some selected beams the cover plate was substituted by the use of a flange transition, as shown in Fig. 2.5. The transition was made by increasing either the flange thickness or width. The fatigue strength at 2,000,000 cycles was found to range from 11.3 to 14.5 ksi for the various partial-length cover plate details, while the flange transitions provided a fatigue strength of about 19 ksi.

The main findings regarding beams with partial-length cover plates were as follows:

1- A gradual change in cross section leads to an increase in the fatigue strength.

2- Although tapered partial-length cover plates have greater life than square ended cover plates, the difference is not large.

3- The omission of end transverse welds increases the fatigue life by a small percentage.

4- The most effective way of increasing the fatigue strength is to use gradual transitions in the thickness or the width of the beam flanges.

2.2.2 Task Committee on Flexural Members (1967)

The static and fatigue studies conducted prior to 1967 on steel sections with cover plates were summarized by the ASCE Task Committee on Flexural Members (1967). The effect of various details on the fatigue behavior of steel beams with cover plates was examined. From a review of available fatigue data, it was found that the general mode of failure for these detail types involves crack initiation in the base metal at the toe of the cover plate weld and propagation of the crack through the tension flange.

A number of different end details were studied, as shown in Fig. 2.6. Except for details (a), (b), and (h), only six or seven specimens have been tested for each detail. Both rolled and welded beams were used. Most of the test specimens were fabricated from mild structural steel. High strength steel beams were used for a few tests with detail (a). Except for detail (b), all the specimens were subjected to zero to tension stress cycles.

The results of beams with partial-length cover plates corresponding to details (c), (d), and (e) are shown in Fig. 2.7. The figure indicates that there is no significant difference between the three details.

Moreover, the following configurations were all found to exhibit comparable fatigue lives:

1- Square ended cover-plates with and without end welds.
2- Tapered cover plates with a 1:6 taper to a 1.0 in width at the end, with and without end welds.
3- Cover plates wider than the flange with and without end welds.
4- Cover plates with semi-circular ends, either convex or concave.

The following are some of the recommendations listed by the Task Committee on Flexural Members (1967):

1- For short fatigue lives, using a continuous or an intermittent weld did not have any influence. On the other hand, intermittent welds had lower fatigue strength at longer lives.
2- The cover plate is to be extended beyond the theoretical cut-off points. This extension should be equal to one and a half times the cover plate width when end welds are used, and twice the cover plate width when end welds are not used.
3- The fatigue design of beams with cover plates can be based on the stress range alone. It is suggested that the allowable stress range be 9, 12, and 18 ksi for lives of 2,000,000, 500,000, and 100,000 cycles, respectively.

2.2.3. Fisher, Frank, Hirt, and McNamee (1970)

The effect of weldments on the fatigue strength of steel beams was studied. The test program consisted of 374 steel beams, and of this total number 204 were fabricated with cover plates. Cover plates were welded to the flange with longitudinal fillet welds for the entire cover plate length. Two different conditions were used at the cover plate ends: a transverse end weld at one end and no weld at the other end. There were 86 plain rolled and plain welded beams tested to determine the fatigue strength of these basic members. The remaining 84 beams were fabricated with flange splices. The different details tested in this study are shown in Fig. 2.8.

The design variables in this study were the type of detail, stress condition, and type of steel. The main detail was a square-ended cover plate with or without transverse end welds. The cover plate thickness and width, and the use of more than one cover plate were the variables in the main detail.

The minimum stress, maximum stress, and stress range were the stress variables. Three types of steel were used to evaluate material effects: A36, A441, and A514.

The cover plates were welded longitudinally to the flanges of W14 X 30 beams with 1/4-in fillet welds. The cover plate thicknesses were 9/16-in and 3/4-in. All the tests were conducted using a constant amplitude loading.

It was found that the fatigue life was not influenced by the following factors:

1- Use of an end weld.

2- Use of a cover plate wider or narrower than the flange.

3- The change in the cover plate thickness up to 3/4-in.

4- Using single or double cover plates.

5- Type of steel for a specified welded detail.

However, it was observed that the un-welded end of the cover plates wider than the flange gave smaller lives than the welded ends. The fatigue test data are shown in Fig. 2.9. As a result of this work, AASHTO adopted the allowable Category E S-N line, shown in Fig. 2.9, for the design of base metal at long attachments, such as for partial-length cover plates.

2.2.4. Schilling, Klippstein, Barsom, and Blake (1975)

A total of 159 beams were tested to determine the fatigue strength of cover plates under variable amplitude loading. The objectives of the study were:

1- Obtain fatigue data on welded members under variable amplitude random loading.

2- Develop an analytical method for predicting the fatigue behavior of welded beams under actual loading conditions by using constant amplitude fatigue data.

3- Determine the effect of detail type and steel type on the fatigue behavior.

4- Determine the fatigue behavior of members subjected to a very large number of small variable amplitude stress cycles.

5- Develop effective methods of performing variable amplitude random sequence fatigue tests on large specimens.

All the specimens were identical to the W14 X 30 beams used by Fisher, Frank, Hirt, and McNamee (1970). The beams were fabricated in accordance with three fabrication procedures. In the first procedure, the cover plates were welded first to the flange plates, then the flange plates were welded to the web. This reduces the residual tensile stresses at the end of the

longitudinal fillet weld connecting the cover plates with the flanges, thus giving higher fatigue life values. In the second procedure, the cover plates were longitudinally welded to the preassembled welded beams. No transverse welds were used in the first and second procedures. In the third procedure, transverse welds were used for the two previous procedures. For the variable amplitude loading, an equivalent constant amplitude stress range was calculated using the following formula:

$$f_{re} = \left(\sum_i \gamma_i f_{ri}^{m}\right)^{\frac{1}{m}} \tag{2.1}$$

where γ_i and f_{ri} are the frequency of occurrence and the corresponding value of the stress ranges, and the value of m is equal to 3. The test results plotted according to Eq. 2.1, shown in Fig. 2.10, indicate that the equivalent stress range for the variable amplitude tests are in excellent agreement with constant amplitude fatigue data.

2.2.5. Grundy and Teh (1985)

The fatigue strength and preferred location of crack initiation at the welded termination of cover plates was studied using the concepts of linear elastic fracture mechanics and finite element methods. Four full scale tests were conducted using girders from an actual bridge. The purpose of the study was to examine the factors that affect the preferred location of fatigue crack initiation and to theoretically evaluate the relative fatigue resistance of beams with tapered cover plates as compared to beams with square-ended cover plates.

It was found that tapering the cover plate does not increase the fatigue resistance of the detail. Tapering of the cover plates does, however, increase the stresses at the cover plate termination. The difference in fatigue lives for tapered and square ended cover plates is not enough to warrant different fatigue categories. It was also found that root cracks would initiate in preference to toe cracks if the weld is particularly small or has little penetration.

2.2.6 Yongii and Yanman (1987)

Fatigue tests on plate girders with tapered and square end welded cover plates were presented. The beam details are shown in Fig. 2.11. It should be noted that a semi-automatic welding process was used to produce the cover plate welds.

The tests were conducted under a loading frequency of 250 cycles/min and with stress ratios of 0.1, 0.3, and 0.5. The S_r - N curves are shown in Fig. 2.12. For the tapered plates, it was observed that the fatigue cracks initiate at the toe of the end weld and propagate toward the two sides of the flange.

It was found that the tapered plates give fatigue lives a little higher than the square end plates. The difference is small, however, and does not require two different categories. It was also found that the stress range, number of cycles, and type of detail are the most important parameters influencing the results. The stress ratio effect was found to be small and can be neglected. It was also found that the slope of the S_r - N curve should be taken as -3.5.

2.3. Improvement of fatigue Strength of Steel Beams with Welded Cover Plates

2.3.1. Fisher, Sullivan and Pense (1974)

A study on repairing fatigue damage was conducted. Three treatment techniques were investigated:

1- Grinding the weld toe to reduce the stress concentration.

2- Air-hammer peening to introduce residual compressive stresses.

3- Remelting the weld toe to remove initial flaws.

In this study, the grinding process was applied to the toe only. No attempt was made to grind the entire weld surface nor to taper the weld end.

A total of 60 beams with square-end cover plates were fabricated from ASTM A36 steel. The beams were identical to those used by Fisher, Frank, Hirt, and McNamee (1970). Three series of tests were conducted. In series I (as-welded beams), treatment of the weld toe was applied prior to any loading. In series II and III (pre-cracked beams), the weld toes were treated after about 75% of the life had expired, or after a visible crack was found. The main variables were the stress range and minimum stress.

The grinding method was found not effective. It increased the fatigue life by only a small amount. Grinding the weld toe removed the discontinuities near the surface, but it was not effective as the crack depth increased. The results, shown in Fig. 2.13, indicate that the grinding process increased the fatigue life to reach Category D for small stress ranges. For high stress ranges, the fatigue life was smaller than the Category D. The early failure of some beams was attributed to the notches caused by the grinding process.

The peening method was found to be more effective than the grinding method. This method was found to be dependent on the magnitude of minimum stress. It was less effective at higher stress range levels and under high minimum stress. This could be explained by the fact that the application of high minimum stresses reduced the compressive residual stresses induced by the peening process. The results, shown in Fig. 2.14, indicate that the peening process increases the fatigue life from Category E to Category D for low minimum stresses. It is to be noted that the peening process is effective only for cracks with depths smaller than 0.125-in.

Remelting was found to be the most effective method. It increased the fatigue life of the details from Category E to Category C, as shown in Fig. 2.15. Remelting can be used for cracks up to 0.18-in deep.

2.3.2. Hausammann, Fisher, and Yen (1983)

The effect of peening on the fatigue strength of steel beams with welded cover plates was studied. An analytical study of the effect of peening intensity, yield strength, and R-ratio on the maximum repairable crack depth was performed using linear elastic fracture mechanics models. Cracks initially penetrate into the flange in the heat affected zone at the weld toe. This zone has high tensile residual stresses that decrease the threshold range of stress intensity factor making the fatigue crack to grow at low applied stress ranges.

The influence of air-hammer peening was investigated. Visual inspection indicates that the peened surface becomes smoother by applying more peening passes and by peening at low air pressures. It was found that the threshold crack length, for which no crack growth occurs, depends on the depth of the residual compressive zone, the minimum stress, and the stress range. The higher the minimum stress and stress range the lower the threshold crack length. The yield strength of the base metal has a small influence on the threshold crack length. Peened beams with crack lengths larger than the threshold value showed almost no increase in the fatigue life. Peening is either successful and prevents further crack growth, or else little fatigue life increase results. The results of the analytical study agree well with the observations made during the tests conducted by Fisher, Sullivan, and Pense (1974). Cracks up to 0.1-in deep could be successfully repaired by peening.

2.3.3. Sahli, Albrecht, and Vannoy (1984)

The fatigue strength of beams with retrofitted cover plates was experimentally examined. A total of 15 W14 X 30 beams were tested under 20 and 30 ksi stress range, and 32.5 ksi maximum stress. The test set-up is shown in Fig. 2.16. The retrofitting was applied for three different conditions:

1- Before any load application (non-cracked beams)

2- After about 1/2 of the tension flange cross section had been cracked (half pre-cracked beams)

3- After the full tension flange cross section had been cracked (fully pre-cracked beams).

The cracks in the web were stopped by drilling a hole at the crack tip and inserting a high strength bolt in the hole.

Results show that the mean fatigue life for non-cracked details exceeded the Category B mean strength, and was 18.2 times higher than the Category E mean strength. The combined mean life for the half pre-cracked and fully pre-cracked beams was smaller than the Category B mean, but was 12.9 times higher than the Category E mean. The following recommendations were proposed:

1- The retrofit shall consist of a high strength bolted friction type splice connection.

2- The splices for the non-cracked details shall be designed for the flange portion of the moment only; those of the pre-cracked details shall be designed for the total moment.

3- The retrofitted details can be designed in accordance with Category B.

4- If a crack appears in the web, it should be stopped by installing a high strength bolt in a hole drilled through the crack tip. If the crack exceeds 1/8 of the beam depth, a web splice should be provided.

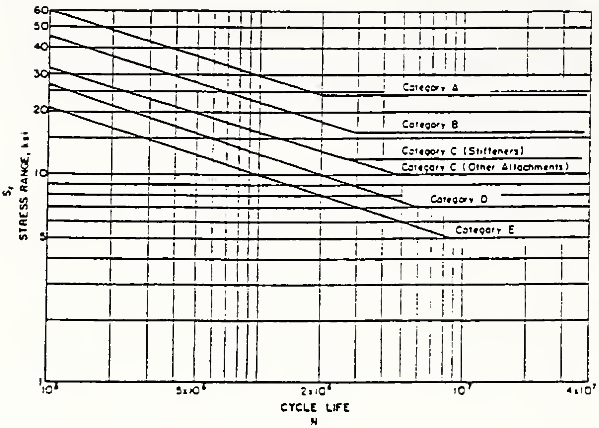

Fig. 2.1. Design Stress for AASHTO Specifications.
(Fisher and Yen (1977))

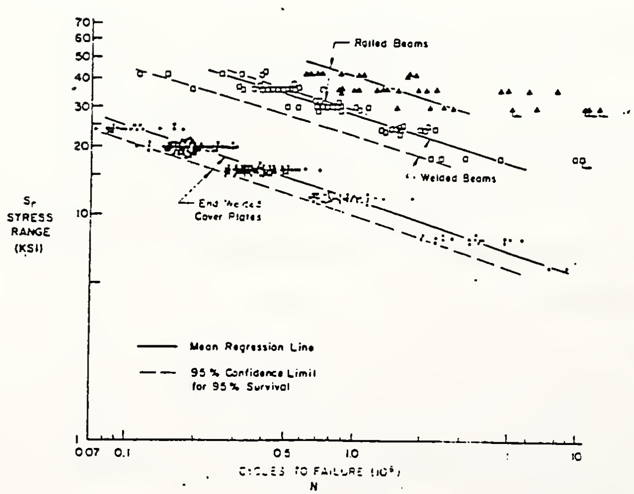

Fig. 2.2. Fatigue Strength of Rolled, Welded, and Cover-Plated Beams.
(Fisher and Yen (1977))

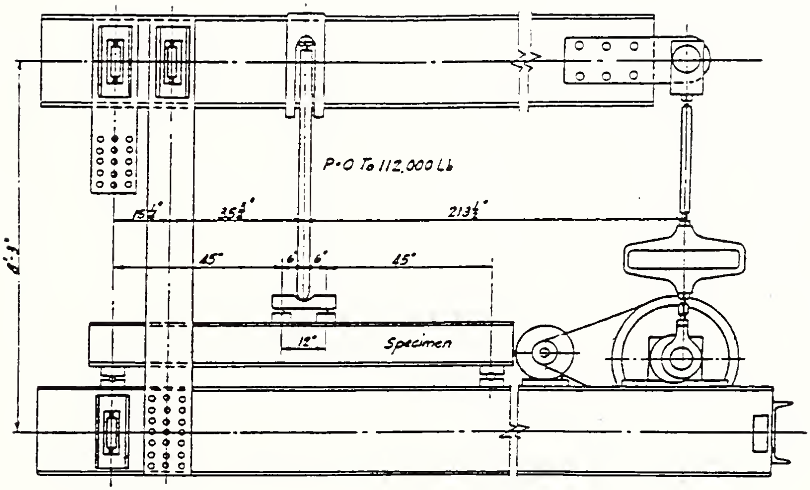

Fig. 2.3. Illinois Fatigue Testing Machine.
(Munse and Stallmeyer (1962))

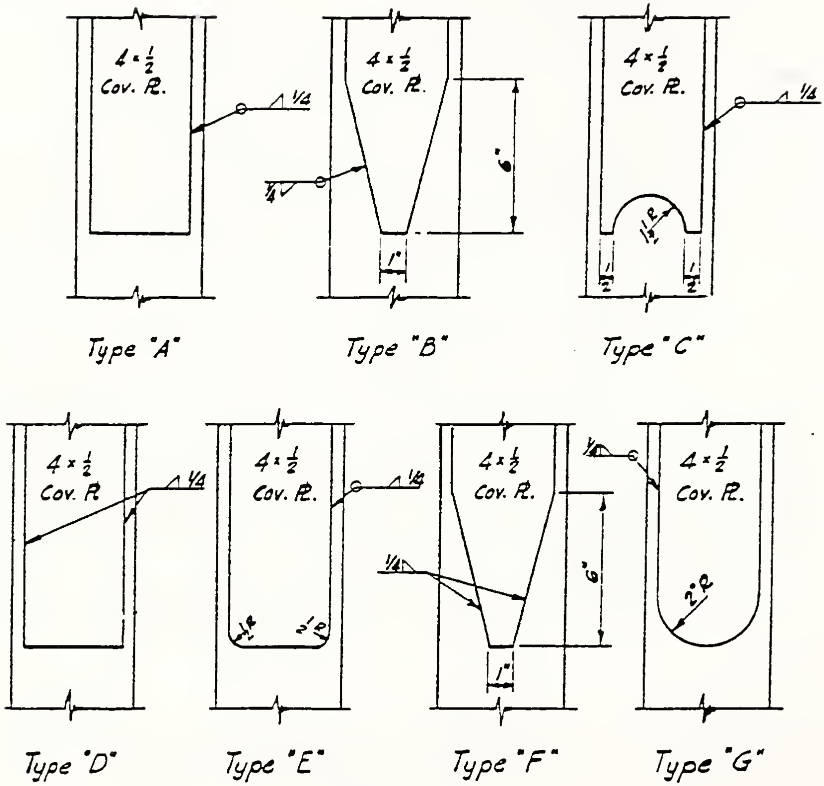

Fig. 2.4. Cover Plate Details.

(Munse and Stallmeyer (1962))

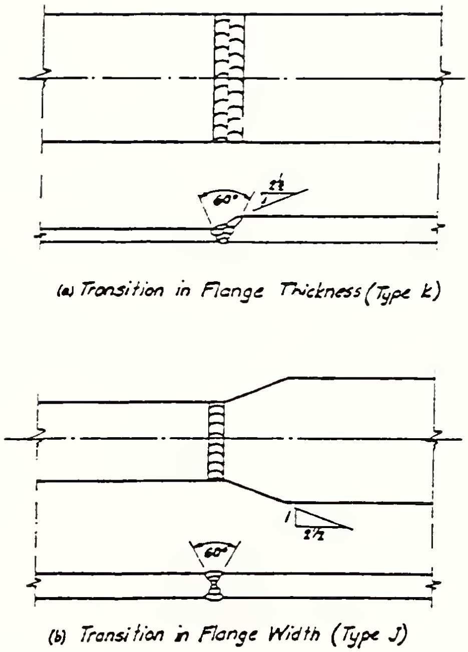

Fig. 2.5. Flange Transition Details.
(Munse and Stallmeyer (1962))

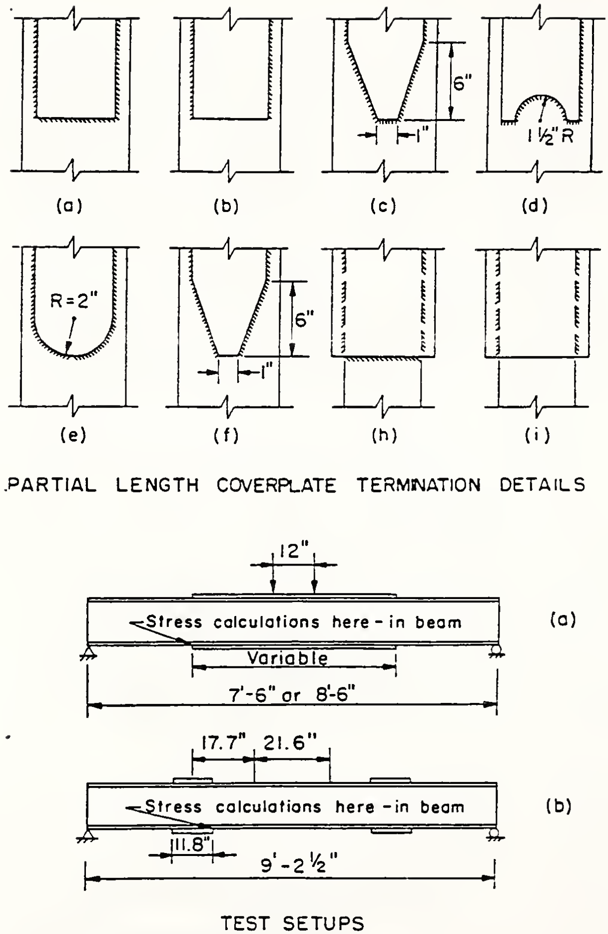

Fig. 2.6. Cover Plate Details.

(Task Committee on Flexural Members (1967))

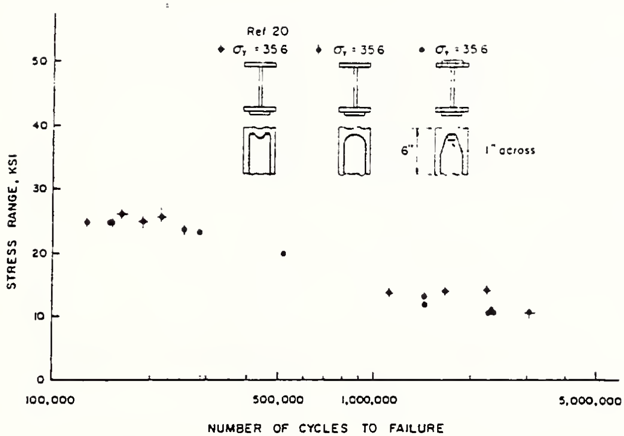

Fig. 2.7. Partial Length Cover Plates Results.

(Task Committee on Flexural Members (1967))

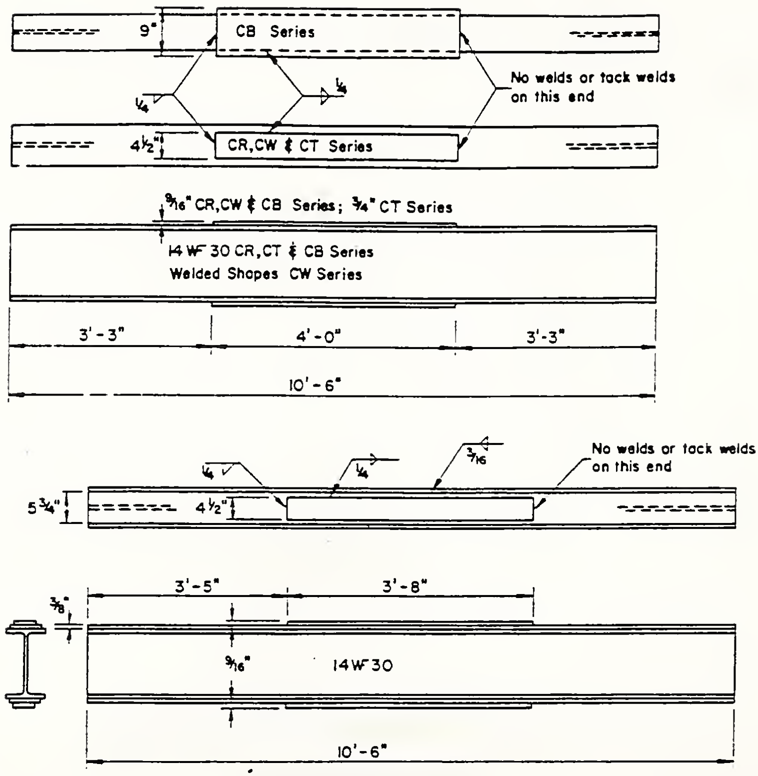

Fig. 2.8. Test Details.

(Fisher, Frank, Hirt, and McNamee (1970))

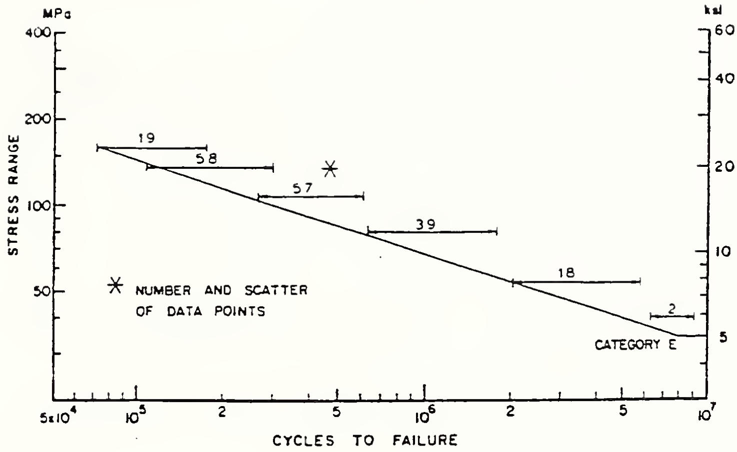

Fig. 2.9. Square-Ended Cover Plates.

(Fisher, Frank, Hirt, and McNamee (1970))

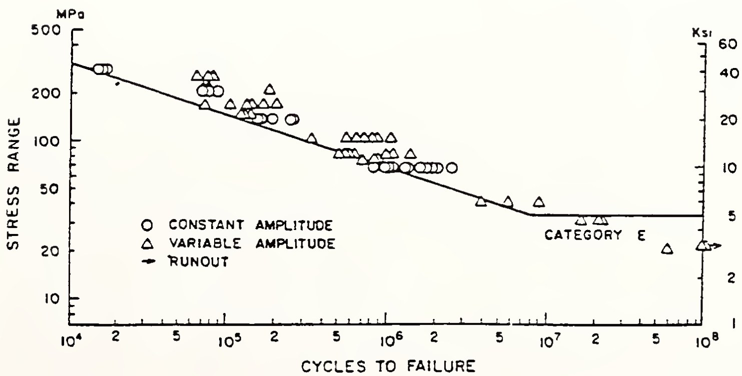

Fig. 2.10. Variable Amplitude Test Results.

(Schilling, Klippstein, Barsom, and Blake (1975))

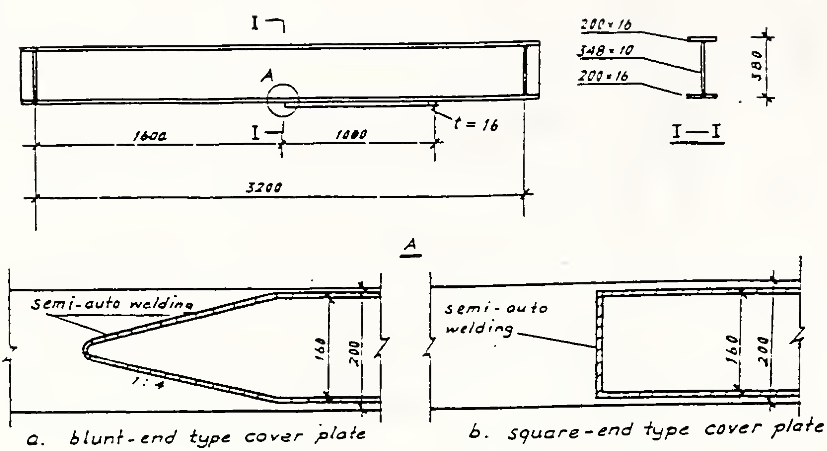

Fig. 2.11. Beams Details.

(Yongii and Yanman (1987))

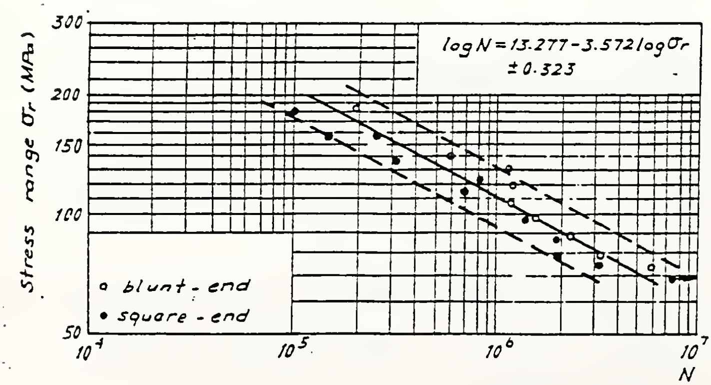

Fig. 2.12. Test Results.

(Yongii and Yanman (1987))

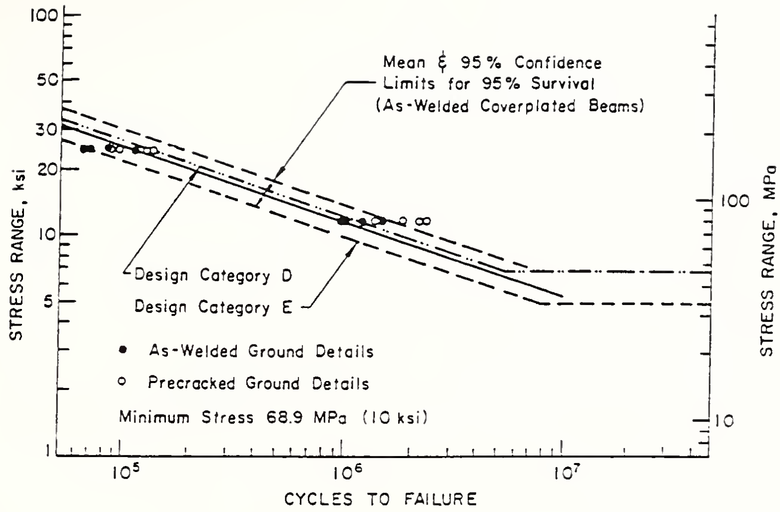

Fig. 2.13. Results of Ground Details.

(Fisher, Hausammann, Sullivan, and Pense (1970))

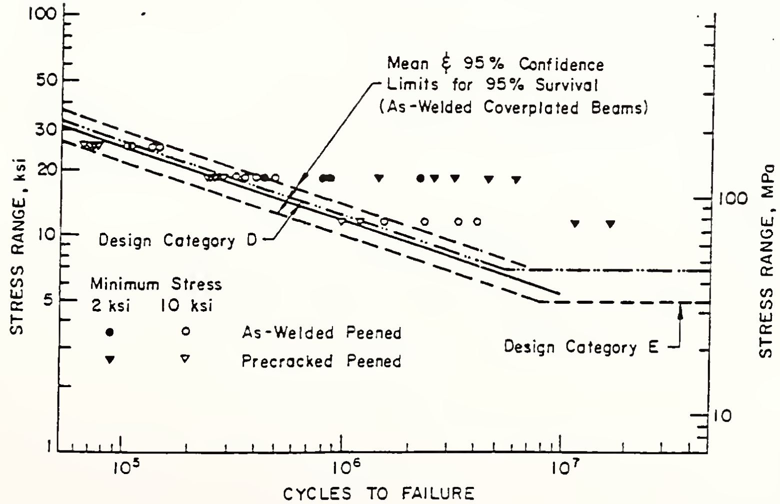

Fig. 2.14. Results of Peened Details.

(Fisher, Hausammann, Sullivan, and Pense (1970))

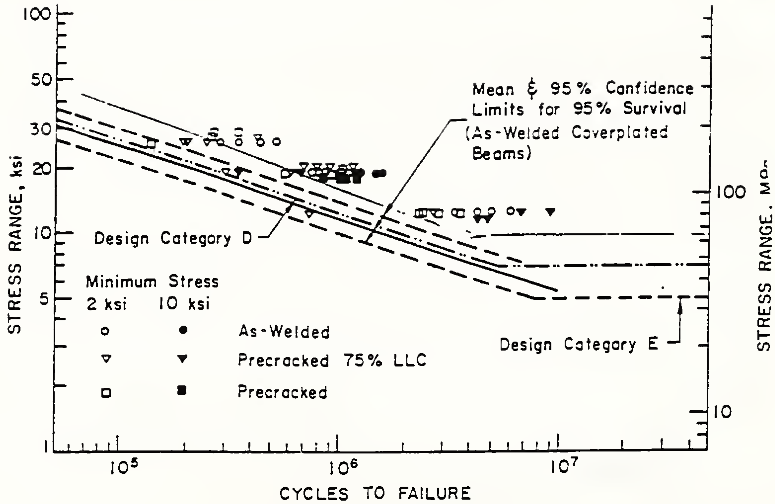

Fig. 2.15. Results of Remelted Details.

(Fisher, Hausammann, Sullivan, and Pense (1970))

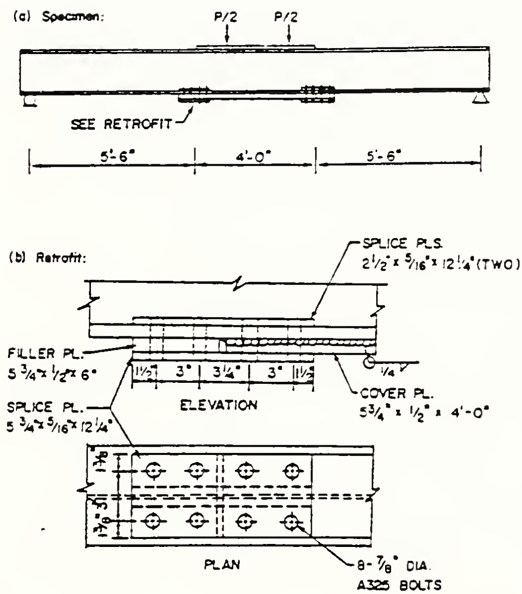

Fig. 2.16. Test Specimen with Retrofitted Cover Plate Ends.
(Sahli, Albrecht, and Vannoy (1984))

CHAPTER 3
SURVEY ON FATIGUE OF STEEL BRIDGES

3.1. Introduction

In order to assess the behavior and performance of steel beams with welded cover plates, a survey on the fatigue of steel bridges was conducted by polling highway bridge engineers throughout the United States. One of the main objectives of the survey was to find out if other states had experienced cracking at the partial-length, tapered cover plate details. The development of fatigue cracks at other details, and the repair techniques utilized to correct the problems encountered were also solicited in the survey.

Although test data might be available for determining the fatigue strength of steel beams with welded cover plates, it was felt that having actual (field) information is extremely important. Beams behave differently in a laboratory set-up than as part of a bridge. Some of the factors that might contribute to this difference are: (1) the presence of several beams in a bridge deck, (2) the participation of a concrete slab deck, (3) the loading type, magnitude, and frequency, (4) the scale effect of beams tested in the laboratory. Moreover, repair methods are generally easier to apply in a laboratory condition than in a field environment.

The survey is mainly divided into four parts. The first part determines whether the completion of the survey is beneficial. If steel bridges are not used, the engineer would sign and return the survey. The second part of the survey deals with the cover plate detail. If cover plate details are not used, the engineer would skip the second part of the survey. The third part is concerned with general inspection methods, while the fourth part of the survey deals with detection of cracks, methods of repair, and effectiveness of these methods. If no fatigue cracks were encountered, the engineer would skip the fourth part of the survey. A blank survey is presented in Appendix A.

Prior to sending out any surveys, telephone contacts were made in all state highway departments to identify the design and inspection engineer who should receive a copy of the survey. The survey packages were then sent out at the end of January, 1992. A return date of February 28, 1992 was reported, providing about one month to complete and return the survey. A total of 51 surveys were sent out; forty-six responses were received - a 90 percent return. One state sent two responses.

The checked responses of the survey are tabulated in Appendix A. Whenever specific comments were written in the survey, these comments are also reported in Appendix A. A detailed discussion of the results and some of the important comments are presented hereafter.

3.2. Discussion

A detailed discussion of the results and the most important comments are presented in the following sections. Each question is presented first, then the discussion of this specific question follows. To make it easier on the reader, it was felt that a repetition of the whole question was necessary prior to the presentation of the results.

3.2.1. Question No.1

"Indicate the approximate percentage of the following bridge types used in your state:
-Steel
-Concrete
-Timber
-Other (Indicate Type:)"

Highway bridges are commonly made of steel and/or concrete. Timber bridges are mainly used for pedestrians and sometimes small traffic - small span crossings. As expected, the survey indicated that concrete and steel are the most commonly used materials in bridge construction. The average percentage of steel bridges in the states is 40.17%. The maximum percentage reported was 100%, while the minimum percentage was 3%. Masonry, aluminum, timber, and iron were included in the given percentages for most of the states.

3.2.2. Question No.2

"The following details are commonly used to increase the section modulus of steel bridge girders:
-Cover plates
-Increase in flange thickness
-Increase in flange width
-All of the above used
-Section modulus not changed at all
-Others "

Several details may be used to increase the flexural capacity of steel bridge girders; these include the use of a cover plate, the increase in flange thickness, and the increase in flange width

- see Fig. 3.1. Thirty-six states have used the cover plate detail in their bridges. Forty-three states commonly use an increase in the flange thickness and forty-two states commonly increase the flange width to increase the flexural capacity of the girder. Most of the states reported that the cover plate detail was used primarily in the past and is no longer used in the current design. Composite construction and increase in the girder depth at the supports were mentioned as alternative methods for increasing the flexural capacity of the girder.

3.2.3. Question No.3

"Cover plate details are mostly:
-Partial Length
-Continuous over the entire girder length
-Both types used "

Cover plates could be of the partial length type or of the full length type - see Fig. 3.2. As previously mentioned, the use of a cover plate is mainly intended to increase the flexural capacity of girders at high moment locations. Thus, the use of a partial length cover plate was common. When fatigue problems associated with this detail started to appear, the cover plate length was extended over most, and sometimes all, of the beam length in an attempt to move the critical fatigue detail (cover plate end) away from the high moment location. Of the 36 states using the cover plate detail, 11 states indicated that they commonly used both the partial-length and the full-length detail, while 24 states reported that they mainly used the partial length detail. One state didn't mention which type was primarily used. The current trend in design is either to avoid the use of cover plates altogether or to use full length details to avoid the fatigue problems associated with the partial length detail. It was reported , in one of the comments, that the partial length cover plate should be within 3' of the end bearings. This means that the cover plate end (critical fatigue detail) is moved far from the high moment location.

3.2.4. Question No.4

"For partial length cover plates, the plates mostly are:
-Welded
-Bolted
-Some details are bolted and the others are welded (give percentages)
-Not applicable "

The cover plate can be attached to the beam flange using welds or bolts. The use of welding was common because of its economy. Welding of partial length cover plates was reported as a common practice in the 36 states using this detail. Bolted connections for the cover plate were reported for 5 states only. The bolts are mainly used to retrofit cover plates to bolted or riveted girders. Bolts, rather than welding, are used at the terminal location of the cover plate, in the current practice - see Fig. 3.3.

3.2.5. Question No.5

"The most common welding process used for welded partial length cover plates is:
-Shielded Metal Arc Welding
-Submerged Arc Welding
-Flux Core Arc Welding
-Gas Metal Arc Welding
-Other (Specify)
-Not Applicable "

The most common welding process used to attach the cover plates to the beam flange was the submerged arc welding method. Twenty-seven states indicated that submerged arc welding was commonly used for welding cover plates, while seventeen states indicated that shielded metal arc welding was commonly used. Flux core and gas metal arc welding were rarely used. It should be noted that 20 to 30 years ago, when most of these details were fabricated, the flux core and the gas metal arc welding were not commonly used in the construction industry.

3.2.6. Question No.6

"For welded partial length cover plates, the plate ends are generally:
-Tapered
-Rounded
-Square
-Other (Specify) "

In an attempt to reduce the stress concentration, several different geometries were used at the cover plate ends: tapered, rounded, and square - see Fig. 3.4. The most common shape of the welded, partial-length cover plate detail is the tapered end geometry, with 32 states reporting that they had used this detail. Four states mentioned that they mainly used the tapered cover plate detail in the past practice, and that the recent trend is to use the square-ended detail.

The tapered cover plate provides a smoother transition for stresses than the square-ended cover plates. On the other hand, costs involved in fabricating the tapered shape are higher than for the square shape. Only four states indicated the use of rounded cover plate ends.

3.2.7. Question No.7

"The cover plates used with the girders are generally:
-Wider than the girder flange
-More narrow than the girder flange
-Neither wider nor narrower than the girder flange, both types are common "

Cover plates could be narrower or wider than the flange - see Fig. 3.5. The cover plates are mostly narrower than the girder flange, as reported by 37 states. In some cases, the bottom plate is wider than the flange while the top plate is narrower. For riveted built-up girders, the cover plate has approximately the same width as the flange.

3.2.8. Question No.8

"The cover plate welds are usually:
-Continuous
-Intermittent
-Both types used (Give percentages) "

The welds used to attach the cover plate to the girder flange can be continuous or intermittent. Thirty-seven states mentioned that the cover plate welds are usually continuous. Only four states mentioned the use of intermittent welds. The use of intermittent welds cause more fatigue problems than the use of continuous welds as a result of the numerous fatigue critical locations at the beginning and end of the intermittent weld beads. The saving in weld material, when using intermittent welds, is usually not big.

3.2.9. Question No.9

"The ends of the cover plates are typically:
-Welded
-Not welded
-Both welded and unwelded details are used "

Three different conditions are used primarily at the cover plate ends: full-end weld, return-end weld, and no-end weld - see Fig. 3.6. Thirty-four states reported that generally the cover

plate ends are welded to the girder flange. Use of an unwelded end detail was also mentioned by 10 of the states.

3.2.10. Question No.10

"Have any fatigue problems developed at the cover plates details in your state bridges?
-Yes (Specify below. Attach a sketch as needed)
-No "

Fatigue problems at the cover plate details were reported in 16 states, which is about 44 percent of the states using the cover plate details. These problems occurred at the ends of the cover plate weld.

3.2.11. Question No.11

"What are the normal inspection periods?
-Two years
-Other (Specify) "

The average normal inspection period was 1.9565 years. Most of the states inspect their bridges periodically at 2 years intervals, as required by the federal regulations. For fracture critical structures the inspection period is sometimes decreased to one year.

3.2.12. Question No.12

"What are the methods used for ordinary (routine) inspections?
-Visual
-Other (Specify below) "

Visual inspection is used for ordinary inspection, as reported by 45 states. Dye penetrant, ultrasonic devices, and magnetic particle inspection, as well as magnifying glasses, are rarely used for routine inspections.

3.2.13. Question No.13

"What is the minimum crack size that you believe can be detected by the inspection procedures used during ordinary inspections?"

It seems that there was some confusion about the meaning of the term *"crack size"*. Some respondents interpreted it as *"crack length"*, while others understood it as *"crack width"*. For the

cases where the answers did not mention whether the length or the width are the specified value, personal judgement was used according to the value indicated. The average crack length that could be detected by the ordinary inspection techniques (visual inspection) is about 0.3 in, while the average width was about 0.02 in. Many answers reflected that the crack is detected by rust stains on the paint or paint cracking. In that case, hairline cracks are usually detectable. The distribution of estimated detectable crack length is shown in Fig. 3.7. It could be seen that most responses indicated a detectable crack length of 0.1-in to 0.3-in.

3.2.14. Question No.14

"Approximate age of the bridges that have developed fatigue cracking problems (please identify the type of detail that developed cracks):

-Less than 5 years
-5 to 10 years old
-10 to 20 years old
-20 to 30 years old
-Mole than 30 years old "

A wide variation in the age of bridges that developed fatigue cracking problems was reported, from less than 5 years old to more than 30 years old. Most of the bridges that developed fatigue cracks were built 20 to 30 years ago, as reported by 23 states. But some fatigue problems were also reported for bridges that were built less than 5 years ago (as mentioned by four states). It should be noted that the bridge age is not a sufficient indication on how good the detail is. The amount of traffic that the bridge sees is of an extreme importance. One way of measuring the amount of traffic passing over a bridge is the average daily truck traffic (ADTT). Fatigue problems due to out of plane bending at lateral bracing attachments with the girder were reported by many states. Fatigue cracks at the cover plate ends were reported in bridges constructed 10-20 years ago. Figure 3.8 shows the distribution of the bridge age when a fatigue crack was observed.

3.2.15. Question No.15

"If during ordinary inspections a crack was detected or suspected to exist, what additional nondestructive methods are typically used in this case?

-Visual with Magnifying Glass
-Ultrasonic
-Radiographic

-Dye Penetrant
-Acoustic Emission
-Magnetic Particle
-Other (Specify:) "

When a crack is detected, the most common techniques for additional inspection are dye penetrant, magnifying glass, and ultrasonic evaluation, as reported by 35, 31, and 24 states, respectively. Magnetic particle was also reported to be used in 17 states. Radiographic and acoustic emission methods are seldom used (as mentioned by 3 states).

3.2.16. Question No.16

"What is the approximate minimum crack size that your inspectors can detect when using the aforementioned NDT methods?"

Again, there was some confusion about the term *"crack size"*. Personal judgement was also used to differentiate between the crack length and width. The average minimum crack length detected is 0.2-in, while the average width is about 0.02-in. It should be noted that the crack length detected is dependant on the type of method used in the inspection. The average numbers are calculated without regard to the NDT methods used. Most of the responses indicated several methods for the inspection, but gave only one crack size. Generally, the respondents indicated that ultrasonic devices are capable of detecting smaller cracks than visual inspection aided by a magnifying glass. Many respondents exhibited considerable confidence on the possibility of detecting "any crack".

3.2.17. Question No.17

"What criteria are used to evaluate the need for repair of the fatigue cracks which are detected?"

Member location, redundancy of the structure, crack growth, and the stress range were cited as the most important factors that would dictate the action taken upon the detection of a crack. In a few states, a consultant was retained to determine the need and type of repair required. A few answers indicated that some action is always taken when a crack is detected.

3.2.18. Question No.18

"Which of the following repair techniques have been utilized to eliminate or minimize fatigue crack growth (please identify detail type):
-Use of splice plates in cracked region
-Use of large diameter cores to remove cracks
-Use of peening
-Use of gas-tungsten arc remelting
-Removal and replacement of cracked members
-Other (Specify below) "

The use of splice plates in cracked region, large diameter cores to remove cracks, and replacement of cracked members were reported to be commonly used by 28, 23, and 17 states respectively. In 12 states, peening was also used, but was reported to be used with other repair methods and not alone. Gas-tungsten arc remelting was mentioned to be used in two states only. Grinding the cracked regions to remove the crack and rewelding was mentioned as a commonly used technique in 3 states. It was advised that grinding should not be done perpendicular to the line of stress. Another technique mentioned for repair of beam web cracks consisted of drilling the crack tip and monitoring the crack to make sure it is not growing and propagating through the hole.

3.2.19. Question No.19

"Provide specific details, procedures, or comments that you believe should be noted for the repair techniques that you have used. Feel free to attach any sketches or specifications used for detail repair if you believe that these would be useful."

Most of the answers to this question referred to their response to the previous question. It was mentioned that some of the splice plate repairs can cover up and hide the cracks, making it very difficult to monitor the crack growth after the repair has been completed. It was also mentioned that the location of the crack is very critical when using holes to remove the crack tip. Many answers reported that cracks had propagated through the drilled holes and, therefore, the crack should be monitored after repair.

3.2.20. Question No.20

"How effective was the repair technique?
-Very effective (crack stopped)
-Not effective
-Not in service long enough to judge "

The repair techniques were reported to be effective if the crack was totally eliminated by grinding or drilling. Otherwise, the crack would eventually grow again. Several states indicated that the repairs had not been in service long enough to judge their effectiveness.

3.2.21. Question No.21

"Since the repair, have any new cracks been detected?
-Yes
-No "

Only seven states reported that new cracks had been detected after repair. In most cases, the new cracks developed when out-of-plane bending caused cracks to propagate through the arresting holes.

3.2.22. Question No.22

"Indicate the size and location of cracks detected after repair."

The answers reflected that the new cracks had a similar size and location as the original flaws. In most cases the crack propagated through the arresting hole.

3.2.23. Question No.23

"How was the additional cracking detected?"

The new cracks were mainly detected visually, when new cracks were observed to propagate beyond the arresting holes.

3.2.24. Question No.24

"What did you do?"

In general, the repair technique (hole drilling) was repeated to repair the new crack.

3.3 Summary

A number of states have observed fatigue cracking at the ends of welded, partial-length tapered cover plate details. as a result of these problems, this detail is not generally used in new bridge construction. However, many bridges with this detail are in use throughout the country.

The main repair method reported for this detail involves the use of bolted splice plates.

A number of problems were reported from fatigue cracks at details subjected to out-of-plane bending. In this case, cracks propagated in the web at the connection of diaphragms or lateral bracing with the girder. The repair technique that was widely used for this type of cracks was to drill a hole at the crack tip. It seems that this method did not prevent the crack from growing through the hole. The probable reason behind this is that the crack tip was not completely eliminated during the drilling process, and/or additional out-of-plane bending caused cracks to re-form.

Peening the weld toe is not used as a separate repair method. To be effective, peening must be conducted when the cracks are very small.

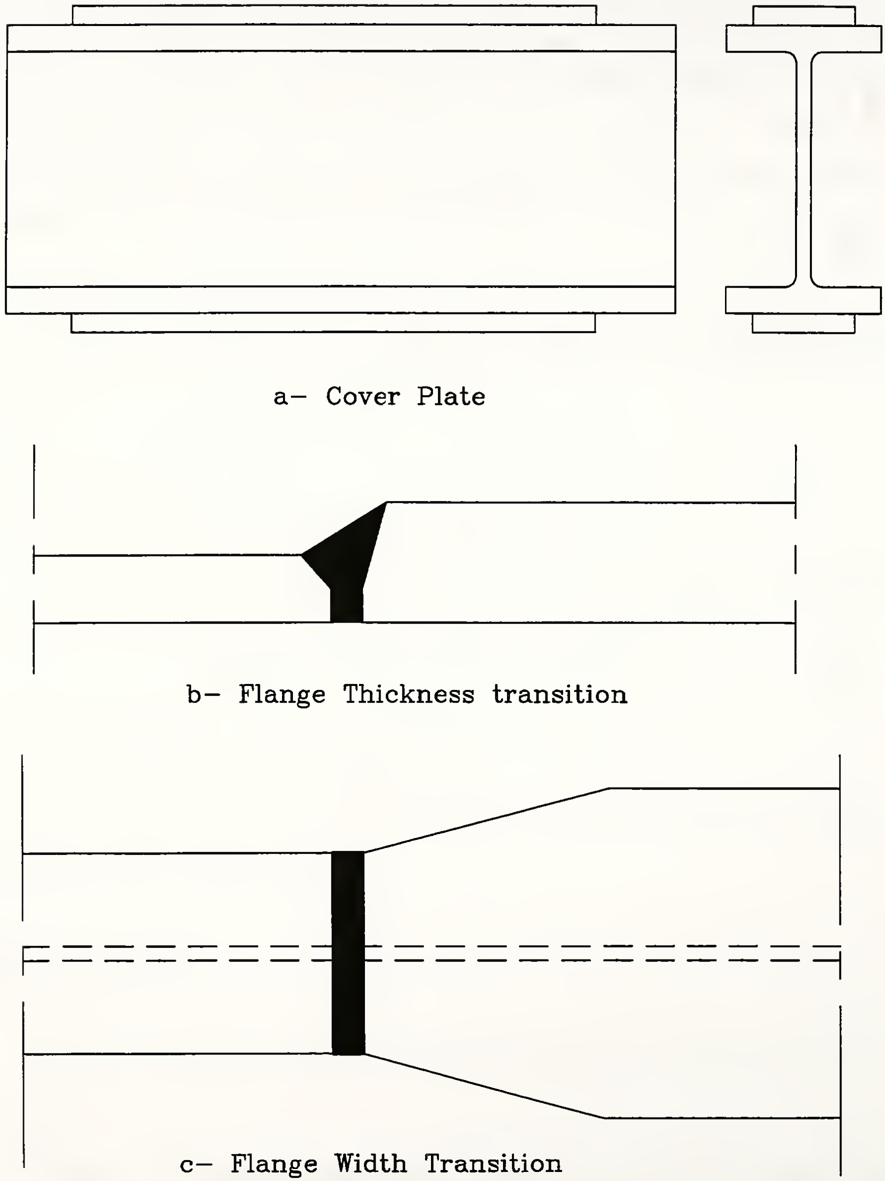

Fig. 3.1. Methods of Increasing the Flexural Capacity of Steel Girders.

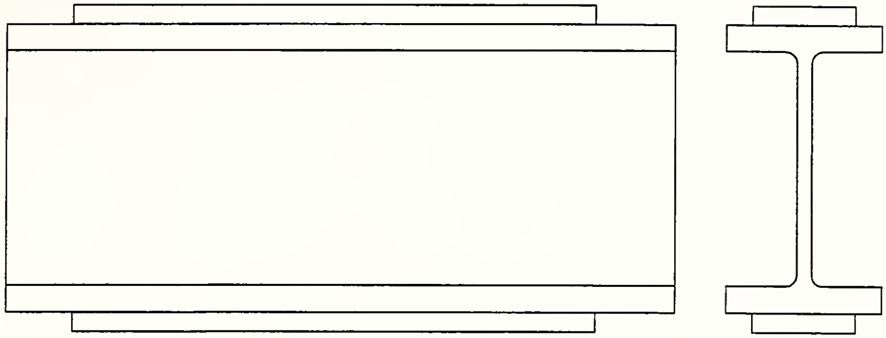

a– Partial Length Cover Plate

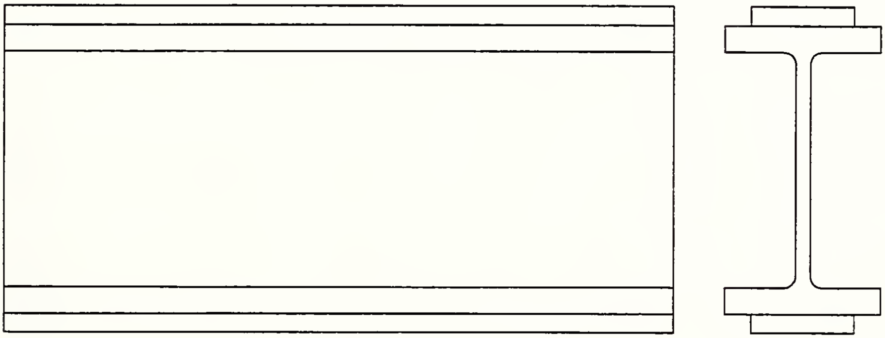

b– Full Length Cover Plate

Fig. 3.2. Partial and Full Length Cover Plate Options.

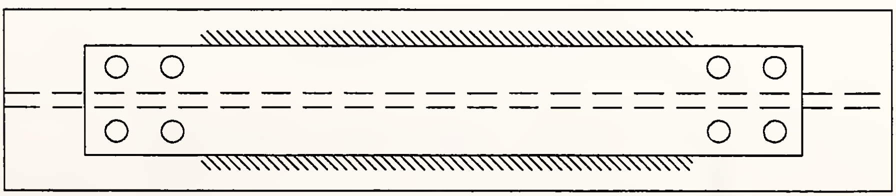

Fig. 3.3. Use of Bolts at Terminal Locations.

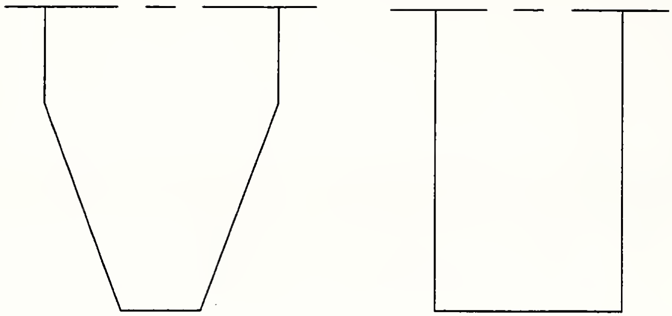

a– Commonly Used Details

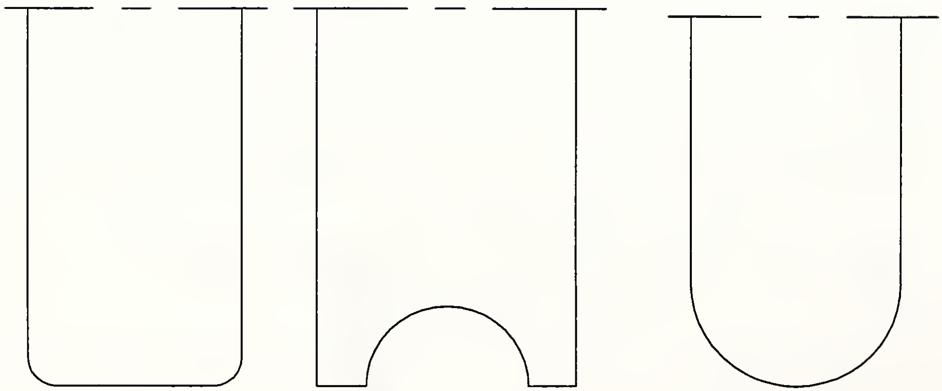

b– Rarely Used Details

Fig. 3.4. Cover Plate End Details.

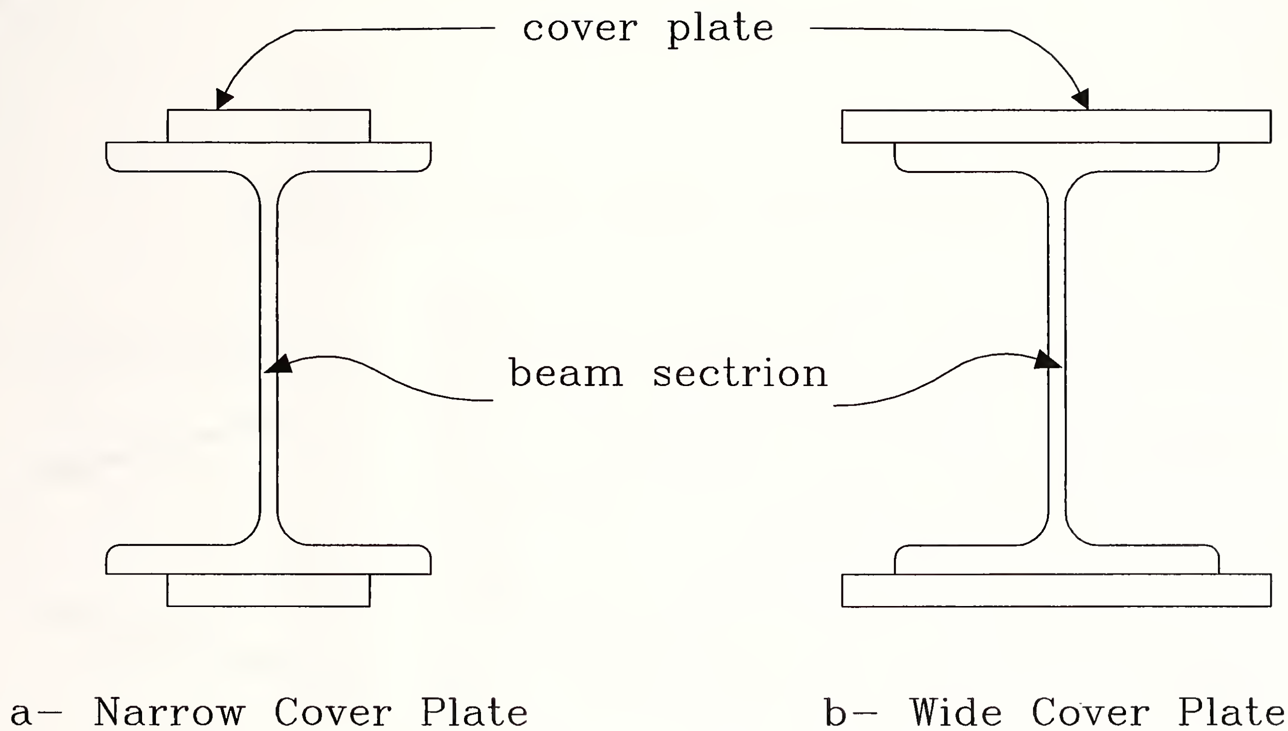

Fig. 3.5. Cover Plate Width.

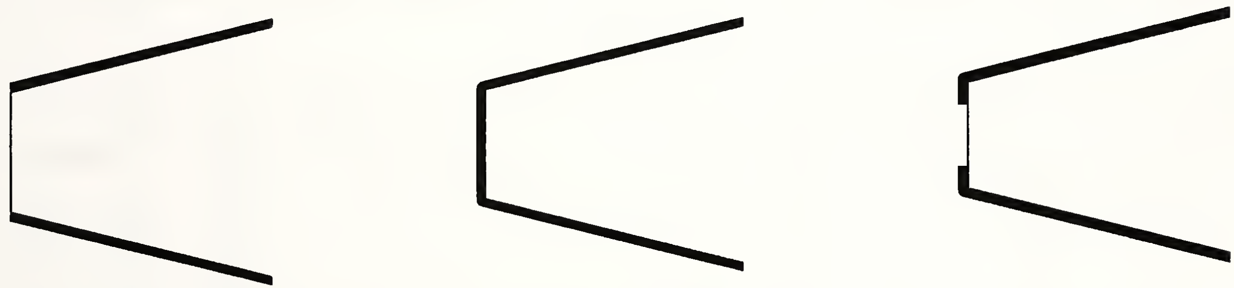

No end weld Full end weld Return end weld

Fig. 3.6. End Weld Conditions.

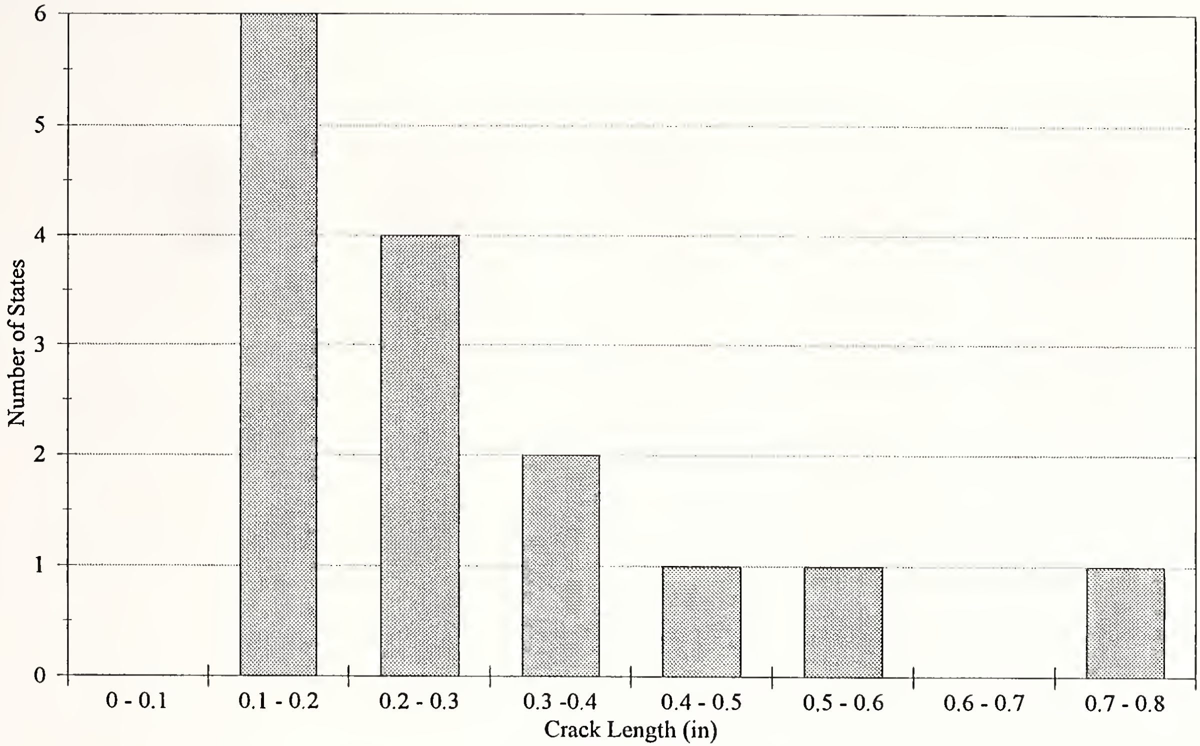

Figure 3.7. Detectable Crack Size Distribution by Visual Inspection.

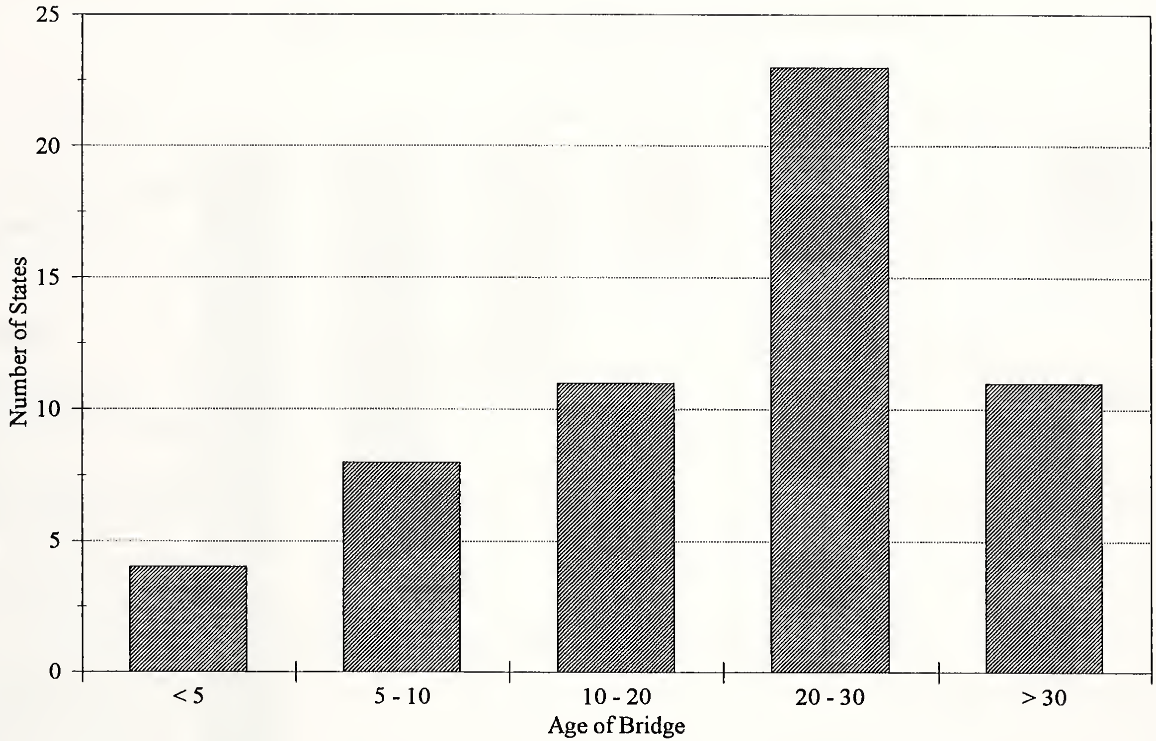

Figure 3.8. Age of Bridge that Developed Fatigue Cracks.

CHAPTER 4
EXPERIMENTAL PROGRAM

4.1. Design Variables

The design variables for the experimental study can be divided into three categories: cover plate width, end weld type, and repair method. Most of the test specimens were subjected to the same constant amplitude load range. The test specimen matrix showing combinations of the test variables studied is given in Table 4.1.

Thirty three W 14 × 30 beams were tested during the experimental phase of the study to fulfill the study objectives. The beams, fabricated from ASTM A36 steel, were 16-ft - 6-in long, tested on a 16-ft span. The beam configuration and specimen dimensions, shown in Fig. 4.1, were similar to the test specimens utilized by Sahli, Albrecht, and Vannoy (1984) on square ended cover plates. Tapered cover plates, 60-in long and 0.5-in thick, were welded to both flanges of the beams.

Two different tapered cover plate widths were studied, as shown in Fig. 4.2. The narrow cover plate $''N''$ was 5.5-in wide, and was not as wide as the beam flange, while the wide cover plate $''W''$ was 8-in wide. These two widths were chosen to model the range in detail widths used in Indiana - see Fig. 1.1.

Three different cover plate end weld conditions were used: no-end weld $''N''$, full end weld $''F''$, and return end weld $''R''$. The different end conditions are illustrated in Fig. 4.3. A survey conducted prior to starting the test program (discussed in detail in Chapter 3) indicated that these three end conditions were used, and that the return end weld was the most common detail in Indiana as well as other states.

Three repair methods were investigated: a friction type bolted splice plate connection, air hammer peening of the weld toes at the cover plate ends, and a partial bolted splice connection that combines both air hammer peening and the bolted splice connection without the bottom splice plate. Two splice plate thicknesses, 5/16-in and 7/16-in, were studied for the bolted splice plate connection. Only 7/16-in thick splice plates, however, were used for the partial bolted splice connection.

Prior to repair, all test beams were subjected to a constant amplitude load range that produced a stress of 20.0-ksi at the extreme fibers of the bare beam section adjacent to the cover plate ends. After repair, only two test specimens were subjected to a 15.0 ksi stress range, while the remaining 31 specimens were subjected to the same load cycle that was used during the pre-cracking phase.

4.2. Fabrication

All test beams were fabricated by Farnsworth Steel Inc. at their fabrication shop in Indianapolis, IN in May 1992. The fabricator was told to use the same procedures that would be used in normal bridge fabrication. Shop drawings, indicating the particular features and details for each specimen, were prepared by the fabricator.

Steel for both the specimens and the cover plates was ASTM A36. The mechanical properties and chemical composition of the steel was supplied by the manufacturer and is listed in Appendix B. Tension coupons were cut from the excess steel and tested to determine the mechanical properties. The results obtained are listed in Appendix B. Also, four cubes were cut from the steel for chemical analysis; the chemical composition is also listed in Appendix B.

Eleven 51-ft long W 14 × 30 beams were cut to the required 16-ft - 6-in length to obtain the 33 test specimens for the testing program. Nineteen beams were needed for the bolted splice portion of the study, eight beams for peening, and 6 beams for partial bolted splice repair. Ten of the eleven 51-ft long beams were obtained from the same heat of steel.

All the plate components, with the same width, were taken from the same heat of steel. The plates were cut to the tapered geometry required for the cover plates and the tapered surfaces ground to remove any surface burrs. All the plates were manually welded to the beam flanges using the Gas Shielded Flux Cored Arc Welding procedure. Carbon dioxide was used as the shielding gas. DC Miller welder machines were used to supply the electrical energy required by the welding process. Flux core wires, E70T-1 5/64-in diameter were used as electrodes to obtain the required 5/16-in weld size.

The geometric position of the plate components were marked first on the beams. C-clamps were then used to hold the plates in position so that the plates could be tack welded to the beam flanges. No preheat was utilized prior to the tack welding. The tacks were placed roughly at a 10-in interval with one tack at the beginning and end of each taper. Stick welding was used for

tack welds with 1/8-in diameter E7018 electrodes. The approximate voltage and amperage used in the tack welding were 35 volts and 300 amperes, respectively.

No preheat was used prior to welding. All welds were deposited in the flat position in one pass to obtain the required 5/16-in weld size. The weld size was measured with a weld gage and an additional pass was placed if the weld size was smaller than required. For the narrow cover plate specimens, the upper plate was first welded to the upper flange according to the specific weld detail, then the beam was turned over and the sequence repeated. In the case of the wide plate specimens, the tapered part of the upper plate was first welded to the upper beam flange, then the straight part of the lower plate was welded to the lower flange. No weld was placed in the last 1-in of both the tapered and straight parts of the cover plate to simulate the actual weld shape used in Indiana - see Fig. 1.1. The beam was then turned over and the same procedure repeated.

Three welders were involved in the fabrication of the return end weld specimens during the period of monitoring the beam fabrication. The sequence of welding varied from one welder to another. The voltage and amperage were also different from one welder to another and even with the same welder. The voltage ranged from 24 to 29 volts, while the amperage ranged from 320 to 440 amperes. The wire feed rate ranged from 13 to 16.5 ft/min depending on the welder. The voltage and amperage values were obtained from the welding machine and were checked periodically during weld placement. To measure the wire feed rate, each welder was asked to press on the feed button in his gun, prior to welding, for a specific time, measured with a stop watch. The length of the wire was measured and the wire feed rate was calculated according to the wire length and feed time.

The observed welding procedure is summarized as follows:

1- Use an air chisel to remove slag from the tack welds.

2- Mark the no-weld positions.

3- Clean the weld surface using a wire brush prior to welding (occasionally).

4- Knock on the weld gun to remove any molten wires inside.

5- Weld the cover plate to the beam flange.

6- Use an air chisel to remove slag from the weld.

7- Clean the weld surface with a wire brush.

8- Measure the weld size with a weld gauge.

After a period of time, the gun nozzle was placed in a nozzle dip to prevent weld from building up in the nozzle.

The average heat input, based on the observed welding variables, was 49.5 KJ/in. It should be noted that there was a wide variation in the heat input from one welder to another, and even from one weld line to another for the same welder. The heat input ranged from 55.5 to 63.8, 32.9 to 38.4, and 29.1 to 55.3 KJ/in. for welders 1, 2, and 3, respectively. It should be noted that the previously mentioned ranges are based upon measurements of the voltage, amperage and deposition rate for 5, 1, and 3 beams for welders 1, 2, and 3, respectively.

4.3. Experimental Procedure

All beam specimens were tested on a 16-ft - 0-in span with four-point loading, as shown in Fig. 4.1. A 55-kip MTS servo-hydraulic linear actuator was used to apply the required loading in each of the two test frames used during the test program. A spreader beam, placed on top of the test beam, distributed the load from the actuator to the test specimen. The distance between loading points was 2-ft - 0-in, with a roller used between the test beam and spreader beam. Figure 4.4 shows photographs of the test setup.

The test beams were first cycled until a visible crack was detected through either visual inspection with a 10X magnifying glass or ultrasonic detection. The pre-cracking was achieved by subjecting the test beams to sinusoidal load cycles, with an R-ratio of 0.05, that produced a stress range of 20.0 ksi in the bare beam section adjacent to the cover plate end. In the case where cracks were detected at only one of the two ends of the beam, a temporary splice plate connection was used to arrest further crack growth in that end. This temporary splice plate connection consisted of one plate 24-in × 6-in × 1-in, and two plates 24-in × 2-in × 1-in. The thick plates were clamped to the cracked end by means of heavy duty C-clamps. When both ends were cracked, the beam was repaired using one of the repair procedures to be investigated. The test was continued with the same cyclic load (except for two specimens) until the necessary number of load repetitions had been applied.

The first repair method investigated involved the use of a friction type bolted splice plate connection. The splice connection, shown in Fig. 4.5, was designed to compensate for the cracked flange by assuming that the flange is completely severed at the end of the cover plate. Using this assumption, a splice plate thickness of 5/16-in was selected so that the maximum stress did not

exceed 20 ksi. Moreover, because the splice plates needed to be quite long to extend beyond the taper, it was believed that the combination of the plate flexibility and the fact that the tension flange was not fully cracked (as assumed) would mean that significant stresses would still exist at the cover plate end. Consequently, it was postulated that splice plates thicker than those required for the maximum stress limitation would be needed to reduce the stress at the cover plate ends. To study this effect, splice plate thicknesses of 7/16-in were also tested. A total of 19 specimens were repaired using the bolted splice plate connection. Initially, only 3 specimens were to be repaired using the 7/16-in splice plates. As the tests progressed, it was evident that neither of the two splice plate thicknesses were able to completely prevent subsequent crack growth, especially when the initial crack, prior to repair, was large. In order to study the effect of splice plate thickness in more detail, it was decided to test some of the remaining beams repaired with a 5/16-in splice on one end and a 7/16-in splice on the other end. In these cases, the 7/16-in splice was attached to the end with the larger initial crack size. Although some of the full bolted splice plate beams were repaired using both the 5/16-in and the 7/16-in details, at least one of each beam configuration was repaired using the 5/16-in splice at both ends. After repair, eighteen specimens were subjected to the same pre-cracking load cycling, while one specimen was subjected to a 15.0 ksi stress range with an R-ratio of 0.05.

The second repair method consisted of air hammer peening the cover plate end weld toes. Figure 4.6 shows a sketch of the peening area. A total of 8 specimens were peened, five after pre-cracking and three prior to pre-cracking. These three beams were cycled for 75,000 cycles under 20.0 ksi stress range, and then inspected to confirm that no cracks had developed. The 75,000 cycle pre-loading was selected so that the cover plate end welded detail had experienced a significant number of loading excursions, but not so many cycles such that a detectable crack would initiate. The purpose of these tests was to evaluate the effectiveness of peening prior to significant crack initiation. A pre-cycle of 75,000 cycles was used, however, to model damage which may occur in actual bridges which have been in service for a number of years, but which have not yet developed a detectable fatigue crack.

The third repair method involved the use of both air hammer peening and a friction type splice plate connection - see Fig. 4.7. All of the six beams repaired using the partial bolted splice method were pre-cracked prior to repair. After repair, five specimens were subjected to the same load cycle used during the pre-cracking stage (20-ksi stress range at the cover late end), while

one specimen was subjected to a load cycle that would cause a 15-ksi stress range at the end of the cover plate in the beam prior to repair.

During the first stages of the experimental phase, compression flange cracks developed at the cover plate ends in the top of the beam. It is believed that these cracks occurred as a result of tensile residual stresses at the cover plate ends from the welding procedure. The tensile residual stress subjects the compression flange adjacent to the weld toe to stress cycles that are partially in tension, although all the external load stresses would be entirely compressive. Another factor that might have contributed to the compression crack initiation is the lateral movement of the compression flange. The flanges were connected to the loading frame through the use of a series of straps near the loading points. But due to the non-straightness of the beam section, most of the specimens had some lateral sway during the cyclic loading. After a couple of compression flange cracks developed, the compression flange at the cover plate ends was peened prior to cycling to prevent the initiation of compression cracks. The peening process was successful in reducing the occurrence of these compression cracks.

4.4. Repair Methods

The following sections describe briefly each of the repair methods investigated during the experimental phase of this study. A description of the step-by-step procedure used for each repair method is presented in Appendix C.

4.4.1. Bolted Splice Repair

The use of bolted splice plates allows a portion of the flange force to be transmitted away from the cover plate ends, and consequently away from the crack location. In other words, the amount of stress that contributes to further crack propagation is reduced. Four high-strength bolts were needed at each end of the splice plate to develop the flange tension force in a slip-critical connection. The connection involves the use of either 5/16-in or 7/16-in thick ASTM A36 steel plates, 7/8-in diameter ASTM A325 bolts and ASTM A563 grade C nuts. A magnetic drill, shown in Fig, 4.8, was used for hole drilling. Figure 4.9 shows a typical beam end after hole drilling and a typical beam end after installation of the splice plates.

The bolt lay-out was selected to keep the splice plate length to a minimum for the narrow cover plate detail. The bolts center lines were 1 1/2-in, and 4 1/2-in from the cover plate end -

see Fig. 4.10. During testing, it was observed that the filler plate was too close to the cover plate end weld (usually the actual weld size is larger than the requested 5/16-in size). Thus, it is recommended that the first row of bolts be at a distance 1 3/4-in from the cover plate ends. On the other hand, the bolt center lines were 1/2-in and 3 1/2-in from the intersection of the taper and straight portions of the cover plate - see Fig. 4.10. The 1/2-in distance was chosen to prevent the bolt hole from intersecting with the taper portion of the cover plate. In the case of the wide cover plate detail, the bolts could be moved closer because of the cover plate geometry. However, it was decided to keep the bolt spacing the same for both the narrow and wide cover plate detail to keep the splice plate length constant.

4.4.2. Peening Repair

Peening is a procedure that introduces compressive residual stresses that are effective in either delaying the initiation of fatigue cracks or halting the propagation of existing cracks. There are two distinct peening methods: air hammer peening and shot peening. Air hammer peening involves the use of a hardened tool which is inserted in a pneumatic air hammer to impact the work piece - see Fig. 4.11. Shot peening, meanwhile, uses shot of different materials and sizes propelled at the weld toe area by air pressure or centrifugal force. The equipment generally includes a means of collecting the shot and sieving to extract and discard the damaged shot. Shot peening is a more controlled process than air hammer peening, as the latter is greatly influenced by the operator. On the other hand, shot peening requires the use of sophisticated equipment and trained personnel. Shot peening equipment and treatment procedures are discussed in more detail by Welsch (1990).

Air hammer peening was selected for use in the present study due to its simplicity of use. The peening tool utilized is similar to the tool described in the weld peening requirements of the Connecticut Department of Transportation. Based on studies by Hausammann et al. (9183), six passes of the peening tool at 40-psi pressure were used to treat the weld toe material at the end of the cover plate. An example of the surface deformation after peening treatment is shown in Fig. 4.12.

4.4.3. Partial Bolted Splice Repair

The partial bolted splice repair technique is a procedure that involves both the use of a bolted splice plate connection along with the use of air-hammer peening at the weld toe - see Fig. 4.7. In the partial bolted splice plate detail, the bottom fibers of the tension flange at the weld toe are peened. Moreover, two splice plates are used on the top fibers of the tension (bottom) flange to assist in transferring a portion of the flange force away from the weld toe region. There are two main advantages of this repair procedure over the conventional friction type splice plate connection. First, the bottom fibers of the flange are accessible to visual inspection, such that any further propagation of existing cracks could be monitored. Second, the partial bolted splice connection provides a greater clearance between the top of the road surface and the bottom of the bridge structure clearance due to the absence of a bottom splice plate.

Table 4.1. Test Specimen Matrix.

Specimen	Cover Plate		End Weld			Repair Condition[4]			
	NP	WP	REW	FEW	NEW	FBS	FBS2	PW	PBS
DB1[1]	✓		✓			2			
DB2[1]	✓		✓			2			
DB3[1]	✓		✓			2			
NR1	✓		✓			2			
NR2	✓		✓				2		
NR3	✓		✓				2		
NR4	✓		✓				2		
NR5[2]	✓		✓					2	
NR6[2]	✓		✓					2	
NR7[3]	✓		✓						2
NR8[3]	✓		✓				2		
NR9	✓		✓					2	
NR10	✓		✓					2	
NR11	✓		✓						2
NR12	✓		✓						2
WR1		✓	✓			2			
WR2		✓	✓			1	1		
WR3		✓	✓			1	1		
WR4		✓	✓					2	
WR5		✓	✓					2	
WR6		✓	✓						2
WR7		✓	✓						2
NF1	✓			✓		2			
NF2	✓			✓		1	1		
NF3	✓			✓		1	1		
NF4	✓			✓				2	

Table 4.1. Test Specimen Matrix. (cont.)

Specimen	Cover Plate		End Weld			Repair Condition[4]			
	NP	WP	REW	FEW	NEW	FBS	FBS2	PW	PBS
NF5	✓			✓					2
WF1		✓		✓		1	1		
WF2		✓		✓		2			
WF3		✓		✓		1	1		
NN1	✓				✓	2			
NN2	✓				✓	1	1		
NN3[2]	✓				✓			2	

[1] *Beams from Different Heat of Steel*

[2] Beams peened prior to cracking

[3] Beams cycled at 15.0 ksi stress range after repair

[4] Number of ends with this condition

Notes:

NP	=	Narrow Cover Plate
WP	=	Wide Cover Plate
REW	=	Return End Weld
FEW	=	Full End Weld
NEW	=	No End Weld
FBS	=	Full Bolted Splice with 5/16-in plates
FBS2	=	Full Bolted Splice with 7/16-in plates
PW	=	Peened Weld
PBS	=	Partial Bolted Splice

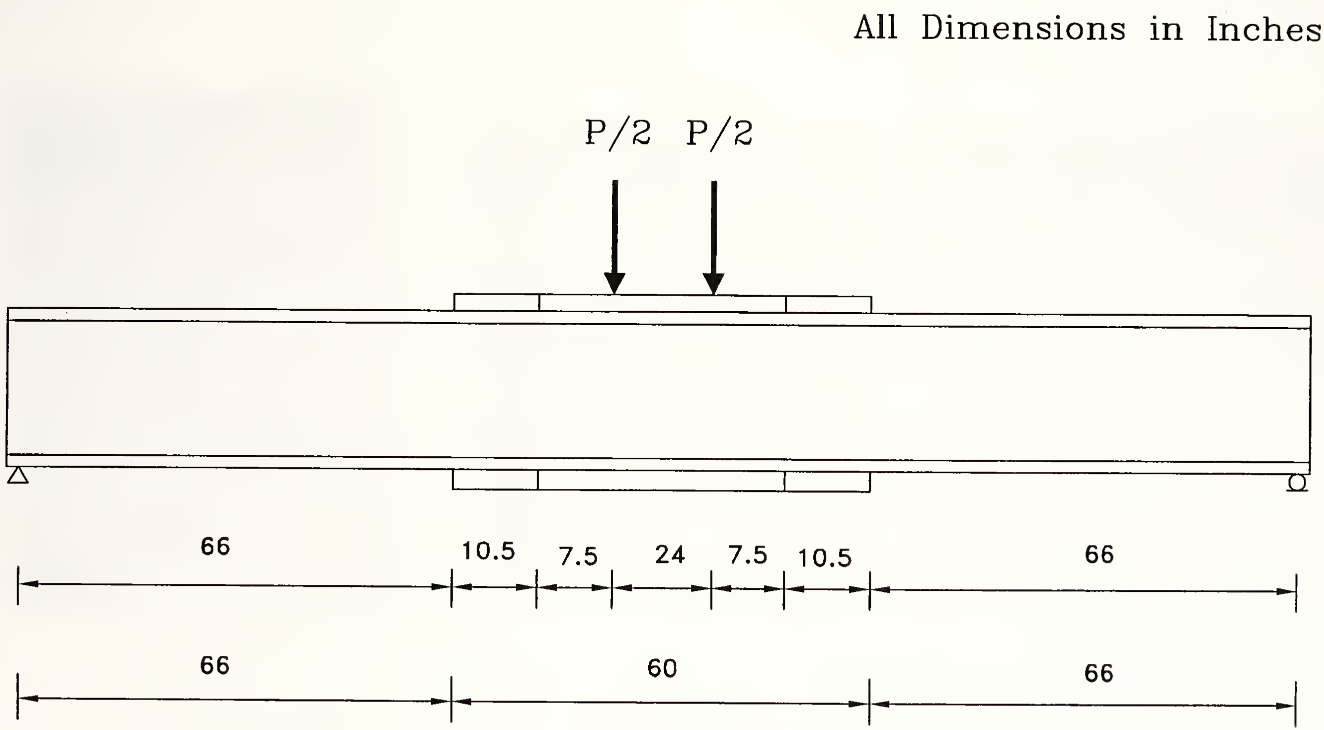

Fig. 4.1. Specimen Configuration and Loading.

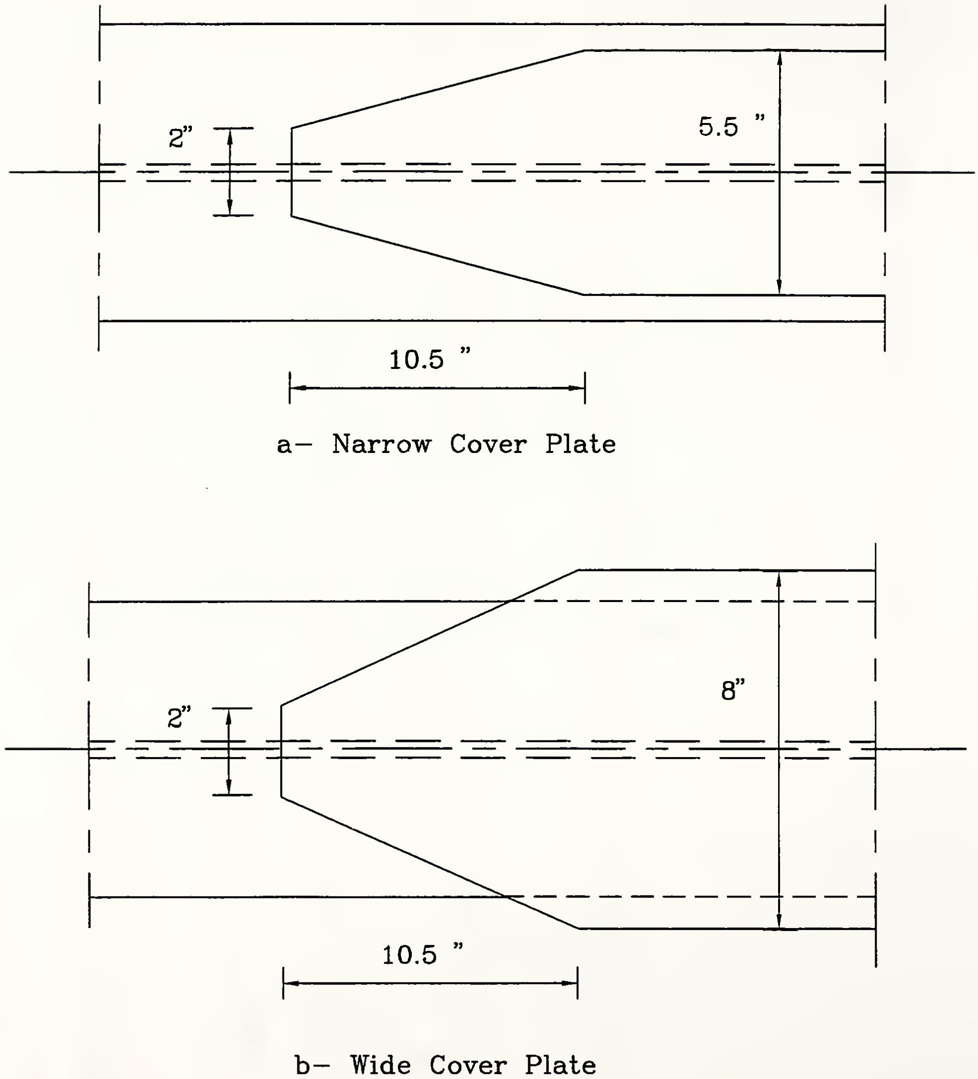

Fig. 4.2. Tapered Cover Plate Detail.

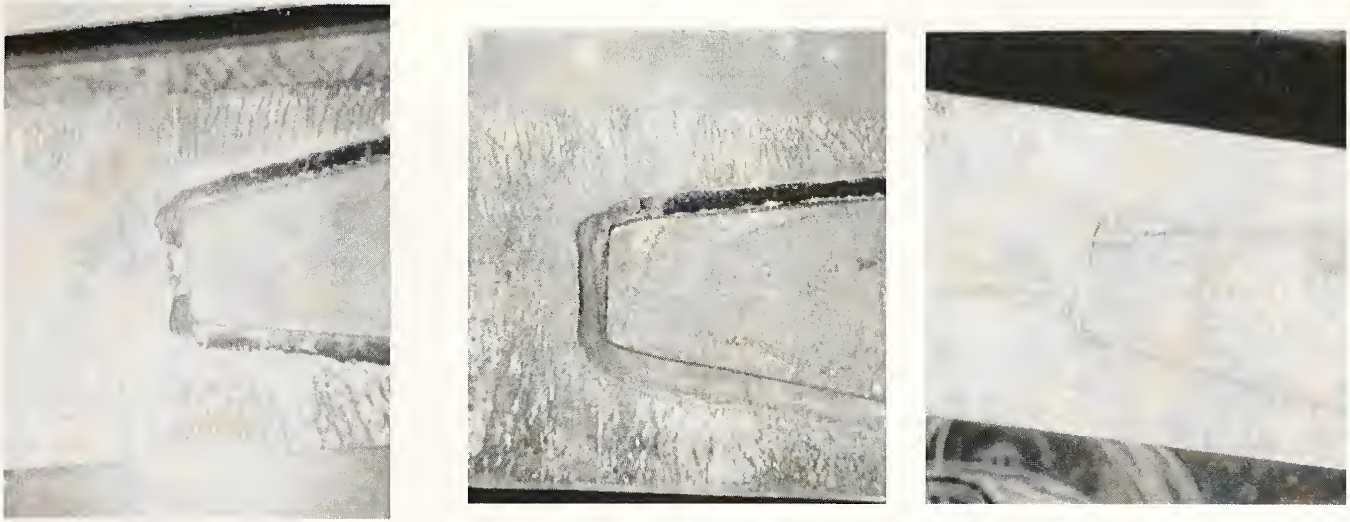

(a) Return End-Weld (b) Full End-Weld (c) No End-Weld

Fig. 4.3. End Weld Conditions.

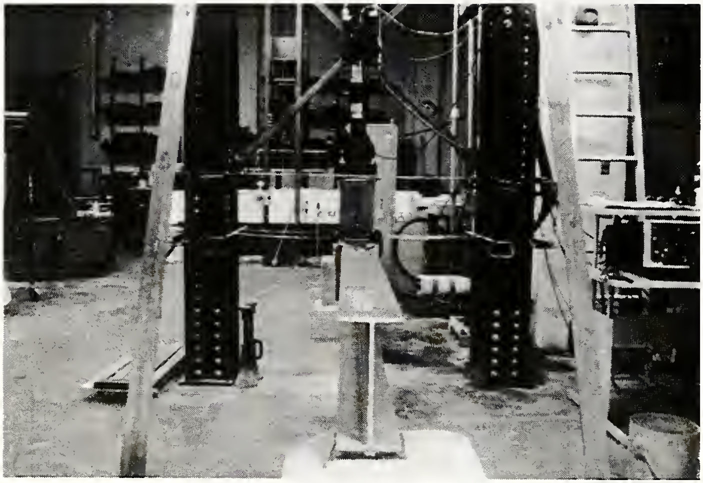

(a) General View

(b) Loading Actuator and Spreader Beam.

Fig. 4.4. Test Set-Up.

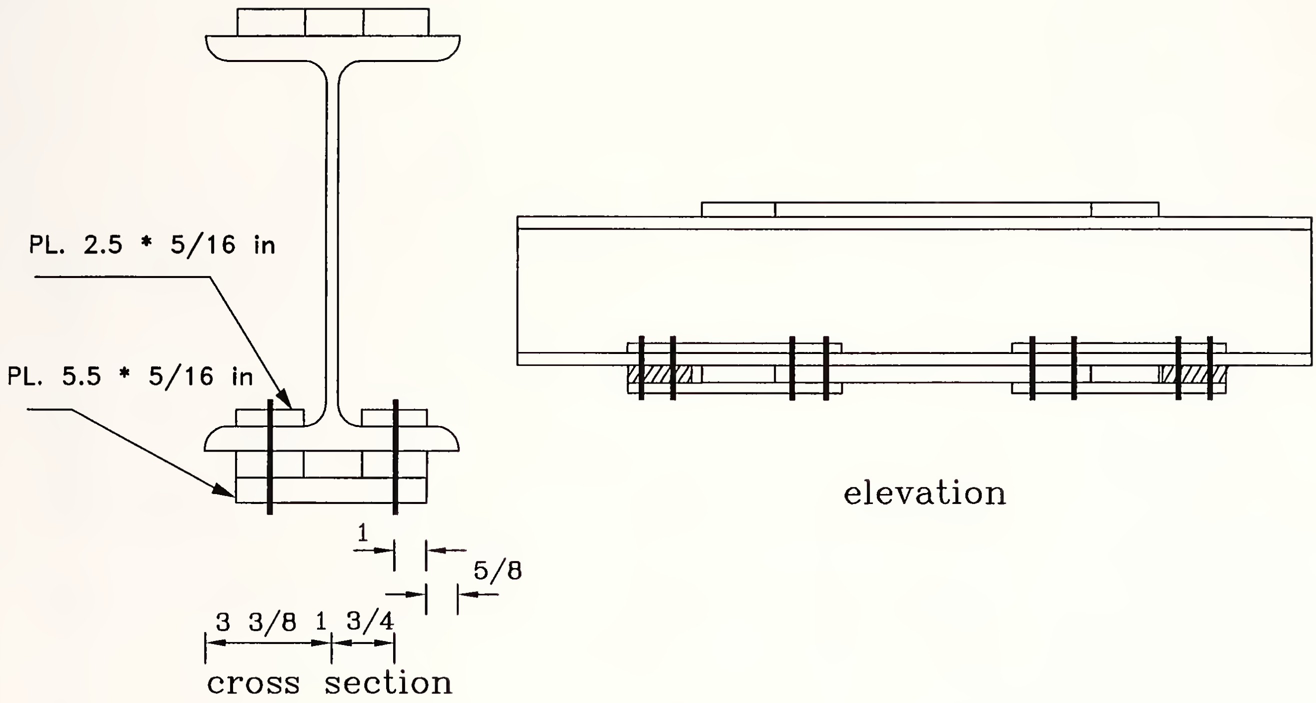

Fig. 4.5. Full Bolted Splice Connection.
(Elevation and Cross Section)

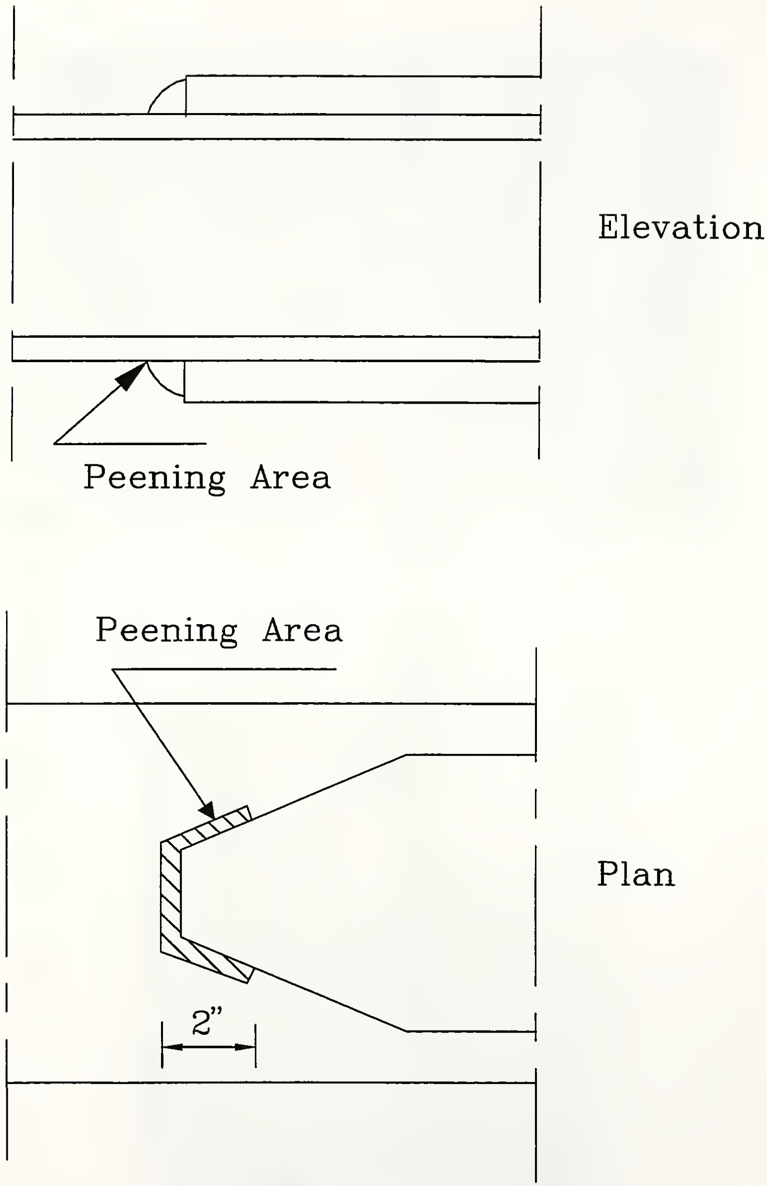

Fig. 4.6. Peening Area.

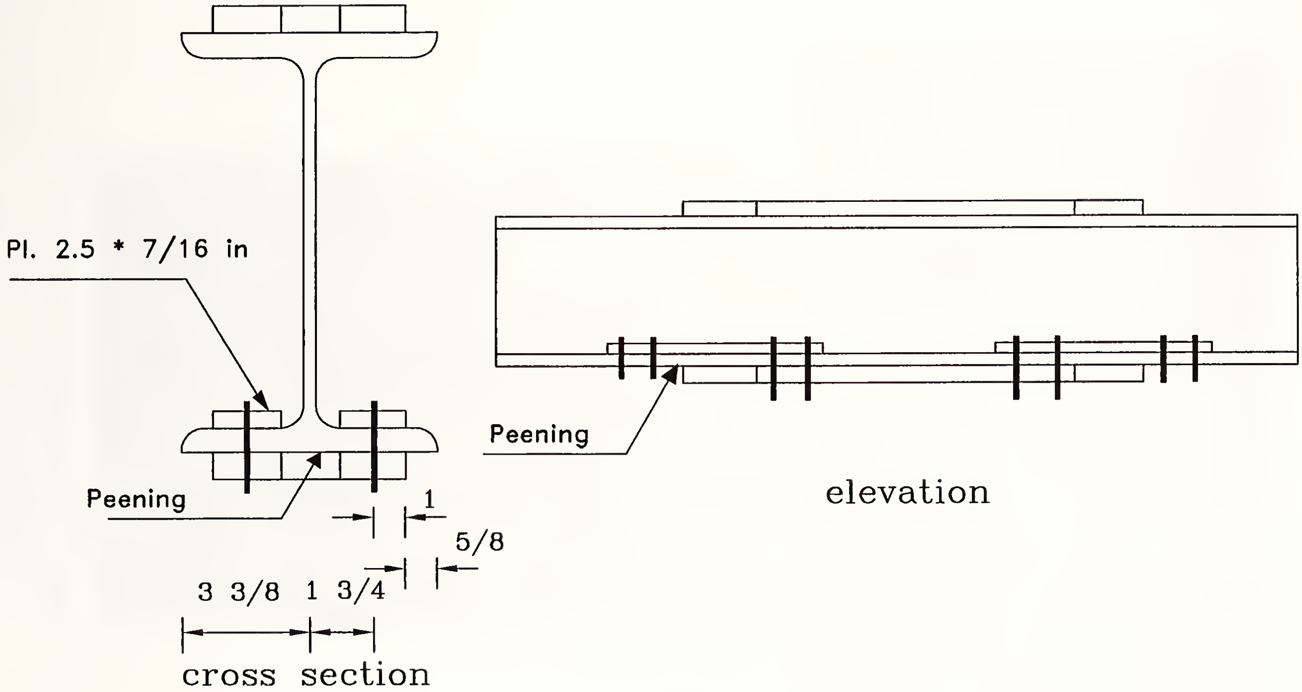

Fig. 4.7. Partial Bolted Splice Connection.
(Elevation and Cross Section)

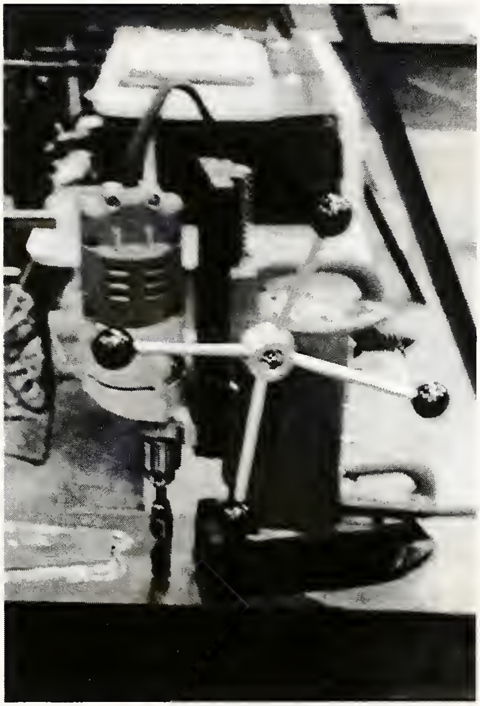

Fig. 4.8. Magnetic Drill.

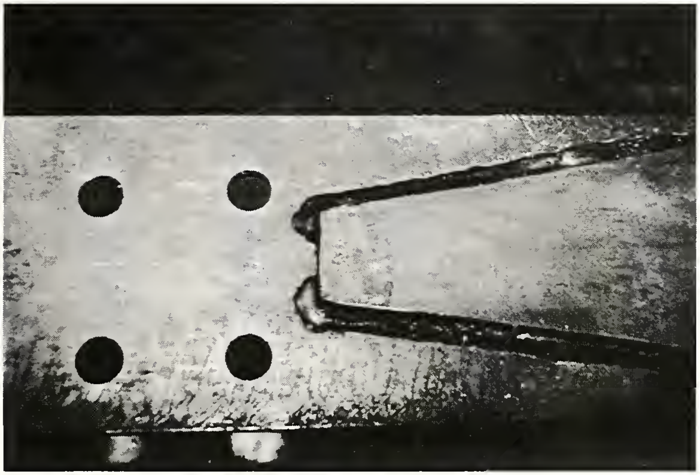

(a) Drilled Holes.

(b) Splice Plates Installation and Bolt Tightening.

Fig. 4.9. Bolted Splice Repair.

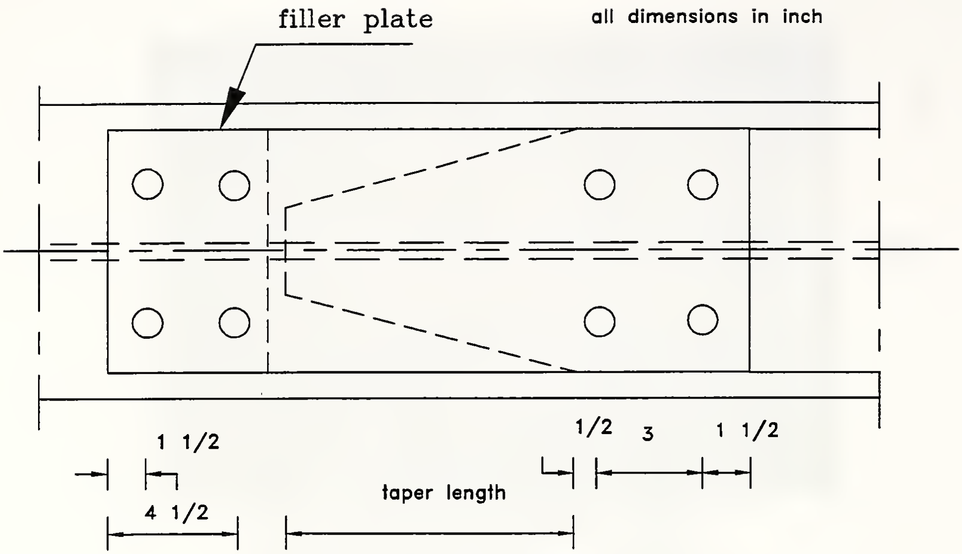

Narrow Cover Plate

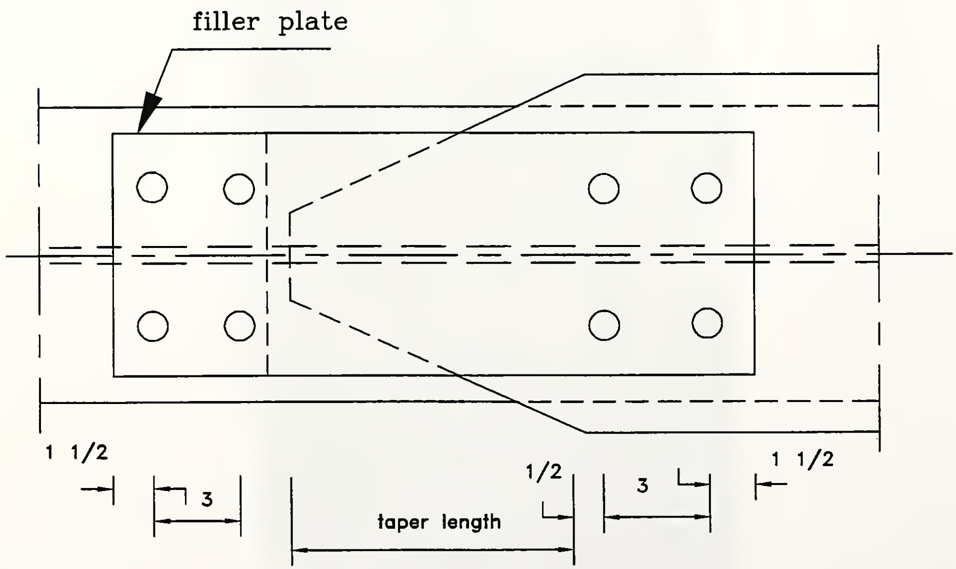

Wide Cover Plate

Fig. 4.10. Bolted Splice Plate Lay-Out.

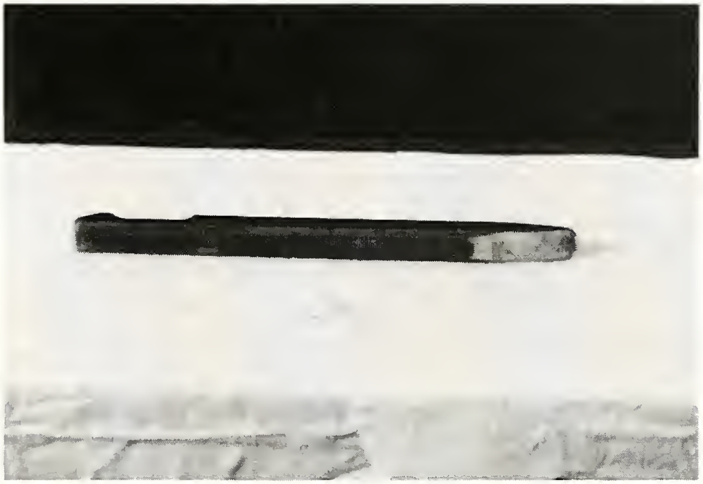

(a) Peening Tool.

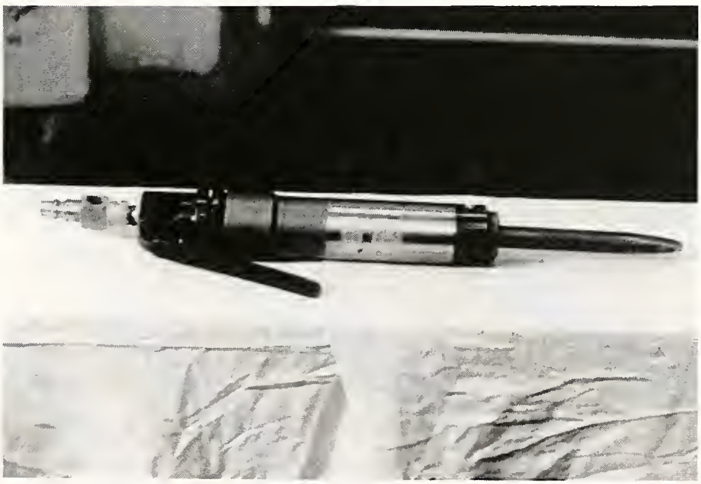

(b) Pneumatic Air-Hammer.

Fig. 4.11. Air-Hammer Peening Equipment.

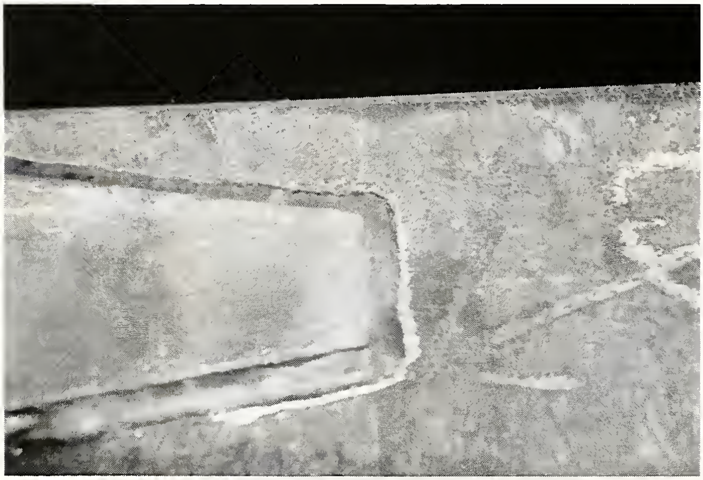

Fig. 4.12. Typical Peened Weld Toe.

CHAPTER 5
CRACK DETECTION

5.1. General Comments

As previously mentioned, thirty-three W 14 × 30 steel beams with welded, tapered partial-length cover plates were tested. All specimens were subjected to a loading that produces a 20.0-ksi stress range at the extreme fibers of the bare beam section at the cover plate ends. The applied load was sinusoidal in shape with a frequency of 2.0 HZ and an R-ratio of 0.05.

The loading of the beams was stopped upon detection of "visible" cracks at both cover plate ends. One of the repair procedures studied (bolted splice, peening, or partial bolted splice) was then applied to the test beam. The cover plate ends were checked for fatigue cracks every 20,000 cycles using visual inspection with a 10X magnifying glass and ultrasonic detection. The ultrasonic detection was not successful in early crack detection. Cracks were first detected visually, and then the existence of these cracks was confirmed using the ultrasonic equipment. In the case of beams repaired using the peening procedure, the crack size prior to repair is extremely important in determining the remaining fatigue life. Thus, for beams to be repaired with the peening procedure, inspection was conducted at a 5,000 cycles interval prior to crack detection.

When cracks were detected at only one of the two ends of the beam, a temporary splice plate connection was used to arrest further crack propagation in that end. The temporary splice plate connection consisted of one plate 24-in × 6-in × 1-in, and two plates 24-in × 2-in × 1-in. The 1-in thick plates were connected to the beam flange with eight heavy duty C-clamps. This temporary splice connection was removed after cracks were detected at the other end of the test beam.

The following sections present a detailed discussion for the first three specimens tested, including the comments encountered during the crack detection phase. Then, the crack detection results are discussed. Finally, the test results are compared with test results obtained by other investigators. The detected crack sizes and the number of cycles to crack detection are presented in Table 5.1 for all test specimens. A detailed summary of the detected crack sizes and number of loading cycles sustained for each test specimen are given in Appendices D and E, respectively.

Reference is made in the following comments and in Table 5.1 to the two frames utilized in the test program. The two frames were slightly different, although both supported a 55-kip linear actuator at mid-span of the frame cross-beam. The columns in the west frame were spaced 6-ft - 0-in center-to-center, while the east frame columns were spaced at 4-ft - 6-in center-to center.

The specimen identification code for the test beams consists of two letters and one number. The first letter indicates the type of cover plate ("N" for narrow, and "W" for wide), the second letter indicates the type of end weld ("R" for return end-weld, "F" for full end-weld, and "N" for no end-weld), and the number is the beam number for this specific configuration. Although all beams were ASTM A36, three were fabricated from a different heat of steel. These three beams, which are of the narrow cover plate and return end-weld type, are denoted DB1, DB2, and DB3.

5.2. Comments for Test Beams

Specimen DB1

Specimen DB1 was the first beam to be tested. The test was conducted in the east frame. The required 20-ksi stress range at the cover plate end was obtained by a loading cycle having a sine-wave shape with a 1.34-kip lower peak and a 26.79-kip upper peak. When first loading the beam statically, a lateral movement of the spreader beam was observed at 9 kips. The spreader beam was then replaced by a wider one, but the lateral movement was still observed at about the same load value. It should be noted that the test beam was attached to the loading frame through the use of straps to prevent the lateral movement of the beam; the straps are quite flexible and offer little vertical load resistance. It was then decided to use a second set of straps to connect the spreader beam to the loading frame. A total of about 3,400 cycles were applied to the beam while adjusting the required load and frequency of application. The loading cycle was finally selected to have a sine-wave form with a 2 HZ frequency. It was intended to use this beam as a dummy beam to solve anticipated problems in the test set-up.

In order to assess the actual behavior of the beam and to compare the test results with the behavior computed using elastic analysis, ten strain gages and three LVDTs were connected to the beam. The placement of these transducers is shown in Fig. 5.1. The deflections were

measured at mid-span of the beam and the two ends of the cover plate. The LVDTs were connected to the bottom cover plate at mid-width (i.e., under the beam web). Two strain gages were connected to the beam web at 5-ft - 0-in from the supports and 1.5-in above the bottom flange. Four strain gages were connected to the beam flanges at 5-ft - 0-in from the supports (two at each end, and one on each flange); these gages were connected at mid-width of the flange. Two strain gages were connected to the middle of the bottom flange at 3-ft - 0-in from the supports. The remaining two gages were connected to the middle of the bottom cover plate width at 7-ft - 6-in from each support. The strains and deflections were measured every 20,000 cycles. All measurements were taken using a static load cycle equivalent to the cyclic loading (1.34-kips minimum to 36.8-kips maximum). Measurements were taken at the minimum load, maximum load, and at multiples of 5-kips between the minimum and maximum loads.

The deflection and strain values measured prior to cyclic loading are shown in Figs. 5.2 and 5.3, respectively. It can be seen in both figures that the measured values agree well with those analytically calculated using elastic beam theory.

The maximum values of the measured deflection and strain are shown in Fig. 5.4. The results show a maximum variation of about 0.02-in in the measured maximum deflection and 30 micro-strain for the measured strain. This fluctuation could be attributed to the sensitivity of the strain gages and LVDTs.

A total of 4 cracks were believed to be present at the 4 return end weld positions after 120,000 cycles of loading. It should be noted that since this was the first beam member tested, only visual inspection was used for crack detection. The crack sizes recorded at that time were: 3/8-in, 1/2-in, 1/2-in, and 3/8-in long at the toe of the southwest, southeast, northwest, and northeast sides of the cover plate end welds, respectively. (As noted later, these indications were not actually cracks but, instead, crevices at the weld toe that were mistaken as cracks.)

Specimen DB2

This beam is similar to specimen DB1. The beam was tested in the west frame using the same procedure as DB1. This time, however, ultrasonic detection was used in conjunction with visual inspection to confirm the existence of cracks. In order to ensure the existence of a crack, it was felt that both the ultrasonic and visual inspection should indicate its presence. This detection procedure was used for all subsequent beams. At 200,000 cycles, a total of 3 cracks

were observed in the beam. Crack lengths of 3/16-in, 3/16-in, and 1/8-in were detected in the tension flange at the northwest, southwest, and southeast ends of the cover plate, respectively - see Fig. 5.5.

Specimen DB3

This beam was tested in the west frame. In an effort to avoid the development of compression cracks (encountered during testing of specimens DB1 and DB2), the ends of the cover plate on the compression side of the beam were air hammer peened prior to load application. For specimen DB3, and all subsequent specimens, a light, one pass peening with a pressure of about 30-psi was utilized. The peening process reduces the tensile residual stresses caused by welding through compressive residual stresses induced at the weld toe. At 200,000 cycles, a total of three cracks were observed in the tension flange of the beam. The measured crack lengths were: 7/32-in, 1/4-in, and 1/8-in at the northwest, southwest, and southeast sides, respectively.

5.3. Discussion of Results

Out of the 33 beams tested, 29 were pre-cracked prior to repairing the cover plate end using one of the repair procedures investigated. Of these 29 beams, 12 were of the narrow cover plate return end-weld (NR-type), 2 of the narrow cover plate no end-weld (NN-type), 5 of the narrow cover plate full end-weld (NF-type), 3 of the wide cover plate full end-weld (WF-type), and 7 of the wide cover plate return end-weld (WR-type). All of the beams were subjected to a 20-ksi stress range on the bare beam cross section adjacent to the end of the cover plate until cracks were detected.

The minimum, average, and maximum number of cycles at first crack detection was 120,000 cycles, 154,600 cycles, and 240,000 cycles, respectively. Fig. 5.6 summarizes the number of cycles at first crack detection for the test beams. The range of cycles for first crack detection is shown for each beam type tested. It should be noted that the results of Specimen DB1 were not included (no cracks were found at the end of test). The average number of cycles to first crack detection was 165,400 cycles, 166,500 cycles, 182,000 cycles, 145,500 cycles, and 139,000 cycles for beam types NR, NN, NF, WF, and WR, respectively. Generally, beams with wide cover plates were observed to initiate cracks sooner than beams with narrow cover plates. The

lowest and highest number of cycles at first crack detection were for the WF and NR beam types, respectively. The NR specimens exhibited the widest range of number of cycles to first crack detection. This may be explained by the fact that most of the specimens were of the NR-type.

The minimum, average, and maximum detected crack length for all beams was 1/16-in, 19/64-in, and 3/4-in, respectively. The average detected crack length for the NR, NN, NF, WF, and WR beam types was 17/64-in, 15/64-in, 13/32-in, 21/64-in, and 9/32-in, respectively. Fig. 5.7 shows the detected crack length for 29 of the 30 beams (Specimen DB1 was not included). Typically, each beam had four potential crack length values corresponding to the northwest, northeast, southwest, and southeast ends of the cover plate - see Fig. 5.5. In the case of the full end weld detail, some of the beams initiated more than two cracks at the same end. In that case an extra point was added with the third crack length.

Figure 5.8 compares the detectable crack length with the number of loading cycles which had been applied prior to detection of that crack. It is evident that the wide cover plate type consistently initiated detectable cracks earlier than the narrow cover plate type. From the results of the 30 beams, the expected (average) detectable crack length for the NR, NN, NF, WF, and WR types are about 0.275-in, 0.25-in, 0.40-in, 0.325-in, and 0.30-in, respectively. The average number of cycles till detection of these cracks is about 160,000 cycles, 160,000 cycles, 180,000 cycles, 140,000 cycles, and 140,000 cycles for the NR, NN, NF, WF, and WR types, respectively.

Figure 5.9 shows the applied stress range versus the number of cycles to first crack detection for 29 of the 30 beams (Specimen DB1 was not included) along with AASHTO Category B, E, and E' design curves. For most beams, the first crack was detected after Category E design life value. It should be noted that a Category E design life in AASHTO gives the total fatigue design life (crack initiation and crack propagation) for a cover plate detail. It should be noted that the design curve is parallel to the mean S-N curve, but shifted about two standard deviations.

The Category B, E, and E' fatigue design curves, shown in Fig. 5.9, correspond to the following conditions: Category B is for built-up plates or shapes connected by continuous full penetration groove welds or continuous fillet welds parallel to the direction of stress; Category E is for base metal at ends of partial length welded cover plates narrower than the flange, with or without welds across the ends, or plates wider than the flange with welds across the ends for

flanges less than 0.8-in thick; and Category E' is for base metal at the ends of partial length welded cover plates wider than the flange without welds across the ends or plates wider than the flange with welds across the end if the flange is thicker than 0.8-in. At a stress range of 20-ksi, the Category E', E, and B design life values are 48,850 cycles, 134,000 cycles, and 1,489,000 cycles. The minimum number of cycles to first crack detection of the NR, NN, NF, WF, and WR beam types was 165,000 cycles, 140,000 cycles, 180,000, 134,000 cycles, and 140,000 cycles, respectively. Although based on only one stress range, the test results suggest that detectable fatigue crack will be present at the end of tapered cover plates after the application of a number of loading cycles equivalent to a Category E design life.

5.4. Comparison with Other Tests

Fisher, Frank, Hirt, and McNamee (1970) tested 204 steel beams with welded square ended cover plates. Two different conditions were used at the cover plate end: a transverse weld and no weld. The cover plate thickness and width, and the use of more than one cover plate were the design variables studied. The stress variables included minimum stress, maximum stress, and stress range. Three types of steel were used to evaluate material effects: ASTM A36, A441, and A514.

The results of the tests by Fisher et al. (1970) are plotted in Fig. 5.10 along with first crack detection results obtained in the present study. It should be noted that the NCHRP-102 results (Fisher et al., 1970) correspond to complete failure of the beams, while the present study results correspond to first crack detection. It can be seen that first crack detection of the welded tapered cover plates (present study) falls within the scatter-band of data for fracture of the welded square ended cover plates (NCHRP-102). This suggests that the fatigue strength of the tapered cover plates is slightly higher than the cyclic life for square ended cover plates, since additional loading cycles would be necessary to propagate the small detected cracks to failure. The average fatigue life of steel beams with welded square ended cover plates subjected to 20.0-ksi stress range was found to be about 197,000 cycles (Fisher, et al.; 1970); the average number of cycles to first crack detection, from the present study, was about 176,000 cycles.

Munse and Stallmeyer (1962) studied the effect of detail geometry and type on the fatigue behavior of welded flexural members. These tests included details such as splices, stiffeners, cover plates, and attachments. The cover plate details included in the study were square, tapered,

and rounded end geometries, both with and without a transverse end weld. The test specimens were fabricated from ASTM A373 steel and were subjected to a stress range from zero to full tension. A comparison between the test results in the present study and all cover plate tests conducted by Munse and Stallmeyer (1962) is given in Fig. 5.11. Again, it should be noted that the present study results correspond to first crack detection, while Munse and Stallmeyer results correspond to complete failure of the specimen. As expected, it can be seen that first crack detection results (present study) fall below the mean life line obtained for the cover plates tested to failure by Munse and Stallmeyer (1962). This mean life was found to be about 449,000 cycles for cover plates subjected to a 20.0-ksi stress range, while the average number of cycles to first crack detection (present study) was about 175,500 cycles.

Figure 5.12 shows a comparison between first crack detection results (present study) and the results of the tapered cover plates with welded ends and un-welded ends (Munse and Stallmeyer, 1962). The first crack detection results fell considerably below the complete failure results of the tapered cover plates with welded and un-welded ends. The average life of the tapered cover plate detail with welded and un-welded ends, when subjected to a 20.0-ksi stress range, was found to be about 408,000 cycles, and 664,000 cycles, respectively. Fig. 5.12 shows that the fatigue life of un-welded cover plate ends is slightly higher than that of welded ends. Comparison with the results of Munse and Stallmeyer (1962) suggest that the present study results fall within the scatter of the tapered cover plate detail results. Moreover, it is believed that if the propagation life was added to the first crack detection life, the present study results would be close to the complete failure results obtained by Munse and Stallmeyer (1962).

Yongii and Yanman (1987) conducted fatigue tests on plate girders with tapered and square-end welded cover plates. The tests were conducted with R-ratios of 0.1, 0.3, and 0.5 to study the effect of the minimum stress on the fatigue life of specimens. Semi-automatic welding was used to weld the cover plates to the tension flange of the plate girder. A total of 10 girders were tested, 5 girders with square-end and 5 with tapered cover plates. The test results are plotted in Fig. 5.13 along with first crack detection results obtained in the present study. It should be noted that the present study results correspond to first crack detection, while Yongii and Yanman results correspond to failure of the specimen. As expected the first crack detection results fall below the complete failure results of both the square-end and tapered cover plates. As before if the life to propagate the detected cracks to failure is added to the cyclic life to initiate the cracks,

then the results of the present study would be close to the results obtained by Yongii and Yanman (1987).

Grundy and Teh (1985) conducted four full scale fatigue tests using girders from an actual bridge. The girders contained a welded tapered cover plate that was wider and thicker than the flange. The fillet weld leg connecting the cover plate to the flange was smaller than half the cover plate thickness. The girders were assumed to be relatively undamaged as they were subjected to a relatively low stress history. The girders were subjected to a relatively low stress range (6.0-ksi to 8.0-ksi stress range). The results of the four tests are shown in Fig. 5.14 along with the first crack detection results from the present study. The test results were greater than the Category E design life, and relatively close to the endurance limit value of 5.0-ksi for redundant members.

Table 5.1. Crack Detection Results.

Specimen	End	Crack Size (in)		Number of Cycles to Crack Detection	Comments
		W	E		
DB1[1]	N	---	---	---	
	S	---	---	---	
DB2[2]	N	3/16	---	200,000	
	S	3/16	1/8	200,000	
DB3[2]	N	7/32	---	200,000	
	S	1/4	1/8	200,000	
NR1[2]	N	17/32	---	240,000	
	S	5/16	3/8	240,000	
NR2[1]	N	5/8	1/2	180,000	
	S	3/8	3/8	180,000	
NR3[2]	N	---	3/8	200,000	
	S	---	7/16	200,000	
NR4[1]	N	7/32	11/16	165,000	
	S	3/8	5/16	165,000	
NR5[1]	N	---	---	---	Specimen cycled for 75,000 cycles. No cracks detected.
	S	---	---	---	
NR6[2]	N	---	---	---	Specimen cycled for 75,000 cycles. No cracks detected.
	S	---	---	---	
NR7[1]	N	1/16	---	130,000	
	S	5/32	---	130,000	
NR8[2]	N	1/8	7/32	130,000	
	S	5/32	3/32	130,000	
NR9[1]	N	1/4	3/8	120,000	
	S	3/32	1/8	120,000	

Table 5.1. Crack Detection Results. (cont.)

Specimen	End	Crack Size (in)		Number of Cycles to Crack Detection	Comments
		W	E		
NR10[2]	N	1/8	5/16	160,000	
	S	---	1/8	160,000	
NR11[2]	N	1/16	---	120,000	
	S	1/2	---	120,000	Two 1/4-in cracks were detected at the southwest side.
NR12[1]	N	5/16	1/8	140,000	
	S	3/8	---	140,000	
NN1[2]	N	3/16	---	160,000	
	S	1/4	---	199,000	
NN2[1]	N	---	3/16	167,000	
	S	---	5/16	140,000	
NN3[1]	N	---	---	---	Specimen cycled for 75,000 cycles. No cracks detected.
	S	---	---	---	
NF1[2]	N	1/2	3/8	200,000	A third crack 1/2-in long was observed in the middle of the full end-weld detail.
	S	9/16	1/4	200,000	
NF2[1]	N	1/8	1/4	180,000	A third crack 1/2-in long was observed in the middle of the full end-weld detail.
	S	3/8	5/8	180,000	A third crack 3/8-in long was observed in the middle of the full end-weld detail.
NF3[2]	N	9/32		200,000	
	S	1/2	3/8	180,000	A third crack 1/4-in long was observed in the middle of the full end-weld detail.

Table 5.1. Crack Detection Results. (cont.)

Specimen	End	Crack Size (in)		Number of Cycles to Crack Detection	Comments
		W	E		
NF4[1]	N	5/32		140,000	
	S	1/8		140,000	
NF5[2]	N	1/2		200,000	
	S	1/2	3/4	200,000	A third crack 1/2-in long was observed in the middle of the full end-weld detail.
WF1[1]	N	1/8	1/2	145,000	A third crack 1/2-in long was observed in the middle of the full end-weld detail.
	S	5/32	1/2	180,000	
WF2[2]	N	5/32	---	134,000	
	S	3/16	3/32	134,000	
WF3[2]	N	7/32		140,000	
	S	7/16		140,000	
WR1[1]	N	5/32	3/16	143,000	
	S	3/16	3/8	143,000	
WR2[2]	N	1/4	3/32	140,000	
	S	13/32	1/4	140,000	
WR3[1]	N	3/16	15/32	140,000	
	S	1/4	3/16	140,000	
WR4[2]	N	3/8	---	140,000	
	S	5/16	1/4	140,000	
WR5[1]	N	3/8	3/16	120,000	
	S	1/2	1/4	120,000	

Table 5.1. Crack Detection Results. (cont.)

Specimen	End	Crack Size (in)		Number of Cycles to Crack Detection	Comments
		W	E		
WR6[2]	N	1/4	3/8	150,000	
	S	---	1/4	150,000	
WR7[1]	N	3/16	5/16	140,000	
	S	13/32	1/4	140,000	

[1] Specimen tested in the east frame.

[2] Specimen tested in the west frame.

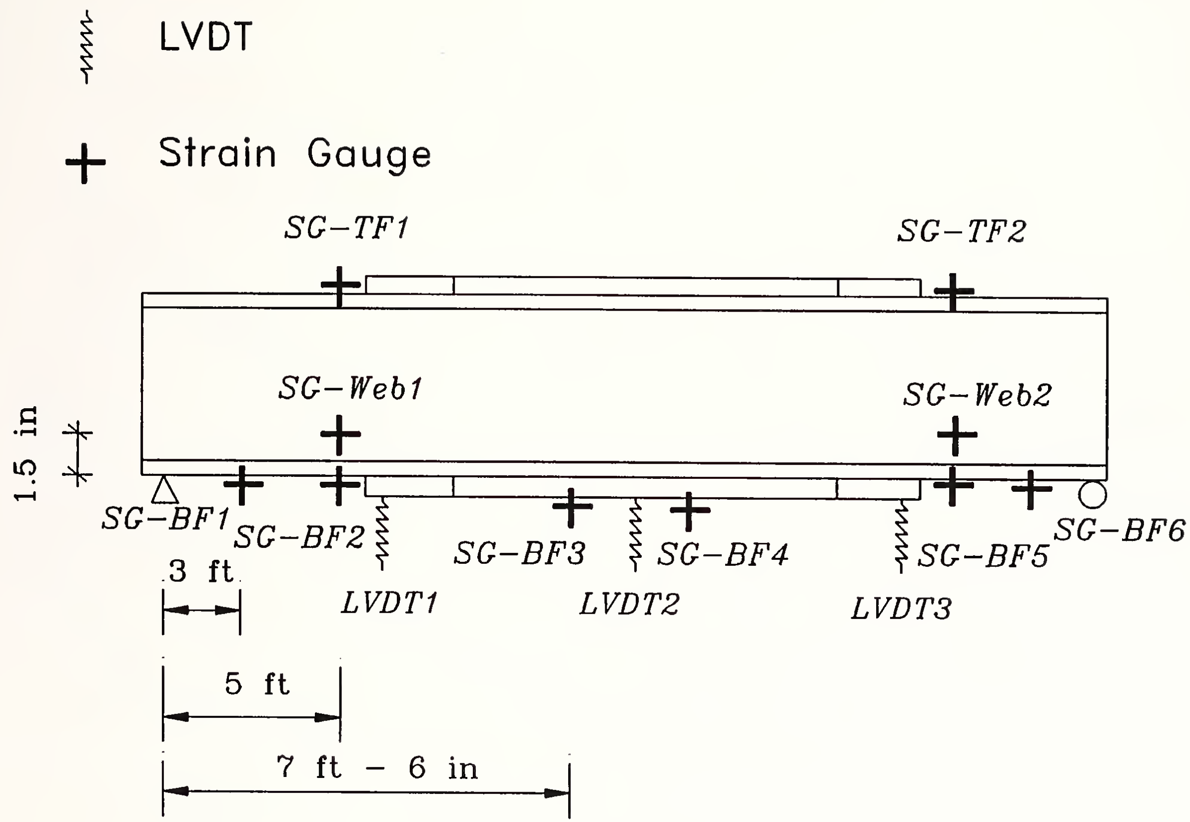

Fig. 5.1. Lay−Out of Strain Gages and LVDTs.

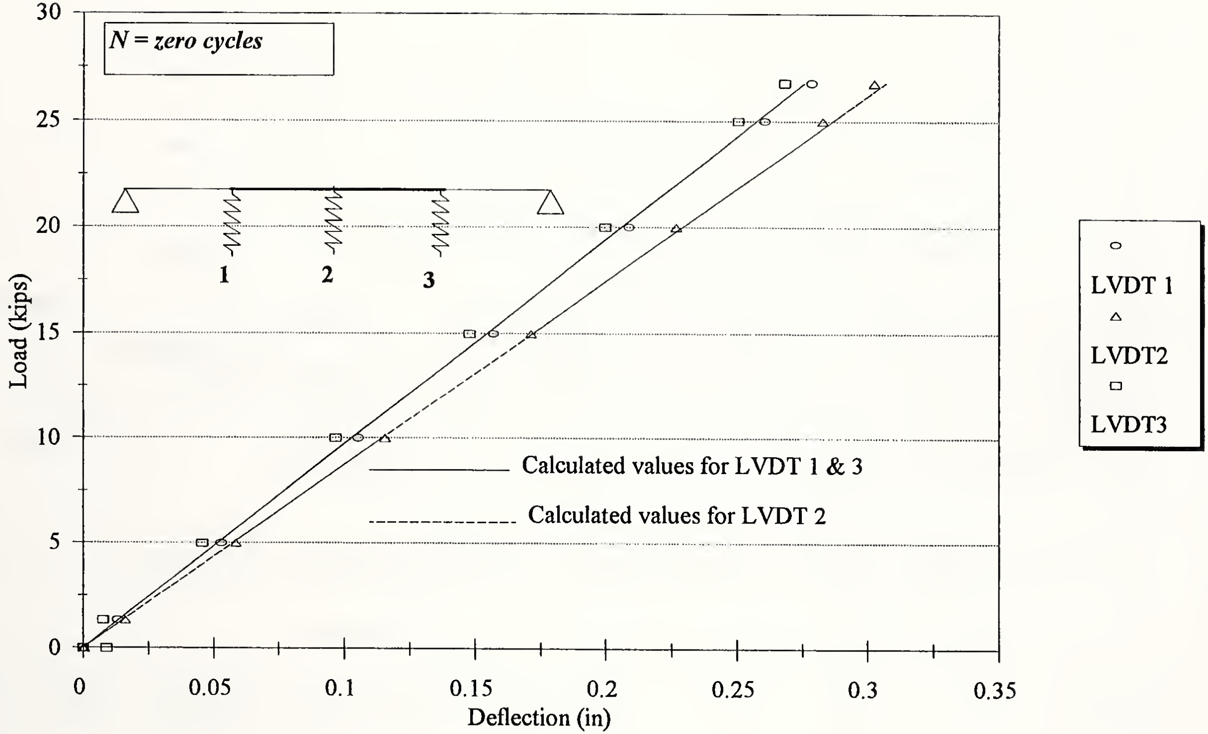

Fig. 5.2. Load-Deflection Relationship.

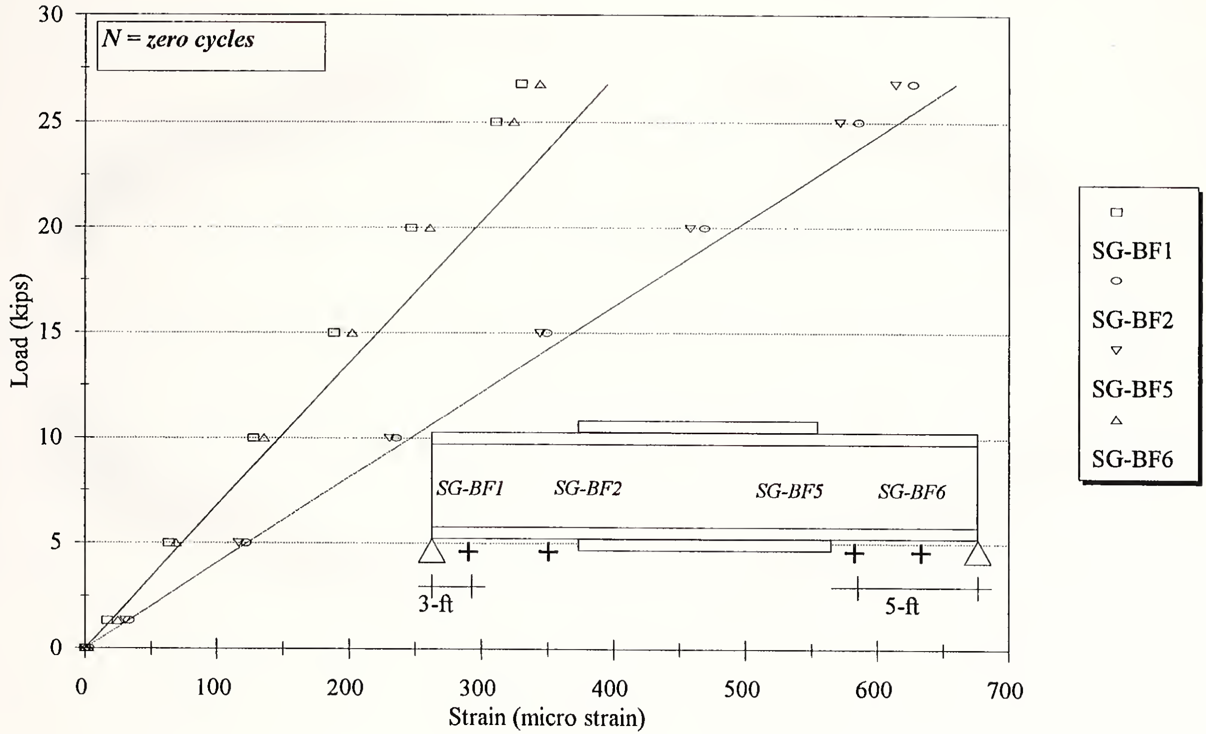

Fig. 5.3. Load-Strain Relationship.

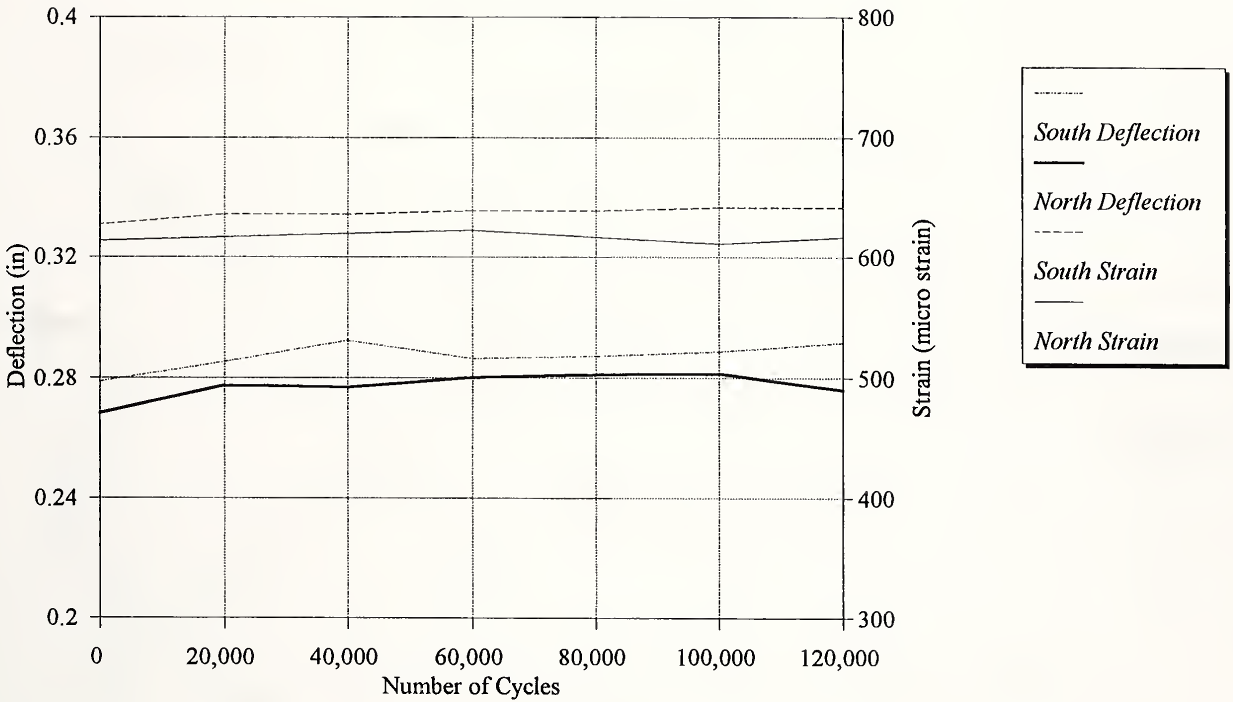

Fig. 5.4. Change in the Maximum Deflection and Strain with the Number of Cycles.

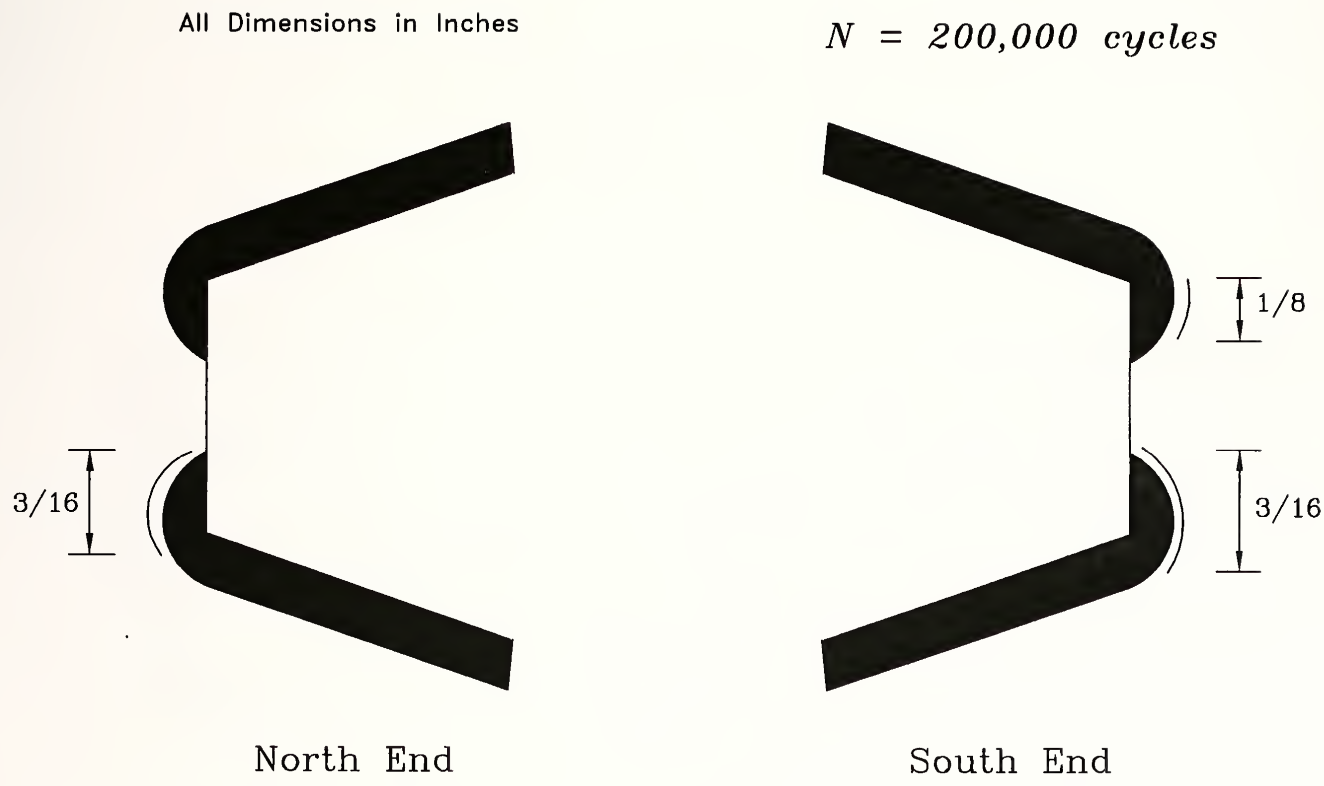

Fig. 5.5. Crack Locations Prior to Repair.
(Specimen DB2)

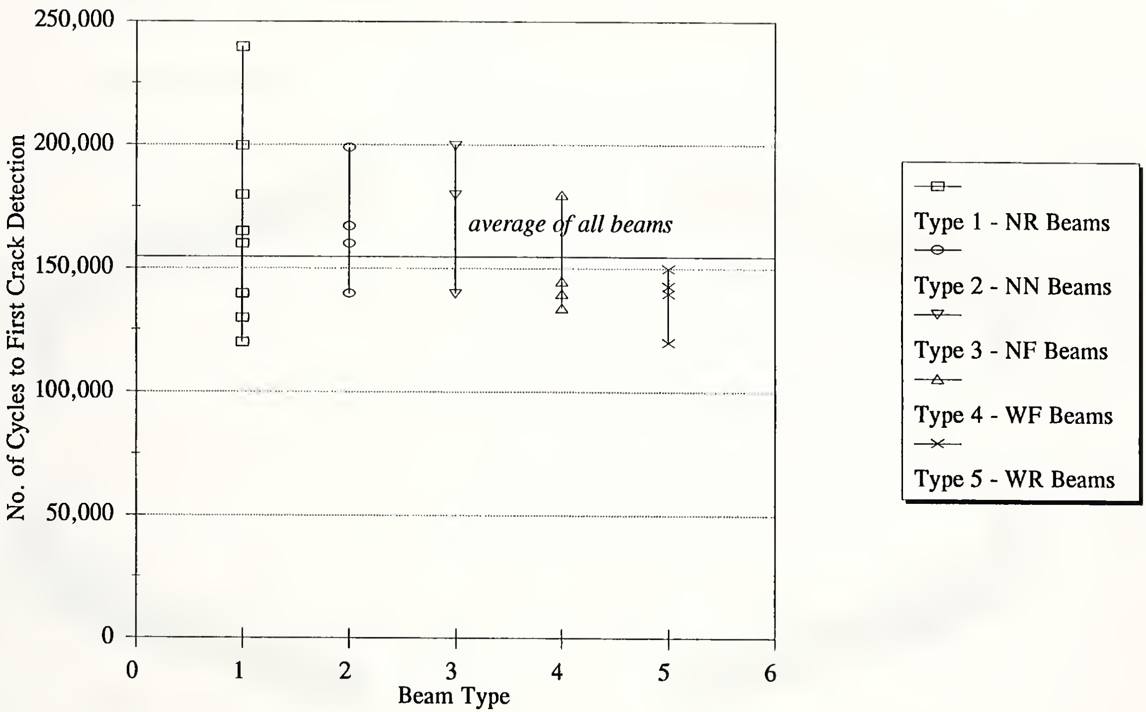

Fig. 5.6. Number of Loading Cycles to First Crack Detection.

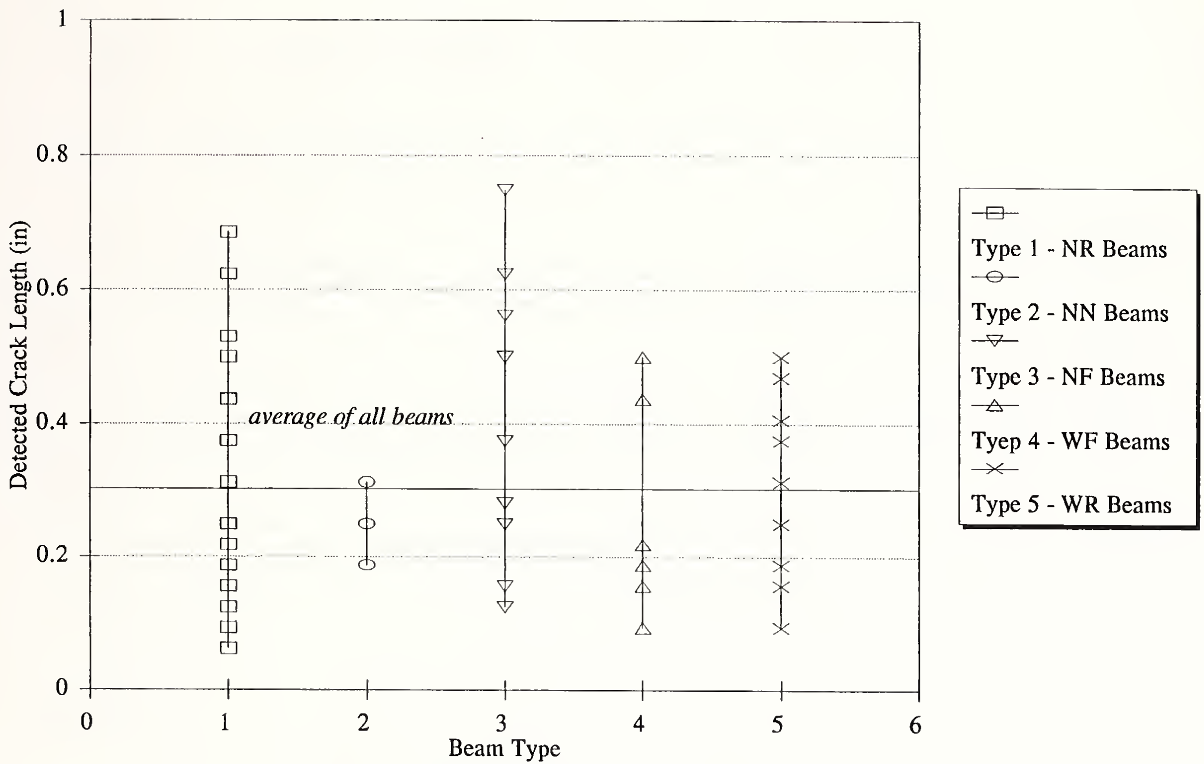

Fig. 5.7. Length of Detected Crack Size prior to Repair.

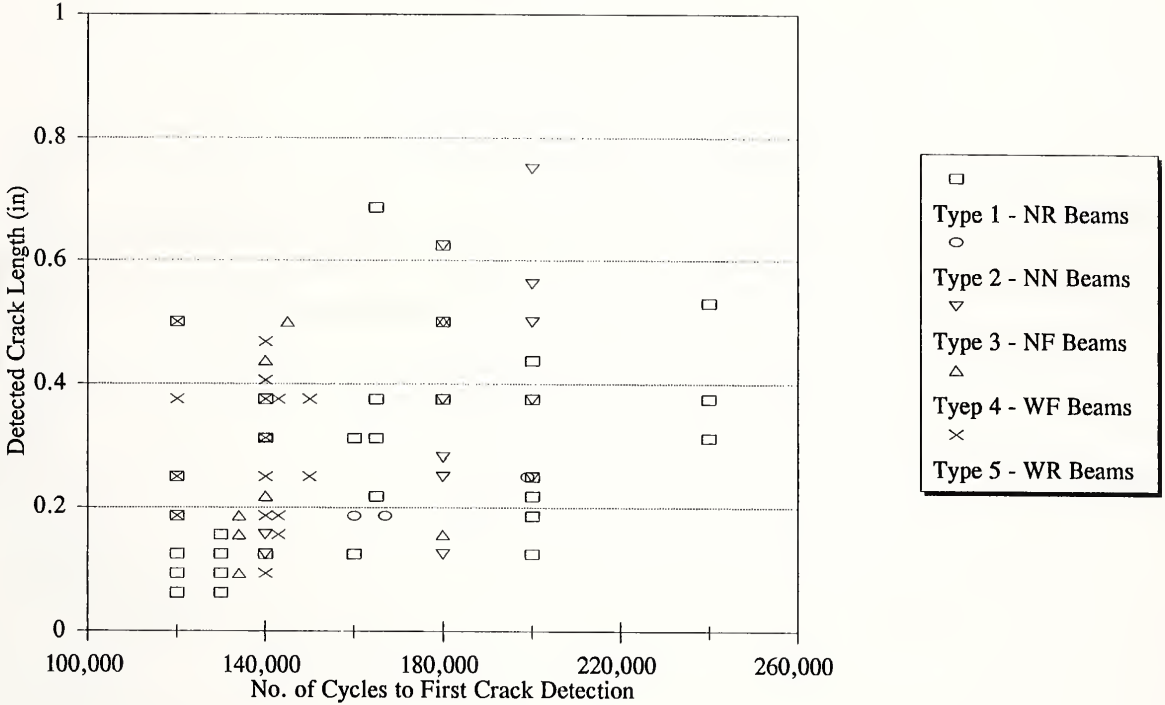

Fig. 5.8. Detected Crack Length versus Number of Cycles.

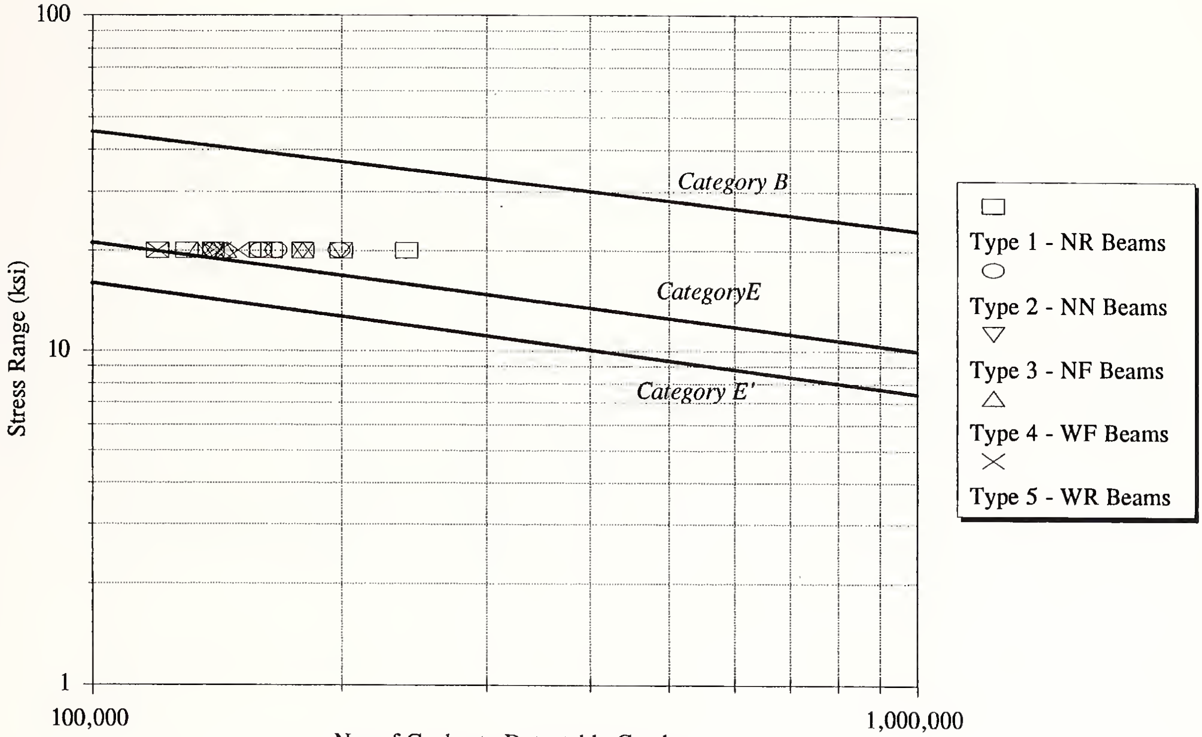

Fig. 5.9. Stress Range versus Number of Cycles to Detectable Crack.

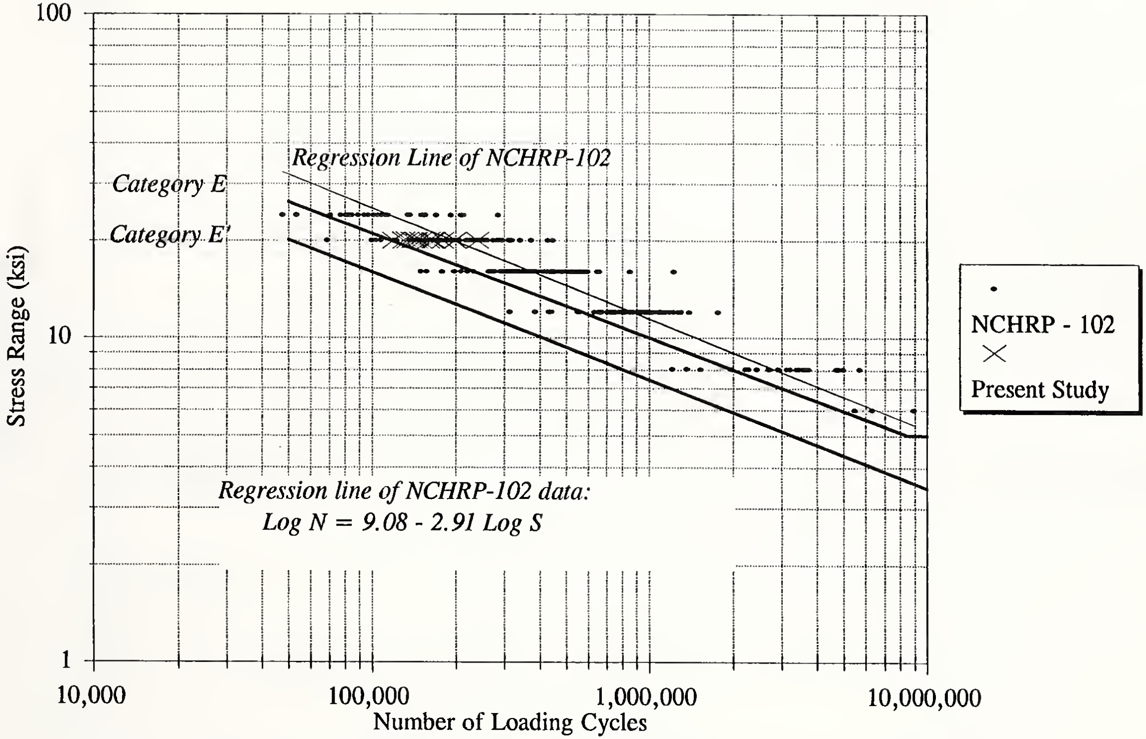

Fig. 5.10. Comparison with Test Results from NCHRP-102 (Fisher et al., 1970)

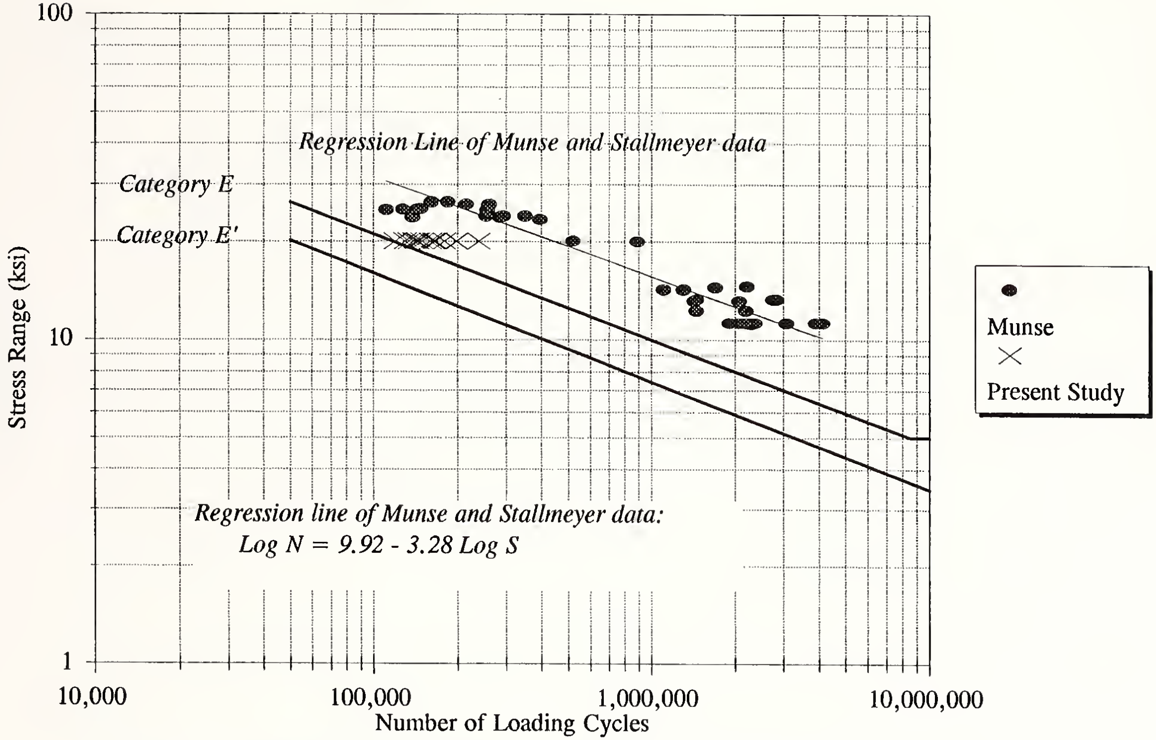

Fig. 5.11. Comparison with Test Results from Munse and Stallmeyer (1962)
(all Data)

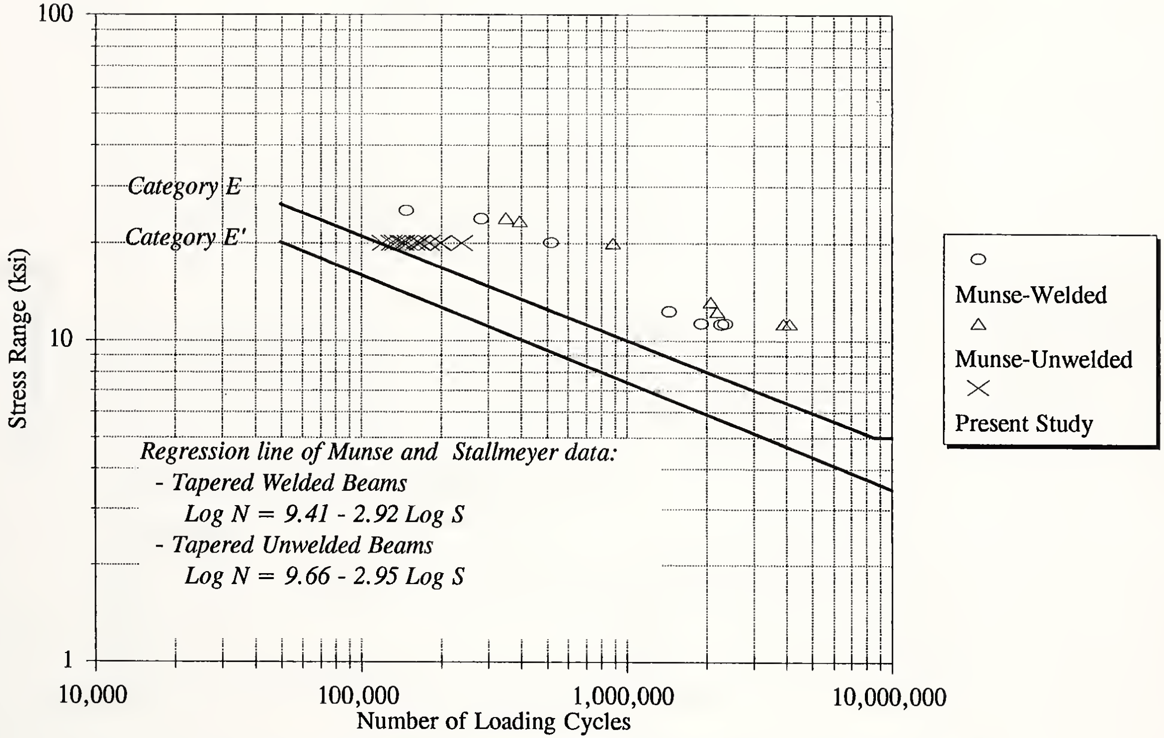

Fig. 5.12. Comparison with Test Results from Munse and Stallmeyer (1962).
(Beams with Tapered Cover Plates)

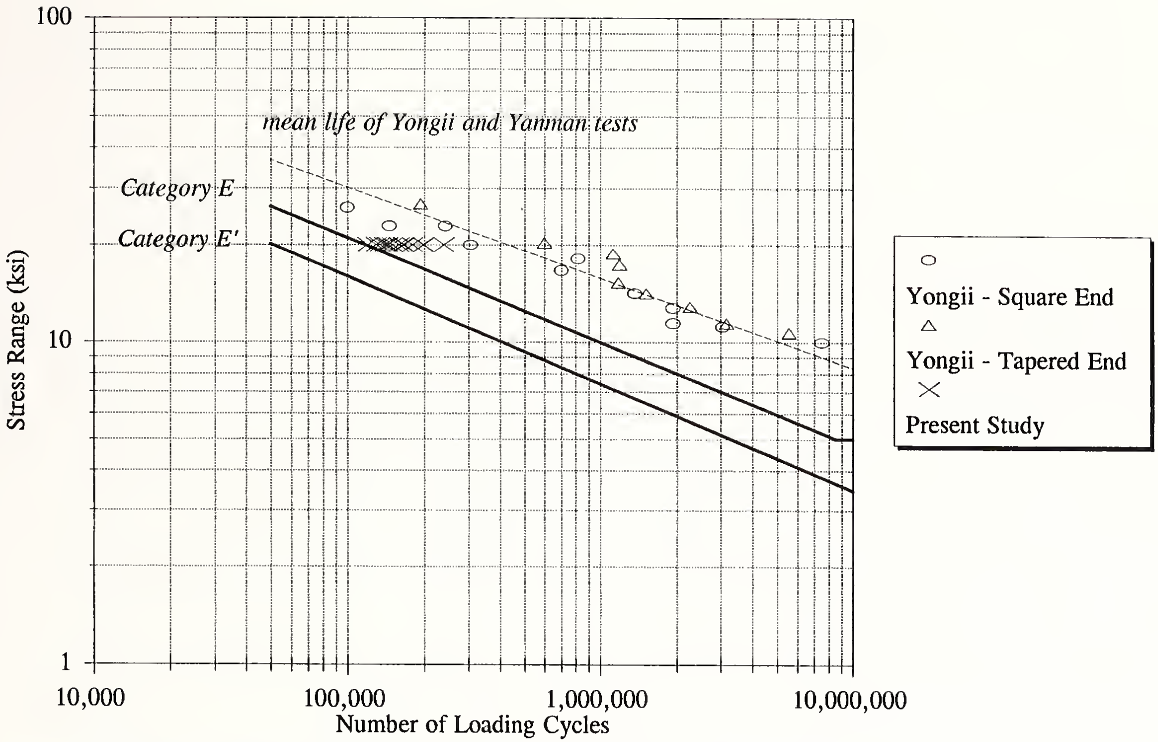

Fig. 5.13. Comparison with Test Results from Yongii and Yanman (1987).

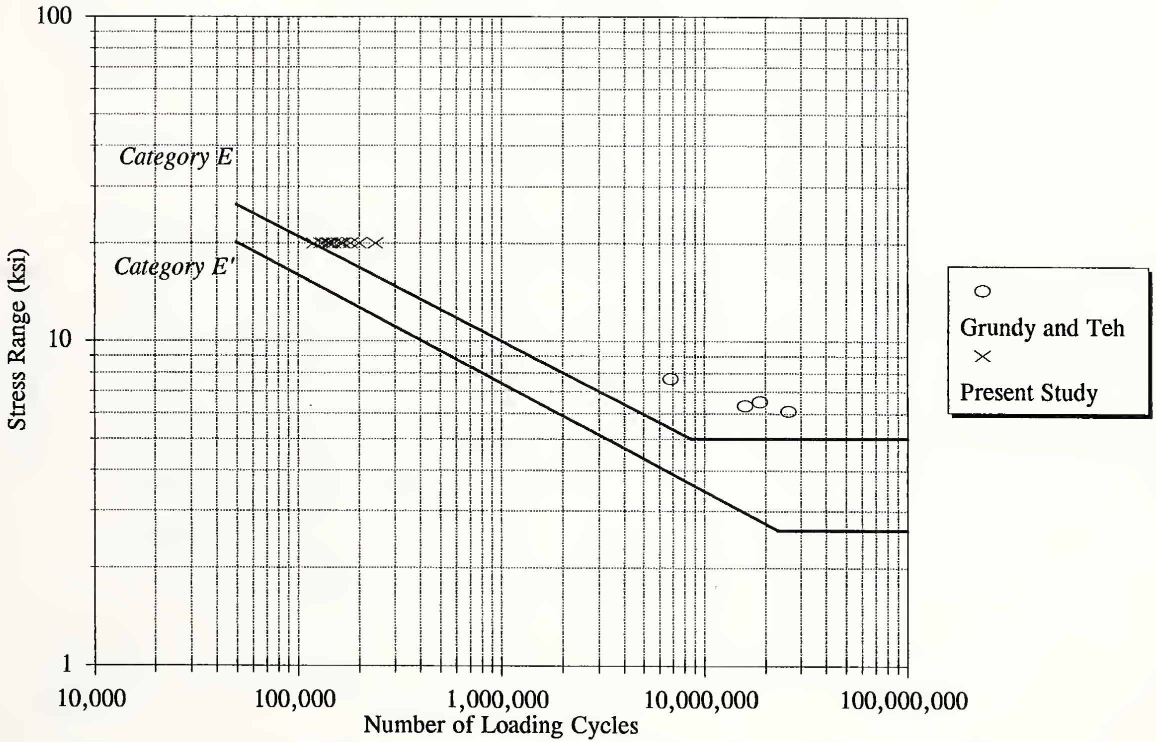

Fig. 5.14. Comparison with Test Results from Grundy and Teh (1985).

CHAPTER 6
BOLTED SPLICE REPAIR

6.1. General Comments

A study by Sahli, Albrecht, and Vannoy (1984) on the repair of beams with welded cover plates using bolted splice plates indicated that this detail has a fatigue life described by Category B in the AASHTO Specifications (Standard Specifications for Highway Bridges, 1989). It should be noted that square ended cover plates were used in the study. Sahli et al. (1984) recommended that the splice plates need to be designed for the full design moment if the flange is pre-cracked; for non-cracked flanges the splice plates need to be designed only for the portion of the design moment not carried by the web.

In the present study, 19 beams were repaired using a friction type bolted splice plate connection after pre-cracking. Out of the 19 beams, 18 were subjected to a loading that produces a 20.0-ksi stress range at the extreme fibers of the bare section at the cover plate ends (same as the pre-cracking load). The remaining beam was subjected to a 15.0-ksi stress range. It should be noted that the endurance limit of Category B details, as suggested by the AASHTO Specifications (1989), is 16.0-ksi.

The fatigue design life of Category B of the AASHTO Specifications (1989) with a 20.0-ksi stress range is about 1,500,000 cycles. For those tests that exhibited a cyclic life in excess of Category B (i.e., greater than about 1,500,000 cycles), the loading was continued until at least 1,800,000 cycles - roughly 20% more life than Category B.

The bolted splice plate connection was designed to carry the full bending moment at the cover plate end, along with the compression flange and the web (i.e. the tension flange was assumed to be completely severed). The design yielded a splice plate thickness of 5/16-in. Because the splice plates needed to be quite long to extend beyond the cover plate taper, it was believed that the combination of the plate flexibility and the fact that the tension flange was not completely severed would mean that significant stress would still exist at the cover plate end. Thus, a thicker splice plate connection (7/16-in thick) was also tested to investigate the effect of splice plate flexibility.

The following sections discuss the test results for each specimen. Then, comprehensive results of the bolted splice repair connection are presented and compared with other test results

obtained from the literature. Finally, conclusions from the test results of the bolted splice repair are presented. A detailed summary of the measured crack sizes and number of loading cycles sustained for each specimen are given in Appendix D. Table 6.1 shows the number of loading cycles applied after repair until fracture of the flange, along with the total number of cycles applied after repair.

6.2. Comments for Test Beams

6.2.1. Specimen DB1

After pre-cracking, the beam was repaired using the 5/16-in bolted splice plate detail and the test was restarted from zero cycles. Assuming that the tension flange is completely severed, the stress range values at the top flange and the bottom splice were found to be 19.3-ksi and 18.4-ksi, respectively. These calculations were made using simple elastic beam theory.

As previously mentioned, 10 strain gages and three LVDTs were connected to specimen DB1 to assess the actual behavior of the beam - see Fig. 5.1. The maximum values of the measured deflection and strain after repair are shown in Fig. 6.1. Very little variation is observed in the maximum values of the measured strain and deflection. It should be noted that the strain values correspond to the maximum strain in the compression flange obtained from the strain gages connected at the cover plate ends. The strain gages connected to the tension flange at the cover plate ends were lost due to the installation of the splice plate connection.

At 1,375,000 cycles, the compression flange on the north end was found to be fractured. A 5 49/64-in long flange crack penetrated into the web for about 2-in from the fillet - see Fig. 6.2. The compression crack is undoubtedly due to tensile residual stresses induced during the welding process in addition to the lateral movement of the beam at the end of the cover plate. It should be noted that straps are connected to the beam near the loading points and prevent most lateral movement. A small lateral movement, however, can sometimes still be observed at the end of the beams.

The compression flange on the north end was repaired using a 7/16-in bolted splice plate detail, and the test was resumed. The computed stress ranges at the top and bottom of splice plates, assuming that both flanges were completely severed, were found to be 13.7-ksi and 16.6-ksi, respectively. These stresses were computed at a section passing through the cover plate end.

At 1,800,000 cycles the test was stopped and the splice plates were removed from the tension flange on the north and south ends. No cracks could be detected through visual inspection with a 10X magnifying glass, or ultrasonic detection. It should be noted that while trying to detect cracks, the beam was loaded to open any existing crack tips in order to facilitate the inspection. Dye penetrant was also used to inspect the weld toe along the cover plate end, but no cracks were detected.

The main finding of this beam is that the use of the splice plate repair technique, even with the smaller thickness (5/16-in) splice plate, was apparently effective in reducing the stress at the weld toe and preventing fatigue crack initiation.

6.2.2. Specimen DB2

After pre-cracking, the beam was repaired with the 5/16-in bolted splice plate detail and the test was resumed. At about 670,000 cycles after repair, two cracks were observed in the compression flange at the end of the cover plate. These cracks were 1 19/64-in and 39/64-in long at the north and south ends, respectively. Both cracks were towards the east side of the beam. The weld toe and cracks were air hammer peened and the test was resumed. The north compression flange fractured at 951,000 cycles, the crack length was 6 9/16-in long and propagated under the fillet for about 3-in in the web. The top flange on both ends was then repaired using the 7/16-in splice plate and the test was resumed.

At 1,800,000 cycles the test was stopped and the splice plates on the tension flange were removed to measure the crack sizes. In order to measure the cracks at the end of the test their size was first evaluated using a 10X magnifying glass without any load application. If the crack was large, no load or very small load was applied to the beam while measuring its length. On the other hand, if the crack was small a high load and sometimes a cyclic load might be required in order to obtain accurate measurements. It was discovered that the use of a high static load or cyclic load during crack measurement resulted in a very accurate assessment of the crack size; the use of no load or a small load often resulted in crack size measurements that were smaller than the actual crack sizes due to closure of the crack tip ends. For this particular beam (DB2), the crack in the south end grew to 3 39/64-in in length (both east side and west side cracks coalesced). It was believed that since the crack was relatively large, there was a possibility that the beam could fracture if a large load static or cyclic was applied. Thus crack measurements

were obtained with no load application. Dye penetrent was also used to measure the final crack lengths; Fig. 6.3 shows a photograph of the dye penetrent usage on the south tension flange of specimen DB2. Dye penetrent was successful in showing the final crack length. The crack on the northwest side was measured to be 3/16-in long; no growth was observed.

In order to measure crack depths, the tension flanges were removed by flame cutting and the crack surface was exposed by fracturing the flange portion removed. The flanges were dipped in liquid nitrogen to reduce their temperature and produce a corresponding decrease in the material fracture toughness. A 15 lb hammer was then used to fracture the flanges at the end of the cover plate. Subsequent measurements on the fracture surface indicated that the crack was 3 5/8-in long at the south end, a difference of 1/64-in from measurements prior to fracturing the flange. Two cracks were found at the north end with lengths of 15/32-in and 1/2-in for the west and east sides, respectively. The depths of the cracks were found to be 9/64-in and 7/64-in for the west and east sides, respectively. The south end crack depth was found to be 3/8-in (same as the thickness of the flange). The difference in crack sizes before and after breaking the flange can be attributed to the fact that the measurements taken prior to breaking the flange were conducted under no load.

6.2.3. Specimen DB3

After pre-cracking, the beam was repaired using the 5/16-in bolted splice repair detail, and the test was resumed. At 1,800,000 cycles after repair, the test was stopped. No compression cracks were observed. Upon removal of the splice plates, the final crack sizes were measured to be 3/8-in, 29/32-in, and 29/32-in for the northwest, southwest, and southeast sides, respectively. No load was applied to the beam while measuring the crack lengths. The tension flanges were removed and fractured using the same procedure noted for specimen DB2. The measured crack lengths after breaking the flange were: 1 25/64-in, 1 3/32-in, 61/64-in, and 1 1/2-in for the northwest, northeast, southwest, and southeast sides, respectively. Crack depths were found to be 3/8-in, 9/32-in, 9/32-in, and 5/16-in for the NW, NE, SW, and SE sides, respectively.

6.2.4. Specimen NR1

After pre-cracking, the beam was repaired using the 5/16-in bolted splice plate detail. In order to estimate the actual stresses in the splice plate connection and the percentage of load transferred through the splice plates, a total of 10 strain gages, 5 each on the north and south sides, were attached to the splice plates - see Fig. 6.4. These gages were located near the end of the cover plate weld (position of the initiated cracks). Static measurements were taken periodically.

The maximum stress at the lower fibers of the bottom splice plate, calculated assuming that the flange is completely severed, was found to be 19.3-ksi. Since the flange was not completely severed at the time of repair, both the flange and the splice plates actually contributed in resisting the applied moment. Therefore, based upon a linear extrapolation of the bottom splice plate stresses, the stress in the lower fibers of the tension flange would be 17.7-ksi (assuming that the flange is not contributing in carrying the applied moment). It should be noted that the assumption of the flange being completely severed is only for design purposes; in reality, the flange is only partially severed due to the existence of the crack.

The maximum stress at the lower fibers of the bottom splice plate, just after repair, is estimated to be about 9.3-ksi (based on the measured strain and a modulus of elasticity of 29,000- ksi for steel). Again using linear extrapolation, the stress at the lower fibers of the tension flange would be 8.0-ksi. On the other hand, assuming that the bottom flange is fully effective and contributes in carrying the applied moment, the maximum stress at the lower fibers of the bottom splice plates was found to be about 12.8-ksi. The estimated stress (based on strain measurements) is smaller than the calculated stress. The splice plates are relatively flexible due to the large distance between the bolts in the taper region. This reduces their contribution in carrying the load. Figures 6.5 and 6.6 show the maximum measured strains with the applied number of cycles after repair for the south and north ends, respectively. Assuming that the tension flange was completely severed, the splice plates would be required to carry a maximum force of about 57- kips. From the strain measurements, the maximum force carried by the splice plates, just after repair, was found to be about 26.5-kips. Figures 6.5 and 6.6 show that the measured strain values increase with the applied number of cycles. This could be attributed to the fact that the crack sizes increase with the applied number of cycles. This, of course, reduces the flange portion that contributes in carrying the applied moment, therefore the splice plates

carry higher loads. Figure 6.6 suggests that a rapid growth of the crack sizes at the north end might have started at about 1,100,000 cycles.

At 1,564,000 cycles after repair, while taking a static measurement of the strains, the north flange fractured. Just after that, the bottom west gage on the north side was found to be damaged. After the north flange fractured, only the splice plates remained to carry the applied moment. The measured strains at the top gages and the bottom east gage indicated that a stress of about 17.4-ksi was carried by the splice plates - see Fig. 6.6. The bottom middle gage indicated a stress of about 24.7-ksi at that position, suggesting a non-uniform stress distribution with its peak under the web (middle of the beam width). The north end crack propagated about 3.5-in into the web. A hole was drilled in the web at the end of the crack tip and the test was resumed.

Strain measurements for the south end suggest a rapid growth of the flange cracks at about 1,800,000 cycles after repair. It should be noted that the east side strain gages recorded higher strain values than the west side gages. At 1,940,000 cycles, a crack propagated about 1.5-in into the web at the south end of the beam. The south flange east side fractured at 2,000,000 cycles and the test was stopped; only about 1-in of the flange remained non-fractured at the west side. The maximum stress (based upon measured strains) recorded after the end of the test at the lower fibers of the bottom splice were 15.4-ksi, 12.8-ksi, and 11.6-ksi at the east, middle, and west sides, respectively.

6.2.5. Specimen NR2

After pre-cracking, the beam was repaired using the 7/16-in bolted splice plate detail. At 1,952,000 cycles a compression crack through the return weld on the northwest side was observed. The crack propagated 9/16-in beyond the return weld. The crack was peened and the test resumed. At 2,000,000 cycles, it was decided to use the 1-in thick temporary repair plates at the north top end of the beam - see Fig. 6.7. Assuming that both the tension and compression flanges were completely severed, the stress range at the lower fibers of the bottom splice plate was calculated to be 11.8-ksi. This corresponds to a stress of about 10.7-ksi at the lower fiber of the tensile flange.

At 2,500,000 cycles the test was stopped and the compression crack was of the same initial length. The final crack sizes for the tension cracks were 3 23/32-in and 3 5/8-in long for

the north and south ends, respectively. No loading was applied during these measurements as the cracks coalesced. After breaking the flanges, as previously explained, the crack length at the north and south sides were found to be 3 13/16-in, and 3 7/32-in respectively. The crack depth for both sides was through the flange (3/8-in). It should be noted that the measured crack size at the south end after breaking the flange was smaller than the measured size before breaking the flange. In this particular case, the fracture surface (using the liquid nitrogen procedure outlined earlier) did not follow the complete path of the crack. Thus, a small portion of the crack was missing from the fracture surface, and consequently the measured size was smaller than the actual one.

6.2.6. Specimen NR3

After pre-cracking, the beam was repaired using the 7/16-in bolted splice repair detail. Ten strain gages were used at similar positions as for specimen NR1. Assuming that the tension flange was completely severed, the maximum stress at the lower fibers of the bottom splice plate was calculated to be 15.3-ksi. Using linear extrapolation (as explained for specimen NR1), the maximum stress at the lower fibers of the tension flange would be about 13.2-ksi. The maximum stresses at the lower fibers of the bottom splice plate (based on the measured strains and a modulus of elasticity of 29,000-ksi for steel), just after repair, were 7.3-ksi and 6.1-ksi for the south and north ends, respectively. The corresponding maximum stresses at the lower fibers of the tension flange (using linear extrapolation) were 6.2-ksi and 5.6-ksi for the south and north ends, respectively. These values correspond to a decrease of 33% to 40% from the 5/16-in splice plate detail. It should be noted that the 7/16-in splice detail represents an increase of about 30% in the area of used steel compared to the 5/16-in detail. On the other hand, assuming that the tension flange is fully effective and contributes in carrying the applied moment, the maximum stress at the lower fibers of the bottom splice plate was calculated to be about 11.1-ksi.

The measured strains versus the number of cycles after repair are shown in Figs. 6.8 and 6.9 for the south and north ends, respectively. These figures demonstrate that the strain values did not change considerably with the number of cycles.

At 1,883,000 cycles after repair, a compression crack 2 15/16-in long was observed at the southeast side of the beam. The 1-in thick temporary repair plates were installed and the test was resumed. Analytical calculations showed that the use of the 1-in thick plates on the compression

flange decreased the maximum stress at the lower fibers of the bottom splice plate by a factor of 0.77. Careful examination of the measured strains indicate a decrease of about 0.84 and 0.75 for the west side gages after the use of the 1-in thick plates. The east side gages readings remained unchanged. It should be noted that there exists two counteracting processes, the use of the 1-in thick plates decreases the stresses, while the flange crack growth increases the stresses.

At 3,000,000 cycles, the test was stopped and the compression crack was found to have the same length. The final tension cracks were 2 3/8-in, 2-in, 1 1/8-in, and 1 3/4-in long for the northwest, northeast, southwest, and southeast sides, respectively. The northeast crack had two branches with a length of 2-in and 2 3/16-in, respectively. It should be noted that the cracks at the east and west sides crossed but did not coalesce (Fig. 6.10). After breaking the flanges, using the previously mentioned procedure, the crack lengths were found to be 2 11/32-in, 2-in, 1 5/32-in, and 1 11/32-in for the northwest, northeast, southwest, and southeast sides, respectively. Although the fracture surface did not pass through the second branch of the northeast side crack, its length was estimated to be 2 3/8-in.

6.2.7. Specimen NR4

After pre-cracking, the beam was repaired using the 7/16-in bolted splice plate detail. At 1,870,000 cycles, a crack was observed in the northeast web fillet of the beam. The test was stopped at 2,000,000 cycles after repair. The cracks coalesced on the north end to form a single crack 3-in long. The final crack lengths were 1 17/32-in and 1 13/32-in at the southwest and southeast sides, respectively. A third crack 11/32-in long formed between the two return welds in the south end, closer to the cover plate end. After breaking the flanges, the crack lengths were found to be 3-in, 1 1/2-in, and 1 7/16-in for the north, southwest, and southeast sides, respectively. The fracture surface did not pass through the crack that formed between the return welds at the south end.

6.2.8. Specimen NR8

After pre-cracking, the beam was repaired using the 7/16-in splice plate connection. Bridge girders are usually subjected to stress ranges smaller than the allowable static stress of 20.0-ksi. To investigate the effect of the stress range on the fatigue strength of steel beams with welded tapered cover plates, repaired using the bolted splice plate connection method, this

specimen (only) was subjected to a stress range of 15.0-ksi. It should be noted that the Category B endurance limit is 16.0-ksi.

At 7,134,000 cycles after repair, a 3 1/2-in long crack was observed in the south compression flange at the cover plate end. The crack initiated at the weld toe and extended 3/8-in into the web. A 5/16-in splice plate connection was then used to prevent the compression crack from further propagation, and the test was resumed. At 8,352,000 cycles after repair, the compression crack extended about 2 13/32-in into the web. A 15/16-in diameter hole was then drilled at the crack tip in the web, a 7/8-in bolt was installed in the hole, and the test was resumed. At 10,096,000 cycles after repair, a 1 1/4-in long crack was observed in the north compression flange at the cover plate end. The crack initiated at the northeast weld root, and extended into the flange. At 10,782,000 cycles after repair, the north compression flange fractured, and the crack extended about 6-in into the web. The test was then stopped.

Four cracks 1-in, 28/32-in, 3/4-in, and 11/16-in long were found at the northwest, northeast, southwest, and southeast sides of the tension flange, respectively. These crack measurements were done with no load applied to the beam. After breaking the flanges, the final crack lengths at the northwest, northeast, southwest, and southeast sides were found to be 7/8-in, 13/16-in, 27/32-in, and 3/4-in, respectively. The measured crack depths were 5/32-in, 7/32-in, 9/64-in, and 3/32-in for the northwest, northeast, southwest, and southeast cracks, respectively. Figure 6.11 shows a photograph of the north flange fracture surface after breaking the flange. Both northwest and northeast cracks have a penny shape, and they both initiated at the weld toe.

6.2.9. Specimen NN1

After pre-cracking, the beam was repaired using the 5/16-in splice plate connection and the test was resumed. At 1,333,000 cycles after repair, a compression crack 1-in long was observed at the southeast side of the beam. The 1-in temporary repair plates were attached to the compression flange and the test was resumed. At 1,800,000 cycles, the test was stopped and the final tension flange crack lengths were 25/32-in, 15/16-in, and 1 1/2-in for the northwest, northeast, and southwest sides, respectively. It is to be noted that these crack lengths are measured from the end of the cover plate and do not include any cracks that might have propagated beneath the cover plate. After breaking the flanges, the crack lengths were found to be 1 1/8-in, 1 13/32-in, and 1 1/2-in for the northwest, northeast, and southwest sides,

respectively. Two additional cracks 1 2/32-in and 28/32-in long were found under the cover plate at the south end.

6.2.10. Specimen NN2

In order to compare the effectiveness of the 5/16-in and 7/16-in splice plates, it was decided to repair the beam using a 5/16-in splice at the north end (smaller crack) and a 7/16-in splice at the south end (larger crack). At 995,000 cycles after repair, a compression crack 1 19/32-in long was observed at the southeast side of the beam. The 1-in temporary repair plates were attached to the compression flange and the test was resumed. At the end of the test (1,800,000 cycles after repair), the tension flange crack lengths were 1 1/16-in, 2-in, 1/2-in, and 7/16-in for the northwest, northeast, southwest, and southeast sides, respectively. After breaking the flanges, the crack lengths were found to be 1 19/32-in, 2 22/32-in, 5/8-in, and 13/32-in for the northwest, northeast, southwest, and southeast sides, respectively. The crack depths were 3/8-in and 9/32-in for the north and south end cracks, respectively. It should be noted that neither the 5/16-in nor the 7/16-in splice plates prevented the initial cracks from propagated.

6.2.11. Specimen NF1

As this beam was the first of its detail, the 5/16-in splice plates were used to repair both ends and the test was restarted from zero. At 476,000 cycles after repair, a crack propagated into the web fillet at the north end of the beam. At 650,000 cycles, this crack propagated 1-in into the web. At the same time, a crack was observed in the web fillet at the south end of the beam. At 720,000 cycles, these cracks were 1 1/4-in and 1/2-in into the web at the north and south ends, respectively. At 820,000 cycles, the north end crack appeared beyond the splice plates at the west side and was 1 7/8-in into the web. At the same time, the south end crack was about 7/8-in into the web. At 860,000 cycles, the north end crack propagated to 2 1/4-in in the web while fracturing the west side of the flange. Meanwhile, the south end crack propagated about 1-in into the web. At 883,000 cycles, holes were drilled at the crack tip ends for both north and south ends - see Fig. 6.12. The north flange fractured while restarting the test. At 1,049,000 cycles, the southeast side flange was severed, and at 1,179,000 cycles, the entire flange fractured. At 1,340,000 cycles, the web cracks were observed to have passed the drilled holes in the web and propagated to 5 3/8-in and 3 25/32-in long at the north and south ends, respectively; new

web holes were then drilled. The test was stopped at 1,800,000 cycles. It was decided that for any future drilled hole in the web, a bolt be inserted in the hole and tightened by hand to assist in preventing subsequent crack propagation.

6.2.12. Specimen NF2

To examine the effect of the splice plate thickness, the north side (smaller crack) was repaired with a 5/16-in splice detail, while the south side (larger crack) was repaired with a 7/16-in splice detail. The north end cracks coalesced and propagated 5/8-in, 1 9/32-in, and 1 5/8-in into the beam web at 810,000, 982,000, and 1,055,000 cycles, respectively. The north end flange fractured at 1,095,000 cycles while the crack grew to 2 1/8-in into the web. A hole was drilled at the end of the crack tip, and a bolt was placed in the hole. At 1,306,000 cycles, the south end crack propagated into the east side of the web fillet. At 1,457,000 cycles, a 1 1/8-in long compression crack propagated through the full end weld detail at the southwest side of the beam. The 1-in thick temporary repair plates were then attached to the compression flange and the test was resumed. At the end of the test, 1,800,000 cycles, the measured tension crack length at the south side was 3 9/32-in. After breaking the south end flange, the crack was found to be 3 11/32-in long. It should be noted that neither of the splice plates prevented the initial cracks from propagating, although the growth was substantially larger for the 5/16-in splice plate than for the 7/16-in splice plate. This could be seen from the fact that the 5/16-in splice plates were used to repair a smaller crack (7/8-in total) than the 7/16-in splice plate (1 3/8-in total), but the 5/16-in end fractured at 1,095,000 cycles while the 7/16-in end did not show any signs of distress until 1,306,000 cycles when a crack appeared in the web fillet.

6.2.13. Specimen NF3

After pre-cracking, the north end was repaired using a 5/16-in splice, while a 7/16-in splice was used for the south end. At 1,346,000 cycles after repair, the north end crack propagated into the web fillet, and at 1,680,000 cycles the north flange fractured and the crack propagated 2-in into the web. When the test was stopped,at 1,800,000 cycles, the north end crack had propagated 2 1/2-in into the web. The south flange cracks coalesced for a final length of 3-in. After breaking the south end flange, the crack was found to be 2 31/32-in long. Here again, similar to specimen NF2, it could be seen that the crack growth was substantially greater for the

beam end with the 5/16-in splice plates than for the end with the 7/16-in splice plates.

6.2.14. Specimen WF1

After pre-cracking, the north end was repaired using the 7/16-in splice plates while the 5/16-in splice plates were used to repair the south end. At 515,000 cycles after repair, the south cracks propagated into the web fillet. At 690,000 cycles, this crack propagated 1-in into the web. The south flange was found to be fractured at 900,000 cycles and the crack had propagated 2 13/32-in into the web. A 15/16-in hole was drilled at the crack tip, a 7/8-in A325 bolt was placed in the hole, and the test was resumed.

The north end crack was found to have propagated 1-in, 1 7/16-in, and 1 3/4-in into the web at 1,025,000, 1,200,000, and 1,377,000 cycles, respectively. A hole, similar to the south end, was then drilled and the test was resumed. The north end flange fractured completely at 1,744,000 cycles. The test was stopped at 1,800,000 cycles after repair. The same observation as for specimens NF2 and NF3 could be made; the beam end with 7/16-in splice plates were found to have a slower crack growth rate than the end with 5/16-in splice plates.

6.2.15. Specimen WF2

After pre-cracking, both ends were repaired using a 5/16-in splice. At 1,002,000 cycles, the north crack was found to have propagated into the web fillet while the south crack was about 27/32-in into the web. At 1,143,000 cycles, the cracks were 1-in and 1 3/4-in into the north and south ends of the web, respectively. At 1,315,000 cycles, the south flange fractured and the crack was 2 3/4-in into the web. At the same time the north end crack was 2-in in the web. A 15/16-in hole was drilled at the crack tip on both sides. A 7/8-in diameter bolt was placed in the hole, and the test was resumed. At 1,485,000 cycles, the north end flange completely fractured. Although both flanges had fractured, the test was continued until 1,800,000 cycles of loading had been applied.

6.2.16. Specimen WF3

After pre-cracking, the north and south ends were repaired using a 5/16-in and a 7/16-in splice, respectively. The north end crack was found to have propagated 1 3/32-in and 1 3/4-in into the web at 967,000, and 1,154,000 cycles, respectively. At 1,324,000 cycles, the north end

flange fractured while the crack propagated 3-in into the web. A 15/16-in hole was drilled at the crack tip, a 7/8-in bolt was placed in the hole, and the test was resumed. At 1,473,000 cycles, the south side crack propagated into the web fillet. At the end of the test (1,800,000 cycles) the south crack was 4 1/32-in long. After breaking the south end flange, the crack length was found to be 4-in. Again, it was observed that the beam end with 5/16-in splice plates exhibited a greater crack growth rate than the end with 7/16-in splice plates.

6.2.17. Specimen WR1

After pre-cracking, both sides were repaired using the 5/16-in splice connection. At 820,000 cycles, the north end crack propagated into the web fillet, and at 1,008,000 cycles, the crack was 1 3/8-in long in the web. At 1,174,000 cycles, the north flange fractured completely and the crack had propagated 2 3/4-in into the web. At the same time, the south flange crack propagated into the web fillet. A 15/16-in hole was drilled at the crack tip, a 7/8-in bolt was placed in the hole, and the test was resumed. At 1,324,000 cycles, the south crack propagated 1 5/8-in into the web. At 1,495,000 cycles, the south flange fractured completely and the crack had grown 3 1/4-in into the web. The same web repair procedure was applied, and the test was continued until 1,800,000 cycles had been applied.

6.2.18. Specimen WR2

After pre-cracking, the north end was repaired using the 5/16-in splice connection, while the south end was repaired using the 7/16-in splice connection. At 1,350,000 cycles, the north end crack propagated into the web fillet. At 1,520,000 cycles, the northwest side of the tension flange fractured and the crack grew 1 7/8-in into the web. At 1,561,000 cycles, the north end tension flange fractured completely and the crack propagated 2 1/4-in into the web. A 15/16-in hole was drilled at the crack tip, a 7/8-in bolt was placed in the hole, and the test was resumed. At the end of the test, 1,800,000 cycles after repair, the final crack length at the southwest and southeast sides were found to be 1 19/32-in and 31/32-in, respectively. It should be noted that the southwest side crack had two branches, as shown in Fig. 6.13. After breaking the south end flange, the crack lengths were found to be 1 5/8-in and 1 1/32-in for the southwest and southeast sides, respectively. Here again, it could be seen that the beam end with the 5/16-in splice plates had a crack growth rate higher than that for the beam end with the 7/16-in splice plates.

6.2.19. Specimen WR3

After pre-cracking, the north and south end flanges were repaired using the 7/16-in and the 5/16-in splice plates, respectively. At 1,000,000 cycles after repair, the south end crack propagated into the web fillet. At 1,170,000 cycles after repair, the southeast side of the tension flange fractured while the crack grew 1 7/8-in into the web. At 1,211,000 cycles, the south end tension flange fractured completely and the crack had propagated 2 3/8-in into the web. A 15/16-in hole was drilled at the crack tip, a 7/8-in bolt was placed in the hole, and the test was resumed. At the end of the test (1,800,000 cycles) the north end cracks coalesced into a single crack 3 9/32-in long. It was also discovered at the end of the test that the north end compression flange was completely severed and the crack had propagated 4-in into the web. After breaking the north end flange, the crack was found to be 3 11/32-in long.

6.3. Discussion of Results

As previously discussed, two splice plate thicknesses were selected for the bolted splice repair procedure: 5/16-in and 7/16-in plates. A total of 23 ends were repaired using the 5/16-in splice plate detail (all of which were subjected to 20.0-ksi stress range), while the remaining 15 ends were repaired with the 7/16-in splice plate detail (two of which were subjected to a 15.0-ksi stress range, and the remaining 13 ends were subjected to a 20.0-ksi stress range).

Specimen DB1 is of particular importance. The test results suggest that if a cover plate end weld detail is repaired with a bolted splice prior to cracking, it can achieve a Category B design life (about 1,500,000 cycles for a 20-ksi stress range) without much additional damage. Specimen DB1, which had no cracks prior to repair, sustained 1,800,000 after cycles after repair without initiating any cracks. It should also be noted that specimen DB1 was pre-cycled for 200,000 cycles prior to repair, and that these cycles are not included in the 1,800,000 cycle count.

All of the beams, regardless of the crack size prior to repair, carried at least 1,800,000 cycles of loading after repair. When the beam flange fractured, the splice plates were able to carry the load that the flange had carried and still reach the required 1,800,000 cycles. It should be noted that none of the splice plates cracked during the test. Out of the 23 ends repaired with the 5/16-in splice detail, 14 beam flanges fractured and the remaining 9 reached at least 1,800,000 cycles without the flange fracturing. For these non-fractured 9 ends, the maximum total crack size at the beam end prior to repair was 3/8-in long. On the other hand, the minimum total

crack length at a beam end that fractured while repaired with the 5/16-in splice detail was 5/32-in. Out of the 15 ends repaired with the 7/16-in splice plate detail only one beam flange fractured. The total crack length at that end, prior to repair, was about 1-in (specimen subjected to 20.0-ksi stress range). The maximum total crack length at a non-fractured end repaired with the 7/16-in splice detail was 1 1/8-in; this beam carried 2,500,000 cycles after repair under a 20.0-ksi stress range before the test was stopped. The maximum total crack length at a beam end repaired with the 7/16-in splice plate detail that reached 3,000,000 cycles (with a 20.0-ksi stress range) without fracturing was 7/16-in.

Figure 6.14 shows the stress range versus the number of loading cycles applied after repair for the NR beams. It should be noted that this is not an S-N curve since only two of the repaired ends actually fractured. In the case of a compression flange fracture, the number of cycles shown in Fig. 6.14 represents the number of cycles until repair of a compression flange crack. At that time, the stress in the tension flange was altered by the compression flange repair. Out of the eight NR beams (16 ends), eight ends were repaired with 5/16-in plates and eight ends were repaired using 7/16-in plates. The beam flange fractured for only two ends repaired with the 5/16-in splice plate detail: one at 1,564,000 cycles and the other at 2,000,000 cycles. Six ends repaired with the 5/16-in splice plate detail reached 1,800,000 cycles after repair without the flange fracturing. Out of the eight ends repaired with the 7/16-in splice plate connection, six were subjected to 20.0-ksi stress range. These six ends were divided as follows: two ends were subjected to 2,000,000 cycles after repair, two ends carried 2,500,000 cycles after repair, and two ends sustained 3,000,000 cycles after repair. All of these ends reached the specified number of cycles without the beam flange fracturing. The two beam ends subjected to a 15.0-ksi stress range and repaired with the 7/16-in splice connection reached 7,143,000 cycles and 10,782,000 cycles without fracturing.

Figure 6.15 illustrates the stress range versus the number of cycles applied after repair for the NN beams. The two NN beams (4 ends) were repaired using the 5/16-in splice plate detail. All four ends reached 1,800,000 cycles without the beam flange fracturing. Again, the number of cycles shown in Fig. 6.15 corresponds to the end of test, tension flange fracture, or repair of the compression flange using a splice connection.

Figure 6.16 shows the stress range versus the number of cycles after repair for the NF beams. Out of the three NF beams tested (6 ends), four ends were repaired using the 5/16-in splice plate detail and two ends were repaired with the 7/16-in splice plate detail. All of these beams carried 1,800,000 cycles of loading. However, the beam flanges repaired using the 5/16-in splice plate detail all fractured prior to reaching 1,800,000 cycles. The beam flanges fractures occurred at 1,049,000 cycles, 1,179,000 cycles, 1,095,000 cycles, and 1,680,000 cycles - these values are indicated in Fig. 6.16. The two ends repaired with the 7/16-in splice plate detail did not fracture.

Figure 6.17 details the stress range versus the number of cycles after repair for the WF beams. Out of the three WF beams (6 ends), four ends were repaired using the 5/16-in splice plate detail and two ends were repaired with the 7/16-in splice plate detail. All of these beams were subjected to 1,800,000 cycles of loading without failure. All ends repaired using the 5/16-in splice plate detail fractured prior to reaching 1,800,000 cycles: at 900,000 cycles, 1,485,000 cycles, 1,315,000 cycles, and 1,324,000 cycles. One of the two ends repaired with the 7/16-in splice plate detail fractured at 1,744,000 cycles after repair, while the other end reached 1,800,000 cycles without fracturing.

Figure 6.18 shows the stress range versus the number of cycles after repair for the WR beams. Out of the three WR beams (6 ends), four ends were repaired using the 5/16-in splice plate detail and two ends were repaired with the 7/16-in splice plate detail. All of these beams were subjected to 1,800,000 cycles. Again, all beam flanges repaired using the 5/16-in splice plate detail fractured prior to reaching 1,800,000 cycles: at 1,174,000 cycles, 1,495,000 cycles, 1,561,000 cycles, and 1,211,000 cycles. The beam flange at the two ends repaired with the 7/16-in splice plate detail did not fracture.

Figure 6.19 compares the number of loading cycles applied after repair of the pre-cracked flange until fracture of the flange or end of test, whichever comes first, for 18 of the 19 beams tested (only specimens subjected to 20.0-ksi stress range are shown). When the compression flange fractured and was repaired with a splice plate, the number of cycles to compression flange repair was used (after repair of the compression flange, the stress in the tension flange was altered). It can be seen that all of the NR and NN type beams sustained more loading cycles than the Category B design life without the beam tensile flange fracturing. The NF, WF, and WR beam results were scattered around the Category B design life value. It should be noted that

although some of the beam flanges fractured prior to reaching the Category B design life value, the splice plates were able to carry the load and the tests were continued until the beams reached at least 1,800,000 cycles.

A comparison between the 5/16-in and 7/16-in thick splice plate details is shown in Fig. 6.20 for specimens tested with 20.0-ksi stress range. Again, the number of cycles to compression flange repair was used whenever appropriate. It can be seen that all beam flanges repaired with the 7/16-in splice plate detail reached the Category B design life without fracturing. The beam flanges repaired with the 5/16-in splice plate detail were not as consistent, with a number of the beam ends fracturing at load repetitions less than the Category B design value.

6.4. Comparison with Other Test Results

Sahli, Albrecht, and Vannoy (1984) tested fifteen W14 × 30 steel beams at 20.0-ksi and 30.0-ksi stress ranges to investigate the fatigue strength of cover plate ends retrofitted with splice plates and high strength bolts in friction. The test specimen consisted of a W14 × 30 steel beam with two 5 3/4-in × 1/2-in × 4-ft - 0-in long square-ended cover plates. The cover plates were welded all around to the beam flanges. Out of the 15 tested beams, seven were retrofitted with splice plates prior to any loading, three were pre-cracked with the crack through half of the flange thickness, and 5 were pre-cracked with the crack through the entire flange thickness. The test results of the fifteen beams are shown in Fig. 6.21, along with the results from the present study. It should be noted that in the present study the splice plates were added after a fatigue crack was first detected. Also, the test results from the present study correspond to either failure of the flange or the end of test (whichever comes first), except in the case of a compression flange repair. In that case, the number of cycles to compression flange repair is used. As mentioned earlier, although all of the tests were stopped after 1,800,000 cycles of loading, no failure of the splice plates was observed throughout the tests. On the other hand, the results of Sahli, Albrecht, and Vannoy (1984) correspond to either failure of the flange or the splice plates.

A distinct difference in the dominate failure mode was observed between tapered and square-end cover plates. It is believed this is attributed to the significant flexibility of the splice plate connection used with the taper cover plate: due to differences in length, the splice plates used by Sahli et al. (1984) were four times stiffer than those used in the present study. This higher flexibility reduces the force carried by the splice plate and, consequently, increases the

stresses in the flange at the weld toe. This would explain why significant crack growth occurred in the present study, while little additional crack growth was observed in the tests by Sahli et al. (1984).

6.5. Conclusions of Test Results

Nineteen W14 × 30 steel beams were tested to examine the fatigue resistance of beams with welded partial-length, tapered cover plates which have been repaired with bolted splice plates. Based upon the experimental test results and corresponding observations, the following general conclusions can be stated:

1- Neither the 5/16-in nor the 7/16-in full bolted splice plates completely prevented subsequent crack growth, except for the case of repair prior to initiating a crack (DB1).

2- It appears that the splice plate thickness has a notable influence on the crack growth rate. Thicker plates increase the effective moment of inertia and decrease the stresses in the beam flange. Consequently, the cracks grew considerably slower when 7/16-in splice plates were used rather than 5/16-in plates. Only one of the flanges repaired using the 7/16-in plate completely fractured (WF1 at 1,744,000 cycles), although the ends repaired with this specific detail had initial crack sizes larger than those in the ends repaired using the 5/16-in plate.

3- The initial crack size is a very important factor in determining the remaining life of the specimen and plays a significant role in controlling when complete fracture of the flange occurs.

4- Both the 5/16-in and the 7/16-in splice plates significantly improved the fatigue life of the various cover plate details. In both cases, the splice plate detail enabled the beams with pre-cycled fatigue cracks to sustain more additional loading cycles than Category B design strength - roughly 1,500,000 cycles at 20-ksi stress range.

5- Even if the initial fatigue cracks cause the beam flange to fracture completely, the 5/16-in splice plates carried the flange force and enabled the detail to sustain a number of loading cycles after beam flange fracture. In one case, the beam carried about 900,000 cycles of 20-ksi stress range after fracture of the flange.

6- Beams with the wide cover plate detail were found to initiate cracks sooner than beams with the narrow cover plate detail.

7- Compression cracks frequently appeared in the tested beams even when the compression side was peened prior to testing. Three out of four non-peened ends exhibited compression cracks. This ratio drops to 6 out of 32 when the cover plate ends are peened prior to cycling.

Table 6.1. Number of Loading Cycles Applied to Test Beams After Repair with Bolted Splice.

Specimen	End	Number of Loading Cycles		Comments
		Flange Fracture	Total Applied	
DB1	N[1]	1,375,000	1,800,000	Compression flange fractured.[4]
	S[1]	---	1,800,000	Flange did not fracture.
DB2	N[1]	951,000	1,800,000	Compression flange fractured.
	S[1]	951,000	1,800,000	Compression flange fractured.
DB3	N[1]	---	1,800,000	Flange did not fracture.
	S[1]	---	1,800,000	Flange did not fracture.
NR1	N[1]	1,564,000	2,000,000	Hole drilled in web at crack tip.
	S[1]	2,000,000	2,000,000	
NR2	N[2]	2,000,000	2,500,000	Compression flange fractured.
	S[2]	---	2,500,000	Flange did not fracture.
NR3	N[2]	---	3,000,000	Flange did not fracture.
	S[2]	1,883,000	3,000,000	Compression flange fractured.
NR4	N[2]	---	2,000,000	Flange did not fracture.
	S[2]	---	2,000,000	Flange did not fracture.
NR8[3]	N[2]	10,782,000	10,782,000	Compression flange fractured.
	S[2]	7,134,000	10,782,000	Compression flange fractured.
NN1	N[1]	---	1,800,000	Flange did not fracture.
	S[1]	1,333,000	1,800,000	Compression flange fractured.
NN2	N[1]	---	1,800,000	Flange did not fracture.
	S[2]	995,000	1,800,000	Compression flange fractured.
NF1	N[1]	1,049,000	1,800,000	Two holes drilled in web at crack tip.
	S[1]	1,179,000	1,800,000	Two holes drilled in web at crack tip.

Table 6.1. Number of Loading Cycles Applied to Test Beams After Repair with Bolted Splice. (cont.)

Specimen	End	Number of Loading Cycles		Comments
		Flange Fracture	Total Applied	
NF2	N[1]	1,095,000	1,800,000	Hole drilled in web at crack tip.
	S[2]	1,457,000	1,800,000	Compression flange fractured.
NF3	N[1]	1,680,000	1,800,000	
	S[2]	---	1,800,000	Flange did not fracture.
WF1	N[2]	1,744,000	1,800,000	Hole drilled in web at crack tip.
	S[1]	900,000	1,800,000	Two holes drilled in web at crack tip.
WF2	N[1]	1,485,000	1,800,000	Hole drilled in web at crack tip.
	S[1]	1,315,000	1,800,000	Hole drilled in web at crack tip.
WF3	N[1]	1,324,000	1,800,000	Hole drilled in web at crack tip.
	S[2]	---	1,800,000	Flange did not fracture.
WR1	N[1]	1,174,000	1,800,000	Hole drilled in web at crack tip.
	S[1]	1,495,000	1,800,000	Hole drilled in web at crack tip.
WR2	N[1]	1,561,000	1,800,000	Hole drilled in web at crack tip.
	S[2]	---	1,800,000	Flange did not fracture.
WR3	N[2]	---	1,800,000	Flange did not fracture.
	S[1]	1,211,000	1,800,000	Hole drilled in web at crack tip.

[1] 5/16-in splice repair connection.

[2] 7/16-in splice repair connection.

[3] Specimen subjected to 15.0-ksi stress range.

[4] Stress in tension flange altered after compression flange repair.

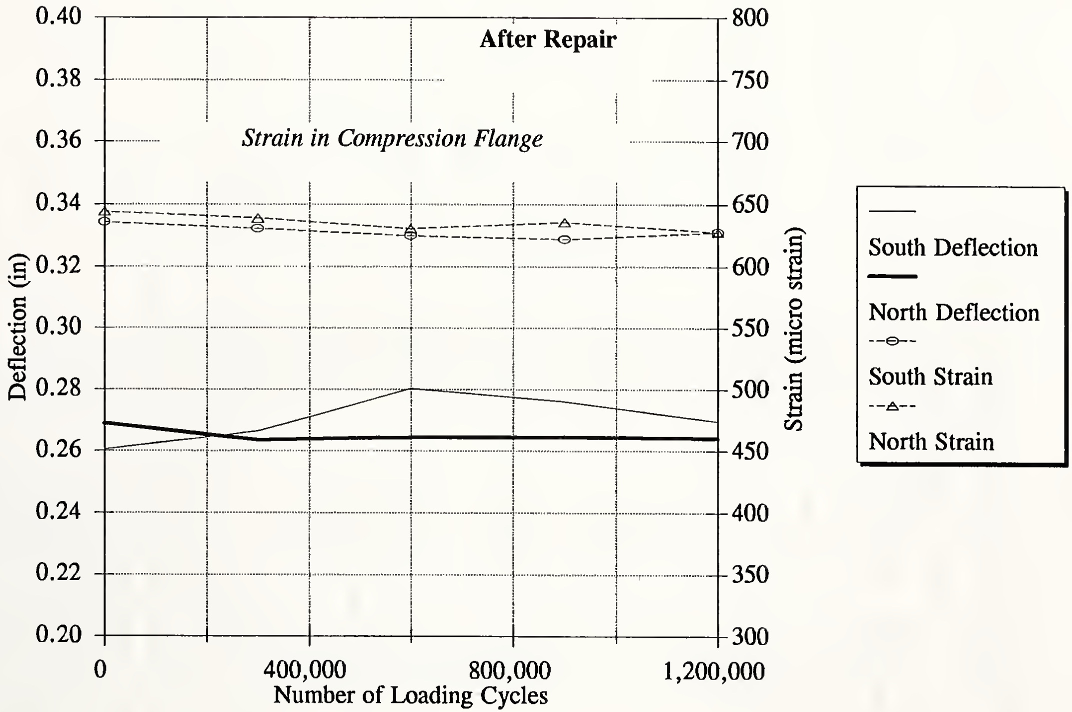

Fig. 6.1. Change in the Maximum Deflection and Strain with the Number of Cycles.

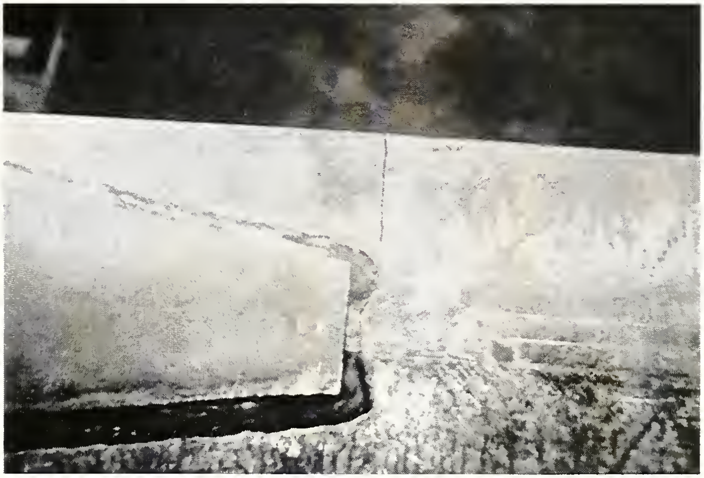

Fig. 6.2. Compression Flange Crack - Specimen DB1.
(1,375,000 Loading Cycles After Repair)

Fig. 6.3. Crack Measurement Using Dye Penetrent Method - Specimen DB2 South End.

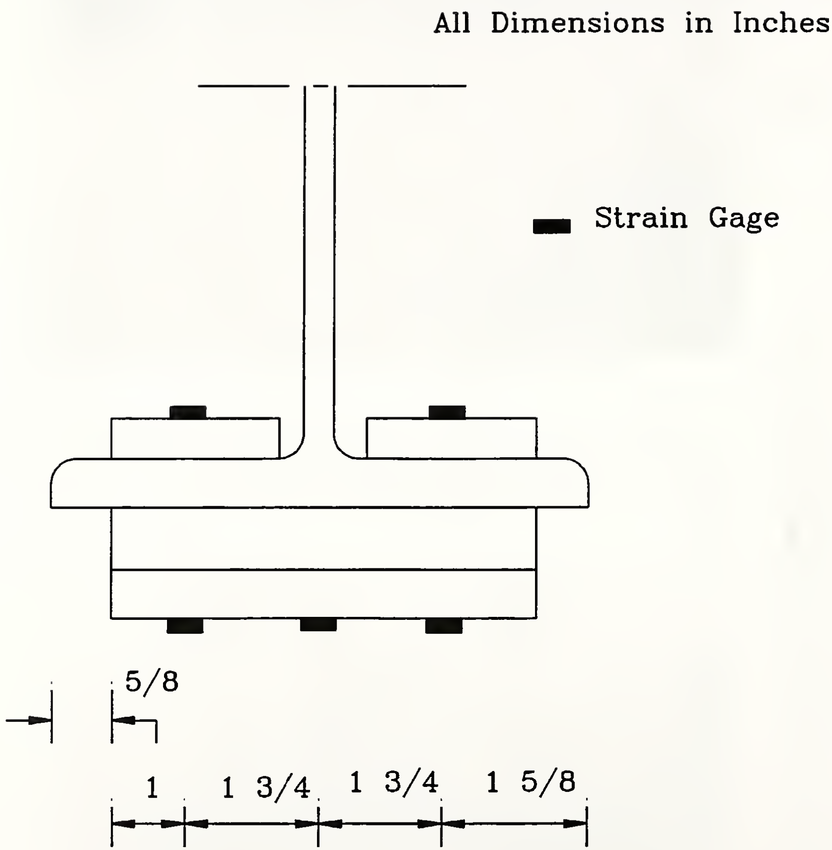

Fig. 6.4. Strain Gage Locations.
(Specimens NR1 and NR3)

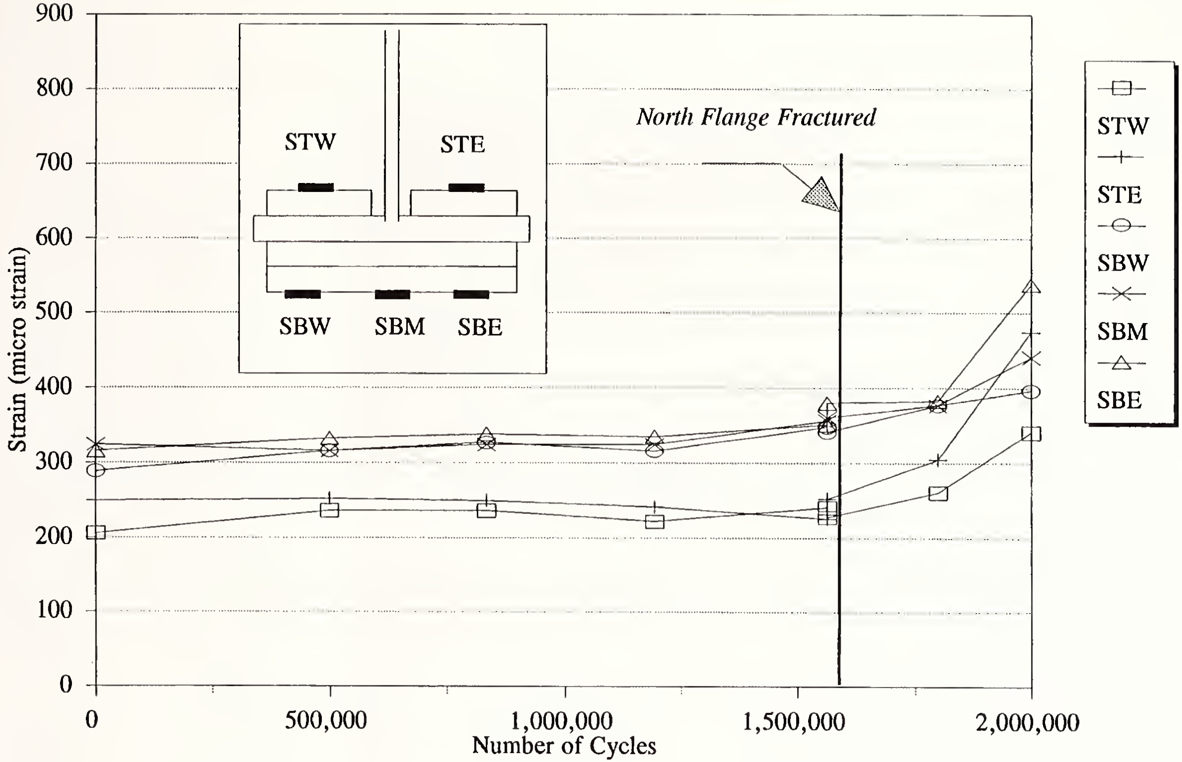

Fig. 6.5. Strain Measurements for 5/16-in Splice Plate - South End.
(Specimen NR1)

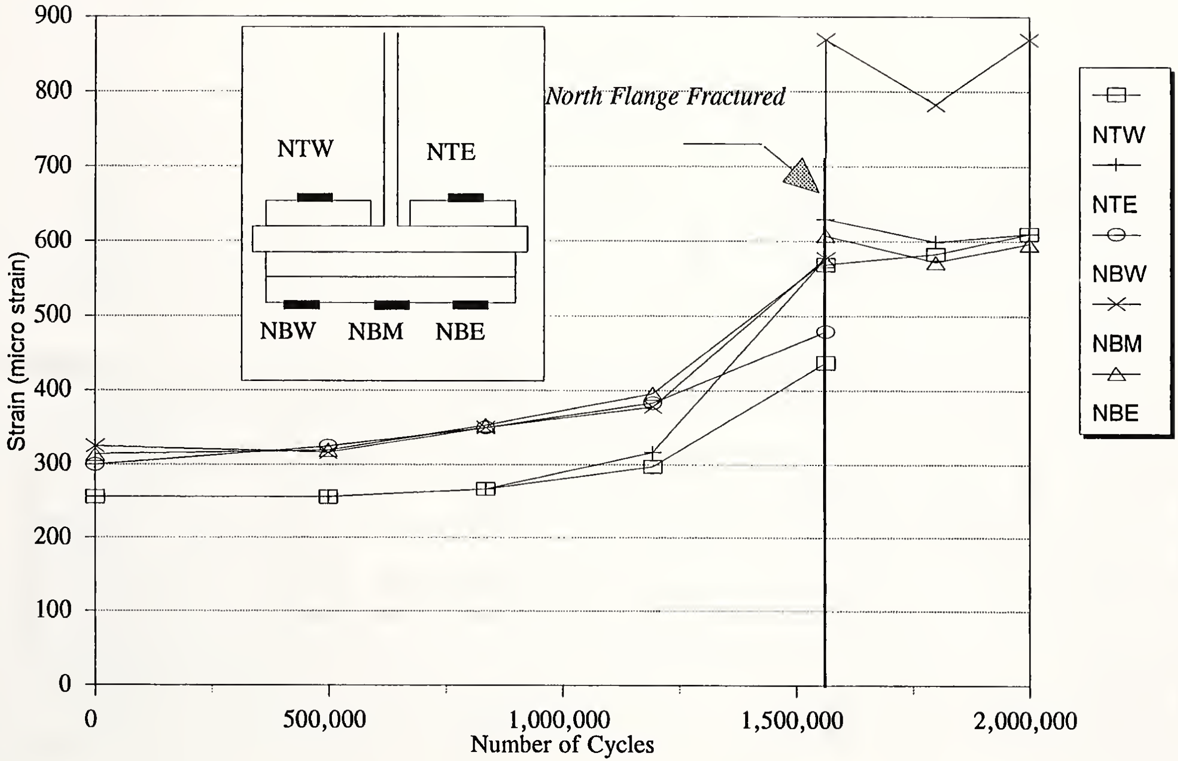

Fig. 6.6. Strain Measurements for 5/16-in Splice Plates - North End. (Specimen NR1)

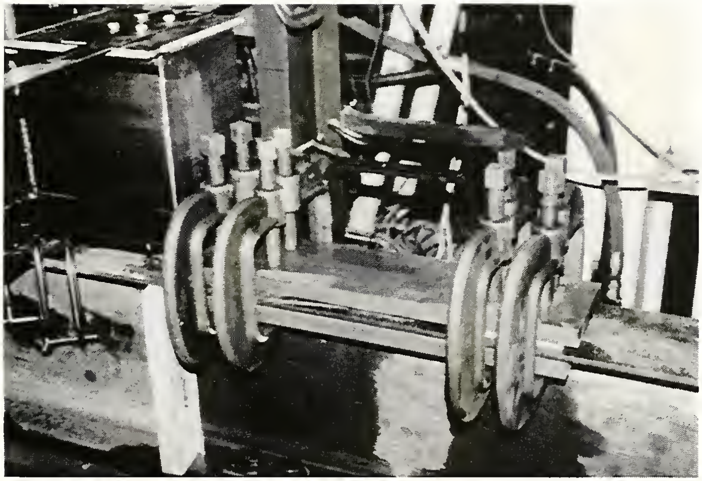

Fig. 6.7. 1-in Thick Temporary Repair Connection.
(Specimen NR2 North - Compression Flange)

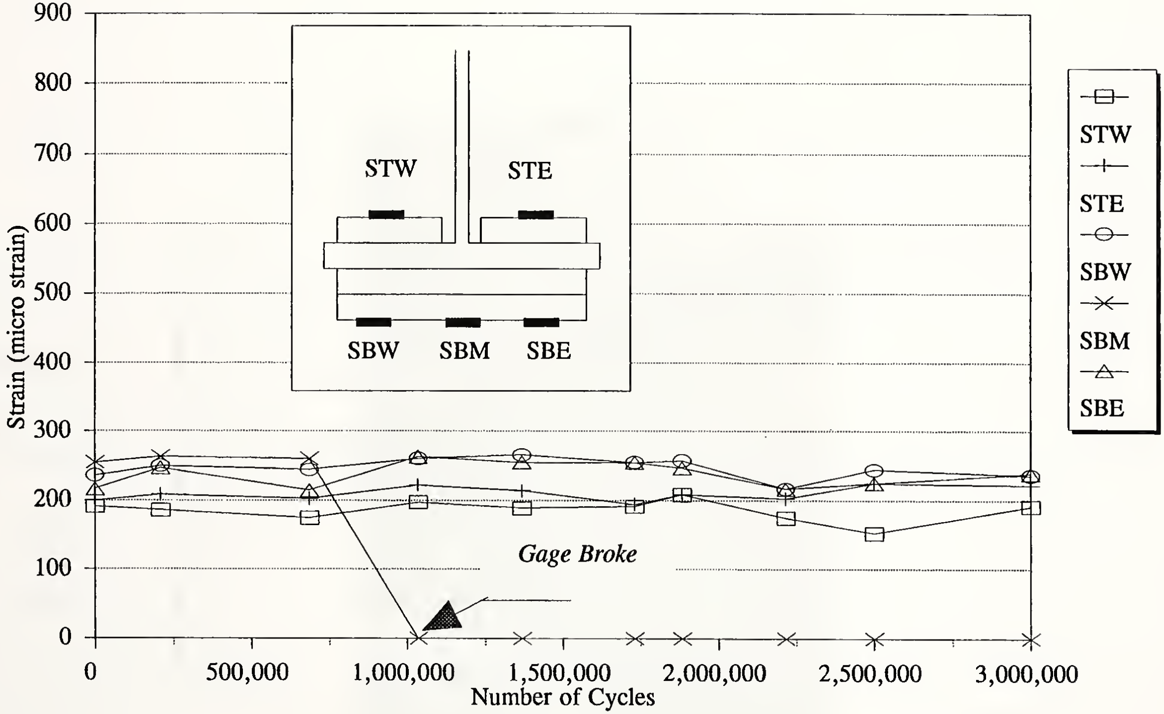

Fig. 6.8. Strain Measurements for 7/16-in Splice Plates - South End.
(Specimen NR3)

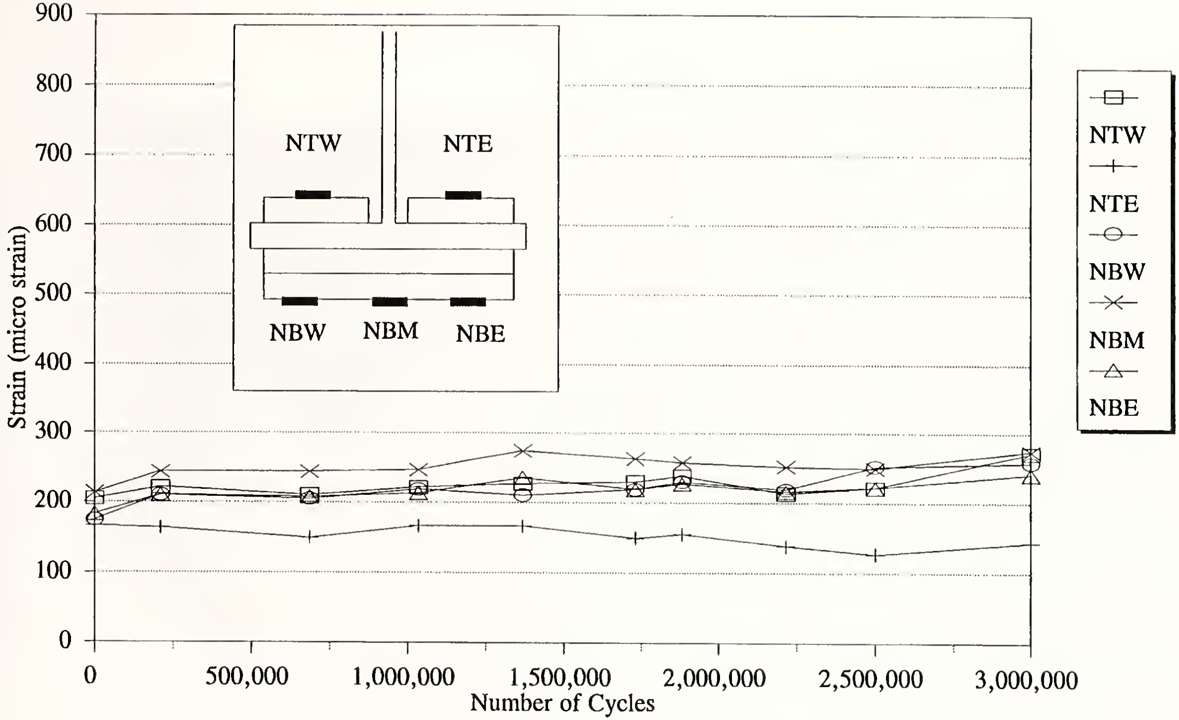

Fig. 6.9. Strain Measurements for 7/16-in Splice Plates - North End.
(Specimen NR3)

Fig. 6.10. Non-Coalesced Cracks - Specimen NR3 North End.

Fig. 6.11. Fracture Surface - Specimen NR8 North End.

Fig. 6.12. Drilled Web Hole at Crack Tip - Specimen NF1 North End.

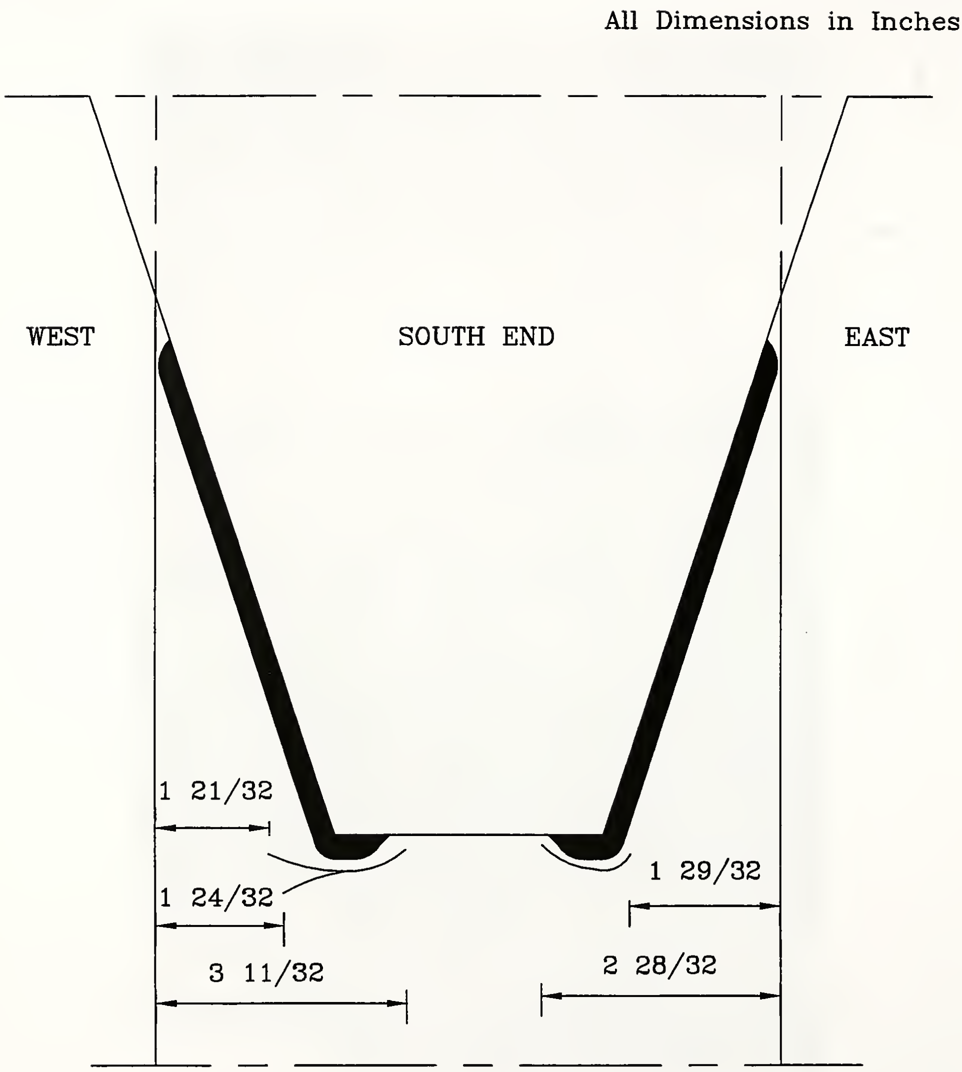

Fig. 6.13. Final Crack Length.
(Specimen WR2)

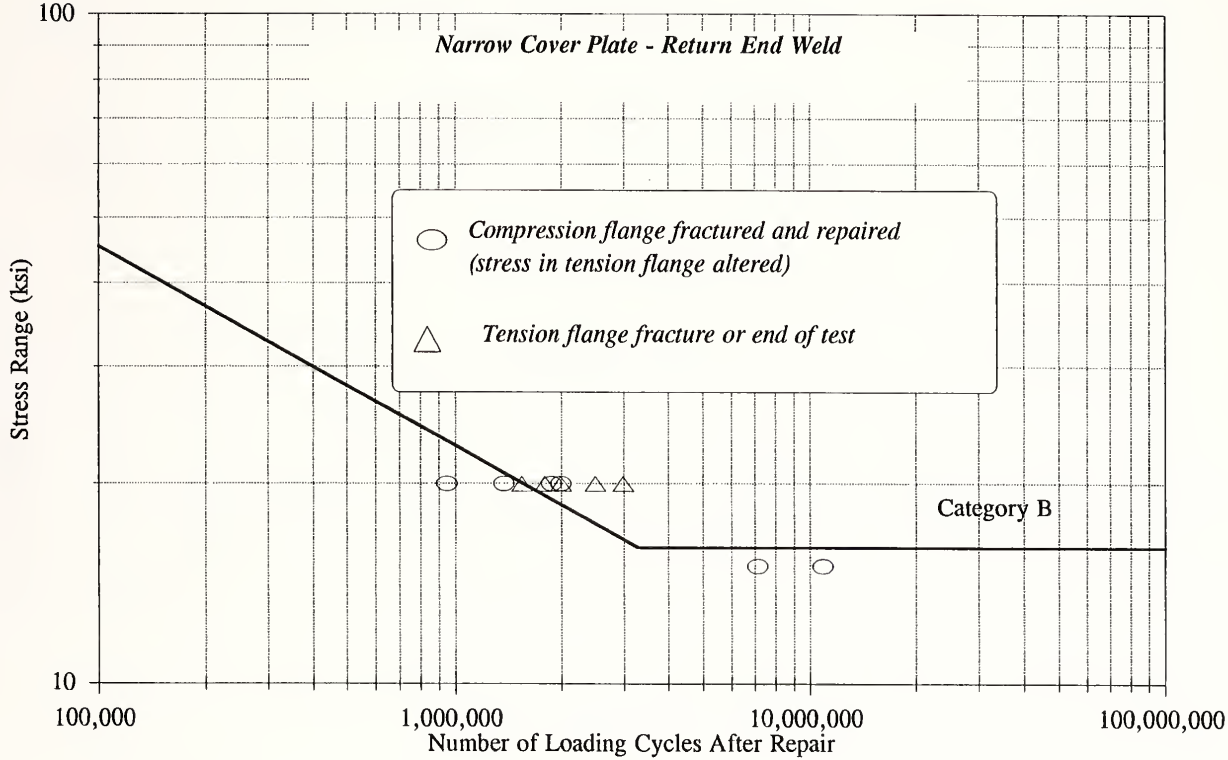

Fig. 6.14. Stress Range versus Number of Loading Cycles after Repair.
(NR-Specimens)

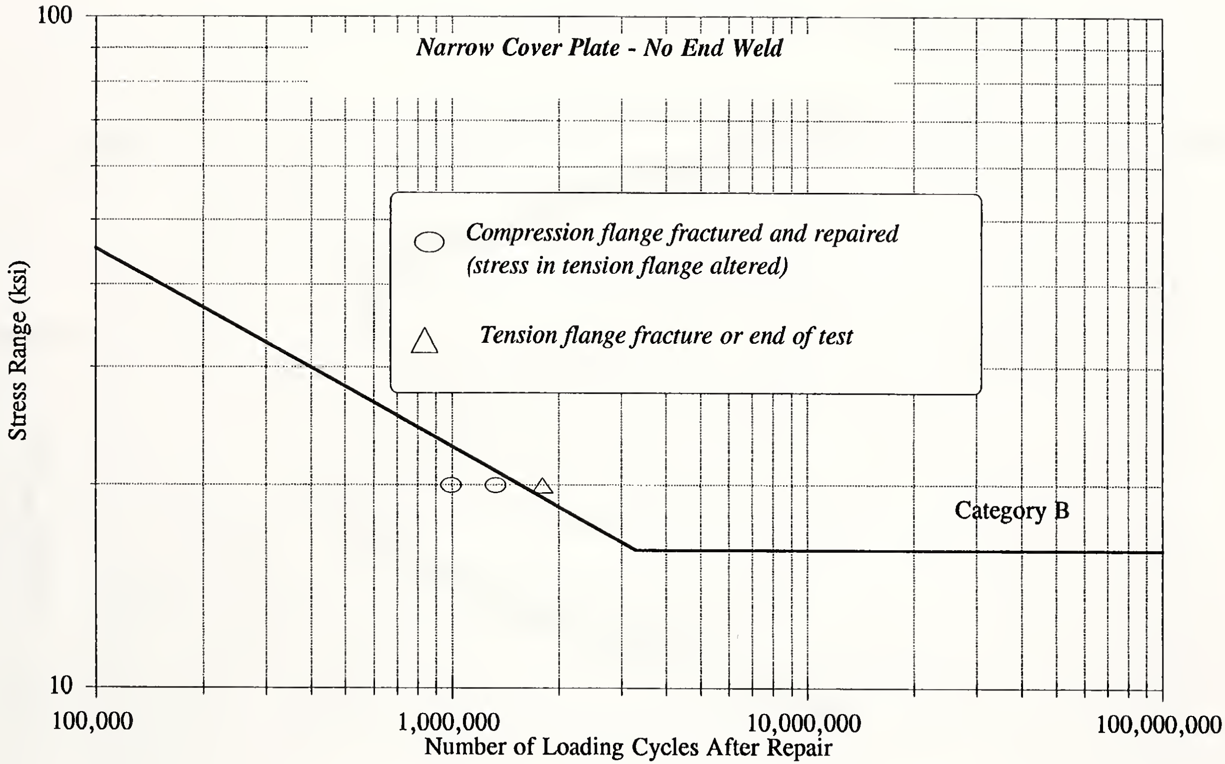

Fig. 6.15. Stress Range versus Number of Loading Cycles after Repair.
(NN-Specimens)

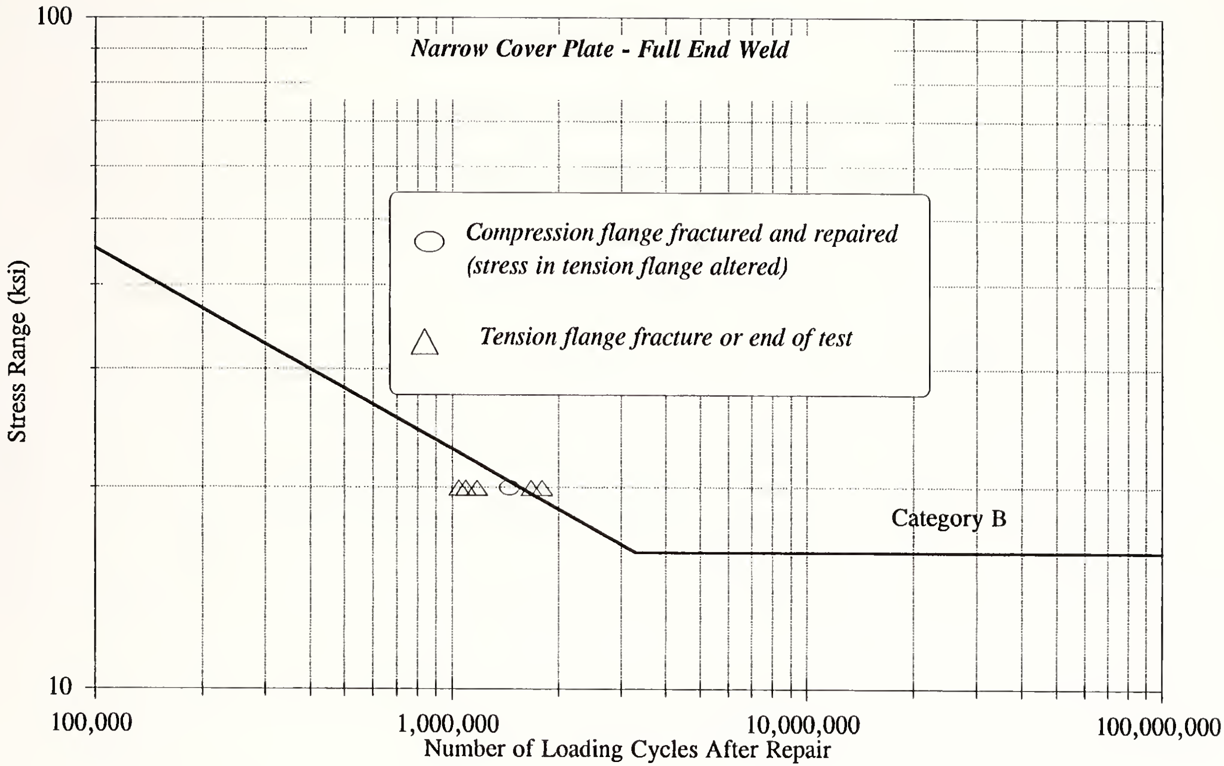

Fig. 6.16. Stress Range versus Number of Loading Cycles after Repair.
(NF-Specimens)

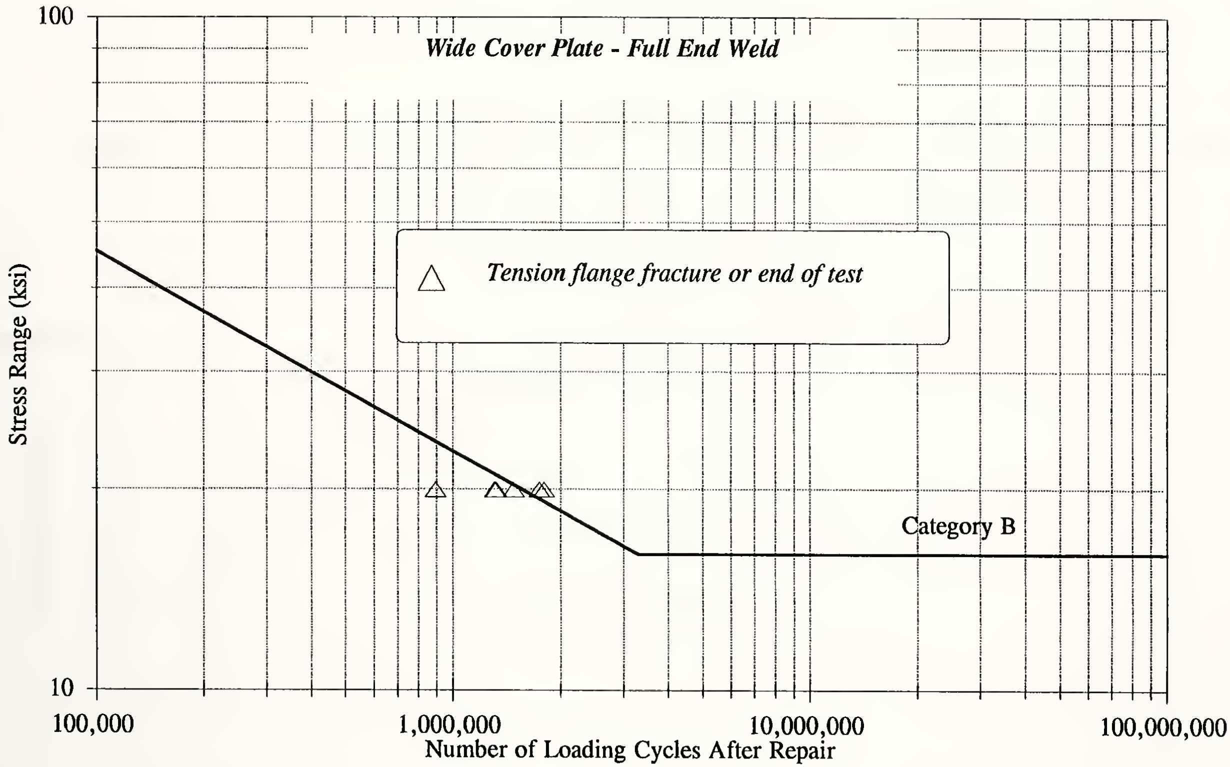

Fig. 6.17. Stress Range versus Number of Loading Cycles after Repair.
(WF-Specimens)

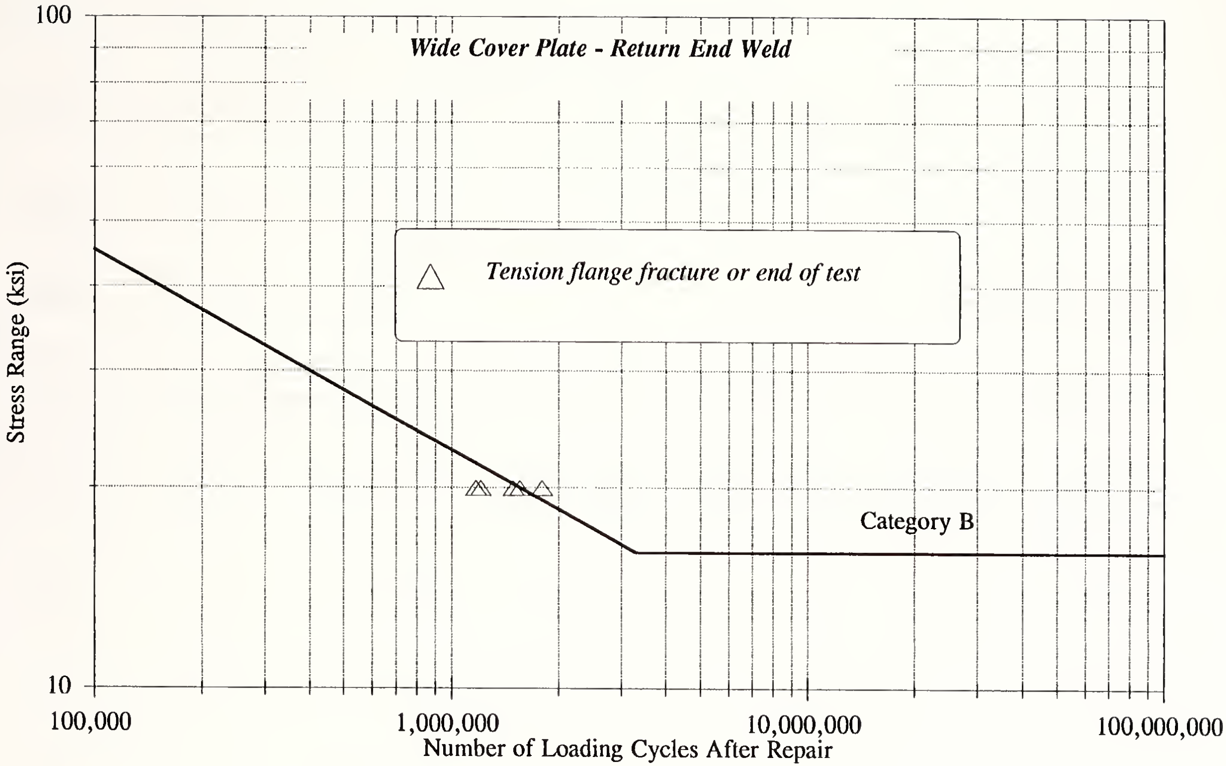

Fig. 6.18. Stress Range versus Number of Loading Cycles after Repair.
(WR-Specimens)

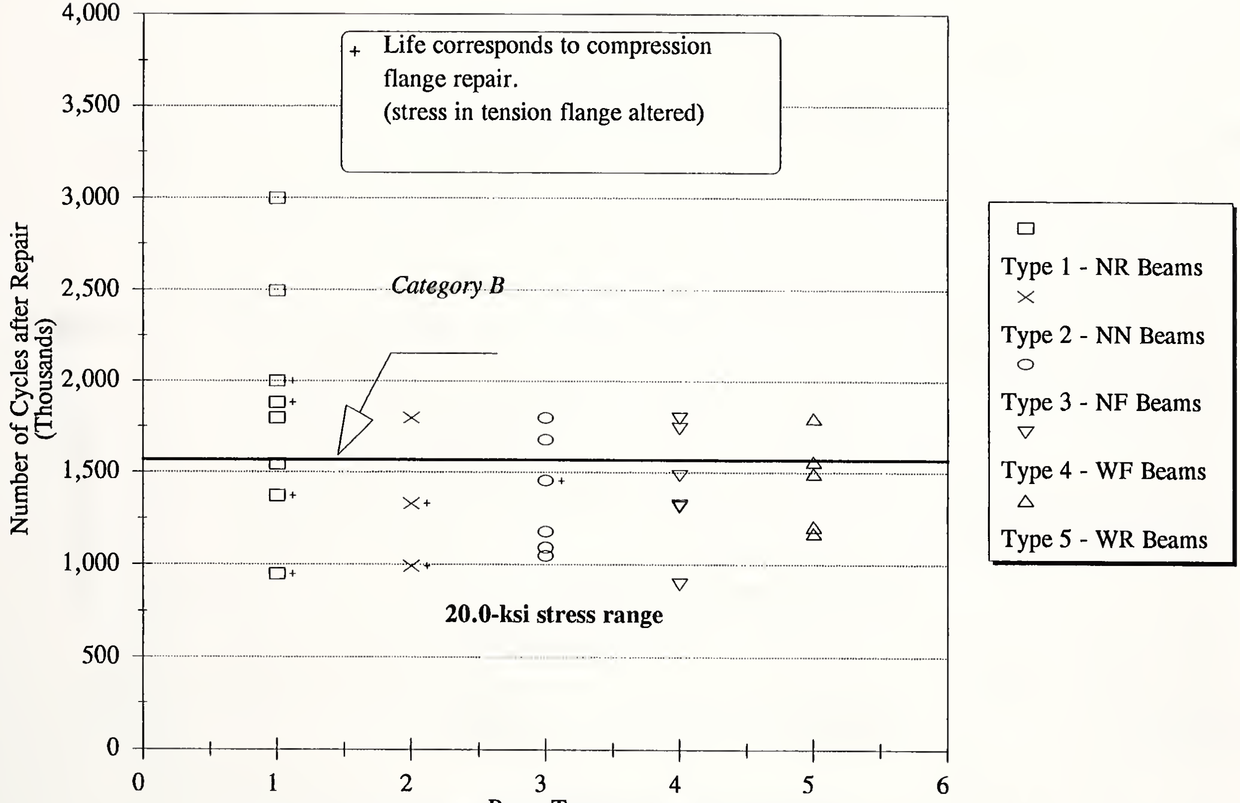

Fig. 6.19. Number of Loading Cycles Applied after Repair.

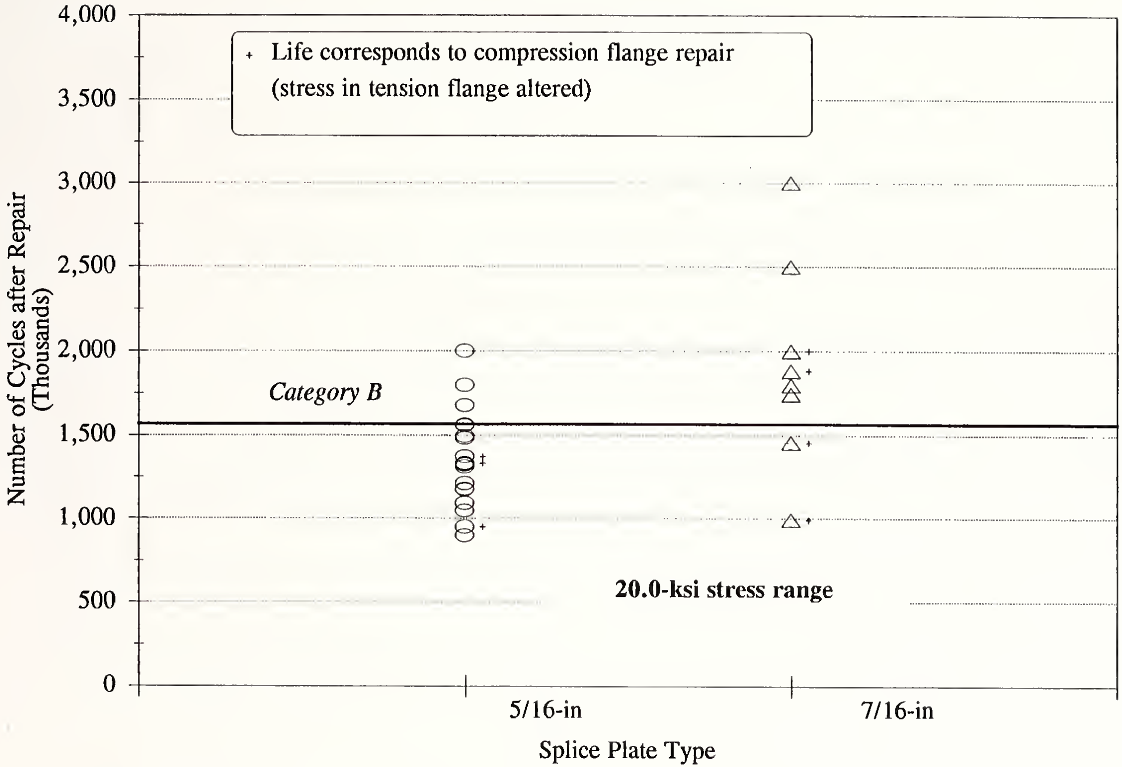

Fig. 6.20. Number of Loading Cycles after Repair versus Splice Plate Thickness.

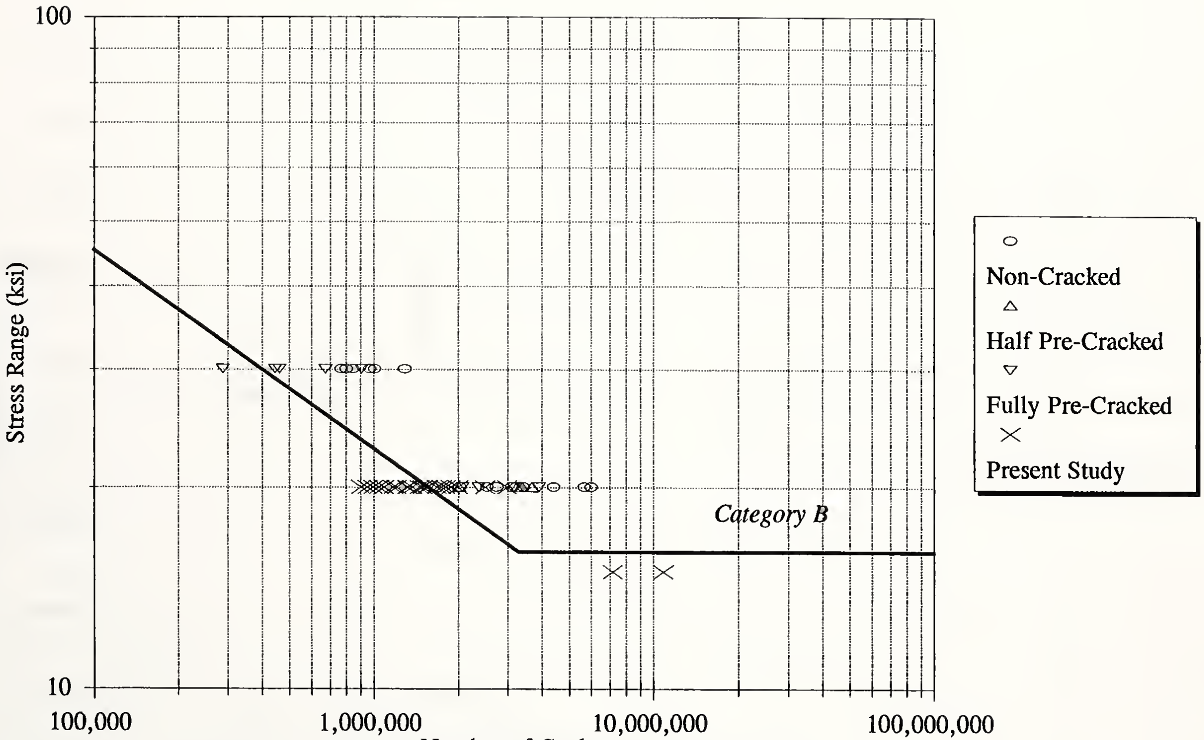

Fig. 6.21. Comparison with Test Results of Sahli, et al. (1984)
(Square Ended Cover Plates)

CHAPTER 7
PEENING REPAIR

7.1. General Comments

Previous studies on the repair of beams with welded cover plates using air-hammer peening by Hausammann, Fisher, and Yen (1983) indicated that fatigue cracks with depths up to about 0.1-in could be successfully repaired. Cracks with larger depths could not be repaired successfully using the peening procedure. As previously mentioned, peening introduces compressive residual stresses at the weld toe area. If the crack depth is greater than the compressive residual stress zone, then the crack tip is in a tensile residual stress region and peening could actually accelerate fatigue crack propagation.

Fisher, Sullivan, and Pense (1974) studied the effect of air-hammer peening to repair fatigue damage of steel beams with welded, square-end cover plates. Three series of tests were conducted. In the first series (as-welded beams), peening was conducted prior to any loading. In the second and third series (pre-cracked beams), peening was applied after about 75% of the life had expired and after a visible crack was present at the cover plate end weld toe, respectively. The effect of air-hammer peening on the fatigue life was found to depend on the minimum stress and the stress range. The method was found to be less effective when the detail was subjected to a large stress range and a high minimum stress. The results obtained suggest that air-hammer peening can increase the fatigue life from Category E to Category D for low values of minimum stress. The results also indicated that peening was effective only for crack depths less than 1/8-in.

In the present study, eight beams were repaired using the air-hammer peening method. Five specimens were peened after cracks which were visibly detected developed at the cover plate end weld. The remaining three specimens were peened after 75,000 cycles of loading under 20.0-ksi stress range. The 75,000 cycles simulate the damage that may occur in bridge girders which have been in service for a number of years, but which have not yet developed a detectable fatigue crack.

To facilitate the peening operation, the test beams were turned over (tension flange on top) prior to peening. Peening was performed using a hardened tool in a pneumatic hammer operated at 40.0-psi. The peening area, including the end weld and 2.0-in of the fillet weld parallel to the beam length, was peened with 6 passes.

The following sections summarize the pertinent comments recorded during the tests for each specimen. Then, the results of the peening repair method are presented and compared with other test results obtained from the literature. Finally, conclusions from the beam test results are presented. Table 7.1. shows the number of loading cycles applied after repair by peening until fracture of the flange. A mcre detailed summary of the measured crack sizes and number of loading cycles sustained for each specimen is given in Appendix D.

7.2. Comments for Test Beams

7.2.1. Specimen NR9

After pre-cracking, the tension flange was peened using the previously described procedure. At 264,000 cycles after repair, the north end cracks coalesced to form one crack 3 15/32-in long. At 275,000 cycles, the north end crack was 4 5/32-in long and had propagated into the web fillet. The 1-in thick temporary repair plates were then attached to the north end of the tension flange, and the test was resumed.

At 400,000 cycles after repair, the south end cracks coalesced to form a single crack 4 7/32-in long. At that time, the 1-in thick temporary repair plates were removed from the north end of the beam and the test was resumed.At 401,000 cycles (i.e. after only 1,000 cycles of loading), the north and south end cracks were 5 1/2-in and 5 5/8-in long, respectively, while they propagated about 1-in and 1 13/16-in into the web. The test was then stopped since the cracks were growing very rapidly.

7.2.2. Specimen NR10

After pre-cracking, the tension flange was peened and the test was resumed. At 432,000 cycles after repair, the south end crack was 4 7/8-in long while it had propagated to about 11/16-in into the web. At 436,000 cycles (i.e. after 4,000 more cycles of loading), the south end crack was 6 1/8-in long and had propagated about 1 7/8-in into the web. The 1-in thick temporary repair plates were then attached to the south end of the tension flange, and the test was resumed. At 506,000 cycles after repair, a crack 5 3/4-in long was present in the north end flange. Also, the crack had propagated about 1 1/8-in into the web. The test was then stopped.

7.2.3. Specimen NF4

After pre-cracking, the beam was peened and the test was resumed. At 352,000 cycles after repair, a crack was observed at the southeast side of the beam. This crack propagated into the web fillet, but could only be seen from the top portion of the bottom flange. Only 1 15/32-in of the southeast side of the flange remained un-cracked. Peening of the weld toe area prevented visual detection of the crack from the bottom of the flange. At 369,000 cycles, the south end crack was 5 11/16-in long and propagated about 1 7/16-in into the web. The 1-in thick temporary repair plates were then attached to the south end tension flange, and the test was resumed.

At 584,000 cycles after repair, a 3 7/8-in long crack propagated about 7/8-in into the web at the north end of the beam. At 590,000 cycles, the south end crack was 5 1/4-in long and had propagated about 1 1/8-in into the web. The test was then stopped.

7.2.4. Specimen WR4

After pre-cracking, the beam was peened and the test was resumed. At 145,000 cycles after repair, a 1/2-in long crack was found at the northeast weld; this crack did not occur at the weld toe (like all other cracks), but severed the return part of the weld and apparently propagated from an internal flaw in the weld material. The crack location is shown in Fig. 7.1.

At 216,000 cycles after repair, the south end cracks coalesced to form a 6 1/16-in long crack that propagated about 2 7/8-in into the web. The 1-in thick temporary repair plates were then attached to the south end tension flange. A 15/16-in hole was drilled at the crack tip, and a 7/8-in bolt was placed in the hole to delay further propagation of the crack in the web. The test was then resumed.

At 257,000 cycles after repair, the northwest side crack propagated into the web fillet. This crack could be seen only from the top fibers of the tension flange; only 1 23/32-in of the northwest tension flange was not cracked - see Fig. 7.1. Again, peening the weld toe area prevented visual detection of the crack from the bottom fibers of the flange. At 300,000 cycles after repair, the north side cracks coalesced to form a 6 1/4-in crack that propagated about 2 3/4-in into the web - see Fig. 7.1. The test was then stopped.

7.2.5. Specimen WR5

After pre-cracking, the beam was peened and the test was resumed. At 160,000 cycles after repair, a 5 1/16-in long crack was found in the south end flange; only 1 11/16-in remained non-cracked at the southeast side of the flange. That crack propagated into the web fillet. Five hundred cycles later, the crack propagated about 1-in into the web. The 1-in thick temporary repair plates were then attached to the south end tension flange, and the test was resumed.

At 222,000 cycles after repair, a 5 1/16-in long crack was observed in the north end flange. This crack propagated from the weld toe in the northwest side of the flange and coalesced with a crack that formed in the northeast side return weld (similar to Specimen WR4); only 1 11/32-in remained non-cracked from the northeast side of the tension flange. The north end crack propagated about 1 1/8-in into the web. At 223,000 cycles, the north end crack propagated about 2 1/2-in into the web. The test was then stopped.

7.2.6. Specimen NR5

After 75,000 of loading, the peening procedure was applied and the test was resumed. At 1,186,000 cycles after repair, two crack were observed at the south end of the beam. A 2 11/16-in long crack was detected at the south east side weld toe, and a 2 1/2-in long crack propagated through the southwest side weld return. These two cracks passed in different planes without coalescing - see Fig. 7.2. The 1-in thick temporary repair plates were then attached to the south end tension flange, and the test was resumed.

At 1,509,000 cycles after repair, a 5-in long crack was observed passing through the weld returns in the north end tension flange (Fig. 7.2); the crack had also propagated into the web fillet. At 1,511,000 cycles, the crack grew to 5 3/8-in in length, and propagated about 1 1/2-in into the web. The test was then stopped.

7.2.7. Specimen NR6

After 75,000 loading cycles, the cover plate end welds were peened and the test was resumed. At 881,000 cycles after repair, two cracks 1 3/32-in and 1 7/16-in long were observed through the return welds in the northwest and northeast side, respectively. At 1,006,000 cycles, these cracks coalesced to form a 6 1/2-in long crack that propagated about 3 3/4-in into the web. A 15/16-in hole was drilled at the crack tip, and a 7/8-in diameter bolt was placed in the hole

to delay further propagation of the crack. The 1-in thick temporary repair plates were then attached to the north tension flange and the test was resumed.

At 1,508,000 cycles after repair, a 3/4-in long crack was observed through the weld return in the southwest side of the tension flange. At 1,702,000 cycles, the crack grew to 1 1/4-in in length, and at 1,759,000 cycles after repair the south end crack grew into the southeast return weld to form a 4 5/32-in long crack. At 1,773,000 cycles, the south end crack was 5 1/8-in long and propagated about 3/4-in into the web. Four hundred cycles later, the crack propagated about 1-in into the web. Since rapid crack growth was evident, the test was stopped.

7.2.8. Specimen NN3

Peening was applied to the cover plate ends after 75,000 cycles of loading. Although there was no weld across the cover plate end, the 2-in width of the cover plate end was peened, as well as the weld toe along the cover plate, according to the previously discussed procedure.

At 304,000 cycles after repair, a 4 1/2-in long crack was observed in the north end tension flange and propagated into the web fillet. At 308,000 cycles, the north end crack was 5-in long. The 1-in thick temporary repair plates were then attached to the north end flange, and the test was resumed. At 413,00 cycles after repair, a 5 1/16-in long crack was observed in the south end tension flange; the crack had also propagated into the web fillet. The test was then stopped.

7.3. Discussion of Results

Two different conditions were investigated during this phase of the study. Out of the eight beams tested, five were first pre-cracked and then peened, while the remaining three were peened prior to pre-cracking. The five pre-cracked beams included two NR beams, one NF beam, and two WR beams. On the other hand, the three non-cracked beams included two NR beams and one NN beam. All of the beams were subjected to a constant-amplitude loading cycle that produced a 20.0-ksi stress range on the bare beam section at the end of the cover plate.

Figure 7.3 shows the stress range versus the number of loading cycles applied after repair for the five pre-cracked beams. It can be seen that there is considerable scatter in the fatigue life of the peened beams. This range in cyclic life extends from Category E design life (134,000 cycles) to Category C design life (550,000 cycles). The wide cover plate beams generally exhibit the lowest fatigue life. This might be attributed to the fact that the wide cover plate beams

initiated longer detectable cracks than the narrow cover plate beams. The data in Fig. 7.3 suggests that peening existing cracks can improve the fatigue life of the cover plate detail to a Category D level for the NR and NF beam types. Only Category E life was achieved for the WR beam type. These category levels represent the approximate lower bound for the number of loading cycles that can be applied after peening repair and are exclusive of the cycles applied prior to cracking.

Specimen WR5 is of particular importance. The total initial crack length on the south end was 3/4-in (one crack 1/2-in long and another 1/4-in long). Upon resuming the cyclic loading after the cracks were peened, the beam barely passed the Category E design life. The test results suggest that peening is not very effective for cracks longer than about 1/4-in to 3/8-in.

The crack depth, which is related to crack length, is the critical factor that controls the effectiveness of peening. If the crack is deeper than the compressive residual stress zone induced during peening, then the procedure in not effective in delaying further crack propagation. Hausammann, Fisher, and Yen (1983) found that cracks deeper than about 0.1-in could not be successfully peened. Assuming a crack length to depth ratio of about 4, the maximum crack length that could be successfully peened is about 0.4-in. This crack length agrees with the test results in the present study.

The three beams which were peened prior to pre-cracking were subjected to 75,000 loading cycles at 20.0-ksi stress range on the bare beam at the end of the cover plate. The beams were checked to make sure no cracks were present, then peening was applied to the cover plate ends. The pre-cycling of these three beams was conducted to simulate the loading history of bridge girders that had sustained a significant number of loading cycles but had not yet initiated fatigue cracks. The 75,000 cycles was intentionally chosen lower than the lowest number of cycles to first crack detection (120,000 cycles) to make sure that no cracks had initiated at the end of the pre-cycling.

Figure 7.4 shows the stress range versus the number of cycles applied after repair for the three non-cracked beams. The test results of the two NR beams suggest that peening of non-cracked beams can improve the fatigue life of the detail to a Category B' level. Peening was applied along the weld toe only, and will not influence cracks that emanate from internal weld flaws. In both beams, the fatigue crack propagated through the weld, cutting the weld return into two parts; unless otherwise mentioned, all the previous cracks initiated at and propagated from the weld toe.

Specimen NN3 test results reached the fatigue design life of Category D only. The no end-weld detail is significantly different than the return and full end-weld details. The welds in the latter details are fully accessible to treatment by peening, while the weld end in the no end-weld detail is very difficult to peen in those regions adjacent to the tapered cover plate. Also, cracks in the no-end weld detail can propagate under the cover plate which is an inaccessible area for peening. Thus, peening is expected to be less effective in the case of the no end-weld detail.

Figure 7.5 shows the number of applied cycles (to failure) after repair for the eight beams tested. It can be seen that the NR beams peened prior to cracking have a much greater fatigue life (the four details for the two beams exceeded Category B') than the corresponding NR beams peened after cracking. The NN beam peened prior to cracking demonstrated that peening only marginally improved the fatigue life of that detail to a Category D level. The NR and NF beams peened after pre-cracking suggest that peening also improved the fatigue life of the detail, such that the beam was able to sustain an additional number of loading cycles equivalent to a Category D design life. Peening was not very effective in improving the fatigue life of the WR type beams, since additional loading cycles could be applied after repair to a Category E level only. It must be noted, however, that these beams had long fatigue cracks at the weld toe, and long cracks generally have corresponding crack depths that do not respond well to repair by peening.

7.4. Comparison with Other Tests

Fisher, Sullivan, and Pense (1974) tested sixty W 14 × 30 steel beams with welded square ended cover plates. The beams, fabricated from ASTM A36 steel, were tested under constant amplitude cyclic loading. Three repair procedures were investigated: (1) grinding the weld toe to reduce the geometrical stress concentration, (2) air-hammer peening the weld toe to introduce compressive residual stresses, and (3) remelting the weld toe using a gas tungsten arc process. Different values of minimum stress and stress range were used during the tests. The repair methods were applied to the test beams for three basic conditions: (1) as-welded beams, (2) pre-cycled beams until 75% of the lower confidence limit of the as-welded detail was reached, and (3) pre-cycled beams until the detection of visible cracks. These three conditions are denoted PA, PL, and PV for the peening repair procedure, respectively. The results of the 24 peening beams tested by Fisher, et al. (1974) are shown in Fig. 7.6, along with the results of eight peened beams from the present study.

Fisher, et al. (1974) found that the minimum stress has a large influence on the fatigue life of peened specimens. Two minimum stress values were investigated: 2.0-ksi and 10.0-ksi. The ratio between the average number of loading cycles after peening of specimens tested under 2.0-ksi minimum stress to specimens tested under 10.0-ksi minimum stress was about 2.8 for the PA specimens tested at a 18.6-ksi stress range. This ratio was about 22.5 and 19.1 for the PL specimens tested under 12.0-ksi and 18.6-ksi stress range, respectively. As results of PA and PL specimens suggested the importance of minimum stress level, some of the PV specimens were peened while loaded with the minimum stress value (applied during the test). The ratio between the average number of loading cycles, applied after peening, of specimens tested at a 2.0-ksi minimum stress to specimens tested at a 10.0-ksi minimum stress was about 0.8 for the PV specimens tested at a 18.6-ksi stress range for beams peened while loaded with the minimum stress value. On the other hand, the ratio between the average number of loading cycles of PV specimens peened under minimum stress to specimens peened under no stress was about 28.8 for beams tested at a 18.6-ksi stress range and a 10.0-ksi minimum stress.

An R-ratio of 0.05 was used for all tests conducted in the present study. Using a linear regression analysis of the data by Fisher et al. (1974), the average fatigue life for the PA, PL, and PV specimens tested at a 20-ksi stress range was found to be about 353,700 cycles, 216,300 cycles, and 211,000 cycles, respectively. The average fatigue life from the present study, however, was about 352,000 cycles for specimens peened after the detection of visible cracks, and 1,369,000 cycles for specimens peened after 75,000 cycles of loading but with no initial cracks. The results of the present study do not agree well with the results obtained by fisher et al. (1974).

7.5. Conclusions of Test results

Eight W14 × 30 steel beams were tested to examine the fatigue resistance of beams with welded partial-length, tapered cover plates which have been repaired using air-hammer peening procedure. Based upon the experimental test results and corresponding observations, the following general conclusions can be stated:

1- Peening is somewhat effective for repairing pre-cracked narrow cover plated beams if the crack length is smaller than about 1/4-in to 3/8-in. In that case, peening can extend the fatigue life of the detail such that an additional number of loading cycles roughly equivalent to a Category D level can be applied prior to failure.

2- Peening was found to be very effective method in increasing the fatigue life of non-cracked cover plate ends for the return end-weld detail. Tests demonstrated that peening improves the fatigue strength of the detail to the Category B' level. Similar results would be expected for the full end weld cover plate detail, although no tests were conducted with this detail condition.

3- Peening is not recommended for the no end-weld detail. Cracks may grow under the cover plate in the unaccessible region. In that case, only small improvement on the fatigue life can be expected.

4- Peening induces surface deformations in the work area, and cracks may initiate from these indentations. Thus, careful examination of the work area should be conducted after the peening procedure. If any cracks are found, peening should be continued until these cracks are no longer visible.

5- Wide cover plate details were found to initiate larger detectable cracks, at fewer number of load applications, than the narrow cover plate weld details. Unless the cracks detected prior to repair are small (less than 1/4-in to 3/8-in long), then peening is not recommended.

Table 7.1. Number of Loading Cycles Applied to Test Beams.

Specimen	End	Number of Loading Cycles for Flange Fracture	Comments
NR9	N	265,000	1-in thick plates were used.
	S	401,000	
NR10	N	506,000	
	S	436,000	1-in thick plates were used.
NF4	N	590,000	
	S	369,000	1-in thick plates were used.
WR4	N	300,000	
	S	216,000	1-in thick plates were used.
WR5	N	223,000	
	S	160,000	1-in thick plates were used.
NR5[1]	N	1,511,000	
	S	1,186,000	1-in thick plates were used.
NR6[1]	N	1,006,000	1-in thick plates were used.
	S	1,733,000	
NN3[1]	N	308,000	1-in thick plates were used.
	S	413,000	

[1] Specimen Peened after 75,000 of loading cycles, but prior to cracking.

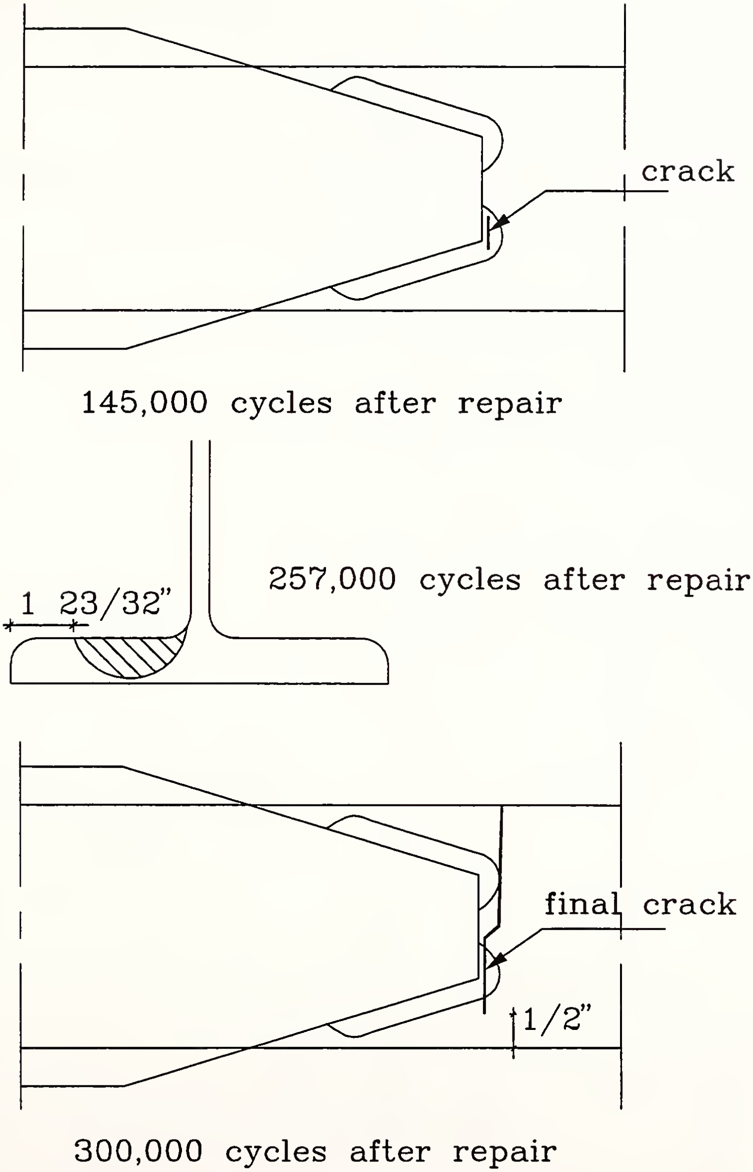

Fig. 7.1. Crack Location – Specimen WR4.
(North End)

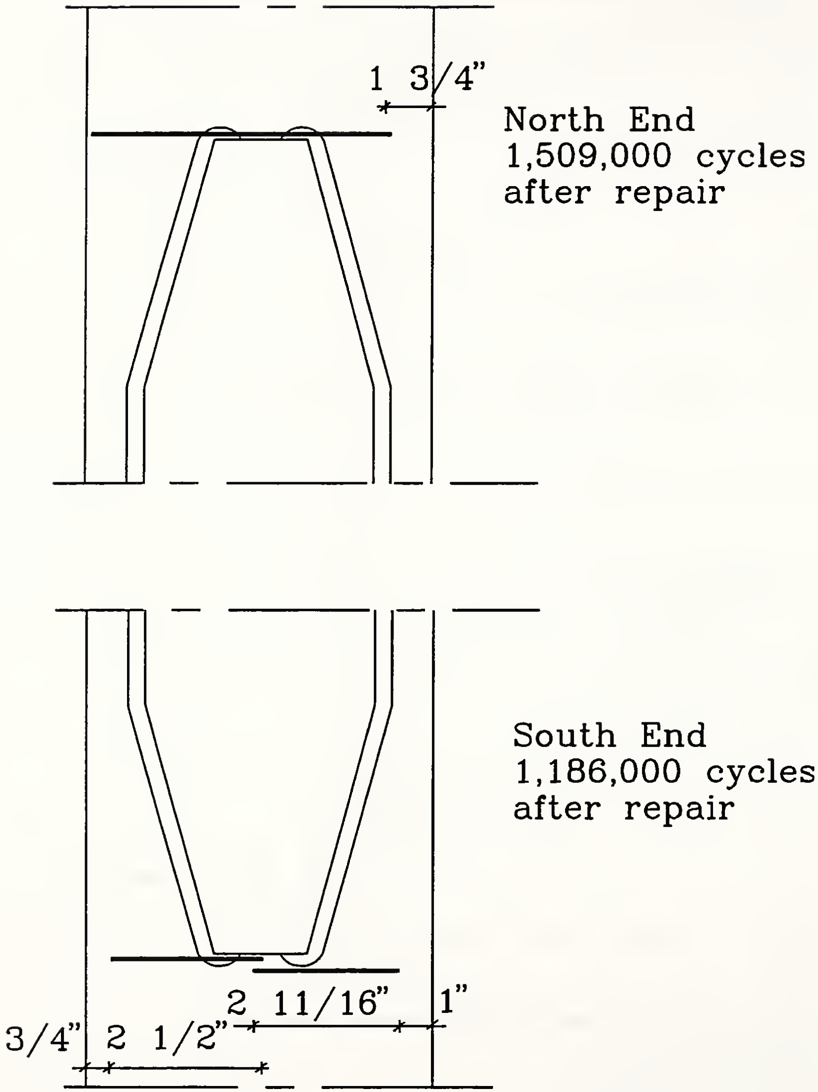

Fig. 7.2. Crack Shape – Specimen NR5.
(End of Test)

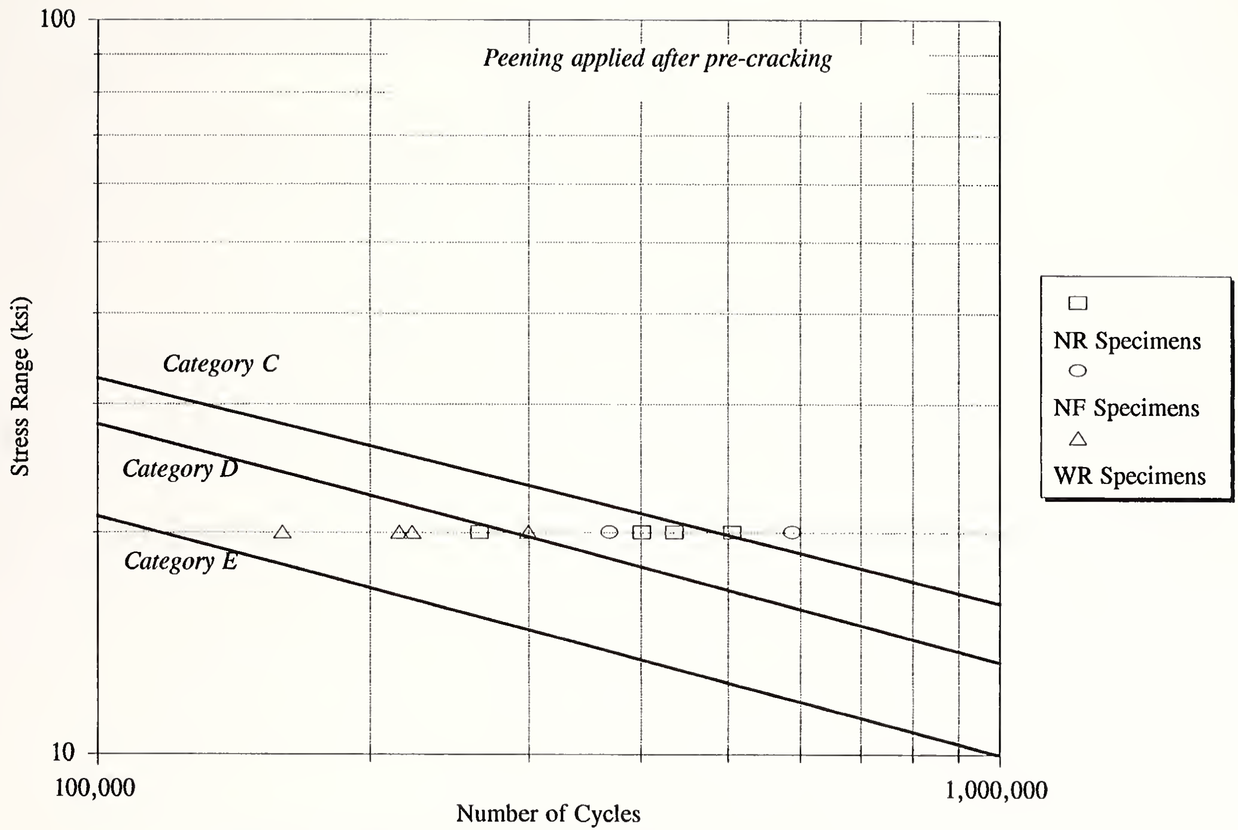

Fig. 7.3. Stress Range versus Number of Loading Cycles after Repair.

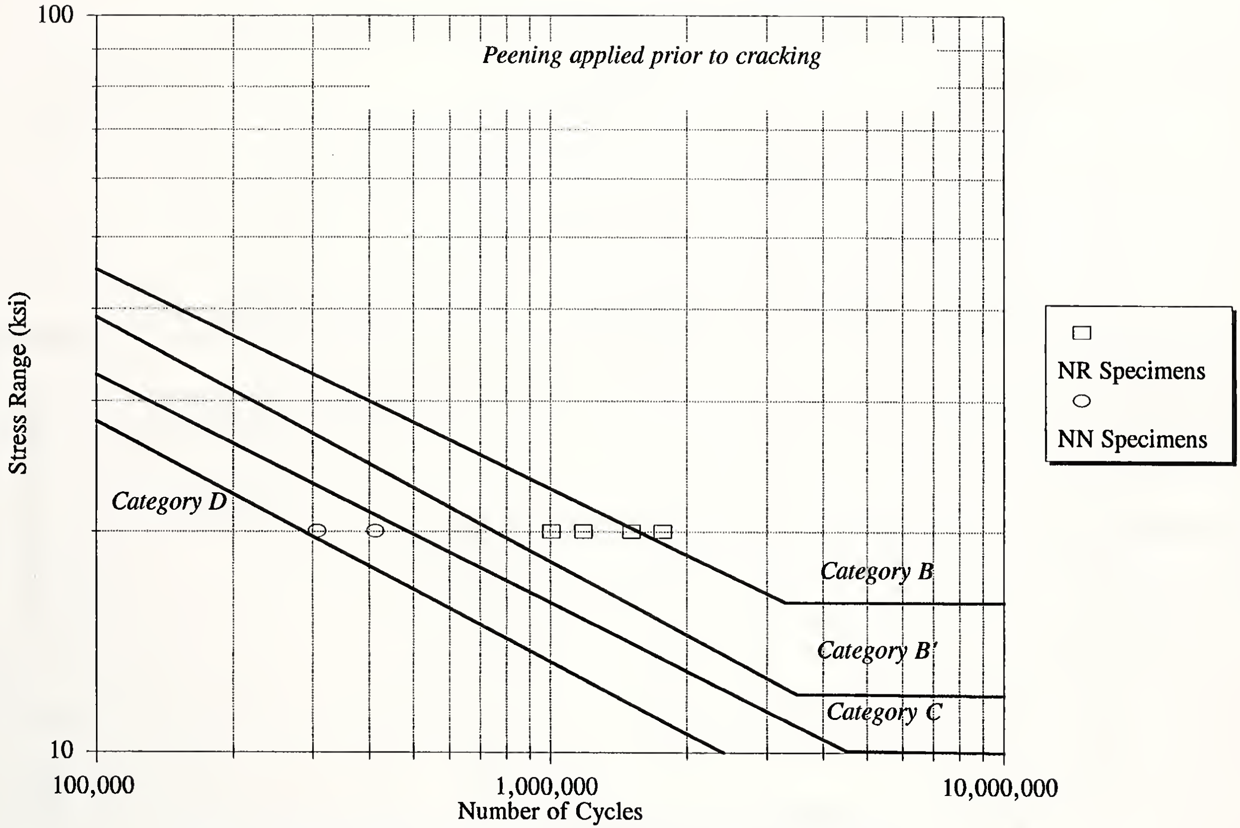

Fig. 7.4. Stress Range versus Number of Loading Cycles after Repair.

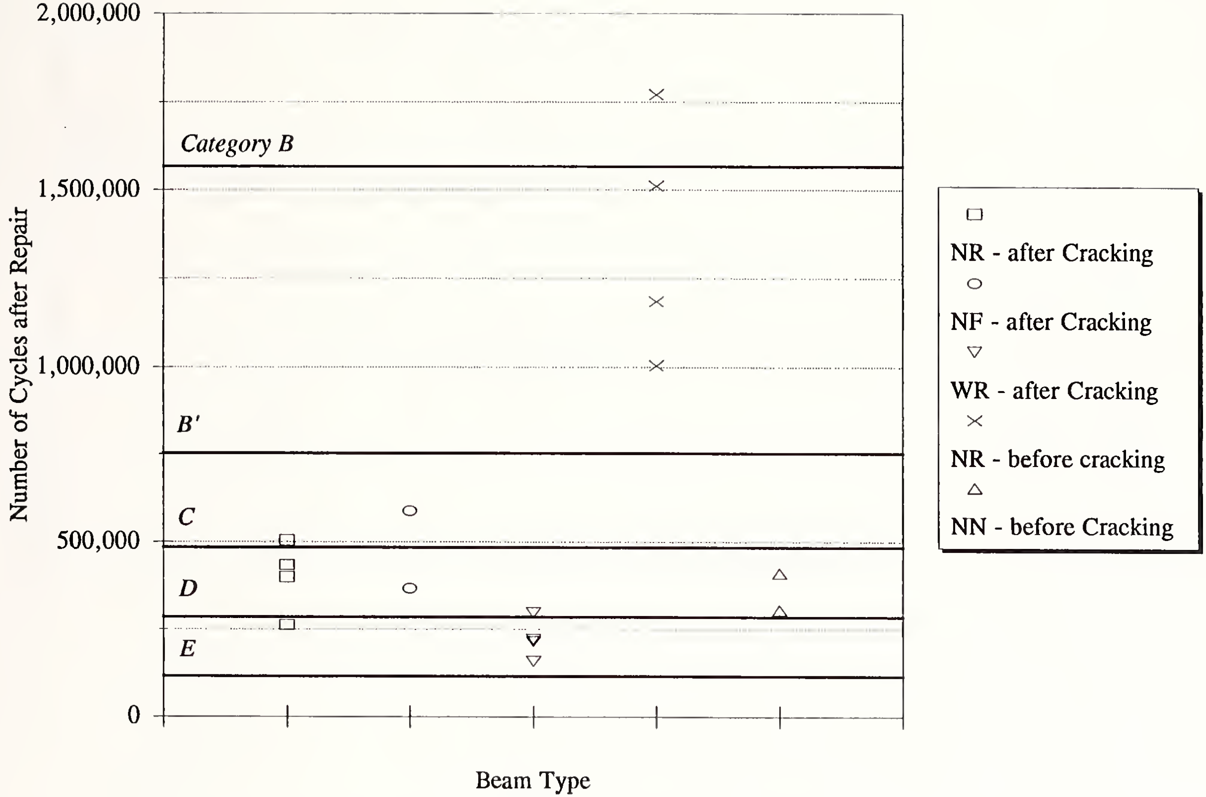

Fig. 7.5. Number of Loading Cycles Applied after Repair for 20.0-ksi Stress Range.

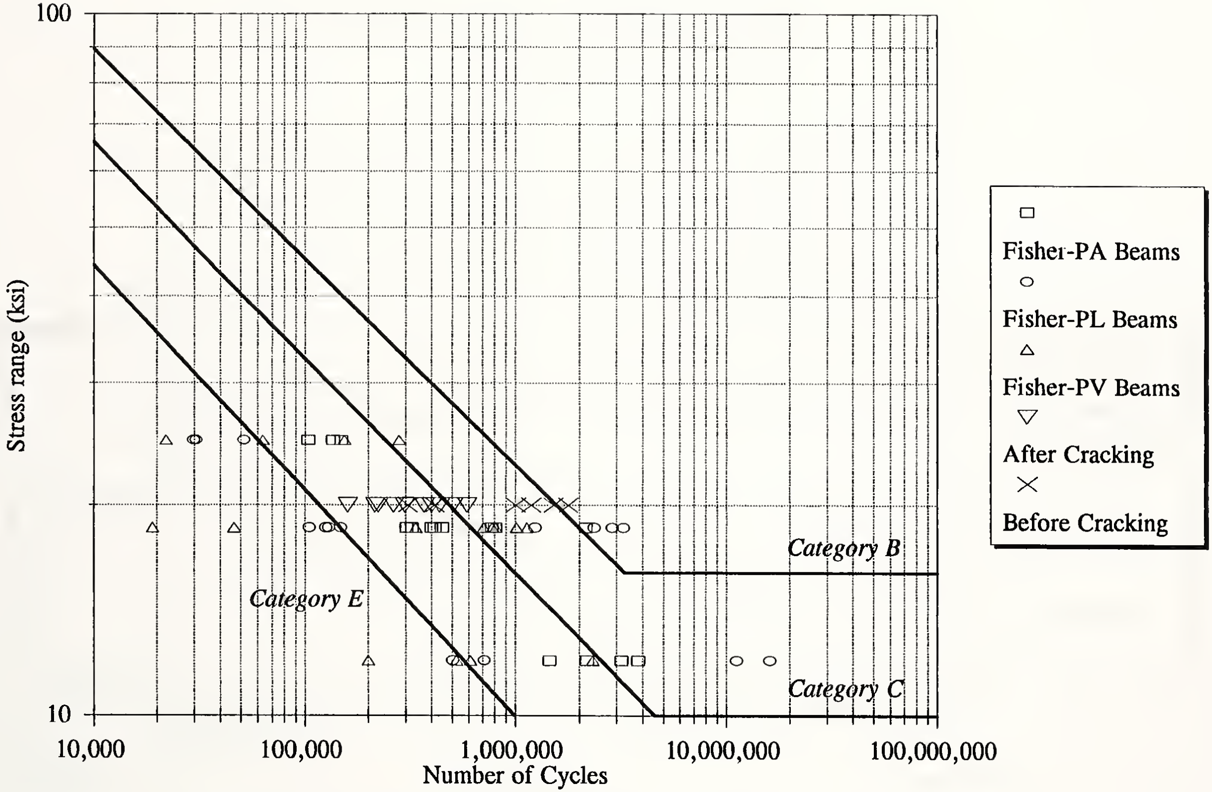

Fig. 7.6. Comparison with Test Results of Fisher et al. (1974).

CHAPTER 8
PARTIAL BOLTED SPLICE REPAIR

8.1. General Comments

The partial bolted splice repair is a combination of the bolted splice and peening repair methods. The partial bolted splice repair involves the use of a bolted splice plate connection above the flange (bottom splice plate omitted) and peening of the cover plate end welds. In this case, a portion of the flange force is diverted away from the cover plate end weld through the splice plates. The amount of force transmitted through the splice plates is smaller than in the case of a regular bolted splice plate connection due to the omission of the bottom splice plate. Thus, the stress at the cover plate end is larger than the stress in a regular bolted splice connection.

The partial bolted splice connection has two advantages over the regular bolted connection. First, if clearance is a problem under a bridge girder then the use of a partial bolted splice plate connection would use less space beneath the girder. Second, the cover plate end weld area is accessible in the case of a partial bolted splice connection. Also, any further crack propagation can be monitored.

In the present study, six beams were repaired using the partial bolted splice method. All six beams were first pre-cracked under 20.0-ksi stress range before repair. The repair consisted of two plates 2 1/2-in × 21 1/2-in × 7/16-in thick connected to the upper fibers of the tension flange, with the web between the two plates. The cover plate end welds were also peened with 6 passes at 40.0-psi pressure. The bolt pattern for the partial bolted splice was the same as for the regular bolted splice plate detail.

After repair, five beams were tested under a 20.0-ksi stress range (same as pre-cracking load), while the remaining specimen was tested under a 15.0-ksi stress range. Loading was applied to all specimens until fracture of the flange occurred. Moreover, although the flanges fractured, the tests were usually continued until a specific number of cycles was attained or until the cracks had propagated through most of the web. In order to achieve this, holes were drilled at the web crack tip.

The following sections summarize pertinent comments recorded during the tests for each specimen. Then, the results of the partial bolted splice repair are presented and compared with other test results obtained from the literature. Finally, conclusions from the test results of the

bolted splice repair are presented. Table 8.1 shows the number of loading cycles applied after repair until fracture of the flange, along with the total number of cycles applied after repair. A detailed summary of the measured crack sizes and number of loading cycles sustained for each specimen is given in Appendix D.

8.2. Comments for Test Beams

8.2.1. Specimen NR11

After pre-cracking, the tension flange at both cover plate ends was repaired using the standard repair procedure. At 1,410,000 cycles after repair, the south end crack was 4 19/32-in long and had propagated about 1 1/16-in into the web. At 1,460,000 cycles, the southeast side of the flange fractured, and at 1,480,000 cycles after repair, the south end of the tension flange completely fractured, and the crack propagated about 2 3/4-in into the web. A 15/16-in hole was drilled at the end of the crack tip, a bolt was placed in the hole, and the test was resumed. At 1,660,000 cycles, the south end crack was found to have propagated from the hole to about 6 1/4-in into the web. A second hole was then drilled at the end of the crack tip, a bolt was placed in the hole, and the test was resumed. At 1,851,000 cycles, the south end crack propagated through the second hole to about 7 5/8-in into the web - see Fig. 8.1. A third hole was then drilled at the crack tip, a bolt was placed in the hole, and the test was resumed.

At 1,898,000 cycles after repair, the crack was found to have propagated from the third hole to about 8-in into the web. The splice plates were then removed, and the temporary 1-in thick splice plate connection was clamped to the south end of the tension flange. The south end of the beam collapsed immediately after the test was resumed - see Fig. 8.1. Slippage occurred between the beam and the 1-in splice plates. The test was then stopped and the north end splice plates were removed to measure the crack length. Two cracks 19/32-in and 1 7/16-in long were found at the northwest, and the northeast sides of the flange, respectively. The north end tension flange was removed and fractured using the liquid nitrogen procedure described earlier. Two cracks 5/8-in and 1 1/2-in long were found at the northwest and northeast sides of the flange, respectively. The northwest crack was 1/8-in deep, while the northeast crack was 3/8-in deep (through the full flange thickness).

8.2.2. Specimen NR12

After pre-cracking, the beam was repaired using the standard repair procedure. In order to assess the behavior of the beam and to compare the test results with the behavior computed using elastic analysis, ten strain gages were placed on the beam, five at each cover plate end. The location of these gages is shown in Fig. 8.2. Two strain gages were attached to the lower fibers of the tension flange near the end of the cover plate weld. Two strain gages were attached to each of the four splice plates, one gage at the mid-length of the splice plate, and the other at a section passing through the expected crack initiation location. The cyclic loading was interrupted and a static loading cycle, equivalent to the cyclic loading (1.34-kips minimum to 26.8-kips maximum), was applied to collect the strain measurements. Strain gage measurements were taken at the minimum load, maximum load, and at multiples of 5-kips between the minimum and maximum load.

The maximum strain in the flange and splice plates are shown in Figs. 8.3 and 8.4 for the south and north ends, respectively. The strain gage measurements show a drop of the flange strain and an increase in the splice plates strain with the number of loading cycles. Figure 8.3 indicates a maximum stress of about 19.7-ksi and 8.1-ksi in the south end flange and the splice plates, respectively. On the other hand, the maximum stress in the north end flange and splice plates are about 20.3-ksi, and 7.3-ksi, respectively - see Fig. 8.4. These stress values are estimated from the strain measurements obtained just after the repair was completed, and using a modulus of elasticity of 29,000-ksi. Based upon simple elastic beam theory, and assuming that the flange is fully effective, the maximum stress at the bottom fibers of the tension flange and at the top fibers of the splice plates were calculated to be 14.1-ksi and 12.04-ksi, respectively. Strain gage measurements indicate that the splice plates were not attracting as much stress as assumed by the elastic beam theory. Splice plate flexibility and the lack of full connectivity between the splice plate and the beam are the probable causes of the difference in computed and measured strain values.

At 927,000 cycles after repair, the southwest crack propagated to about 1 3/8-in in length. At 1,045,000 cycles, the south end crack was observed to have a larger opening while no increase in length could be measured. At 1,185,000 cycles, the south end crack was 5-in long and had propagated about 1 1/4-in into the web. Strain measurements indicate a large drop in the strain values measured at mid-width of the flange, and an increase in the strain values in the splice

plates - see Fig. 8.3. Obviously, as the crack was getting larger the load carried by the flange was getting smaller, causing an increase in the load carried by the splice plates. At 1,234,000 cycles, the south flange completely fractured and the crack propagated about 3 1/4-in into the web. The calculated stress at the top fibers of the splice plate, using elastic beam theory and assuming that the bottom flange did not participate, was about 22.0-ksi. Fig. 8.3 shows that the stress at the upper fibers of the splice plates were about 20.9-ksi and 22.6-ksi for the west and east splice plates, respectively.

A 15/16-in hole was drilled at the crack tip, a 7/8-in diameter bolt was placed in the hole, and the test was resumed. At 1,430,000 cycles after repair, the south end crack propagated through the hole to about 6-in into the web. A second hole was then drilled at the crack tip, a bolt was placed in the hole, and the test was resumed. At 1,736,000 cycles, the south end crack propagated through the second hole. At 1,800,000 cycles after repair, the test was stopped. At the end of the test, the south end crack was about 7-in into the web. An increase in the measured strain values after the fracture of the tension flange was observed - see Fig. 8.3. After the flange had fractured, all the stresses were transferred through the splice plates alone. The flange stresses were transferred to the splice plates through friction between the upper fibers of the tension flange and the lower fibers of the splice plates. This friction may have influenced the strain gage located about 1/2-in from the crack location.

The north end of the beam exhibited a behavior similar to the south end. Fig. 8.4 shows the strain measurements with the number of loading cycles. At 1,185,000 cycles after repair, the north end cracks coalesced into a single crack 1 5/8-in long. Strain gage measurements, shown in Fig. 8.4, indicate a large drop in the strain at mid-width of the lower fibers of the tension flange (similar to the south end behavior). At 1,234,000 cycles, the crack propagated to about 3 9/16-in long. At 1,255,000 cycles, the crack was 3 15/16-in long and had propagated about 2 7/32-in into the web. At 1,347,000 cycles, the north flange completely fractured and the crack propagated about 4-in into the web. The strain gage measurements indicate a maximum stress of about 20.9-ksi and 21.7-ksi at the upper fibers of the west and east splice plates respectively. The calculated maximum stress at the upper fibers of the splice plates, assuming the flange is completely fractured, was about 22.0-ksi.

A 15/16-in hole was drilled in the web at the crack tip, a 7/8-in diameter bolt was placed in the hole, and the test was resumed. At 1,610,000 cycles after repair, the crack propagated

through the hole to about 6-in into the web. A second hole was drilled at the crack tip, a bolt was placed in the hole, and the test was resumed. At 1,800,000 cycles, the test was stopped.

Figures 8.3 and 8.4 demonstrate an increase in the splice plate strains even after fracture of the flange. The increase in the splice plate strains might be attributed to the fact that after the flange fractures, the cracks continue growing into the web. Hence, the stiffness of the beam is decreasing, and the strains (or stresses) in the splice plate are increasing. It should be noted that the flange strain gage and the splice plate gages are not in the same plane.

8.2.3. Specimen WR6

After pre-cracking, the beam was repaired using the partial bolted splice method and the test was resumed. At 1,157,000 cycles after repair, the south end crack propagated to about 3 7/16-in in length, severed the west side return weld, and propagated about 3/4-in into the web. At 1,326,000 cycles after repair, the north compression flange fractured. The crack passed through the northwest weld return and propagated about 3 1/4-in into the web. The 1-in thick temporary repair plates were clamped to the north compression flange, and a 15/16-in hole was drilled in the web at the crack tip. Using elastic beam theory, the maximum stress at the bottom fibers of the tension flange drops from about 14.1-ksi to about 11.8-ksi due to the use of the 1-in plates.

Also at 1,326,000 cycles, the south flange fractured and the crack had propagated about 5 1/4-in into the web. A 15/16-in hole was drilled at the crack tip, a 7/8-in bolt was placed in the hole, and the test was resumed. At 1,494,000 cycles after repair, the south end crack propagated through the hole to about 7 3/16-in into the web. A second hole was drilled at the crack tip, a bolt was placed in the hole, and the test was resumed. At 2,100,000 cycles, the south end crack had propagated through the second hole, and at 2,200,000 cycles, the crack was about 8-in into the web. The test was then stopped.

The north flange was flame cut and fractured using the liquid nitrogen procedure described earlier. Two cracks 1-in and 31/32-in long were found at the northwest and northeast sides of the flange, respectively. Both cracks were 3/8-in deep (through the full flange thickness).

8.2.4. Specimen WR7

After pre-cracking, the beam was repaired using the previously discussed procedure. In order to assess the actual behavior of the beam and to compare the test results with the behavior computed using elastic analysis, ten strain gages were attached to the beam. The location of these gages is similar to the gages for Specimen NR12 - see Fig. 8.2. All strain measurements were taken using a static load cycle. The maximum strain in the flange and splice plates are shown in Figs. 8.5 and 8.6 for the south and north ends, respectively. As expected, the strain gage measurements show a drop of the flange strain and an increase in the splice plates strain with the number of loading cycles. Figure 8.5 indicates a maximum stress of about 20.0-ksi and 6.4-ksi in the south end beam flange and the splice plates, respectively. On the other hand, the maximum stress in the north end flange and splice plates are about 20.0-ksi, and 7.8-ksi, respectively - see Fig. 8.6. These stress values are estimated from the strain measurements, obtained just after the repair was completed, using a modulus of elasticity of 29,000-ksi. From simple elastic beam theory, and assuming that the flange is fully effective, the maximum stress at the bottom fibers of the tension flange and at the top fibers of the splice plates were calculated to be 14.1-ksi and 12.04-ksi, respectively. Strain gage measurements indicate that the splice plates were not attracting as much stress as assumed by the elastic beam theory. Again, this is probably attributed to the flexibility and lack of connectivity of the splice plate.

At 479,000 cycles after repair, the south end cracks coalesced to form a 4 3/8-in long crack. At 604,000 cycles, the south end crack fractured while the crack propagated about 4 5/8-in into the web. Strain measurements, shown in Fig. 8.5, indicate a large drop in the strain values measured at mid-width of the flange, and an increase in the splice plate strain values. The same behavior was observed for specimen NR12. As the crack was getting larger the stresses were getting smaller at mid-width of the flange (location of the crack) and larger in the splice plates. The calculated stress at the top fibers of the splice plate (using elastic beam theory) was about 22.0-ksi. Fig. 8.5 indicates that the maximum stress at the top fibers of the splice plates was about 21.46-ksi.

A 15/16-in hole was drilled in the web at the crack tip, a 7/8-in diameter bolt was placed in the hole, and the test was resumed. At the same time (604,000 cycles after repair), the north end cracks coalesced and formed a 3 31/32-in long crack that propagated about 1 1/8-in into the web. At 631,000 cycles, the north end flange completely fractured and the crack propagated about

1 1/2-in into the web. At 686,000 cycles, the north end crack propagated about 4 1/8-in into the web. A 15/16-in hole was drilled, a 7/8-in diameter bolt was placed in the hole, and the test was resumed. At 847,000 cycles after repair, the south end crack propagated through the first hole to about 7 5/8-in into the web. A second hole was drilled, a bolt was placed in the hole, and the test was resumed. At that time the maximum stresses at the upper fibers of the north end splice plates were about 21.5-ksi and 23.8-ksi for the west and east splice plates, respectively - see Fig. 8.6. At 1,313,000 cycles, the north and south end cracks propagated through the holes to about 7-in and 8-in into the web, respectively. The test was then stopped.

As for Specimen NR12, Figures 8.5 and 8.6 show that the splice plate strains increase even after fracture of the flange. The increase in the splice plate strains is likely attributed to the fact that after the flange fractures, the cracks continue growing into the web.

8.2.5. Specimen NF5

After pre-cracking, the beam was repaired using the partial bolted splice method. At 800,000 cycles after repair, the south end fractured while the crack propagated about 3 1/4-in into the web. A 15/16-in hole was drilled in the web at the crack tip, a 7/8-in bolt was placed in the hole, and the test was resumed. At 955,000 cycles, the south end crack propagated through the hole to about 5 15/32-in into the web. At the same time, the north end crack was 3 1/2-in long and propagated about 1/2-in into the web.

At 1,111,000 cycles after repair, the south end crack propagated through the second hole to about 6 3/4-in into the web. The crack tip was still close to the second hole, thus a third hole was not drilled at that time. At the same time, the north end flange fractured and the crack propagated about 4 3/16-in into the web. A hole was drilled in the web, a bolt was placed in the hole, and the test was resumed. At 1,152,000 cycles, the south end crack had propagated 7 1/4-in into the web. The test was then stopped.

8.2.6. Specimen NR7

After pre-cracking, the beam was repaired using the partial bolted splice repair method. Then the test was resumed with a loading cycle that would produce a 15.0-ksi stress range at the flange extreme fibers of the bare beam section.

At 5,446,000 cycles after repair, a 3.0-in long crack was observed at the southwest compression flange weld. The crack severed the return end weld (weld root crack) and propagated about 1/2-in into the web. In an attempt to repair the compression flange without altering the stress in the tension flange, the south compression flange at the cover plate end was prepared for a repair weld. The total flange thickness was removed to form a V-shape opening. Then, the flange was joined using stick welding, and the weld surface was ground smooth with the flange surface to eliminate any stress concentration spots. The cover plate end weld was then peened from the top and the bottom of the flange for 3 complete passes at 40.0-psi pressure.

At 5,750,000 cycles, the south compression flange fractured again at the same position. The crack extended about 7/8-in into the web. It was postulated that the grinding process did not completely remove the crack from the flange. A rectangular hole (about 1-in × 2-in) was cut in the web to eliminate the web crack, then the hole was ground to eliminate any notches. The flange at the cover plate end was ground with an opening of about 1/8-in and 1/2-in at the bottom and top fibers of the flange, respectively. The crack was completely eliminated by the grinding process. In order to join the flange by welding, aluminum backing plates were connected to the flange. The flange was then welded with 8 passes of stick welding using 1/8-in diameter E7018 electrodes. After each welding pass, the weld slag was removed, the weld surface cleaned with a wire brush, and the weld surface peened with 3 passes at 40.0-psi pressure. The weld was then ground smooth with the flange surface to eliminate any stress concentration spots. Figure 8.7 shows the flange surface after welding and after grinding. The beam was then turned over and the inner fibers of the flange were ground. An additional weld pass was needed to completely join the flange at the lower fibers.

The beam was turned over and the test resumed. At 6,540,000 cycles, the south compression flange fractured again. Two cracks 2 1/8-in and 3 1/4-in long were observed at the cover plate end and at 3/4-in away from the cover plate end, respectively. The second crack was at a section passing through the web hole edge. While the first crack was at the middle of the web hole, passing through a notch in the hole.

A 5/16-in bolted splice plate connection was used for the south compression flange, and the test was resumed. At 7,934,000 cycles, a 1 3/32-in long crack propagated from the web hole edge into the web. A 15/16-in diameter hole was drilled at the crack tip, a 7/8-in diameter bolt was placed in the hole, and the test was resumed.

At 8,340,000 cycles, a 5 5/8-in long crack was observed at the north compression flange. The crack severed both the northwest and northeast return end welds (root crack); only 1 1/8-in remained non-fractured at the northeast side of the flange. The test was then stopped, and the tension flanges at both the north and south ends were flame cut and fractured using the liquid nitrogen procedure. Four cracks 1/2-in, 45/64-in, 31/32-in, and 29/64-in long were found at the northwest, northeast, southwest, and southeast sides, respectively. The crack depths were 7/64-in, 3/32-in, 5/32-in, and 5/64-in for the northwest, northeast, southwest, and southeast sides, respectively.

8.3. Discussion of Results

All six beams tested were first pre-cracked and then repaired using the procedure described previously. These six beams included three NR beams, one NF beam, and two WR beams. Five out of the six beams were subjected to a constant-amplitude loading that would produce a 20.0-ksi stress range in the bare beam section adjacent to the end of the cover plate after repair. The remaining beam was subjected to a 15.0-ksi stress range after repair.

Figure 8.8 shows the stress range versus the number of loading cycles, to the fracture of the flange, applied after repair for the six beams. It can be seen that there is considerable scatter in the fatigue life of the WR beams repaired with the partial bolted splice technique. This range in cyclic life extends from Category C design life (550,000 cycles) to higher than Category B design life (1,500,000 cycles). The narrow cover plate beams had a fatigue life larger than the Category B' design life. It should be noted that although the flange may have fractured, the detail was still capable of sustaining some additional loading cycles (Specimen WR6 sustained 874,000 cycles after the flange fractured). The cracks, however, kept on growing with a relatively high rate - higher than for the bolted splice plates investigated during the first phase of the study. Also, it should be noted that intentional efforts were made to slow crack growth in the beam web by drilling a hole through the web to eliminate the crack tip. In some cases, an additional hole was required when the crack propagated beyond the first web hole.

Specimen NF5 is of particular importance. The total initial crack length on the south end was 1 3/4-in (two cracks 1/2-in long and another 3/4-in long). The beam attained the Category C design life. Obviously, the larger the initial crack, the lower the fatigue life of the detail.

Figure 8.9 shows the total number of loading cycles applied after repair for the five beams tested under 20.0-ksi stress range. It can be seen that the NF beam had the lowest fatigue life (Specimen NF5 had a relatively large initial crack size). The figure also shows a relatively large scatter for the WR beams compared with other beam types. It should be noted that most of the beam flanges fractured at a number of cycles lower than the total number of applied cycles - see Table 8.1.

The number of loading cycles applied until flange fracture is shown in Fig. 8.10. It can be seen that the WR-type beams reached the Category C design life, while the NR-type and NF-type beams surpassed the Category B' design life of the AASHTO specifications. The partial bolted splice plate is, thus, an effective repair method.

8.4. Comparison with Other Test Results

No test results were found in the literature for the partial bolted splice repair method. Comparison between the partial bolted splice and the regular bolted splice results obtained during the present study is shown in Fig. 8.11. The number of cycles shown in Fig. 8.11 correspond to the number of cycles until flange fracture. Specimens which encountered a compression flange fracture are denoted with a plus (+) sign beside their results. It should be noted that in the case of a compression flange fracture, the fatigue life reported in Fig. 8.11 correspond to the number of cycles to compression flange repair (stress in tension flange altered).

Fig. 8.11 indicates that the partial bolted splice results are lower than the bolted splice results. However, the difference in fatigue life of the partial bolted splice and the 5/16-in bolted splice connection is small. However, after flange fracture, cracks were observed to grow much faster in the case of a partial bolted splice connection than in the case of a regular bolted splice connection. The regular bolted splice plate connection is stiffer than the partial bolted splice connection. Thus, the bolted splice plate connection can sustain more loading cycles with smaller web crack propagation than the partial bolted splice.

8.5. Conclusions of Test Results

Six W14 × 30 steel beams were tested to examine the fatigue resistance of beams with welded partial-length, tapered cover plates which have been repaired with the partial bolted splice repair method. Based upon the experimental test results and corresponding observations, the following general conclusions can be stated:

1- The partial bolted splice plate repair procedure is an effective method of repairing pre-cracked cover plated beams. The installation of a partial bolted splice after first crack detection can significantly improve the fatigue strength of the detail.It was found that an additional number of loading cycles equivalent to a Category C design life of the AASHTO Specifications could be applied after repair.

2- The partial bolted splice repair did not prevent subsequent crack growth.

3- The initial crack size is a very important factor in determining the remaining life of the specimen and plays a significant role in controlling when complete fracture of the flange occurs. The average size of the cracks at first crack detection was about 5/16-in.

4- Even if the flange fractures, the partial bolted splice plate detail is able to sustain a number of loading cycles after the flange fractures. In one case, the beam carried 874,000 loading cycles of 20.0-ksi stress range after fracture of the flange.

5- The fatigue strength of steel beams (with tapered cover plates), which were repaired with the partial bolted splice repair technique was found to be lower than the fatigue strength of beams (with square ended cover plates) repaired with a slip-critical connection that utilizes splice plates on both sides of the flange.

Table 8.1. Number of Loading Cycles Applied to Test Beams.

Specimen	End	Number of Cycles for Flange Fracture	Total Number of Cycles Applied	Comments
NR11	N	---	1,898,000	Flange did not fracture.
	S	1,480,000	1,898,000	Two holes drilled in web at crack tip.
NR12	N	1,347,000	1,800,000	Two holes drilled in web at crack tip.
	S	1,234,000	1,800,000	Two holes drilled in web at crack tip.
WR6	N	1,326,000	2,200,000	Compression flange fractured.
	S	1,326,000	2,200,000	Two holes drilled in web at crack tip.
WR7	N	631,000	1,313,000	Two holes drilled in web at crack tip.
	S	604,000	1,313,000	Two holes drilled in web at crack tip.
NF5	N	1,111,000	1,152,000	Hole drilled in web at crack tip.
	S	800,000	1,152,000	Two holes drilled at web crack tip
NR7[1]	N	8,340,000	8,340,000	Compression flange fractured.
	S	6,540,000	8,340,000	Compression flange fractured.

[1] Specimen subjected to 15.0-ksi stress range.

(a) 1,851,000 Cycles After Repair

(b) After Beam Collapse - 1,898,000 Cycles

Fig. 8.1. Crack Location - Specimen NR11 South End.

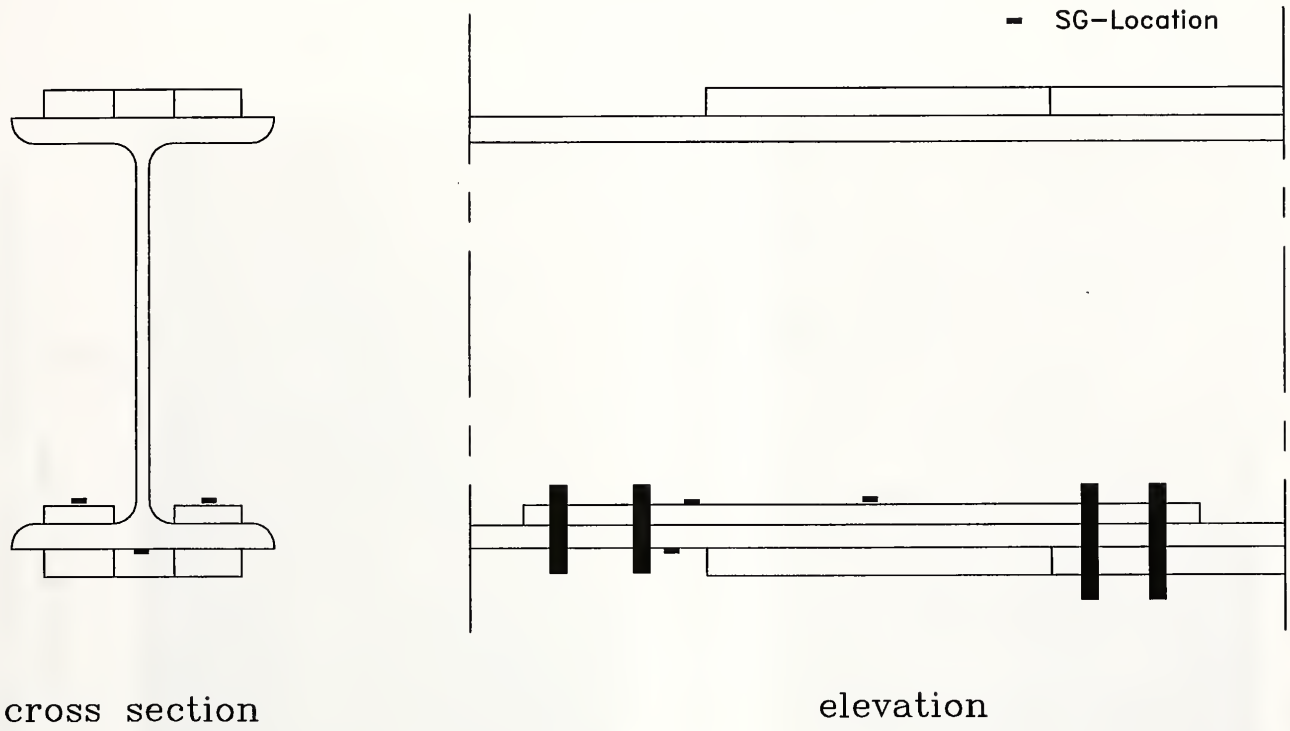

Fig. 8.2. Strain Gage Locations.
(Specimen NR12)

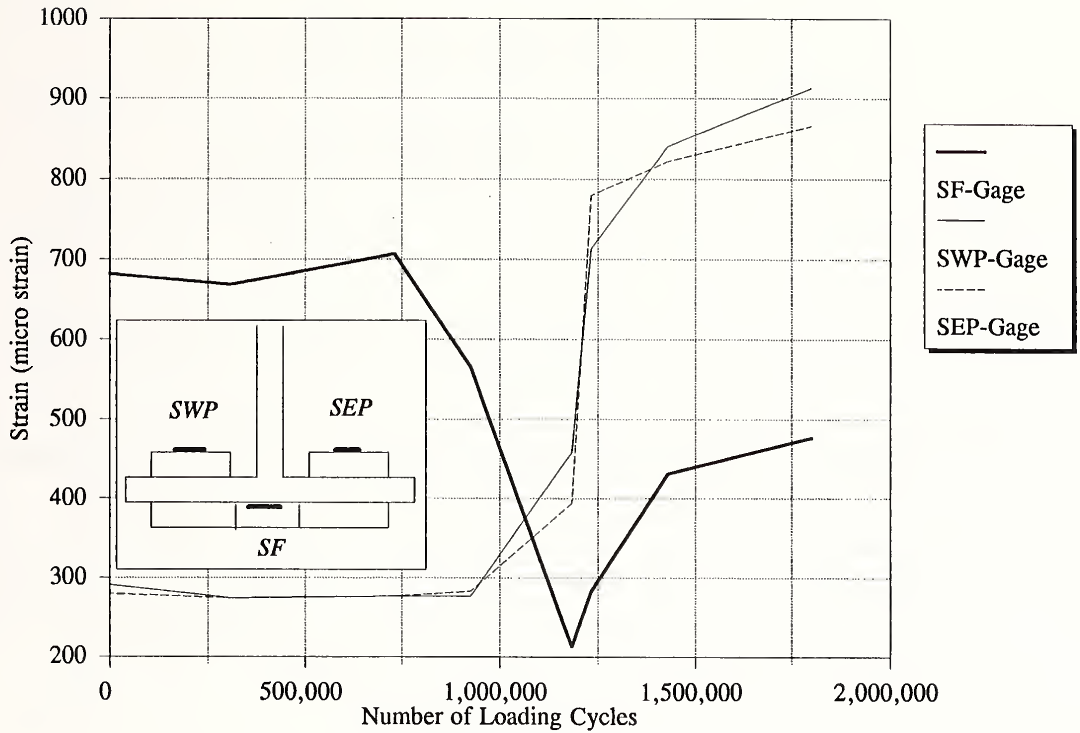

Fig. 8.3. Strain Measurements for Partial Bolted Splice Detail.
(Specimen NR12 - South End)

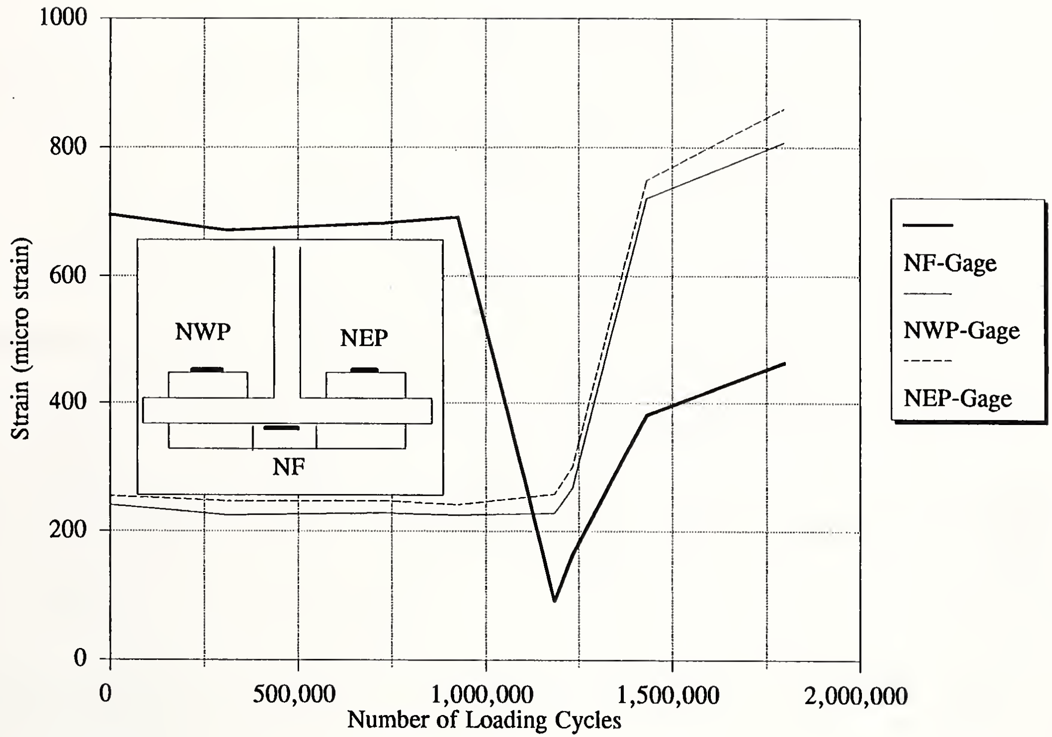

Fig. 8.4. Strain Measurements for Partial Bolted Splice Detail.
(Specimen NR12 - North End)

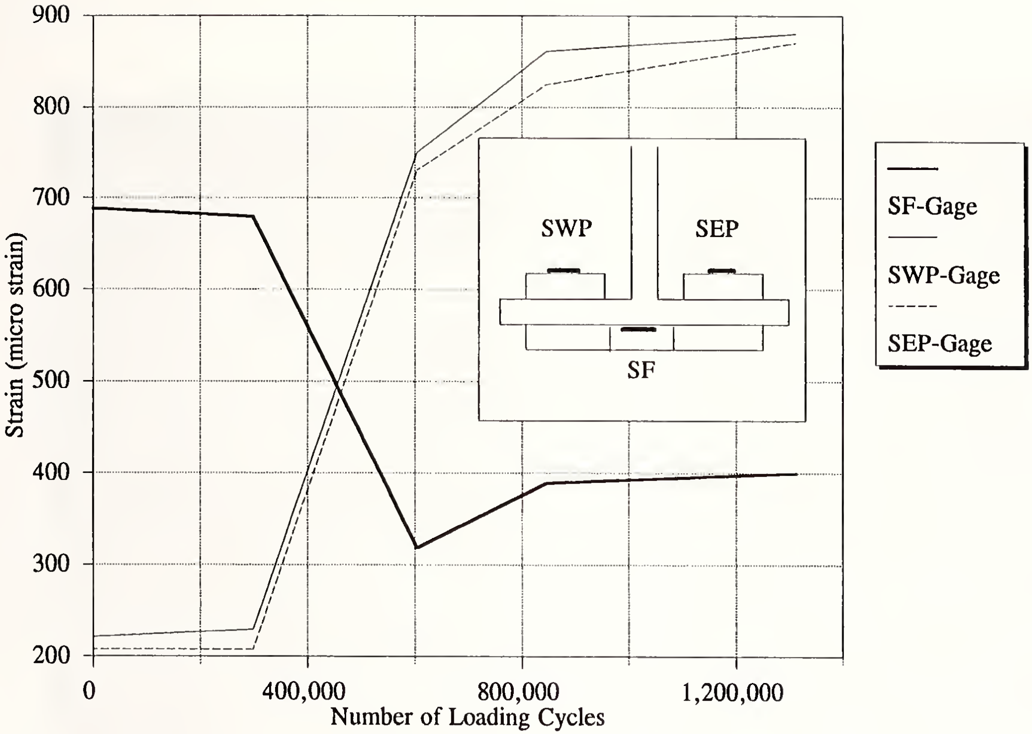

Fig. 8.5. Strain Measurements for Partial Bolted Splice Detail.
(Specimen WR7 - South End)

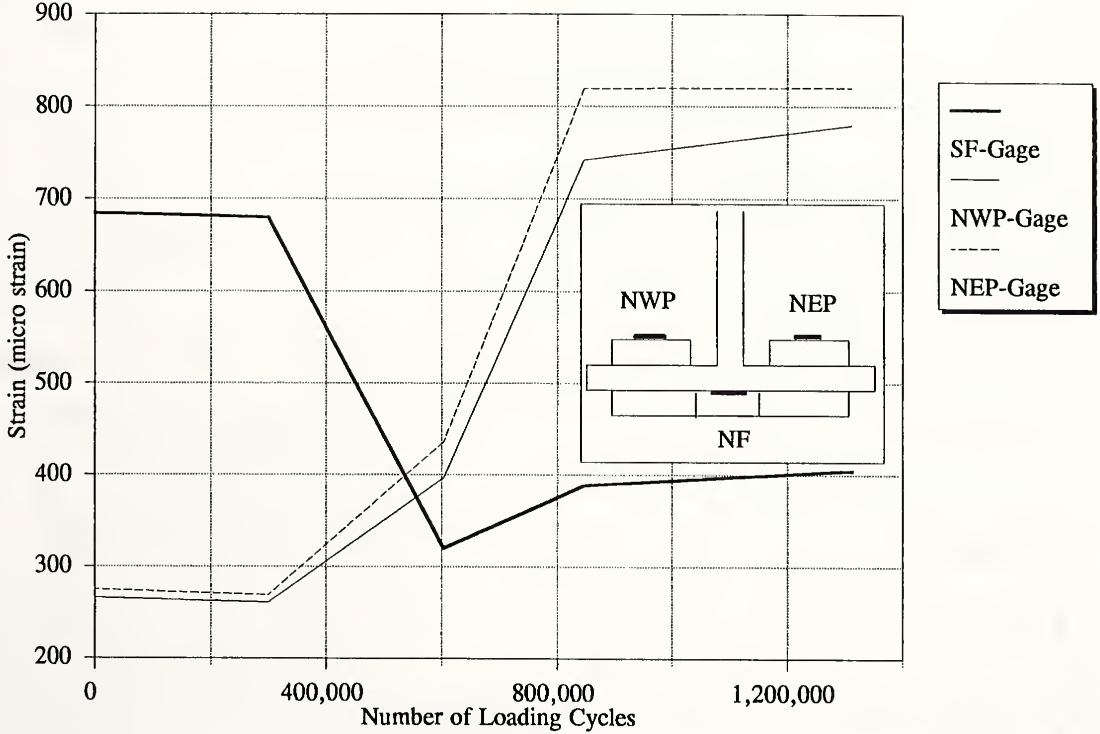

Fig. 8.6. Strain Measurements for Partial Bolted Splice Detail.
(Specimen WR7 - North End)

(a) After Welding

(b) After Grinding

Fig. 8.7. Flange Surface - Specimen NR7 South End.

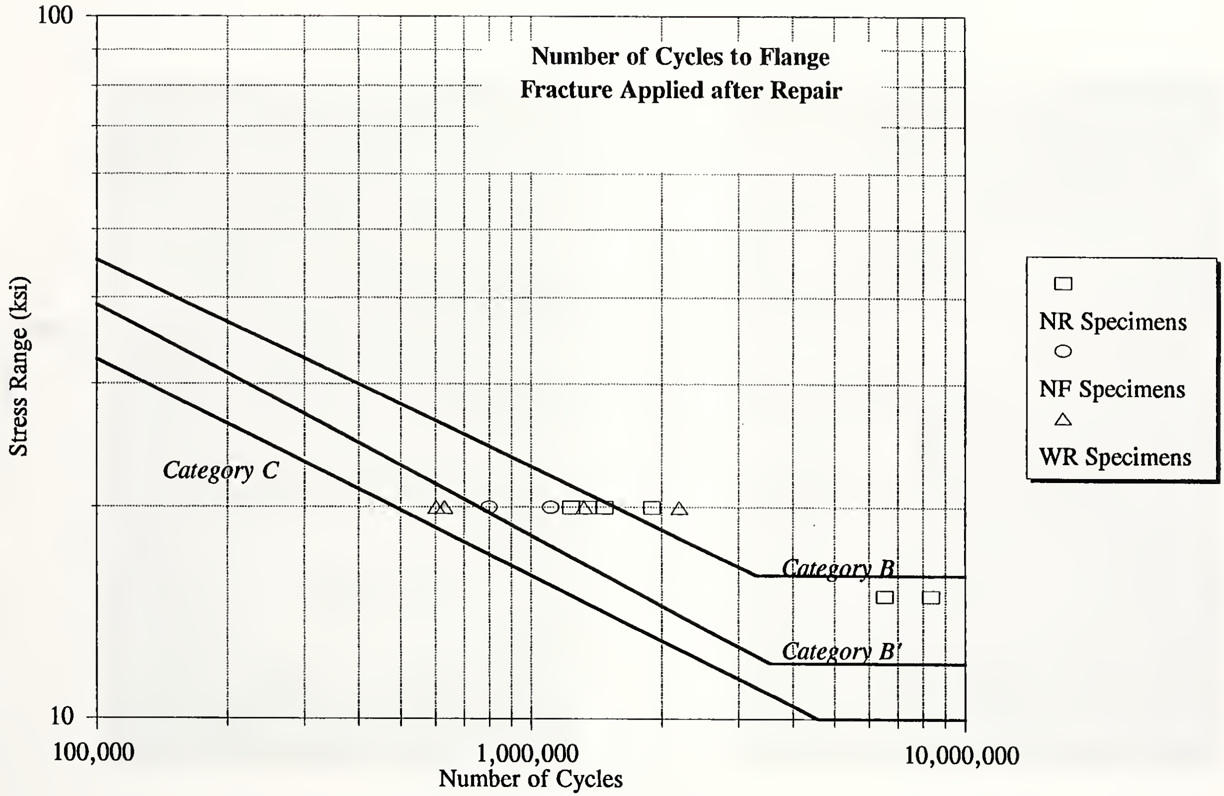

Fig. 8.8. Stress Range versus Number of Loading Cycles.

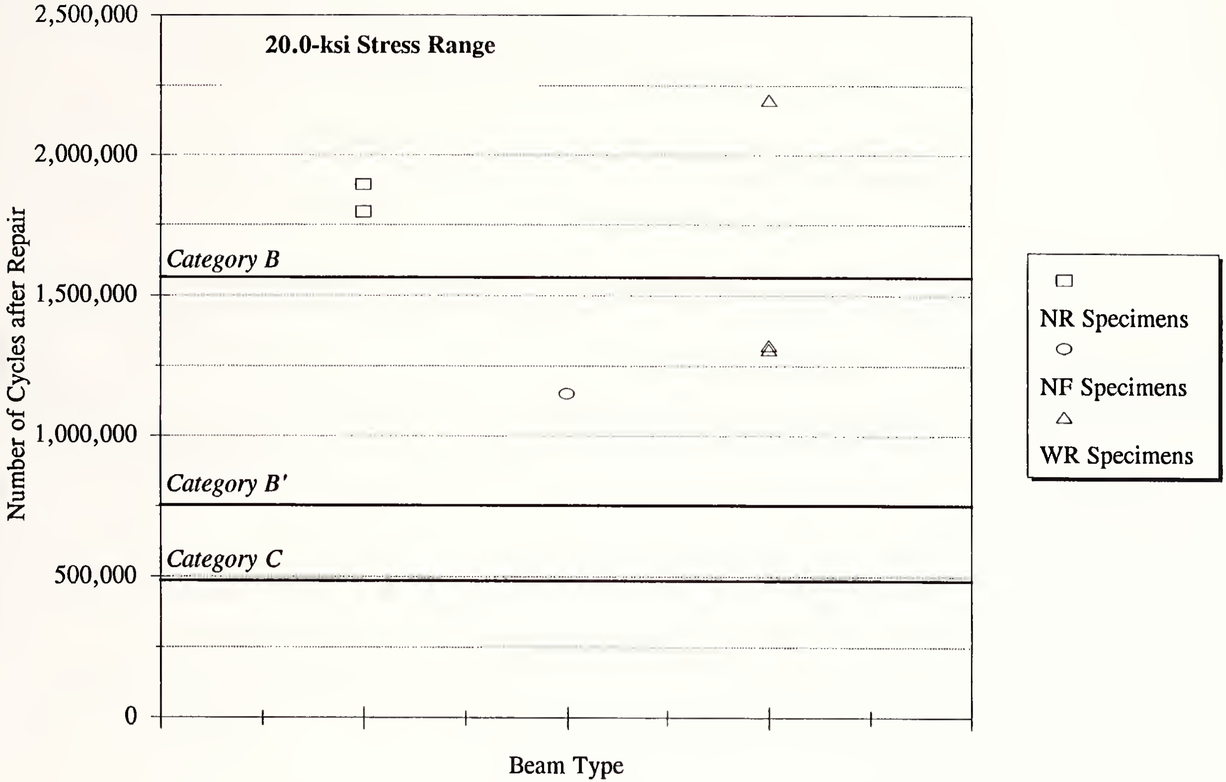

Fig. 8.9. Total Number of Loading Cycles Applied after Repair.

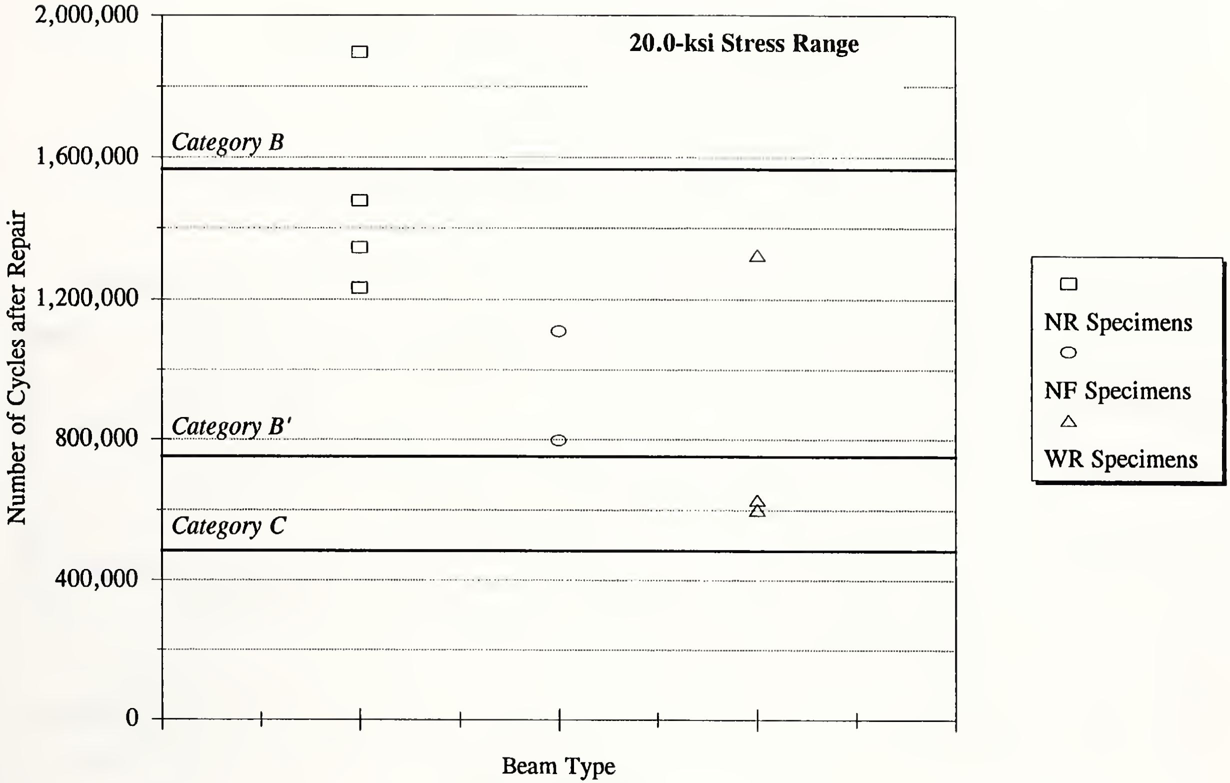

Fig. 8.10. Number of Loading Cycles to Flange Fracture Applied after Repair.

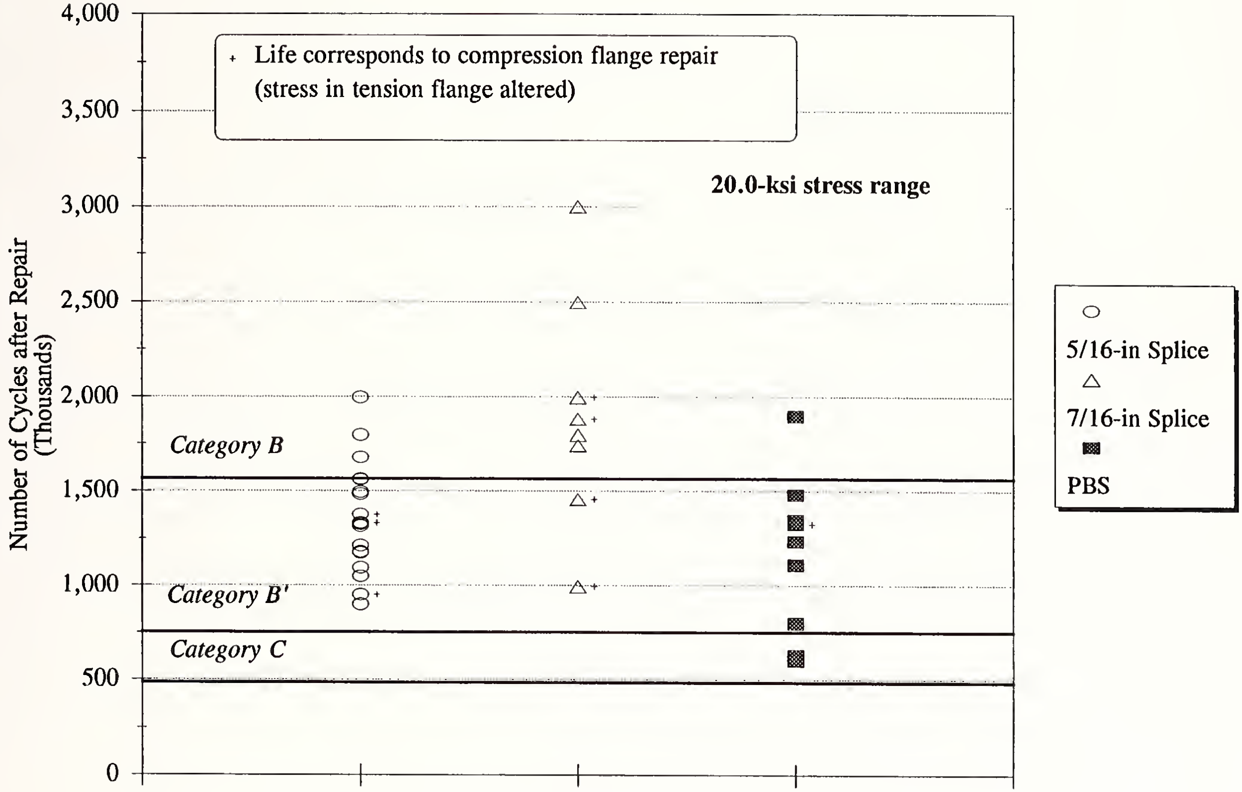

Fig. 8.11. Comparison with Bolted Splice Results.

CHAPTER 9
FATIGUE LIFE CALCULATION OF TAPERED COVER PLATES REPAIRED WITH SPLICE PLATE CONNECTIONS

9.1. Introduction

During the experimental phase of this study it was demonstrated that the use of a friction-type bolted splice connection is an effective method of repairing fatigue cracks at the end of tapered cover plates. It was also found that the splice plate thickness has a large influence on the fatigue life of the repair detail.

Upon detection of cracks, the splice plate connection is used. For static loading, the splice plates are designed to provide a cross sectional area large enough such that the bending moment in the beam at the cracked section can be carried without utilizing the beam tension flange; the beam tension flange is consequently assumed to be completely severed. In most cases, only a small portion of the tension flange (cracked portion) does not contribute in carrying the bending moment. Therefore, the tensile force (flange force prior to repair) is carried by both the splice plates and the non-cracked portion of the tension flange. Only the portion of the force carried by the flange is responsible for further crack growth, while the remaining portion of the force (carried by the splice plates) does not affect the cracked area. Increasing the splice plate thickness increases the amount of force carried by the splice plates and, therefore, increases the fatigue life of the detail.

The fatigue crack propagation life of a cracked bridge girder can be obtained using linear elastic fracture mechanics concepts. Several studies have shown that the stress intensity factor controls the crack growth rate. In order to calculate the crack propagation life the following information is needed:

1- The stress intensity factor for the cracked detail.

2- A model that relates stress intensity factor to crack growth rate.

3- Knowledge of the nominal stress, residual stress, and stress concentration at the studied detail.

4-Knowledge of the initial and final (critical) crack sizes.

The following sections describe a computer program developed to estimate the propagation life of fatigue cracks initiated at the end of welded, tapered cover plates. The various

assumptions utilized in the program are discussed, and a comparison between the fatigue life of test specimens and the corresponding analytical predictions is presented. Finally, the fatigue life of tapered cover plate details which have been repaired are predicted for the typical bridge beam sections using the proposed program.

9.2. Stress Intensity Factor

Exact determination of the stress intensity factor is often difficult to obtain, especially for complicated geometries. Empirical and approximate methods have been proposed to obtain approximate values in cases where exact solutions are not available. Albrecht and Yamada (1977) suggested a simplified method based on the superposition approach. The basic stress intensity factor for a through crack in an infinite plate is used, along with several correction factors to simulate complex geometries as follows:

$$K = F_E \, F_S \, F_W \, F_G \, \sigma \, \sqrt{\pi \, a} \tag{9.1}$$

where F_E, F_S, F_W, and F_G are correction factors that account for elliptical crack shape, free surface, finite width, and non-uniform opening stress, respectively.

Newman and Raju (1981) developed an empirical equation for the Mode I (crack opening) stress intensity factor of elliptical surface cracks in finite plates, subjected to both tension and bending. The solution is presented in Appendix F. It should be noted, however, that this solution does not account for the geometrical stress concentration due to the welded cover plate (non-uniform opening stress).

If the crack growth path is known, the geometrical stress concentration correction factor, F_G, can be expressed as follows:

$$F_G = \frac{2}{\pi} \int_0^a \frac{K_t(x)}{\sqrt{a^2 - x^2}} \, dx \tag{9.2}$$

where $K_t(x)$ is the stress gradient distribution due to the welded cover plate, for a non-cracked detail, along the expected crack trajectory.

The stress gradient distribution, K_t (x), was obtained using a general purpose finite element computer package, ANSYS (1993). The analysis was conducted in two phases. First, the cover plate end and the beam flange were analyzed to obtain the stress concentration factor due to end weld condition and cover plate width. Then, the second phase was conducted to assess the effect of weld geometry. Both phases are discussed in more detail in Appendix G. Linear regression analysis yielded the following equation for the stress gradient distribution at the cover plate end:

$$K_t\,(x) \approx F_1\,[0.8 + 3.615\,e^{(-4.6\,(\frac{x}{t_f})^{\frac{1}{3}})}] \tag{9.3}$$

where F_1 is the effect of end weld condition and cover plate width and is equal to 1.252, 1.214, 1.373, 1.235, and 1.197 for NR, NF, NN, WR, and WF specimens, respectively.

9.3. Propagation Model

There are many models that relate crack growth rate to stress intensity factor range. The most widely used expression for stable crack growth was proposed by Paris (1964). The Paris crack growth relationship is expressed as:

$$\frac{da}{dN} = C \quad \Delta K^m \tag{9.4}$$

where da/dN is the crack growth rate in in/cycle, ΔK is the stress intensity factor range in ksi in$^{1/2}$, and C and m are material constants. Some common values of C and m for various steels are summarized in Table 9.1.

It should be noted that the Paris law neglects the effect of stress ratio on the crack propagation rate. Eason et al. (1988) suggested the following mean-stress model for propagation of cracks in ferrite-pearlite steels:

$$\frac{da}{dN} = 4.16 * 10^{-9}\left(\frac{\Delta K}{2.88 - R}\right)^{3.07} \tag{9.5}$$

where da/dN is the growth rate in in/cycle, ΔK is the stress intensity range in ksi in$^{1/2}$, and R is the ratio of the minimum to maximum stress intensity factors.

9.4. Model Verification

A computer program was developed to estimate the fatigue crack propagation behavior of steel beams with welded tapered cover plates. Due to the complexity of the stress intensity factor solution, a step-by-step analysis was conducted. The program is given in Appendix H, while the algorithm is shown in Fig. 9.1. Comparisons between test specimen results and the corresponding analytical predictions are presented in this section.

The computed fatigue propagation life of the tapered cover plate detail corresponds to the number of loading cycles required to fracture the beam tension flange. This life is obtained in two phases. The first phase corresponds to the number of loading cycles required to propagate an elliptical crack shape and the second phase corresponds to the number of loading cycles required to propagate a through crack shape. The end of the first phase is usually achieved when the crack depth reaches a value equal to the flange thickness. However, several other criteria are also checked prior to the end of the first propagation phase. These are:

1- Crack depth exceeds half the crack length (condition for validity of stress intensity factor solution by Newman and Raju, 1981).

2- Crack length exceeds flange width.

3- Rapid crack growth (growth rate exceeds 0.001 in/cycle).

4- Maximum stress intensity factor exceeds fracture toughness of the material.

If any of the conditions 1 to 4 is achieved prior to the crack depth reaching the flange thickness, only phase one is considered. On the other hand, if the crack depth reaches a value equal to the flange thickness prior to one of the conditions controlling, then the crack is assumed to have the same length (from phase one) but extended all through the flange thickness. Then, the second phase computes the number of loading cycles to propagate the through crack until fracture of the flange. In the second phase, only criteria 2, 3, and 4 are considered.

The initial and final crack sizes were obtained from the experimental phase of the study. For each specimen, the crack sizes (lengths) were measured both prior to applying the repair procedure and at the end of the test (in the case of no flange fracture). Most of the test specimens initiated more than one crack at each end. As the program is limited to a single crack, an equivalent crack approach is proposed to represent the multiple initial cracks. As shown in Fig. 9.2, the equivalent crack is assumed to have a length equal to the summation of all initial crack lengths, and a depth equal to the deepest initial crack.

Only crack lengths were measured during the experimental study. A crack length to depth ratio was assumed to obtain the initial crack depth required for the calculation purposes. It is likely that this ratio changes as the crack length changes. Small cracks probably have a shape closer to a penny crack, although the length may grow faster than the depth due to the higher stress concentration on the flange surface. Since the variation of the crack length to depth ratio is unknown, it was felt that the use of a single value may be more logical, although admitably unrealistic.

A number of small plate specimens with a welded plate were tested during the early stages of the experimental study. The measured crack length to depth ratios were approximately 3.5. Consequently, a ratio of 4.0 was used in all of the analytical predictions.

The final requirement for crack propagation life predictions is an estimate of the nominal stress and residual stress for each repair condition. For the case of peening, the applied nominal stresses can be easily computed using elastic beam theory. All of the test beams repaired using the peening technique were cycled under 20.0 ksi stress range. Thus, the nominal stress range that propagates the cover plate end cracks is 20.0 ksi.

For the bolted splice repair technique, however, the nominal stress contributing to the crack propagation is not as obvious as for of peening. The force carried by the flange prior to repair will be carried by both the splice plates and the flange after repair. Only the portion of the force carried by the flange will affect the crack propagation; the force carried by the splice plates will have no effect on the propagation of cracks in the flange at the cover plate end. Finite element analysis was conducted to estimate the portion of the force carried by the flange and that carried by the splice plates. Appendix I discusses the finite element analysis assumptions and the results obtained.

The residual stress distributions are not well known and are difficult to assess. Thus, simplified models were assumed to represent the complex actual shapes. The fabrication residual stress is assumed to be linear in shape, having a maximum stress at the bottom flange fibers and zero stress at the top flange fibers - see Fig. 9.3. The maximum residual stress value,σ_r, was assumed to be -42.0 ksi ($-F_Y$), -21.0 ksi ($-F_Y/2$), and 0.0 ksi for the full end-weld, return end-weld, and no end-weld conditions, respectively. Hausammann, Fisher, and Yen (1983) suggested an idealized total residual stress distribution due to peening, as shown in Fig. 9.3. A simpler distribution, assumed for the present study, is also shown in Fig. 9.3. A higher compressive

residual stress was utilized by Hausammann et al. (1983) than for the simplified distribution. Both distributions were incorporated in the propagation program.

The residual stress distribution is used to determine the minimum stress intensity factor only and does not affect the stress intensity factor range. It was found that depth of the compression residual stress zone, relative to the initial crack depth, was a dominant factor influencing the crack propagation life. The distribution shape itself has very little effect on the propagation life. As previously mentioned, the crack growth rate depends mainly on the stress intensity range, which can be expressed as follows:

$$\Delta K = K_{max} - K_{min} \qquad \textit{for } K_{min} > 0.0 \tag{9.6a}$$

$$\Delta K = K_{max} \qquad \textit{for } K_{min} < 0.0 \tag{9.6b}$$

$$\Delta K = 0.0 \qquad \textit{for } K_{max} < 0.0 \tag{9.6c}$$

Analytical predictions of fatigue crack growth and the cyclic lives of the test specimens are compared in the following sections. Out of the 33 beams tested, 31 were subjected to a 20.0 ksi stress range at the cover plate end of the bare beam. The remaining two beams were subjected to a 15.0 ksi stress range. The smaller stress range is close to the Category B endurance limit.

All the analytical results discussed hereafter were obtained using the Paris crack growth law with constants for mean propagation rates of ASTM A36 steel (Barsom and Rolfe, 1987). The initial crack length to depth ratio was assumed to be 4.0, and the equivalent crack approach mentioned previously was used to represent multiple cracks. The simplified residual stress distribution for peening was used with a maximum compressive (negative) stress of -42.0 ksi at the surface and a compression zone depth of 0.026".

9.4.1. Bolted Splice Specimens

A total of 19 specimens were repaired using a friction-type bolted splice connection. Eighteen specimens were subjected to a loading that would cause a 20.0-ksi stress range at the cover plate end of the bare beam, while one specimen was subjected to 15.0-ksi stress range loading. As specimen DB1 did not initiate any cracks prior to repair, no comparison could be obtained for that specimen. A total of 9 ends exhibited cracks at the compression flange at the

cover plate end. These ends were repaired using either a friction type bolted splice connection or 1" thick plates along with 8 heavy duty C-clamps. In both cases, the stress in the tension flange was altered after the application of the compression flange repair. Thus, no comparison could be obtained for these ends. Therefore, results from 27 ends only, out of the 38 possible ends, were compared with the analytical predictions.

The north end of specimen NR8 (subjected to a 15.0 ksi stress range) developed a crack in the compression flange at 10,096,000 cycles after repair, and the test was terminated at 10,872,000 cycles. At the end of the test, the tension flange crack sizes were measured. The program predicted a life of 11,579,000 cycles to propagate the initial cracks to their final sizes measured at the end of test. Although the stress in the tension flange was altered after the compression flange repair, this effect can be neglected as the compression flange repair lasted for 776,000 cycles only (about 7% of the total life only). Thus, the analytical prediction compares very well with the test result.

Tables 9.2 and 9.3 show the comparison between the test specimen load history and the corresponding analytical predictions for the 5/16-in and 7/16-in splice repairs, respectively. It should be noted that the experimental load history corresponds to either tensile flange fracture or the end of test, whichever occurred first. The analytical predictions are the corresponding life of the specimen: total life or the life needed to propagate the initial cracks to their final sizes measured from the experiments.

Comparisons between the analytical predictions and the experimental results are also shown in Figs. 9.4 and 9.5 for the 5/16-in and 7/16-in splice repairs, respectively. Lines representing ±100% and ±50% difference in life prediction are also shown in the figures. Most of the points fall within the ±50% band, meaning that the predicted life usually falls within ⅔ and 1.5 times the experimental life. The average ratio between the predicted to the experiment lives was about 0.97 and 1.05 for the 5/16-in and 7/16-in splice repairs, respectively. Considering the large scatter involved with fatigue, the analytical predictions agree reasonably well with the experimental results. It should be noted that the figures do not indicate the results of ends that initiated compression cracks.

9.4.2. Partial Bolted Splice Specimens

The residual stress induced during the peening procedure was assumed to have a constant compressive stress of $-F_Y$ (-42.0-ksi) for a depth of 0.026-in and a constant stress of +3.0-ksi for the remaining flange thickness; the stress distribution is in a self equilibrium state for the W 14 × 30 flange thickness. The compression zone depth was found to be the most influential factor on the predicted propagation life, except when the initial crack depth is larger than the compression zone depth. Hausammann, Fisher, and Yen (1983) suggested a compression residual stress depth somewhere between 2 to 4 times the depth of deformed grains during the peening procedure. During their experimental study, they measured the depth of deformed grains and found that it depends on the number of peening passes and the air pressure used for the peening process. For 40.0 psi air pressure and 6 peening passes (values used in the present study), Hausammann, Fisher, and Yen (1983) found that the depth of deformed grains is between 0.012-in and 0.020-in. This corresponds to a compression zone depth of between 0.024-in and 0.080-in. As a conservative estimate, the compression residual stress depth was chosen to be 0.026-in. Compression zone depths larger than the initial crack depth prevent cracks from growing, which is in contradiction with the experiments.

A total of six beams (12 ends) were repaired using the partial-bolted splice repair procedure. Five beams were subjected to a 20.0-ksi stress range, and one beam was tested with a 15.0-ksi stress range. Both ends of the 15.0-ksi stress range specimen fractured on the compression side prior to the end of test. Therefore, comparison between the analytical predictions and the experimental results could not be conducted. Table 9.4 presents a comparison between test specimen lives and their corresponding predicted analytical lives for the partial bolted splice specimens. The results are also shown in Fig. 9.6. Here again, excellent agreement was found between the analytical predictions and the experimental life. The points fall within the ±50% difference bands, meaning that the analytical prediction lies between ⅔ and 1.5 times the experimental life with an average ratio between the predicted and experimental life of about 1.10.

The initial crack length for specimen NR11-N was very small (5/32-in). Due to the small crack size, the crack length to depth ratio is probably closer to 2.0 than 4.0. The analytical model predicts a life of 5,528,000 cycles and 1,322,000 cycles for a crack length to depth ratio of 4.0 and 2.0, respectively. The experimental life of specimen NR11-N was 1,898,000 cycles, and lies between the two extremes but closer to the 2.0 ratio - again, small cracks are probably semi-

circular in shape, then they grow wider due to the higher stress concentration at the surface. Moreover, a small error in the crack measurement for small cracks has a large influence on the computed life. For example, if the initial crack at specimen NR11-N was 7/32-in long (1/16-in error in measurement) and the crack length to depth ratio was kept at 4.0, the analytical life would be 1,998,000 cycles.

The initial crack sizes for other specimens, being larger than that for Specimen NR11-N, did not have such a large effect on the predicted life. It should be noted that cracks are generally large (0.25-in to 0.50-in) when they are detected in the field.

9.4.3. Peening Specimens

A total of 8 specimens were repaired using the peening repair technique. Five specimens were peened after detectable cracks had initiated at the cover plate ends, while three specimens were peened prior to crack detection. The same residual stress model used for the partial bolted splice specimens was also used for the peening specimens.

The test specimen lives and the analytical predictions for the peening specimens are compared in Table 9.5. The results are also shown graphically in Fig. 9.7. The peening repair results show more scatter than that demonstrated for the bolted splice repair. The larger scatter can be explained partially by the many factors that influence the experimental results: tool orientation, air pressure used during peening, shape and number of indentations induced on the peened surface, and the way the operator handles the tool. Some of the factors influencing the scatter in the analytical predictions include the compression zone depth, the maximum surface compressive stress induced during peening, and the initial crack depth.

It can be observed that the analytical model underestimates most of the experimental lives, especially for the case of large initial cracks. The average ratio of analytical to experimental life was about 0.74. Peening effects are negligible when the crack depth is larger than the compression zone depth. Consequently, peening is not recommended for large cracks that have significant depths; a bolted splice connection would probably be a better choice.

Specimens peened prior to crack detection were assumed to have one crack 0.04-in long by 0.02-in deep for calculation purposes. Using the analytical model, specimens NR5 and NR6 (peened prior to crack detection) were predicted to fail after 212,590,000 cycles. In other words, no propagation is expected in the flange at the cover plate ends for this detail. Since specimens

NR5 and NR6 did not propagate cracks from the weld toe at the cover plate ends, the experimental results appear to agree with the analytical prediction.

9.5. Flange Stress in Girders Repaired with a Friction-Type Bolted Splice Connection

As discussed in the previous sections, a portion of the flange force prior to repair is transmitted through the splice plates and, thus, does not contribute in the propagation process. Therefore, an estimate of the crack propagating force is required for the propagation life calculations. Several factors influence the percentage of the total tension force carried by the splice plates and the flange. Finite element analysis of the test specimens revealed that the following factors influence the force distribution ratio to some extent:

1- Splice Plate Area (A_{sp}).

2- Flange Area (A_{fl}).

3- Cover Plate Area (A_{cp}).

4- Web Area (A_w).

5- Distance between the inner bolt rows of the splice connection (l_{sp}).

6- Splice plate thickness (t_{sp}).

7- Web depth (d_w).

8- Web thickness (t_w).

A simple evaluation of the flange force is complicated by the number of influential factors, and variation of these factors for various beam member sizes.

Discussion with Indiana Department of Transportation engineers indicated that the following range of beams represents nearly all of the bridge girders containing the tapered cover plate detail in Indiana:

- W36 × 136 to W36 × 194
- W33 × 118 to W 33 × 152
- W30 × 99 to W30 × 132
- W27 × 84 to W27 × 114

Also, the cover plate thickness ranged from 3/8-in to 15/16-in. The taper length ranged from 1-ft to 2-ft (1 1/2-ft was the usual taper length), and the cover plate width at the end of taper ranged from 2-in to 4-in (3-in was the usual width).

A general equation was developed to calculate the magnitude of the flange force in the splice region for a given flange force without the splice plate. Finite element analysis was used to determine the flange force for particular beam, splice, and cover plate sizes. To limit the number of finite element runs, the taper length and the cover plate width at the taper end were selected to be 1 1/2-ft and 3-in, respectively. To cover the whole range of beams, three beam sizes were selected for each of the four beam depths to represent the low, high, and middle size for each beam depth.

For each beam analyzed, three cover plate areas were considered as follows:

1- A middle cover plate area (5/8-in thick) with a narrow cover plate detail (about 1-in narrower than the flange width).

2- A low cover plate area (3/8-in thick) with a narrow cover plate detail.

3- A high cover plate area (15/16-in thick) with a wide cover plate detail (about 1-in wider than the flange width).

The last variable considered in the analysis is splice plates area. For each beam depth, the splice plate widths were selected as follows:

- the width of the lower splice plate was selected to be equal to the narrow cover plate width.
- the two upper splice plate widths were chosen to fit on both sides of the web with their edges even with the edges of the lower splice plate.

For each beam depth, a splice plate connection was designed for the middle beam of the beam size range such that the stresses in the lower fibers of the bottom splice plate and the upper fibers of the compression flange do not exceed the allowable stress (20.0-ksi for ASTM A36 steel). The design was conducted assuming that the tension flange was completely severed and does not contribute in carrying the applied bending moment. The splice plate thickness obtained by this procedure, referred to as the design thickness, is used along with thicknesses of 1.25, 1.50, and 2.0 times the design value to represent a wide range in splice plate areas.

Previous finite element runs indicated that changing the beam flange width or thickness has only a small influence on the portion of the force carried by the splice plates, as long as the same flange area is maintained. The same observation was made for the splice plates: changing the width or the thickness, for a given area, has little effect on the splice plate force. Thus, to facilitate the analysis, four main finite element meshes were developed to represent the middle size of each of the four beam depths studied. To analyze the lower and upper sizes for each

depth, the flange width was changed to obtain the appropriate flange area. Also, the splice plate thickness was kept equal to the design thickness, while the splice plate width was changed to obtain the required range of splice plates area. The finite element analysis assumptions are discussed in more detail in Appendix I.

Finite element analysis was conducted to determine the force developed in the beam flange and the splice plates for a wide range of parameters: four beam depths, three flange areas, three cover plate areas, and four splice plate areas. Hence, a total of 144 finite element runs were conducted to obtain the percentage of the total flange force carried by the splice plates (non-propagating force). For simplicity, the total flange force was assumed to be equal to the allowable stress (20.0-ksi for ASTM A36 steel) multiplied by the flange area. The splice plate force was obtained from the finite element analysis. Therefore, the propagating force is the total force minus the splice plate force. The results of the finite element analysis are presented in Appendix J.

Linear regression analysis was then conducted to obtain a general equation relating the splice plate force to the previously mentioned influential factors. To obtain a non-dimensionalized equation, the following factors were considered:

$X_1 = A_{sp} / A_{fl}$ = splice plate area / flange area

$X_2 = A_{cp} / A_{fl}$ = cover plate area / flange area

$X_3 = A_w / A_{fl}$ = web area / flange area

$X_4 = d_w / t_w$ = web depth / web thickness

$X_5 = l_{sp} / t_{sp}$ = distance between inner bolts / splice plate thickness

$Y = F_{sp} / F_{total}$ = splice plate force / total flange force

The following expression was found to best represent the obtained data with a maximum error of about 6.5%:

$$Y = 0.28128573 + 0.31143275\, X_1 - 0.06566232\, X_2 + 0.0011347\, X_5 - 0.03573589\, X_1^2 \qquad (9.7)$$

Other expressions were also considered, but equation 9.7 represented the data with a small error and the fewest parameters. It should be noted that the regression equation was developed for the following range of parameters, and should be only used within that range:

⇒ X_1 ranged from 0.86 to 3.44

⇒ X_2 ranged from 0.34 to 1.62

⇒ X_3 ranged from 1.40 to 2.34

⇒ X_4 ranged from 49.38 to 52.26

⇒ X_5 ranged from 14.73 to 36.00

The use of the regression equation outside the parameter ranges mentioned involves an additional error (approximation) in the flange stress ratio.

9.6. Fatigue Life of Bridge Girders with Bolted Splice Plate Repair

A crack propagation program was used to predict the fatigue life of girders repaired with splice plates. The splice plate force regression analysis equation was incorporated in the propagation program to estimate the nominal flange stress that propagates existing cracks. For a specific bridge girder, with known initial crack sizes and splice plate configuration, the expected fatigue life can be estimated using the program listed in Appendix H. Several examples illustrating the steps involved in fatigue life calculations are presented in Appendix K.

The fatigue propagation life of the middle size of each beam depth commonly utilized by INDOT was computed for the following conditions:

- Three splice plate thicknesses: design thickness (t_D), 1.25 t_D , and 1.5 t_D.
- Four nominal stress ranges at the cover plate ends: 30.0, 20.0, 15.0, and 12.0 ksi.
- Five cover plate geometries: NR, NF, NN, WR, and WF specimens.
- Four initial crack lengths: 1/2-in, 1-in, 1 1/2-in, and 2-in.

Based upon observations of end detail cracking during the experimental program, the NR and WR geometries were assumed to initially have two cracks, the NN beams were assumed to initially have one crack, and the NF and WF geometries were assumed to initially have three cracks. It should be noted that the crack lengths represent the total length of cracks found prior to repair. In other words, the 1/2-in crack represents a single 1/2-in long crack for the no end-weld specimens, two 1/4-in long cracks for the return end-weld specimens, and three 1/6-in long cracks for the full end-weld specimens.

The propagation life predictions are presented in Appendix L. The 1/2-in and 2-in initial crack length results are discussed in more detail in the following sections. It should be noted that all of these results are for special cases (specific beams sizes, splice plate areas, initial crack

values,...etc), and should only be used for these cases. In order to estimate the fatigue crack propagation life of a specific beam geometry, the proposed propagation program listed in Appendix H should be used in conjunction with the appropriate variable values.

The results presented in Appendix L demonstrate that the there is little difference in the fatigue life between the narrow and wide cover plate details. It can also be seen that the full end-weld condition has the highest propagation life, while the no end-weld condition has the lowest fatigue life. This result is due to the initial crack size effect. The no end-weld, return end-weld, and full end-weld specimens were assumed to initially have one, two, and three cracks, respectively. Thus, for the same total initial crack length, the no end-weld detail has a deeper crack than the return end-weld detail which has a deeper crack than the full end-weld detail.

Figures 9.8 and 9.9 show the fatigue propagation life of W36 × 160 girders versus splice plate thickness for a total initial crack length of 1/2-in and 2.0-in, respectively. The fatigue life is shown for four nominal stress ranges: 30.0, 20.0, 15.0, 12.0 ksi. The nominal stress ranges correspond to the stress range that would exist at the end of the cover plate (crack location) with no splice plate attached. For a specific stress range and splice plate thickness, the expected fatigue life can be obtained. For reference, Category B and C design lives are noted on the same figure for the four nominal stress ranges: B-30 indicates the Category B life for a 30-ksi stress range. Also, note that the fatigue category is extended beyond the endurance limit. As an example of using the design charts, if a W36 × 160 girder was inspected and two cracks 1/4-in long each were detected, a splice plate thickness of about 3/4-in is required to obtain a Category B behavior and a thickness of about 3/8-in is required to achieve Category C behavior (assuming that the girder is subjected to 20.0-ksi stress range). It should be noted that the return end-weld results were used in the previous example because two cracks were initially detected. On the other hand, if two cracks 1.0-in long each were detected in the same girder, splice plate thicknesses of about 7/8-in and 9/16-in are required to achieve Category B and C behavior, respectively. The previously mentioned splice plate thicknesses are computed assuming that the splice plates width is the same as the for the design splice plate connection (one plate 11-in × 5/8-in and two plates 5-in × 5/8-in).

Figures 9.8 and 9.9 indicate that, in most cases, the fatigue life of the specimen is lower than the Category B design life. However, it should be noted that the predicted life corresponds only to the number of cycles required to fracture the flange. Results obtained from the

experimental portion of the study also indicated that flange fracture usually occurs after a number of loading cycles less than Category B design life (for the 5/16-in splice plate connection). However, experimental results also indicated that the total life of the detail exceeded a Category B design life since the splice plates were able to carry a number of additional cycles of loading after flange fracture. Thus, the predicted propagation life values agree closely with observations obtained from the experimental program.

Figures 9.10 and 9.11, 9.12 and 9.13, and 9.14 and 9.15 show the fatigue propagation life of W33 ×141, W30 × 116, and W27 × 102 sections, respectively. It should be noted that Figs. 9.8-9.15 are design charts of specific cases and are not intended to cover the entire range of variables. Thus, whenever possible the propagation program should be used to estimate the fatigue life for cases not covered by these charts.

9.7. Summary and Conclusions

A computer program has been developed to predict the crack propagation life of steel beams with welded-tapered cover plates. Due to the complexity of the stress intensity factor solution, a step-by-step analysis was used for the propagation calculations. The crack geometry, stress intensity factor at the crack tips, and growth rates are updated during each step. The program, which is written in FORTRAN language, incorporates four propagation models that could be used for ASTM A36 steel; the user also has a choice for a user's defined value based on the Paris law model. Knowledge of the nominal stress propagating the crack is required for the propagation calculations. The program also incorporates residual stress distributions that are used to model the internal stresses from fabrication and peening. Linear-elastic finite element analysis was conducted to obtain the stress values in the different components of the studied details. The analysis was conducted using a general purpose finite element package (ANSYS, 1993).

A regression equation was developed to estimate the percentage of the stress transmitted through the flange after a friction type splice plate connection is used to connect the flange on each side of the cover plate end detail. The equation predicts the flange stress with a maximum error of about 4% for the range of variables studied. Fatigue life estimation was conducted for various beam sizes, crack lengths, end details, stress ranges, and splice plate thicknesses. Based upon the results, a number of simplified design charts were presented.

All of the previously discussed results were based on the following assumptions:

1. An initial crack length to depth ratio of 4.0.
2. A crack propagation model suggested by Barsom and Rolfe (1987) for mean propagation rates of ASTM A36 steel.
3. Simplified residual stress distributions.
4. An equivalent crack used to represent multiple crack sites.

Based on the analytical and experimental results, the following conclusions were obtained:

1. The proposed analytical model predicts cyclic lives of repaired cover plate details that agree well with the test results of bolted splice, partial bolted splice, and peened repair details.
2. Agreement between the experimental and predicted lives was better for the bolted splice beams and the partial bolted splice beams than for peened beams.
3. The model is conservative and underestimates the propagation life of peened specimens with large initial cracks by a factor of about 2.0.

Table 9.1. Crack Propagation Material Constants.

Reference	C	m	Notes
Barsom and Rolfe (1987)	$3.6 * 10^{-10}$	3.0	Conservative growth rate for ferrite-pearlite steels
Barsom and Rolfe (1987)	$1.0 * 10^{-10}$	3.3	Mean growth rate for ASTM A36 steel
Yamada and Hirt (1982)	$2.5 * 10^{-10}$	3.0	Mean growth rate for ferrite-pearlite steels

Table 9.2. Comparison between Experimental Load History and Analytical Predictions for the 5/16-in Bolted Splice Repair Technique.

Specimen Number	Experiment Cyclic Life	Analytical Cyclic Life	Notes
DB1-N	---	---	Repair applied with no initial cracks.
DB1-S	---	---	Repair applied with no initial cracks.
DB2-N	1,800,000	776,000	Compression flange repaired with 7/16" splice at 950,000 cycles.
DB2-S	1,800,000	1,800,000	Compression flange repaired with 7/16" splice at 950,000 cycles.
DB3-N	1,800,000	1,416,000	Cyclic load stopped.
DB3-S	1,800,000	1,248,000	Cyclic load stopped.
NR1-N	1,563,600	1,017,000	Flange fractured.
NR1-S	2,000,000	1,254,000	Flange fractured.
NN1-N	1,800,000	1,223,000	Cyclic load stopped.
NN1-S	1,800,000	500,000	Compression flange repaired with 1" thick plates at 1,333,000.
NN2-N	1,800,000	1,567,000	Cyclic load stopped.
NF1-N	882,600	1,050,000	Flange fractured.
NF1-S	1,178,800	1,002,000	Flange fractured.
NF2-N	1,095,000	1,078,000	Flange fractured.
NF3-N	1,680,000	1,669,000	Flange fractured.
WF1-S	900,000	918,000	Flange fractured.
WF2-N	1,485,000	1,992,000	Flange fractured.
WF2-S	1,315,000	1,767,000	Flange fractured.
WF3-N	1,324,000	1,650,000	Flange fractured.
WR1-N	1,174,000	1,625,000	Flange fractured.
WR1-S	1,495,000	1,065,000	Flange fractured.
WR2-N	1,561,000	1,398,000	Flange fractured.
WR3-S	1,211,000	1,378,000	Flange fractured.

Table 9.3. Comparison between Experimental Load History and Analytical Predictions for the 7/16-in Bolted Splice Repair Technique.

Specimen Number	Experiment Cyclic Life	Analytical Cyclic Life	Notes
NR2-N	2,500,000	1,733,000	Compression flange repaired with 1" thick plates at 2,000,000 cycles.
NR2-S	2,500,000	2,600,000	Cyclic load stopped.
NR3-N	3,000,000	3,067,000	Cyclic load stopped.
NR3-S	3,000,000	2,050,000	Compression flange repaired with 1" thick plates at 1,883,000 cycles.
NR4-N	2,000,000	1,433,000	Cyclic load stopped.
NR4-S	2,000,000	2,533,000	Cyclic load stopped.
NN2-S	1,800,000	617,000	Compression flange repaired with 1" thick plates at 995,000 cycles.
NF2-S	1,800,000	1,756,000	Compression flange repaired with 1" thick plates at 1,457,000 cycles.
NF3-S	1,800,000	2,025,000	Cyclic load stopped.
WF1-N	1,744,000	2,053,000	Flange fractured.
WF3-S	1,800,000	2,188,000	Cyclic load stopped.
WR2-S	1,800,000	1,713,000	Cyclic load stopped.
WR3-N	1,800,000	1,763,000	Cyclic load stopped.
NR8-N[1]	10,782,000	11,579,000	Compression crack found at 10,096,000 cycles.
NR8-S[1]	10,872,000	7,000,000	Compression flange repaired with 5/16" splice at 7,143,000 cycles.

[1] Specimen subjected to 15.0 ksi stress range at the cover plate end.

Table 9.4. Comparison between Experimental Lad History and Analytical Predictions for the Partial Bolted Splice Repair Technique.

Specimen Number	Experiment Cyclic Life	Analytical Cyclic Life	Notes
NR11-N	1,898,000	5,528,000	Flange fractured.
NR11-S	1,480,000	1,405,000	Flange fractured.
NR12-N	1,347,000	1,342,000	Flange fractured.
NR12-S	1,234,000	865,000	Flange fractured.
NF5-N	955,000	671,000	Flange fractured.
NF5-S	800,000	292,000	Specimen was already fractured when observation was made.
WR6-N	2,200,000	639,000	Compression flange repaired with 1" thick plates at 1,326,000 cycles.
WR6-S	1,326,000	1,355,000	Flange fractured.
WR7-N	631,000	841,000	Flange fractured.
WR7-S	604,000	579,000	Flange fractured.
NR7-N[1]	8,340,000	---	Compression flange fractured.
NR7-S[1]	8,340,000	---	Compression flange fractured.

[1] Specimen subjected to 15.0 ksi stress range at the cover plate end of the bare beam.

Table 9.5. Comparison between Experimental Load History and Analytical Predictions for the Peening Repair Technique.

Specimen Number	Experiment Cyclic Life	Analytical Cyclic Life	Notes
NR9-N	275,000	142,000	Flange fractured.
NR9-S	401,300	396,000	Flange fractured.
NR10-N	506,200	112,000	Flange fractured.
NR10-S	435,700	415,000	Flange fractured.
NF4-N	590,000	309,000	Flange fractured.
NF4-S	369,100	488,000	Flange fractured.
NN3-N[1]	304,000	391,000	Flange fractured.
NN3-S[1]	308,000	391,000	Flange fractured.
WR4-N	300,000	104,000	Flange fractured.
WR4-S	215,500	116,000	Flange fractured.
WR5-N	223,000	99,000	Flange fractured.
WR5-S	160,000	74,000	Flange fractured.
NR5-N[1]	---	---	No crack detected, test stopped.
NR5-S[1]	---	---	No crack detected, test stopped.
NR6-N[1]	---	---	No crack detected, test stopped.
NR6-S[1]	---	---	No crack detected, test stopped.

[1] Specimens peened prior to crack detection.

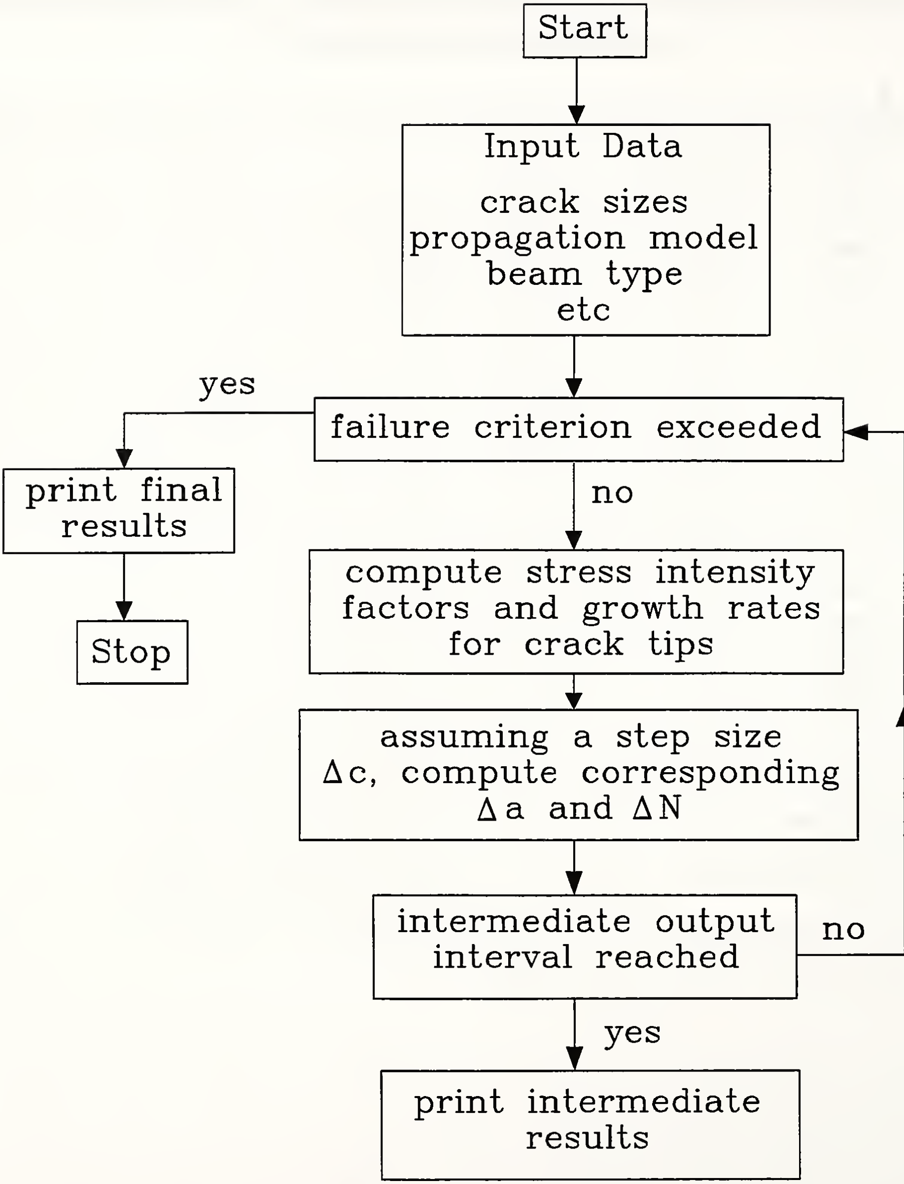

Fig. 9.1. Program Flow Chart.

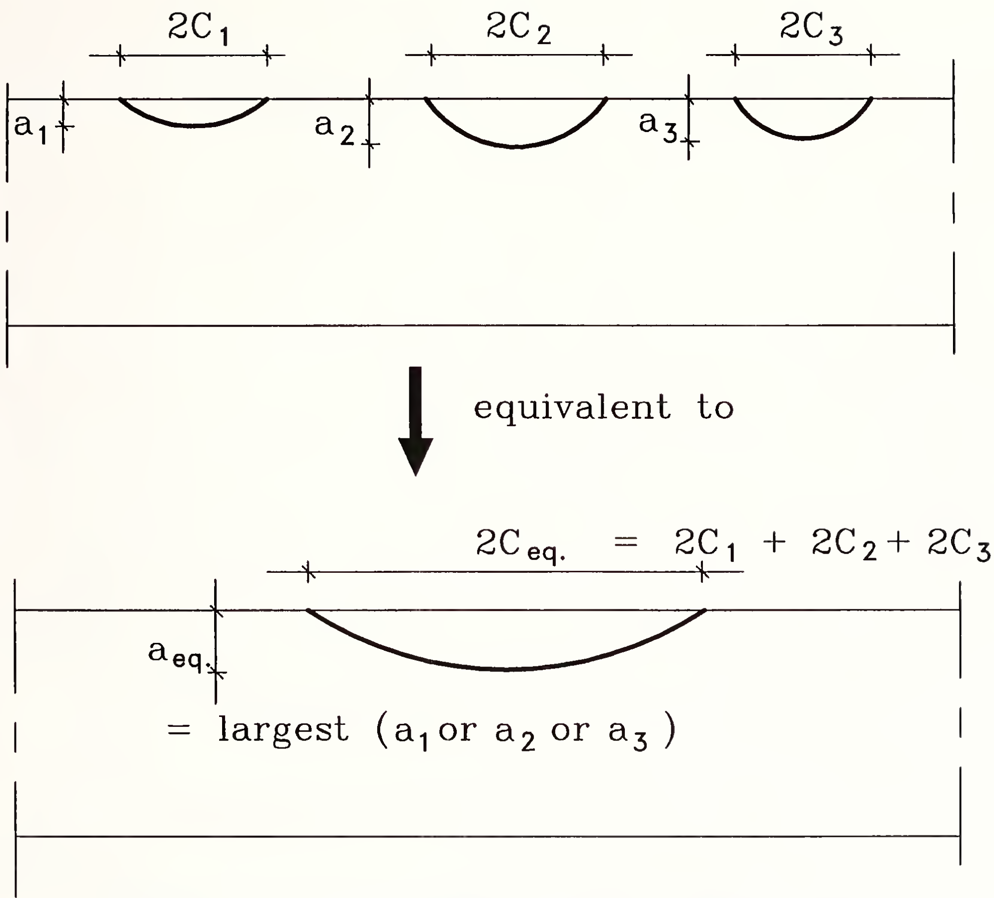

Fig. 9.2. Equivalent Crack Approach.

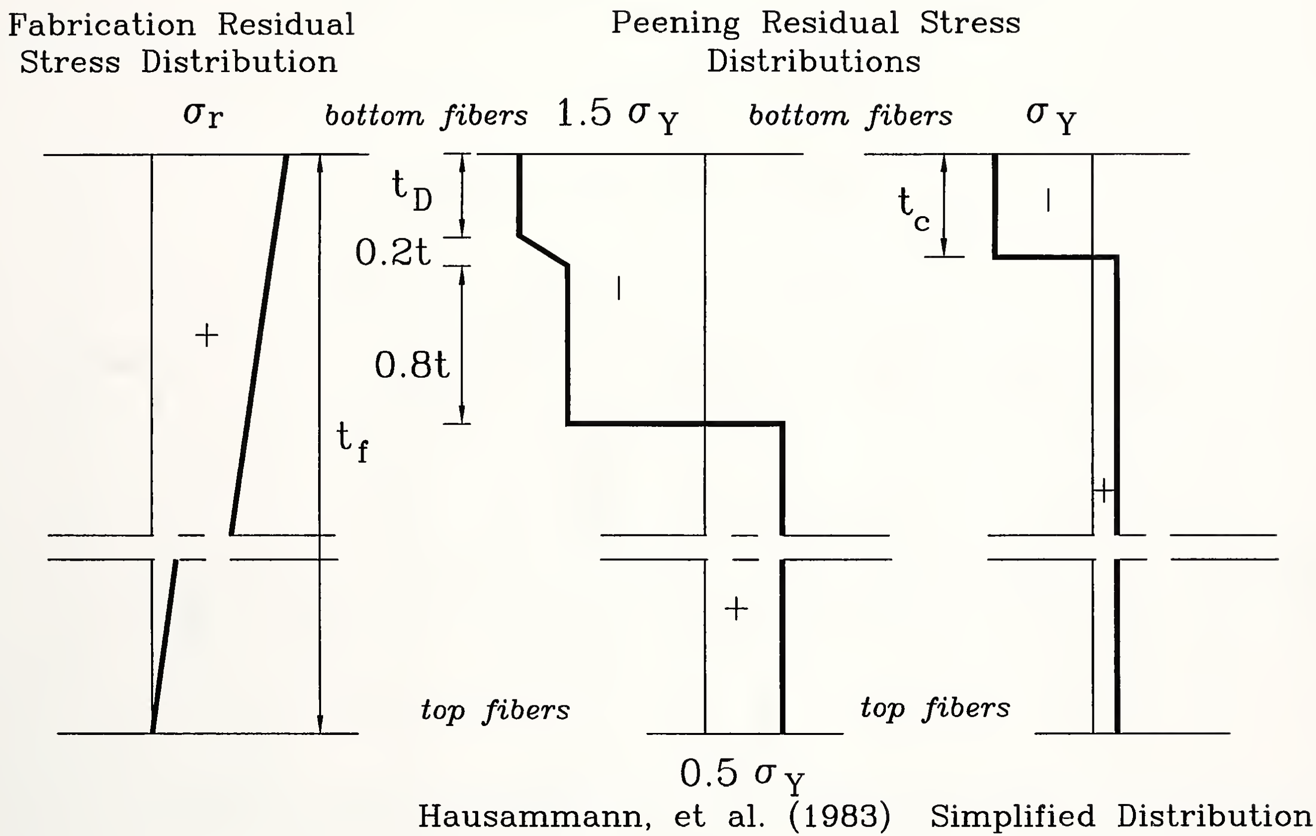

Fig. 9.3. Residual Stress Distributions.

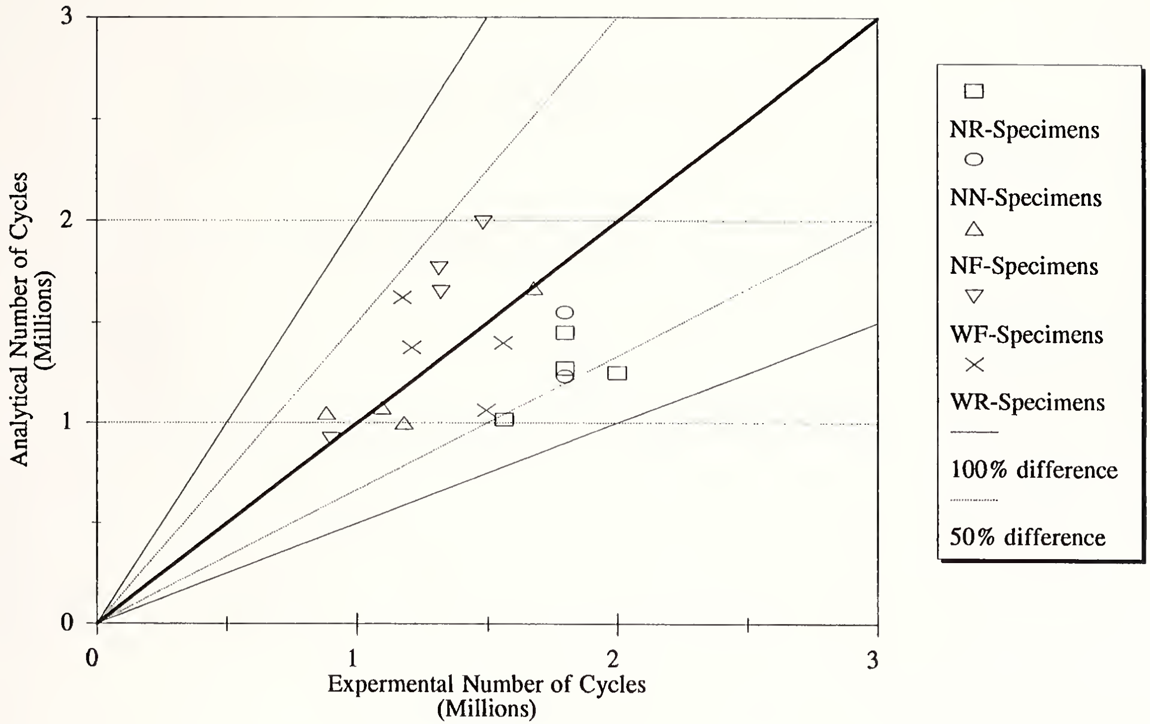

Fig. 9.4. Comparison between Experimental Results and Analytical Results for the 5/16-in Bolted Splice Connection.

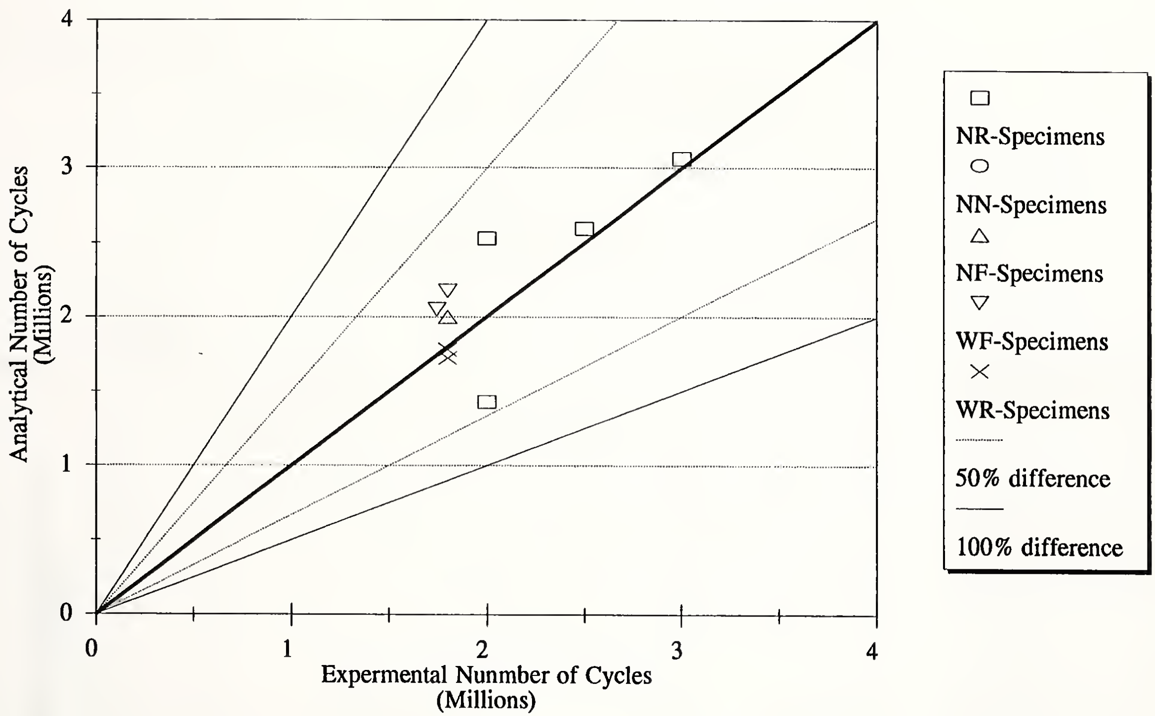

Fig. 9.5. Comparison between Experimental Life and Analytical Prediction for the 7/16-in" Bolted Splice Connection.

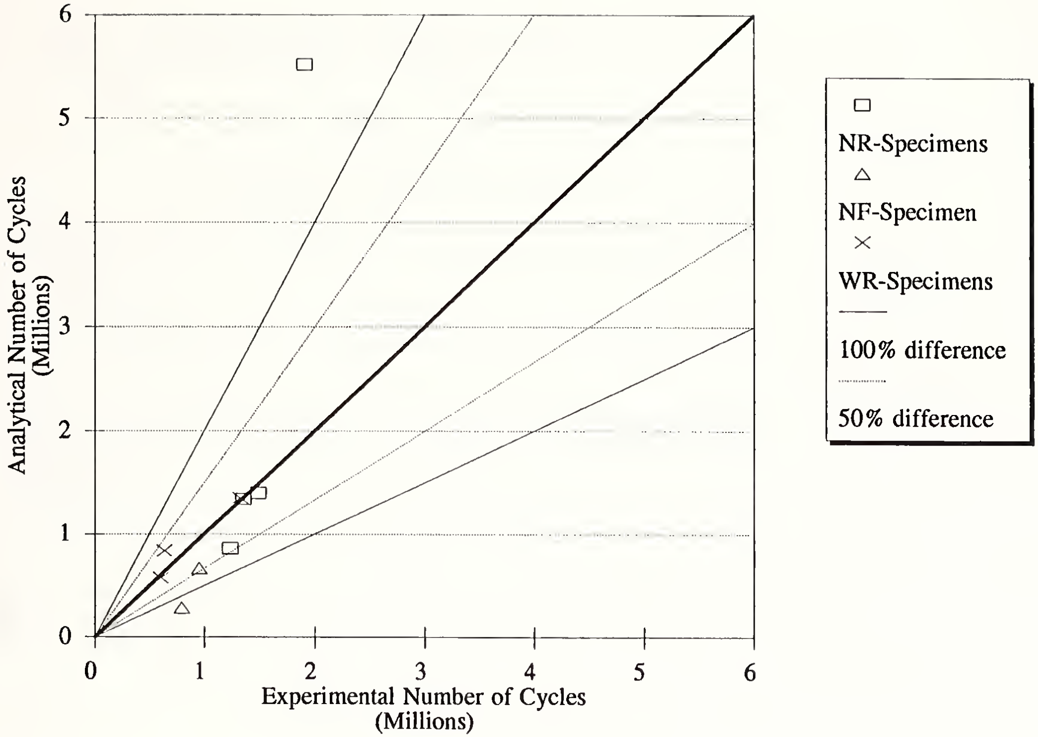

Fig. 9.6. Comparison between Experimental Life and Analytical Prediction for thePartial Bolted Splice Connection.

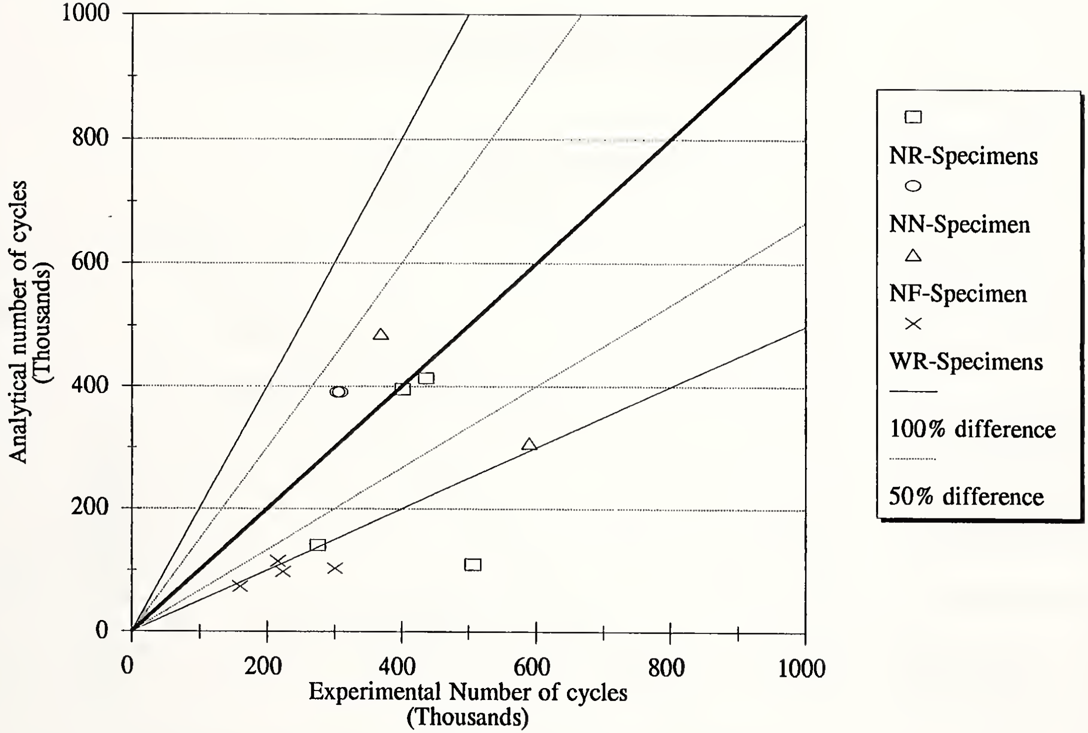

Fig. 9.7. Comparison between Experimental Life and Analytical Prediction for the Peening Repair Technique.

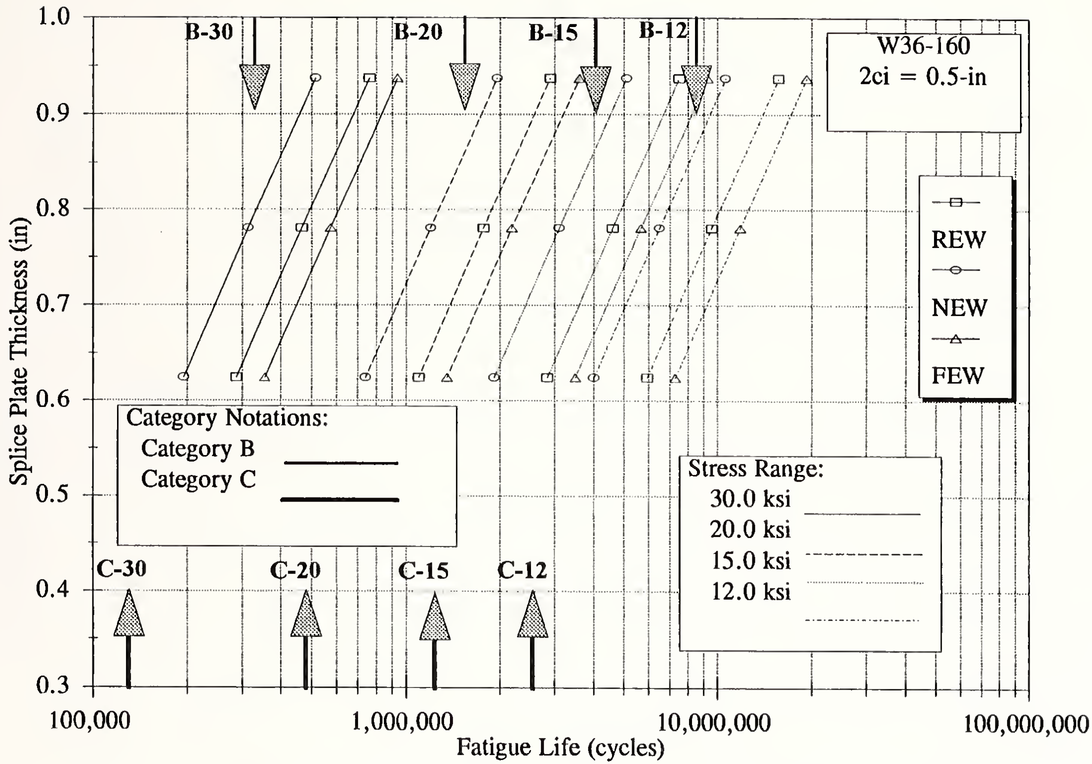

Fig. 9.8. Design Chart - Initial Crack Length 0.5-in.
(W 36 X 160)

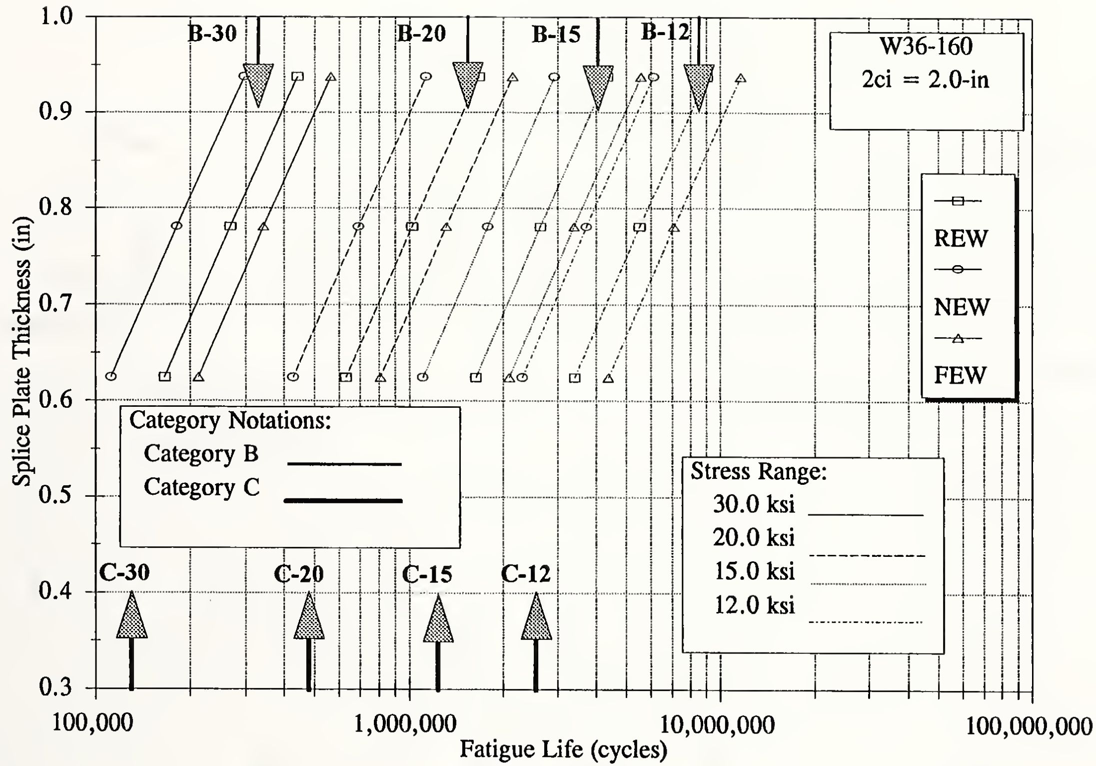

Fig. 9.9. Design Chart - Initial Crack Length 2.0-in.
(W 36 X 160)

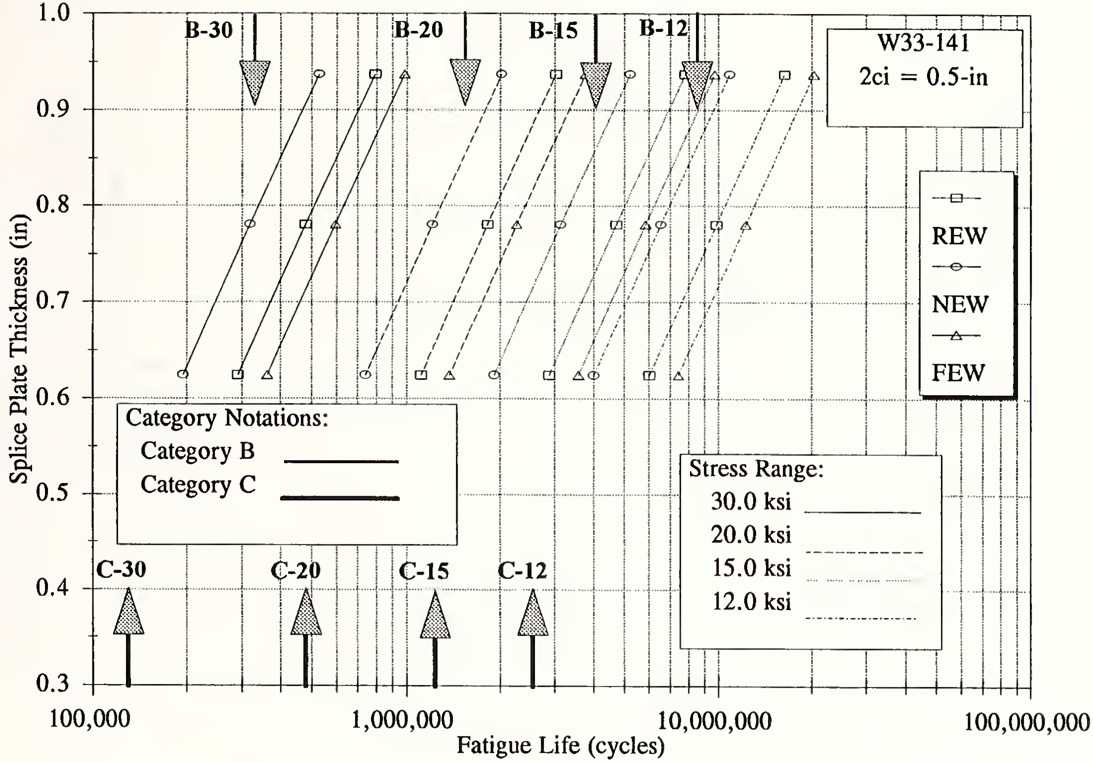

Fig. 9.10. Design Chart - Initial Crack Length 0.5-in.
(W 33 X 141)

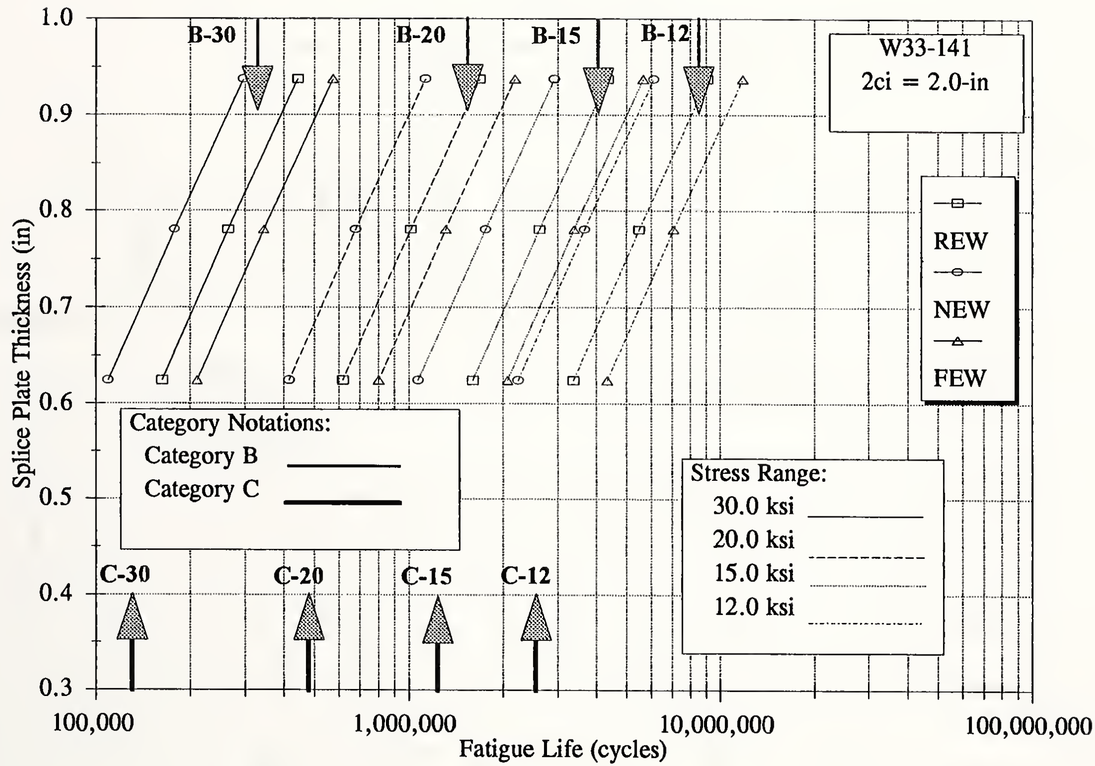

Fig. 9.11. Design Chart - Initial Crack Length 2.0-in.
(W 33 X 141)

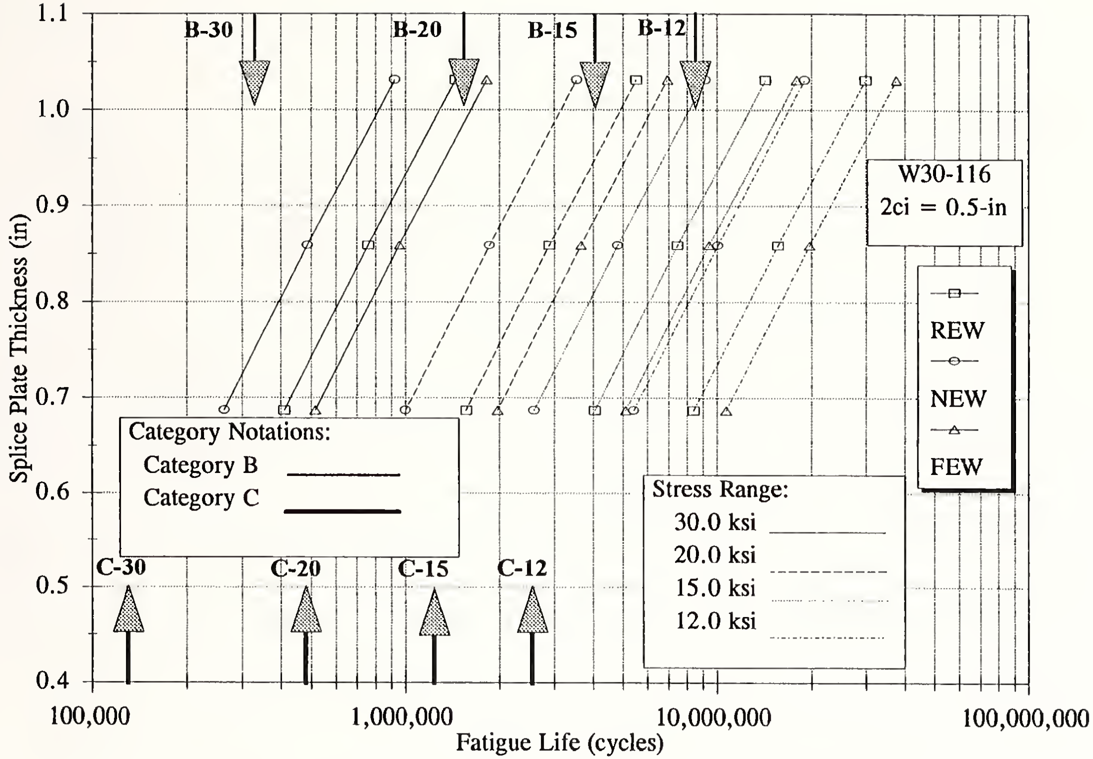

Fig. 9.12. Design Chart - Initial Crack Length 0.5-in.
(W 30 X 116)

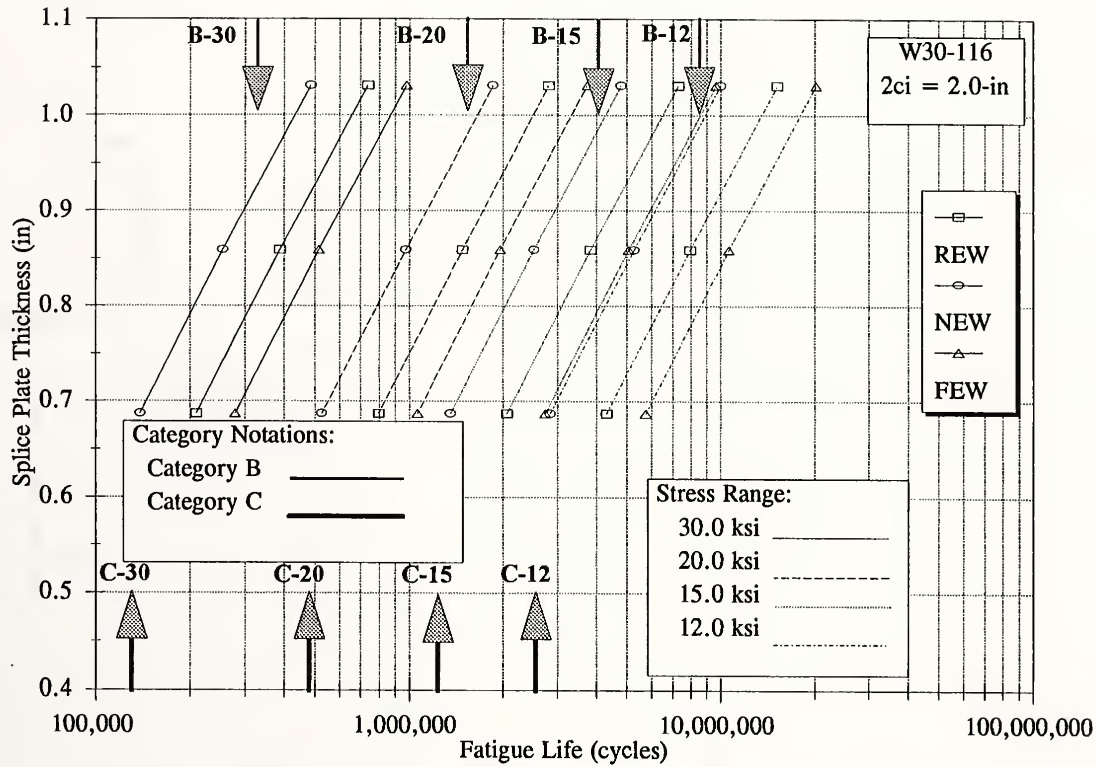

Fig. 9.13. Design Chart - Initial Crack Length 2.0-in.
(W 30 X 116)

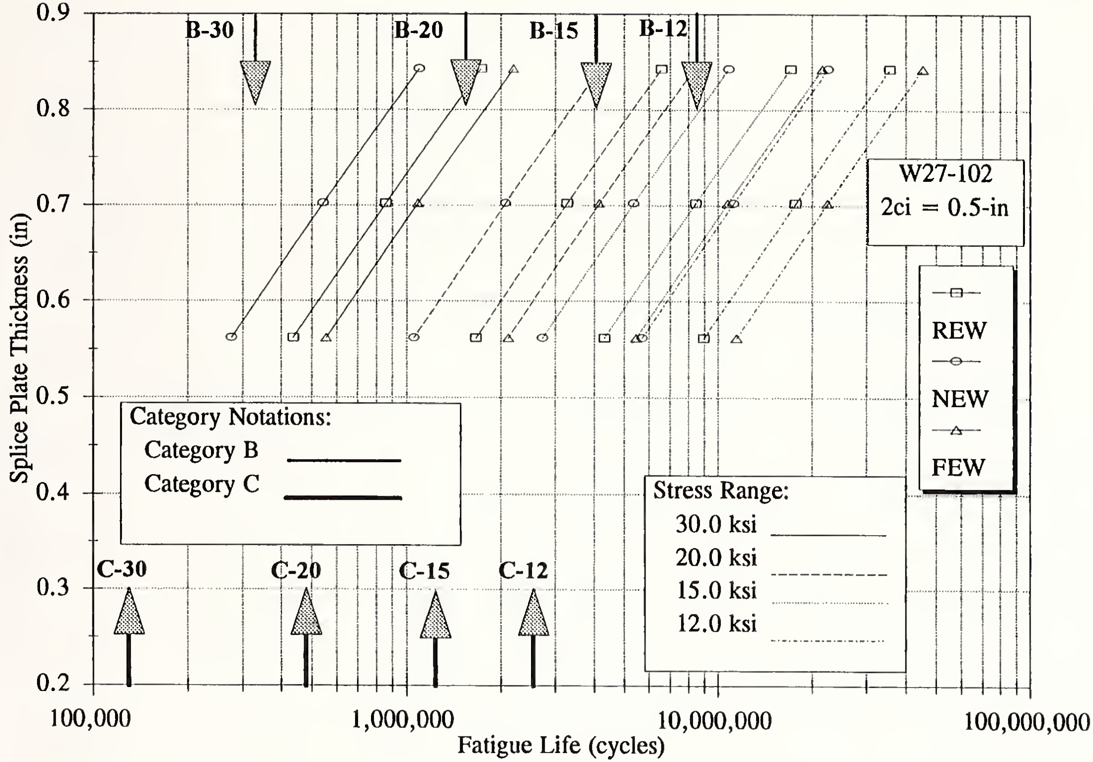

Fig. 9.14. Design Chart - Initial Crack Length 0.5-in.
(W 27 X 102)

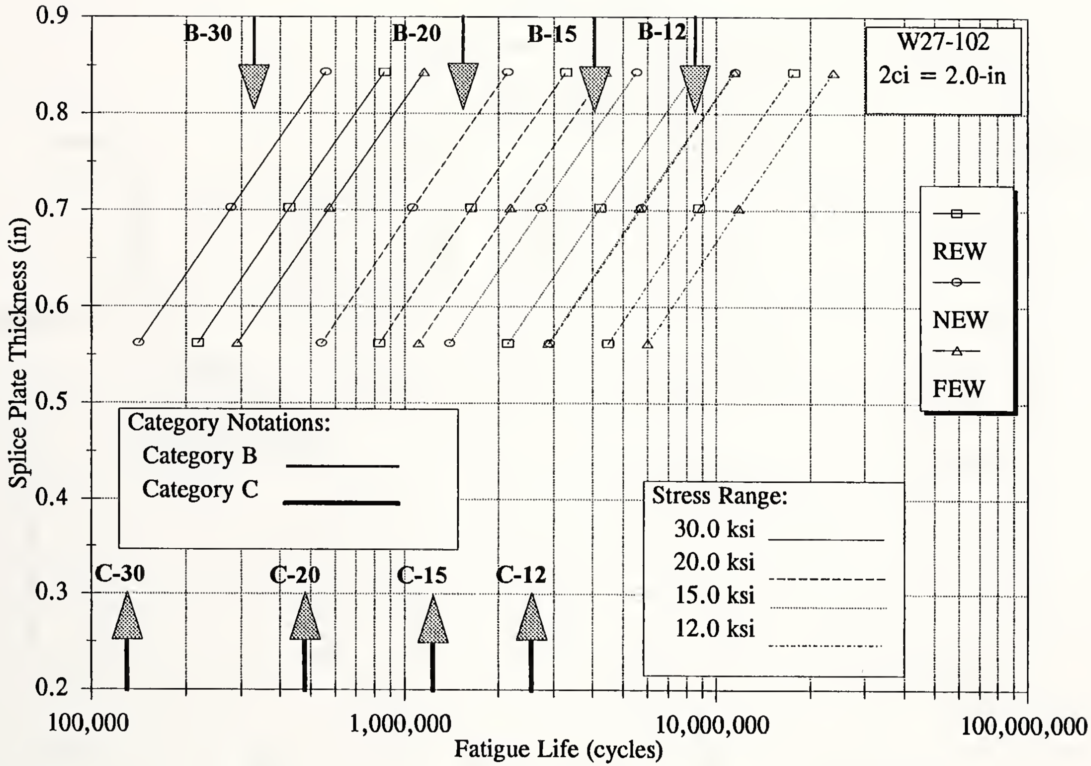

Fig. 9.15. Design Chart - Initial Crack Length 2.0-in.
(W 27 X 102)

CHAPTER 10
CONCLUSIONS, RECOMMENDATIONS, AND FUTURE RESEARCH NEEDS

10.1. Summary and Conclusions

The fatigue strength of steel girders with partial-length tapered, welded cover plates was investigated. Thirty three specimens were tested under constant amplitude, load controlled cycling. After pre-cracking, the cover plate ends were repaired using one of three repair methods: a friction type bolted splice plate connection, air-hammer peening of the weld toe, and a hybrid of the previous two called partial bolted splice. The fatigue strength of the repaired cover plate ends was then evaluated experimentally. To complement the experimental study, a computer program based on crack propagation was developed to estimate the fatigue life of welded cover plate ends repaired with one of the three repair techniques investigated.

Based on the experimental test results and analytical evaluations conducted in conjunction with this study, the following general conclusions can be stated:

1. Welded ends of the tapered cover plate detail consistently develop detectable cracks after a number of loading cycles equivalent to Category E design life.
2. Beams with wide cover plate details were found to initiate larger detectable cracks, at fewer number of load applications, than narrow cover plate weld details.
3. The initial crack size is a very important factor in determining the remaining life of the specimen and plays a significant role in controlling when complete fracture of the flange occurs.
4. Compression cracks frequently appeared in the repaired beams, even when the compression side was peened prior to testing. Three out of four non-peened ends developed compression cracks. This ratio dropped to 6 out of 32 when the cover plate ends were lightly peened prior to cycling.
5. Neither the 5/16-in nor the 7/16-in bolted splice plates completely prevented subsequent crack growth, except when the splice repair was installed prior to crack initiation.
6. Splice plate thickness has a notable influence on crack growth rate after repair. Thicker plates increase the effective moment of inertia and decrease the stresses in the beam flange. Consequently, the cracks grew much slower when 7/16-in splice plates were used

rather than 5/16-in plates. Only one of the flanges repaired using the 7/16-in plate completely fractured, although the ends repaired with this specific detail had initial crack sizes larger than those in the ends repaired using the 5/16-in plate.

7. Both the 5/16-in and the 7/16-in splice plates significantly improved the fatigue life of the various cover plate details. For both thicknesses, the splice plate detail enabled the beams with pre-cycled fatigue cracks to sustain more additional loading cycles than Category B design strength - roughly 1,500,000 cycles at a 20-ksi stress range.
8. When the initial fatigue cracks caused the beam flange to fracture completely, the 5/16-in splice plates were able to pick up the flange force and still carry a significant number of loading cycles after beam flange fracture. In one case, the beam carried about 900,000 cycles of 20-ksi stress range after fracture of the flange.
9. Peening is a moderately effective method for repairing pre-cracked cover plated beams if the crack length is smaller than about 1/4-in to 3/8-in. In that case, peening can extend the fatigue life of the detail such that an additional number of loading cycles roughly equivalent to a Category D level can be applied prior to failure.
10. Peening was found to be a very effective method to increase the fatigue life of non-cracked cover plate ends for the return end-weld detail. Tests demonstrated that peening improved the fatigue strength of the detail to a Category B' level. Similar results would be expected for the full end-weld cover plate detail, although no tests were conducted with this detail condition.
11. Peening is not recommended for the no end-weld detail. Cracks may grow under the cover plate or initiate in regions adjacent to the cover plate which are inaccessible for treatment by peening. In that case, only small improvement of the fatigue life, or perhaps no improvement, can be expected.
12. The partial bolted splice plate repair procedure is an effective method of repairing pre-cracked welded cover plate ends. The installation of a partial bolted splice after first crack detection can significantly improve the fatigue strength of the detail. It was found that an additional number of loading cycles equivalent to a Category C design life could be applied after repair.
13. Similar to the bolted splice detail, the partial bolted splice repair did not prevent subsequent crack growth. However, after the flange fractured the partial bolted splice

plate detail was able to sustain a number of loading cycles. In one case, the beam carried 874,000 loading cycles of 20.0-ksi stress range after flange fracture.

14. Of the repair details investigated in this study, the bolted splice repair was clearly the most effective and produced the greatest repair fatigue life.

10.2. Recommendations for Use in Bridge Construction

The following section presents recommendations obtained from results and observations acquired during this study:

1. The bolted splice plate connection is the most reliable method of repairing cracked cover plate ends. It is recommended that a slip-critical bolted splice plate connection be used to repair cracked cover plate ends whenever possible.
2. It is recommended that peening be used to significantly extend the fatigue life of details with welded, partial-length cover plates that have not developed detectable fatigue cracks.
3. It is recommended that peening be used to only repair cracks that are 1/4-in in length or less.
4. Use of the partial bolted splice plate connection is not recommended unless clearance is the governing factor at the site location. The partial bolted splice connection has a lower fatigue life than the bolted splice connection, and the additional cost of the bottom splice plate is not too significant compared with the increase in fatigue strength obtained.

10.3. Future Research Needs

The following are suggestions for future work on the fatigue behavior of steel beam with welded cover plates:

1. The previously mentioned conclusions and recommendations are based on the results of 33 test specimens. Thirty one specimens were tested under 20.0-ksi stress range while the remaining two specimens were tested under 15.0-ksi stress range. Additional tests conducted at lower stress ranges would model actual bridge conditions and provide more complete information on the long-term viability of the repair details.
2. The computed fatigue crack propagation lives for peened cover plate ends were based on an assumed residual stress distribution near the cover plate weld. To improve the accuracy

of the propagation model, additional tests are needed to better define the residual stress distribution.

3. The cover plate repair detail should be evaluated in the field. Measurements are needed to determine the effectiveness of repair details installed in the field.

LIST OF REFERNCES

LIST OF REFERENCES

1. AISC (1986). Manual of Steel Construction, Load and Resistance Factor Design, First Edition.

2. Albrecht, P., and Yamada, K. (1977). "Rapid Calculation of Stress Intensity Factors", *Journal of the Structural Division*, ASCE, Vol. 103, No. ST2, pp. 377-389.

3. ANSYS (1993). Engineering Analysis System, General Purpose Finite Element Program, Swanson Analysis Systems, Inc., Version 5.0, Houston, Pennsylvania.

4. Barsom, J.M., and Rolfe, S.T. (1987). "Fracture and Fatigue Control in Structures", Applications of Fracture Mechanics, Second Edition, Prentice-Hall, Inc., Englewood Cliffs, New Jersey.

5. Eason, E.D., Gilman, J.D., Jones, D.P., and Andrew, S.P. (1988). "Technical Basis for a Revised Fatigue Crack Growth Rate Reference Curve for Ferritic Steels in Air", Fatigue Initiation, Propagation, and Analysis for Code Construction, Winter Annual Meeting, ASME, Materials Properties Council.

6. Fisher, J.W., Frank, K.H., Hirt, M.A., and McNamee, B.M. (1970). "Effect of Weldments on the Fatigue Strength of Steel Beams", NCHRP Report No. 102, Transportation Research Board, National Research Council, Washington D.C.

7. Fisher, J.W., Sullivan, M.D., and Pense, A.W. (1974). "Improving Fatigue Strength and Repairing Damage", Fritz Engineering Laboratory Report No. 385.3, Office of Research, Lehigh University, December.

8. Fisher, J. W., and Yen, T. B. (1977). "Fatigue Strength of Steel Members with Welded Details", *Engineering Journal*, American Institute of Steel Construction, Vol. 14, No. 4, 118-129.

9. Grundy, P., and Teh, S. (1985). "Fatigue Strength of Beams at Cover Plate Terminations", Metal Structures Conference, Performance of Structures, Melbourne, Institution of Engineers, Australia, pp. 148-153.

10. Hausammann, H., Fisher, J.W., and Yen, B.T. (1983). "Effect of Peening on Fatigue Life of Welded Details", Proceeding of the W.H. Munse Symposium, Behavior of Metal Structures, Research to Practice, ASCE National Convention, Philadelphia, PA, May 17, pp. 70-83.

11. Munse, W.H., and Stallmeyer, J.E. (1962). "Fatigue in Welded Beams and Girders", Bulletin No. 315, Highway Research Board, National Research Council, Washington, D.C.

12. Newman, J.C. Jr., and Raju, I.S. (1981). "An Empirical Stress Intensity Factor Equation for the Surface Crack", *Engineering Fracture Mechanics*, Vol. 15, No. 1-2, pp. 185-192.

13. Paris, P.C. (1964). "The Fracture Mechanics Approach to Fatigue", Fatigue an Interdisciplinary Approach, Syracuse University Press, Syracuse, N.Y., pp. 107-127.

14. Quinn, B. (1991). "The Effect of Profile and Root Geometry on the Strength of Fillet Welds", M.Sc. Thesis, Volumes I and II, Purdue University.

15. Raju, I.S., and Newman, J.C. Jr. (1979). "Stress Intensity Factors for a Wide Range of Semi-Elliptical Surface Cracks in Finite Thickness Plates", *Engineering Fracture Mechanics*, Vol. 11, pp. 817-829.

16. Sahli, A.H., Albrecht, P., and Vannoy, D.W. (1984). "Fatigue Strength of Retrofitted Cover Plates", *Journal of Structural Engineering*, ASCE, Vol. 110, No. 6, 1374-1388.

17. Schilling, C. G., Klippstein, K. H., Barsom, J. M., and Blake, G. T. (1975). "Fatigue of Welded Steel Bridge Members under Variable Amplitude Loading", NCHRP Report No. 188, Transportation Research Board, National Research Council, Washington, D.C.

18. "Standard Specifications for Highway Bridges", (1989). American Association of State Highway and Transportation Officials, 14th Edition, Washington, D.C.

19. Task Committee on Flexural Members (1967). "Commentary on Welded Cover-Plated Beams", *Journal of the Structural Division*, ASCE, Vol. 93, No. ST4, 95-122.

20. Welsch, W.H. (1990). "A Concept for Preventing Repeated Weld Repairs of Bridge Structures", Extending the Life of Bridges, ASTM STP 1100, G.W. Maupin, Jr., B.C. Brown, and A.G. Liechtenstein, Eds., American Society for Testing and Materials, Philadelphia, 44-52.

21. Yamada, K., and Hirt, M.A. (1982). "Fatigue Crack Propagation from Fillet Weld Toes", *Journal of the Structural Division*, ASCE, Vol. 108, No. ST7, pp. 1526-1540.

22. Yongii, S., and Yanman, Y. (1987). "Assessment of Fatigue Safety Behavior of Welded Cover Plate Girders", Proceedings of the 1st German-Chinese Conference, Benijing, ISBN 3-87155-413-8, pp. 185-189.

APPENDICES

APPENDIX A
BRIDGE SURVEY RESULTS

A.1. General

The following sections present the results of the survey on fatigue of steel bridges. First a blank copy of the survey is presented. Then the tabulated results are given for each state. Finally, comments provided by various respondents for each question are presented.

A.2. Steel Bridge Survey

The following pages present a blank copy of the survey on fatigue of steel bridges. A copy of this survey was sent to the bridge engineer in each state highway department in the U.S. Telephone contacts were made in all state highway departments to identify the person who should receive a copy of the survey. The survey packages were sent out at the end of January, 1992. A return date of February 28,1992 was reported, providing about one month to complete and return the survey.

STEEL BRIDGE SURVEY
Please return before February 28, 1992

1. Indicate the approximate percentage of the following bridge types used in your state:
   ______ Steel
   ______ Concrete
   ______ Timber
   ______ Other (Indicate Type: ______________________________)

   If steel is not used for the bridges in your state, please sign and return the survey.

2. The following details are commonly used to increase the section modulus of steel bridge girders:
   ______ a. Cover plates
   ______ b. Increase in flange thickness
   ______ c. Increase in flange width
   ______ d. All of the above used
   ______ e. Section modulus <u>not</u> changed at all
   ______ f. Others (Indicate: ______________________________)

   If cover plate details are not used in your state then skip to Question No. 11.

3. Cover plate details are mostly:
   ______ a. Partial length
   ______ b. Continuous over the entire girder length
   ______ c. Both types used

4. For partial length cover plates, the plates mostly are:
   ______ a. Welded
   ______ b. Bolted
   ______ c. Some details are bolted and others are welded (give percentages)
   ______ d. Not applicable

5. The most common welding process used for welded partial-length cover plates is:
   ______ a. Shielded Metal Arc Welding
   ______ b. Submerged Arc Welding
   ______ c. Flux Core Arc Welding
   ______ d. Gas Metal Arc Welding
   ______ e. Other (Specify: ______________________________)
   ______ f. Not applicable

6. For welded partial length cover plates, the plate ends are generally:
   ______ a. Tapered
   ______ b. Rounded
   ______ c. Square
   ______ d. Other (Specify: ____)

7. The cover plates used with the girders are generally:
   ______ a. Wider than the girder flange
   ______ b. More narrow than the girder flange
   ______ c. Neither wider nor narrower than the girder flange, both widths are common

8. The cover plate welds are usually:
   ______ a. Continuous welds
   ______ b. Intermittent welds
   ______ c. Both types used (Give percentages: __________________________)

9. The ends of the cover plates are typically
   ______ a. Welded
   ______ b. Not welded
   ______ c. Both welded and unwelded details are used

10. Have any fatigue problems developed at the cover plates details used in your steel bridges?
    ______ a. Yes (Specify below. Attach a sketch as needed.)
    ______ b. No

Routine Inspection

11. What are the normal inspection periods?
    ______ a. Two years
    ______ b. Other (Specify: ____________________________________)

12. What are the methods used for ordinary (routine) inspections?
    ______ a. Visual
    ______ b. Other (Specify Below)

13. What is the minimum crack size that you believe can be detected by the inspection procedures used during ordinary inspections?

If no fatigue cracking problems have been encountered in your state, then please:

(1) Note this condition,
(2) sign the survey on the last page,
(3) return the survey in the enclosed, self-addressed envelope.

14. Approximate age of the bridges that have developed fatigue cracking problems (please identify the type of detail that developed cracks):
    ______ a. Less than 5 year old
    ______ b. 5 to 10 years old
    ______ c. 10 to 20 years old
    ______ d. 20 to 30 years old
    ______ e. More than 30 years old

15. If during ordinary inspections a crack was detected or suspected to exist, what additional nondestructive methods are typically used in this case?
    ______ a. Visual with Magnifying Glass
    ______ b. Ultrasonic
    ______ c. Radiographic
    ______ d. Dye Penetrant
    ______ e. Acoustic Emission
    ______ f. Magnetic Particle
    ______ g. Other (Specify: ______________________________)

16. What is the approximate minimum crack size that your inspectors can detect when using the aforementioned NDT methods?

17. What criteria are used to evaluate the need for repair of the fatigue cracks which are detected?

18. Which of the following repair techniques have been utilized to eliminate or minimize fatigue crack growth (please identify detail type):
    ______ a. Use of splice plates in cracked region.
    ______ b. Use of large diameter cores to remove cracks.
    ______ c. Use of peening.
    ______ d. Use of gas-tungsten arc remelting.
    ______ e. Removal and replacement of cracked members.
    ______ f. Other (Specify below)

19. Provide specific details, procedures, or comments that you believe should be noted for the repair techniques that have been used. Feel free to attach any sketches or specifications used for detail repair if you believe that these would be useful.

20. How effective was the repair technique?
    ______ a. Very effective (crack stopped)
    ______ b. Not effective
    ______ c. Not in service long enough to judge

21. Since the repair, have any new cracks been detected?
    ______ a. Yes
    ______ b. No **(If no, please sign and return the survey.)**

22. Indicate the size and location of cracks detected after repair.

23. How was the additional cracking detected?

24. What did you do?

Thank you for your help. Please return the survey in the enclosed envelope by February 28, 1992 to:

Professor Mark D. Bowman
School of Civil Engineering
Purdue University
1284 Civil Engineering Building
West Lafayette, IN 49707-1284

______________________________ ____________________

Signature Date

_____ Check here if you would like to receive a copy of the survey results.

Address for survey results: ______________________________

____

____

____

A.3. Survey Results

The following pages present the results of the survey on fatigue of steel bridges. A total of 51 surveys were sent out, and forty-six responses were received - a 90 percent return. One state sent back two responses. The checked answers are marked "CK", while the non-checked answers are marked "NCK". At the end of states list, the number of checked answers, or number of positive answers are reported. Whenever the answer involved numerical information, the average of the responses is presented at the end of the list. To keep the answers of each state confidential, the name of the state is omitted and the order has been shuffled.

State	% Types of Bridges			Commonly Used Details			
	Steel	Concrete	Timber	Cover Plates	Increase Flange Thickness	Increase Flange Width	Section not Changed
State 1	30	65	5	CK	CK	CK	NCK
State 2	35	35	30	CK	CK	CK	NCK
State 3	41	47	11	CK	CK	CK	NCK
State 4	60	40	0	CK	CK	CK	NCK
State 5	60	30	7	CK	CK	CK	NCK
State 6	63	37	0	CK	CK	NCK	NCK
State 7	12	82	6	CK	CK	CK	NCK
State 8	20	79	1	CK	CK	CK	NCK
State 9	13	86	1	NCK	CK	CK	NCK
State 10	50	50	0	CK	CK	CK	NCK
State 11	36	63	1	CK	CK	CK	NCK
State 12	44	50	0	CK	CK	CK	NCK
State 13	40	60	0	CK	CK	CK	NCK
State 14	19	79	1	CK	CK	CK	NCK
State 15	15	85	0	CK	CK	CK	NCK
State 16	30	40	29	CK	CK	CK	NCK
State 17	68	30	2	CK	CK	CK	NCK
State 18	100	0	0	NCK	NCK	NCK	CK
State 19	65	29	2	CK	CK	CK	NCK
State 20	72	27	1	NCK	NCK	NCK	NCK
State 21	31	49	20	CK	CK	CK	NCK
State 22	30	70	0	CK	CK	CK	NCK
State 23	35	53	12	CK	CK	CK	NCK
State 24	42	56	2	CK	CK	CK	CK
State 25	20	75	5	CK	CK	CK	NCK
State 26	58	35	4	CK	CK	CK	NCK

State	% Types of Bridges			Commonly Used Details			
	Steel	Concrete	Timber	Cover Plates	Increase Flange Thickness	Increase Flange Width	Section not Changed
State 27	33	49	17	CK	CK	CK	NCK
State 28	30	73	7	NCK	CK	CK	NCK
State 29	75	22	2	CK	CK	CK	NCK
State 30	30	70	0	CK	CK	CK	NCK
State 31	51	45	1	CK	CK	CK	NCK
State 32	41	47	12	CK	CK	CK	NCK
State 33	15	80	5	NCK	NCK	NCK	NCK
State 34	38	57	1	CK	CK	CK	NCK
State 35	53	42	3	CK	CK	CK	NCK
State 36	32	67	1	NCK	CK	CK	NCK
State 37	20	70	10	NCK	CK	CK	NCK
State 38	29	70	1	CK	CK	CK	NCK
State 39	72	25	3	CK	CK	CK	NCK
State 40	60	40	0	CK	CK	CK	NCK
State 41	10	85	5	NCK	CK	CK	NCK
State 42	58	40	1	CK	CK	CK	NCK
State 43	25	75	0	NCK	CK	CK	NCK
State 44	46	43	11	NCK	CK	CK	NCK
State 45	3	92	5	CK	CK	CK	NCK
State 46	38	34	20	CK	CK	CK	NCK
Results	40.17	53.87	5.33	36	43	42	2

State	Cover plates are		Partial Length Cover Plates		
	Partial Length	Continuous on Whole Length	Welded	Bolted	Not Applicable
State 1	CK	NCK	CK	NCK	NCK
State 2	CK	NCK	CK	NCK	NCK
State 3	CK	NCK	CK	NCK	NCK
State 4	NCK	CK	CK	CK	NCK
State 5	CK	NCK	CK	NCK	NCK
State 6	CK	NCK	CK	NCK	NCK
State 7	CK	CK	CK	NCK	NCK
State 8	CK	NCK	CK	NCK	NCK
State 9	NCK	NCK	NCK	NCK	NCK
State 10	CK	CK	CK	NCK	NCK
State 11	CK	NCk	CK	NCK	NCK
State 12	CK	CK	NCK	NCK	NCK
State 13	CK	NCK	CK	NCK	NCK
State 14	CK	NCK	CK	CK	NCK
State 15	CK	CK	CK	NCK	NCK
State 16	CK	NCK	CK	NCK	NCK
State 17	CK	NCK	CK	NCK	NCK
State 18	NCK	NCK	NCK	NCK	NCK
State 19	CK	CK	CK	NCK	NCK
State 20	CK	NCK	CK	NCK	NCK
State 21	CK	NCK	CK	NCK	NCK
State 22	CK	NCK	CK	NCK	NCK
State 23	CK	NCK	CK	NCK	NCK
State 24	CK	NCK	CK	NCK	NCK
State 25	NCK	CK	CK	NCK	NCK
State 26	CK	CK	CK	NCK	NCK

State	Cover plates are		Partial Length Cover Plates		
	Partial Length	Continuous on Whole Length	Welded	Bolted	Not Applicable
State 27	CK	NCK	CK	NCK	NCK
State 28	NCK	NCK	NCK	NCK	NCK
State 29	CK	CK	CK	NCK	NCK
State 30	CK	NCK	CK	NCK	NCK
State 31	CK	NCK	CK	NCK	NCK
State 32	CK	NCK	CK	CK	NCK
State 33	NCK	NCK	NCK	NCK	NCK
State 34	CK	CK	CK	CK	NCK
State 35	CK	NCK	CK	NCK	NCK
State 36	NCK	NCK	NCK	NCK	NCK
State 37	NCK	NCK	NCK	NCK	NCK
State 38	CK	NCK	CK	NCK	NCK
State 39	CK	NCK	CK	NCK	NCK
State 40	CK	MCK	CK	NCK	NCK
State 41	NCK	NCK	NCK	NCK	NCK
State 42	CK	CK	CK	CK	NCK
State 43	NCK	NCK	NCK	NCK	NCK
State 44	NCK	NCK	NCK	NCK	NCK
State 45	CK	NCK	CK	NCK	NCK
State 46	CK	NCK	CK	NCK	NCK

Results	35	11	36	5	0

State	Most Common Welding Process Used				Welded Partial Length Cover Plates are		
	Shielded Metal Arc	Submerged Arc	Flux Core Arc	Gas Metal Arc	Tapered	Rounded	Square
State 1	CK	CK	NCK	NCK	CK	NCK	NCK
State 2	CK	NCK	NCK	NCK	CK	NCK	NCK
State 3	NCK	NCK	NCK	NCK	CK	CK	CK
State 4	CK	CK	CK	CK	NCK	CK	NCK
State 5	CK	NCK	NCK	NCK	CK	NCK	NCK
State 6	NCK	CK	NCK	NCK	CK	NCK	NCK
State 7	CK	NCK	NCK	NCK	CK	NCK	NCK
State 8	CK	NCK	NCK	NCK	NCK	NCK	CK
State 9	NCK	NCK	NCK	NCK	NCK	NCK	NCK
State 10	CK	CK	NCK	NCK	CK	NCK	CK
State 11	CK	CK	NCK	NCK	Ck	NCK	NCK
State 12	CK	NCK	NCK	CK	CK	NCK	NCK
State 13	CK	CK	NCK	NCK	CK	NCK	CK
State 14	NCK	CK	NCK	NCK	CK	NCK	NCK
State 15	CK	CK	NCK	NCK	CK	NCK	NCK
State 16	NCK	CK	NCK	NCK	CK	NCK	NCK
State 17	NCK	CK	NCK	NCK	CK	NCK	NCK
State 18	NCK	NCK	NCK	NCK	NCK	NCK	NCK
State 19	NCK	CK	CK	NCK	CK	NCK	NCK
State 20	NCK	CK	NCK	NCK	CK	NCK	CK
State 21	NCK	CK	NCK	NCK	CK	NCK	NCK
State 22	NCK	CK	NCK	NCK	CK	NCK	NCK
State 23	CK	NCK	CK	NCK	CK	NCK	NCK
State 24	NCK	NCK	NCK	NCK	CK	NCK	NCK
State 25	NCK	NCK	NCK	NCK	NCK	NCK	NCK
State 26	NCK	CK	NCK	NCK	CK	NCK	CK

State	Most Common Welding Process Used				Welded Partial Length Cover Plates are		
	Shielded Metal Arc	Submerged Arc	Flux Core Arc	Gas Metal Arc	Tapered	Rounded	Square
State 27	NCK	CK	NCK	NCK	CK	NCK	CK
State 28	NCK	NCK	NCK	NCK	NCK	NCK	NCK
State 29	NCK	CK	NCK	NCK	CK	NCK	CK
State 30	NCK	CK	NCK	NCK	CK	NCK	NCK
State 31	CK	CK	NCK	NCK	NCK	NCK	CK
State 32	NCK	CK	NCK	NCK	CK	NCK	NCK
State 33	NCK	NCK	NCK	NCK	NCK	NCK	NCK
State 34	CK	CK	CK	CK	CK	CK	CK
State 35	NCK	CK	NCK	NCK	CK	NCK	CK
State 36	NCK	NCK	NCK	NCK	NCK	NCK	NCK
State 37	NCK	NCK	NCK	NCK	NCK	NCK	NCK
State 38	CK	CK	NCK	NCK	CK	CK	CK
State 39	NCK	CK	NCK	NCK	CK	NCK	NCK
State 40	NCK	CK	NCK	CK	NCK	NCK	CK
State 41	NCK	NCK	NCK	NCK	NCK	NCK	NCK
State 42	NCK	CK	NCK	NCK	CK	NCK	NCK
State 43	NCK	NCK	NCK	NCK	NCK	NCK	NCK
State 44	NCK	NCK	NCK	NCK	NCK	NCK	NCK
State 45	CK	NCK	NCK	NCK	CK	NCK	NCK
State 46	CK	CK	NCK	NCK	CK	NCK	NCK

Results	17	27	4	4	32	4	13

State	Cover Plates compared to Flange Width are		Cover Plates Welds are		Cover Plate Ends are	
	Wider	More Narrow	Continuous	Intermittent	Welded	Not Welded
State 1	NCK	CK	CK	NCK	CK	NCK
State 2	NCK	CK	CK	NCK	CK	NCK
State 3	NCK	CK	CK	CK	CK	CK
State 4	NCK	CK	CK	NCK	CK	NCK
State 5	CK	CK	CK	NCK	CK	NCK
State 6	CK	CK	CK	NCK	CK	NCK
State 7	NCK	CK	CK	NCK	CK	NCK
State 8	NCK	CK	CK	NCK	CK	NCK
State 9	NCK	NCK	NCK	NCK	NCK	NCK
State 10	NCK	CK	CK	NCK	CK	NCK
State 11	NCK	CK	CK	CK	CK	NCK
State 12	CK	CK	CK	CK	NCK	CK
State 13	NCK	CK	CK	NCK	CK	NCK
State 14	NCK	CK	CK	NCK	CK	CK
State 15	NCK	CK	CK	NCK	CK	NCK
State 16	NCK	CK	CK	NCK	CK	NCK
State 17	NCK	CK	CK	NCK	CK	NCK
State 18	NCK	NCK	NCK	NCK	NCK	NCK
State 19	CK	CK	CK	NCK	CK	NCK
State 20	NCK	CK	CK	NCK	CK	NCK
State 21	NCK	CK	CK	NCK	CK	NCK
State 22	CK	CK	CK	NCK	CK	CK
State 23	NCK	CK	CK	NCK	NCK	CK
State 24	NCK	CK	CK	NCK	CK	NCK
State 25	NCK	CK	CK	NCK	CK	NCK
State 26	NCK	CK	CK	NCK	CK	CK

State	Cover Plates compared to Flange Width are		Cover Plates Welds are		Cover Plate Ends are	
	Wider	More Narrow	Continuous	Intermittent	Welded	Not Welded
State 27	NCK	CK	CK	NCK	CK	NCK
State 28	NCK	NCK	NCK	NCK	NCK	NCK
State 29	CK	CK	CK	NCK	CK	NCK
State 30	NCK	CK	CK	NCK	CK	NCK
State 31	CK	CK	CK	NCK	CK	NCK
State 32	NCK	CK	CK	NCK	CK	NCK
State 33	NCK	NCK	NCK	NCK	NCK	NCK
State 34	CK	CK	CK	NCK	CK	NCK
State 35	NCK	CK	CK	NCK	CK	CK
State 36	NCK	NCK	NCK	NCK	NCK	NCK
State 37	NCK	NCK	NCK	NCK	NCK	NCK
State 38	NCK	CK	CK	CK	CK	CK
State 39	NCK	CK	CK	NCK	CK	NCK
State 40	NCK	CK	CK	NCK	CK	NCK
State 41	NCK	NCK	NCK	NCK	NCK	NCK
State 42	NCK	CK	CK	NCK	NCK	CK
State 43	NCK	NCK	NCK	NCK	NCK	NCK
State 44	NCK	NCK	NCK	NCK	NCK	NCK
State 45	NCK	CK	CK	NCK	CK	NCK
State 46	NCK	CK	CK	NCK	CK	CK
Results	8	37	37	4	34	10

State	Fatigue Problems?	Inspection Period (years)	Method of Inspection	Detectable Crack Size (in)	
				Length	Width
State 1	Yes	2	Visual	NCK	0.0075
State 2	No	2	Visual	0.375	NCK
State 3	No	2	Visual	NCK	NCK
State 4	Yes	2	Visual	NCK	0.005
State 5	Yes	2	Visual	0.125	NCK
State 6	No	2	Visual	NCK	NCK
State 7	No	2	Visual	0.1875	NCK
State 8	No	2	Visual	NCK	Crack Paint
State 9	NCK	2	Visual	NCK	0.015625
State 10	Yes	2	Visual	NCK	0.03
State 11	No	2	Visual	0.75	0.03
State 12	Yes	2	Visual	0.125	NCK
State 13	Yes	2	Visual	NCK	0.01
State 14	No	2	Visual	NCK	0.002
State 15	No	2	Visual	0.25	NCK
State 16	No	2	Visual	NCK	0.03125
State 17	No	2	Visual	NCK	0.039
State 18	NCK	2	Visual	NCK	0.0625
State 19	Yes	2	Visual	NCK	0.03125
State 20	No	2	Visual	NCK	NCK
State 21	Yes	1	Visual	NCK	Break Paint
State 22	Yes	2	Visual	0.25	NCK
State 23	Yes	2	Visual	0.25	Rust Paint
State 24	No	2	Visual	NCK	Hairline
State 25	No	2	Visual	NCK	0.015625
State 26	Yes	2	Visual	0.6	NCK
State 27	No	2	Visual	NCK	Hairline

State	Fatigue Problems?	Inspection Period (years)	Method of Inspection	Detectable Crack Size (in)	
				Length	Width
State 28	NCK	2	NCK	NCK	0.005
State 29	Yes	2	Visual	0.375	NCK
State 30	No	2	Visual	0.157	NCK
State 31	No	1	Visual	0.125	NCK
State 32	Yes	2	Visual	0.125	NCK
State 33	NCK	2	Visual	0.25	NCK
State 34	Yes	2	Visual	NCK	Hairline
State 35	Yes	2	Visual	NCK	NCK
State 36	NCK	2	Visual	NCK	NCK
State 37	NCK	2	Visual	NCK	0.002
State 38	No	3	Visual	NCK	Unknown
State 39	No	2	Visual	NCK	NCK
State 40	No	2	Visual	NCK	2E-05
State 41	NCK	2	Visual	NCK	Rust Stain
State 42	Yes	2	Visual	0.5	NCK
State 43	NCK	1	Visual	NCK	0.03125
State 44	NCK	2	Visual	NCK	hairline
State 45	No	2	Visual	NCK	0.01
State 46	No	2	Visual	NCK	0.01

Results	16	1.9565	45	0.2963	0.0188

State	Age of Bridges Having Fatigue Problems (years)				
	< 5	5 - 10	10 - 20	20 - 30	> 30
State 1	NCK	NCK	NCK	CK	NCK
State 2	NCK	NCK	NCK	CK	NCK
State 3	NCK	CK	NCK	NCK	NCK
State 4	NCK	NCK	CK	NCK	NCK
State 5	NCK	CK	CK	NCK	NCK
State 6	NCK	NCK	NCK	NCK	NCK
State 7	CK	NCK	NCK	NCK	NCK
State 8	NCK	NCK	NCK	NCK	NCK
State 9	NCK	NCK	CK	NCK	NCK
State 10	CK	CK	CK	CK	CK
State 11	CK	CK	CK	CK	NCK
State 12	NCK	NCK	NCK	CK	NCK
State 13	NCK	NCK	NCK	CK	CK
State 14	NCK	NCK	NCK	NCK	NCK
State 15	CK	CK	CK	CK	NCK
State 16	NCK	NCK	NCK	NCK	NCK
State 17	NCK	NCK	NCK	NCK	NCK
State 18	NCK	NCK	CK	NCK	NCK
State 19	NCK	NCK	NCK	CK	CK
State 20	NCK	NCK	NCK	CK	NCK
State 21	NCK	CK	CK	CK	NCK
State 22	NCK	NCK	CK	NCK	NCK
State 23	NCK	CK	NCK	CK	CK
State 24	NCK	NCK	NCK	CK	NCK
State 25	NCK	NCK	NCK	NCK	NCK
State 26	NCK	NCK	CK	CK	CK
State 27	NCK	NCK	NCK	CK	NCK

State	Age of Bridges Having Fatigue Problems (years)				
	< 5	5 - 10	10 - 20	20 - 30	> 30
State 28	NCK	NCK	NCK	CK	NCK
State 29	NCK	NCK	NCK	NCK	CK
State 30	NCK	NCK	NCK	CK	NCK
State 31	NCK	NCK	NCK	CK	NCK
State 32	NCK	NCK	NCK	NCK	CK
State 33	NCK	NCK	NCK	NCK	CK
State 34	NCK	CK	NCK	CK	NCK
State 35	NCK	NCK	NCK	CK	NCK
State 36	NCK	NCK	CK	NCK	NCK
State 37	NCK	NCK	NCK	CK	NCK
State 38	NCK	NCK	NCK	CK	CK
State 39	NCK	NCK	NCK	NCK	NCK
State 40	NCK	NCK	NCK	CK	NCK
State 41	NCK	NCK	NCK	NCK	CK
State 42	NCK	NCK	NCK	NCK	NCK
State 43	NCK	NCK	NCK	CK	NCK
State 44	NCK	NCK	NCK	NCK	CK
State 45	NCK	NCK	NCK	NCK	NCK
State 46	NCK	NCK	NCK	NCK	NCK

Results	4	8	11	23	11

State	Additional Inspection Methods in Case of Crack detection					
	Visual with M.G.	Ultrasonic	Radiographic	Dye Penetrant	Accoustic Emission	Magnetic Particle
State 1	CK	NCK	NCK	CK	NCK	CK
State 2	CK	CK	NCK	CK	NCK	NCK
State 3	CK	CK	NCK	CK	NCK	CK
State 4	CK	CK	NCK	CK	NCK	CK
State 5	CK	NCK	NCK	NCK	NCK	NCK
State 6	NCK	NCK	NCK	NCK	NCK	NCK
State 7	CK	CK	CK	CK	CK	CK
State 8	NCK	NCK	NCK	NCK	NCK	NCK
State 9	NCK	CK	NCK	CK	NCK	NCK
State 10	CK	CK	NCK	CK	NCK	CK
State 11	NCK	CK	NCK	CK	NCK	CK
State 12	CK	NCK	NCK	CK	NCK	NCK
State 13	NCK	CK	NCK	CK	NCK	NCK
State 14	NCK	NCK	NCK	NCK	NCK	NCK
State 15	CK	CK	NCK	CK	NCK	NCK
State 16	NCK	NCK	NCK	NCK	NCK	NCK
State 17	NCK	NCK	NCK	NCK	NCK	NCK
State 18	CK	CK	NCK	CK	NCK	NCK
State 19	CK	CK	CK	CK	NCK	CK
State 20	NCK	NCK	NCK	CK	NCK	NCK
State 21	CK	CK	NCK	CK	NCK	NCK
State 22	CK	NCK	NCK	CK	NCK	NCK
State 23	NCK	CK	NCK	NCK	NCK	NCK
State 24	NCK	NCK	NCK	CK	NCK	NCK
State 25	NCK	NCK	NCK	NCK	NCK	NCK
State 26	CK	NCK	NCK	CK	NCK	NCK
State 27	CK	NCK	NCK	CK	NCK	NCK

State	Additional Inspection Methods in Case of Crack detection					
	Visual with M.G.	Ultrasonic	Radiographic	Dye Penetrant	Accoustic Emission	Magnetic Particle
State 28	CK	NCK	NCK	CK	NCK	NCK
State 29	CK	CK	NCK	CK	NCK	CK
State 30	CK	CK	NCK	CK	NCK	NCK
State 31	CK	NCK	NCK	CK	NCK	CK
State 32	CK	CK	NCK	CK	NCK	CK
State 33	CK	CK	NCK	CK	NCK	CK
State 34	CK	CK	NCK	CK	CK	CK
State 35	CK	CK	NCK	CK	NCK	NCK
State 36	CK	CK	NCK	CK	NCK	NCK
State 37	CK	NCK	NCK	CK	NCK	NCK
State 38	CK	NCK	NCK	CK	NCK	NCK
State 39	NCK	NCK	NCK	NCK	NCK	NCK
State 40	CK	CK	CK	CK	CK	CK
State 41	CK	CK	NCK	CK	NCK	CK
State 42	CK	NCK	NCK	CK	NCK	CK
State 43	CK	CK	NCK	CK	NCK	CK
State 44	CK	CK	NCK	CK	NCK	CK
State 45	NCK	NCK	NCK	NCK	NCK	NCK
State 46	NCK	NCK	NCK	NCK	NCK	NCK
Results	31	24	3	35	3	17

State	Minimum Crack Size Detected by Aforementioned NDT Methods		Criteria Used to Evaluate the need for Repair of Detected Cracks
	Length (in)	Width (in)	
State 1	NCK	0.003	Memeber Location
State 2	0.125	NCK	Memebr Type
State 3	NCK	0.001	Generally repaired
State 4	Any Crack	Any Crack	All Cracks Repaired
State 5	0.375	NCK	Stress Range
State 6	NCK	NCK	NCK
State 7	CK	CK	Crack Growth
State 8	NCK	NCK	NCK
State 9	CK	CK	Consultant
State 10	CK	0.007	Member location
State 11	0.25	0.025	Redundancy
State 12	N/A	N/A	Structure Type
State 13	Any Size by UT	Any Size by UT	Redundancy
State 14	NCK	NCK	NCK
State 15	0.125	NCK	Propagation Rate
State 16	NCK	NCK	NCK
State 17	NCK	NCK	NCK
State 18	NCK	0.0625	Location of Crack
State 19	NCK	0.03125	All Cracks Repaired
State 20	NCK	NCK	Consultant
State 21	Any Size	Any Size	Redundancy
State 22	0.25	NCK	Own Judgement
State 23	NCK	Microscopic	AWS D1.5 90
State 24	NCK	Hairline	Type of Detail
State 25	NCK	NCK	NCK
State 26	0.2	NCK	Generally Repaired
State 27	NCK	< Hairline	Member Location

State	Minimum Crack Size Detected by Aforementioned NDT Methods		Criteria Used to Evaluate the need for Repair of Detected Cracks
	Length (in)	Width (in)	
State 28	NCK	Any Width	Own Judgemenet
State 29	0.125	NCK	All Cracks Repaired
State 30	0.16	NCK	Case-by-Case
State 31	0.125	NCK	Crack Growth
State 32	NCK	NCK	NCK
State 33	NCK	0.0625	Member Location
State 34	NCK	0.001	Memeber Location
State 35	NCK	Hairline	Location
State 36	NCK	NCk	Structure Type
State 37	NCK	0.002	Location
State 38	Unknown	Unknown	NCK
State 39	NCK	NCK	NCK
State 40	NCK	NCK	Member Location
State 41	CK	CK	All Cracks Repaired
State 42	0.2	NCK	Crack Size & Growth
State 43	NCK	Hairline	Memeber Location
State 44	CK	CK	Member Type
State 45	NCK	NCK	NCK
State 46	NCK	NCK	NCK
Results	0.1935	0.0217	35

State	Utilized Repair Techniques					
	Splice Plate	Large Cores	Peening	Remelting	Replace Memeber	Other
State 1	CK	CK	NCK	NCK	CK	CK
State 2	CK	NCK	NCK	NCK	NCK	CK
State 3	CK	CK	CK	NCK	CK	NCK
State 4	CK	CK	CK	NCK	CK	NCK
State 5	CK	CK	CK	NCK	NCK	NCK
State 6	NCK	NCK	NCK	NCK	NCK	NCK
State 7	NCK	NCK	NCK	NCK	NCK	CK
State 8	NCK	NCK	NCK	NCK	NCK	NCK
State 9	CK	CK	NCK	NCK	NCK	NCK
State 10	CK	CK	CK	NCK	CK	CK
State 11	CK	CK	NCK	NCK	CK	CK
State 12	NCK	NCK	CK	NCK	CK	NCK
State 13	CK	NCK	NCK	NCK	CK	CK
State 14	NCK	NCK	NCK	NCK	NCK	NCK
State 15	CK	CK	NCK	NCK	NCK	NCK
State 16	NCK	NCK	NCK	NCK	NCK	NCK
State 17	NCK	NCK	NCK	NCK	NCK	NCK
State 18	CK	NCK	NCK	CK	NCK	CK
State 19	CK	CK	NCK	NCK	NCK	CK
State 20	NCK	NCK	NCK	NCK	NCK	CK
State 21	CK	CK	CK	NCK	NCK	CK
State 22	CK	CK	NCK	NCK	NCK	CK
State 23	CK	NCK	NCK	NCK	NCK	CK
State 24	NCK	NCK	NCK	NCK	CK	CK
State 25	NCK	NCK	NCK	NCK	NCK	NCK
State 26	CK	CK	NCK	NCK	CK	NCK
State 27	CK	CK	NCK	NCK	CK	NCK

State	Utilized Repair Techniques					
	Splice Plate	Large Cores	Peening	Remelting	Replace Memeber	Other
State 28	CK	CK	NCK	NCK	NCK	NCK
State 29	NCK	NCK	NCK	NCK	NCK	CK
State 30	NCK	CK	NCK	NCK	NCK	NCK
State 31	CK	CK	CK	NCK	CK	NCK
State 32	CK	NCK	NCK	NCK	NCK	CK
State 33	CK	CK	CK	NCK	CK	CK
State 34	CK	CK	NCK	NCK	CK	NCK
State 35	CK	NCK	CK	NCK	NCK	CK
State 36	CK	CK	CK	NCK	CK	CK
State 37	CK	CK	NCK	CK	NCK	CK
State 38	NCK	NCK	NCK	NCK	CK	CK
State 39	NCK	NCK	NCK	NCK	NCK	NCK
State 40	CK	CK	NCK	NCK	NCK	NCK
State 41	CK	CK	CK	NCK	NCK	NCK
State 42	NCK	NCK	NCK	NCK	NCK	NCK
State 43	CK	CK	CK	NCK	CK	NCK
State 44	NCK	NCK	NCK	NCK	CK	CK
State 45	NCK	NCK	NCK	NCK	NCK	NCK
State 46	NCK	NCK	NCK	NCK	NCK	NCK

Results	28	23	12	2	17	21

State	How Effective was the Repair Technique			Any New Cracks After Repair
	Very Effective	Not Effective	Not in Service Long Enough	
State 1	CK	NCK	NCK	No
State 2	NCK	NCK	CK	NCK
State 3	CK	NCK	NCK	Yes
State 4	CK	NCK	NCK	No
State 5	NCK	NCK	CK	No
State 6	NCK	NCK	NCK	NCK
State 7	CK	NCK	NCK	No
State 8	NCK	NCK	NCK	NCK
State 9	NCK	NCK	NCK	No
State 10	CK	CK	CK	Yes
State 11	CK	NCK	NCK	Yes
State 12	NCK	NCK	CK	NCK
State 13	CK	NCK	NCK	Yes
State 14	NCK	NCK	NCK	NCK
State 15	NCK	NCK	NCK	NCK
State 16	NCK	NCK	NCK	NCK
State 17	NCK	NCK	NCK	NCK
State 18	CK	NCK	NCK	No
State 19	CK	NCK	CK	No
State 20	CK	NCK	NCK	No
State 21	CK	NCK	NCK	No
State 22	CK	NCK	NCK	No
State 23	NCK	NCK	CK	No
State 24	NCK	NCK	CK	No
State 25	NCK	NCK	NCK	NCK
State 26	NCK	NCK	CK	No
State 27	NCK	NCK	CK	No

State	How Effective was the Repair Technique			Any New Cracks After Repair
	Very Effective	Not Effective	Not in Service Long Enough	
State 28	CK	NCK	NCK	No
State 29	CK	NCK	NCK	No
State 30	NCK	NCK	CK	No
State 31	CK	NCK	NCK	Yes
State 32	NCK	NCK	CK	No
State 33	NCK	CK	NCK	Yes
State 34	CK	NCK	NCK	CK
State 35	CK	NCK	NCK	No
State 36	CK	NCK	CK	No
State 37	NCK	NCK	NCK	NCK
State 38	CK	CK	NCK	Yes
State 39	NCK	NCK	NCK	NCK
State 40	CK	NCK	NCK	No
State 41	NCK	NCK	CK	NCK
State 42	NCK	NCK	NCK	NCK
State 43	CK	NCK	NCK	No
State 44	NCK	NCK	CK	No
State 45	NCK	NCK	NCK	NCK
State 46	NCK	NCK	NCK	NCK
Results	21	3	14	7

State	For the New Crack What is?			
	Size	Location	Method of Detection	Action Taken
State 1	NCK	NCK	NCK	NCK
State 2	NCK	NCK	NCK	NCK
State 3	NCK	CK	Visual	CK
State 4	NCK	NCK	NCK	NCK
State 5	NCK	NCK	NCK	NCK
State 6	NCK	NCK	NCK	NCK
State 7	NCK	NCK	NCK	NCK
State 8	NCK	NCK	NCK	NCK
State 9	NCK	NCK	NCK	NCK
State 10	NCK	CK	Visual	CK
State 11	CK	CK	Visual	CK
State 12	NCK	NCK	NCK	NCK
State 13	CK	CK	Ultrasonic	CK
State 14	NCK	NCK	NCK	NCK
State 15	NCK	NCK	NCK	NCK
State 16	NCK	NCK	NCK	NCK
State 17	NCK	NCK	NCK	NCK
State 18	NCK	NCK	NCK	NCK
State 19	NCK	NCK	NCK	NCK
State 20	NCK	NCK	NCK	NCK
State 21	NCK	NCK	NCK	NCK
State 22	NCK	NCK	NCK	NCK
State 23	NCK	NCK	NCK	NCK
State 24	NCK	NCK	NCK	NCK
State 25	NCK	NCK	NCK	NCK
State 26	NCK	NCK	NCK	NCK
State 27	NCK	NCK	NCK	NCK

State	For the New Crack What is?			
	Size	Location	Method of Detection	Action Taken
State 28	NCK	NCK	NCK	NCK
State 29	NCK	NCK	NCK	NCK
State 30	NCK	NCK	NCK	NCK
State 31	1"	CK	Visual	CK
State 32	NCK	NCK	NCK	NCK
State 33	NCK	NCK	Visual	CK
State 34	NCK	NCK	Inspection	CK
State 35	NCK	NCK	NCK	NCK
State 36	NCK	NCK	NCK	NCK
State 37	NCK	NCK	NCK	NCK
State 38	CK	CK	Visual	CK
State 39	NCK	NCK	NCK	NCK
State 40	NCK	NCK	NCK	NCK
State 41	NCK	CK	Visual	CK
State 42	NCK	NCK	NCK	NCK
State 43	NCK	NCK	NCK	NCK
State 44	NCK	NCK	NCK	NCK
State 45	NCK	NCK	NCK	NCK
State 46	NCK	NCK	NCK	NCK

Results	4	7	9	9

A.4. Survey Comments

The following pages present the comments written in the survey. These comments could not be presented with the result section for clarity. The total question was not repeated prior to each comments. Instead, the question number, a summary of the question, and the different responses were written before any comments related to that response.

Question 1 :

Indicate the approximate percentage of the following bridge types used in your state:

- *Steel*

  Steel beams are normally confined to spans over 140', up to 140' pre-cast prestressed I-beams or box beams are used.

  No new steel bridges in the past 25 years.

- *Concrete*

- *Timber*

  Only for temporary crossings.

- *Other*

  3% metal culverts.

  1% masonary, aluminum, wrought iron, or cast iron.

  6% underfill and stone arch.

  1% corrugated metal.

  1% combination of steel, concrete, and timber.

  4% masonary and iron.

  0.2% tunnel, suspensions.

  5% steel truss.

  2% stone masonary and aluminum.

  1% truss.

  1% aluminum.

  7% prestressed concrete.

4% masonary and aluminum.

2% masonary.

1% various.

8% culverts.

Question 2 :

The following details are commonly used to increase the section modulus of steel bridge girders:

- *Cover plates*

Discontinued around 1972.

Used previous to 1985.

Discontinued in the past 8-10 years, some old bridges still have cover plates.

Existing structures only in-kind replacement to repair impact damage.

Discontinued around 1965.

On rolled beams only (very few in the last 20 years).

Seldom used, discouraged.

Before 1970.

Limited in recent years.

Only in the past practice.

Not commonly used at present, but were used extensively in the past practice.

Not used in the last 20 years.

Rarely.

- *Increase in flange thickness*

New construction.

After 1970.

- *Increase in flange width*

New construction.

Seldom used.

After 1970.

- *All of the above used*

- *Section modulus not changed at all*

    Rolled beams.

- *Others*

    Composite design.

    Composite construction.

    Post tensioning, composite.

    Increase the girder depth at the piers.

    Make the deck composite.

    Composite action.

    Increase in depth (haunched).

    Increase web depth if vertical clearance allows.

<u>Question 3 :</u>

Cover plate details are mostly:

- *Partial Length*

    Discontinued around 1972.

    Used previous to 1985.

    On rolled (WF) beams & built-up girders.

    Before 1975.

    Within 3' of bearings.

    Past practice.

- *Continuous over the entire girder length*

    On built-up girders.

    After 1975.

    Current practice.

- *Both types used*

<u>Question 4 :</u>

For partial length cover plates, the plates mostly are:

- *Welded*

    Discontinued around 1972.

    Used previous to 1985.

    New Construction.

    70%.

    Extended into field splice or abutment bearing.

    Past practice.

    75%.

- *Bolted*

    Retrofitting cover plates to bolted or riveted girders.

    30%.

    Terminal location in current practice.

    25%.

- *Some details are bolted and others are welded (give percentage)*

- *Not applicable*

<u>Question 5 :</u>

The most common welding process used for welded partial length cover plates is:

Unknown.

All permitted.

- *Shielded Metal Arc Welding*

    Current practice at ends, and past practice all welds.

    Occasionally.

- *Submerged Arc Welding*

    Current practice along sides, sometimes "hand held" at ends.

    95%-98%.

- *Flux Core Arc Welding*

- *Gas Metal Arc Welding*

- *Other (Specify)*

  All allowed if F_y is less than 50 ksi.

- *Not applicable*

<u>Question 6 :</u>

For welded partial length cover plates, the plate ends are generally:

- *Tapered*

  Discontinued around 1972.

  When welded to WF beams.

  In the 50's and 60's.

  Old bridges.

  15%.

  Past practice.

- *Rounded*

- *Square*

  For riveted built-up sections.

  Currently used.

  Recent.

  85%.

- *Other (Specify)*

  All three are used.

Question 7 :

The cover plates used with the girders are generally:

- *Wider than the girder flange*

    50%.

    Bottom.

- *More narrow than the girder flange*

    For Wf beams (welded).

    1 1/2" narrower than the flange.

    50%.

    Top.

    Past practice.

    With beams.

- *Neither wider nor narrower than the girder flange, both widths are common*

    For riveted built up girders, approximately equal widths.

Question 8 :

The cover plate welds are usually:

- *Continuous welds*

    95%.

    Not around ends of cover plates.

    Past practice.

    70%.

- *Intermittent welds*

    5%.

    30%.

- *Both types used (Give percentages)*

    Less than 5% intermittent.

Question 9 :

The ends of the cover plates are typically:

- *Welded*

    WF beams.

    Incorporated into field splice or abutment bearing.

    Past practice.

- *Not welded*

    Riveted built-up members.

- *Both welded and unwelded details are used*

Question 10 :

Have any fatigue problems developed at the cover plate details in your steel bridges?

- *Yes (Specify)*

    Small % have cracks at the cover plate ends.

    Cracks.

    Primarily attributable to poor welding practice and bad termination details.

    At the terminal ends of the welds at the tapered cover plate ends.

    In the end weld of cover plate.

    Cover plate ends.

    On a bridge in service for over 25 years, shallow cracks were detected in the weld across the end of the cover plate. The cracks did not extend into the flange and were repaired by grinding off the weld.

    Minor problem at the end of cover plate.

    In welds at ends where the welds were carried around the corner at the cover plate end (built in 1957), this method is not acceptable now.

    At the end weld or the toe.

    Fatigue cracks.

    At the cover plate end, propagates through the bottom flange.

    Very few old bridges.

Weld cracking through throat at end of cover plate, weld pool cracking.

At cover plate ends. One crack was found parallel to the taper weld.

- *No*

Cover plates bridges that have been rehabed have not shown a fatigue problem. When removing decks, the area around the cover plates ends is cleaned, visually inspected, and if crack is suspected dye penetrant is used.

Monitoring old designed bridges with short plates.

<u>Question 11 :</u>

What is the normal inspection period?

- *Two years*

Some are inspected on an annual or semi-annual basis depending on condition.

- *Other (Specify)*

1 year.

Fracture critical, underwater 4 years.

1 year.

1 year for fracture critical structures and when condition dictates. 4 years for concrete box culverts and continuous concrete structures that meet eligibility requirements.

1-5 years depending on several factors.

1 year on non-redundant structures.

1 year on state trunk highways.

<u>Question 12 :</u>

What are the methods used for normal inspection

- *Visual*

From the ground.

Supplemented by dye penetrant inspections.

Dye penetrant at ends of short cover plates.

With magnifying glass, if necessary use dye penetrant.

- *Other (Specify)*

Recently purchased an ultrasonic flaw detector which will be used for inspection of components of steel bridges.

Dye penetrant, magnetic particle, UT on pin and link assemblies.

"Hands on" inspection for questionable areas.

Arms length and closer with magnifying glass for mainline interstates.

<u>Question 13 :</u>

What is the minimum crack size that you believe can be detected by the inspection procedures used during ordinary inspections?

0.005"-0.010".

1/8" - 1/4" long, hairline width.

Sufficient to crack the paint system on the bridge.

Unaided eye 0.03", with magnification 0.02" - 0.01", dye penetrant 0.007", UT less than 0.007".

Depends on crack, available light, and paint condition.

For close inspection (less than 2') smaller than 1/8", for ground inspection with binoculars cracks larger than 1" and would be very rusted over (in this case it would be a guess).

If detail is accessible: 1/4" if lucky on visual, 3/4" most common.

Visual 1/16"-1/64", dye penetrant less than 1/64".

Cracks which break the paint film and show a line of rust.

Fairly small (1/4" or less), in many times it is not the crack itself that is detected, but the rust spot in the paint. An ultrasound testing machine is used, but visual inspection is still the most potential method.

If paint cracking or rust indicates a possible crack then dye penetrant is used. Hairline cracks are detectable.

1/64" easily, sometimes smaller.

Approximately 1-2 cm.

Hairline.

1/4"-1/2".

0.3-0.5 cm.

Hairline cracks, generally rust stain or paint cracking provide early clue.

Unknown.

Generally detected by rust staining. Hard to detect at initial stage due to heavy coat of paint.

0.5" visually, 0.2" with 8x glass.

Rust from crack frequently pinpoint small cracks. Areas subject to cracking are inspected at close ranges.

Hairline.

<u>Question 14 :</u>

Approximate age of the bridges that have developed fatigue cracking problems (please identify the type of detail that developed cracks):

- *Less than 5 year old*

A514 steel tie girder (box) at diaphragm locations.

Out of plane details.

- *5 to 10 years old*

Out of plane buckling at 2-girder cross frames.

Construction or utility supports.

Gusset plate detail.

Cracking in welds attaching lateral bracing gusset plates to girder webs, oversized bracing was vibrating excessively fatiguing the welds at an excessive rate, lateral bracing was removed and welds were ground.

Displacement induced fatigue.

- *10 to 20 years old*

Plug welds, poor welding on details, castings of sheave wheels on vertical lift bridge, flange transition welds (poor quality).

Secondary connections.

Diaphragm connection plates.

Flange crack.

Most common are web cracks at cross frame plate locations. Weld terminations at cover plate ends. Intersection of longitudinal and vertical web stiffeners.

- *20 to 30 years old*

Plug welds, poor welding on details, castings of sleeve wheels on vertical lift bridge, flange transition welds (poor quality).

Web cracks at flange to web coping (A588 steel).

Steel pier cap where the girder pierced the cap, cracks developed at the welds around the girder.

Out of plane bending.

Two girder system (riveted built in 1963), mis-located holes were plugged with welds causing cracks. Ends of cracks were drilled in 1987. Holding up well.

Out of plane bending at vertical stiffener on girder web.

Diaphragm to girder connection.

Lower lateral gusset plate-web welds; floor beam connections.

Load induced fatigue.

Out of plane bending at diaphragms and other welded connection details.

Stiffener & connector plates. Poor weld connections. Obsolete connection detail.

- *More than 30 years old*

Plug welds, poor welding on details, castings of sheave wheels on vertical lift bridge, flange transition welds (poor quality).

Flange cracks at splices, welded diaphragm connections.

Two girder system, cracks found in one of the main girders (riveted construction). Splice plates were bolted across the crack.

Stringer/floor beam connection, crack between web and flange below a web stiffener, flange/web and coping cracks.

<u>Question 15 :</u>

If during ordinary inspections a crack was detected or suspected to exist, what additional nondestructive methods are typically used in this case?

Method based on location.

Method depends upon where the crack is found.

- *Visual with Magnifying Glass*

Most common.

- *Ultrasonic*

Used.

On link hanger pins.

- *Radiographic*

- *Dye Penetrant*

Used.

Seldom used.

- *Acoustic Emission*

Tried on one location.

Special cases only.

- *Magnetic Particle*

On rare occasion.

Most common.

- *Other (Specify)*

Question 16 :

What is the approximate minimum crack size that your inspectors can detect when using the aforementioned NDT methods?

Any surface crack subsequent to propagation.

1/16" - 1/8".

Inspectors use dye penetrant and magnetic particle, other methods require specially trained technicians. The size depends on the sensitivity of the used method.

State inspectors have not used these methods.

Dye penetrant and magnetic particle 1/4" long or 0.002"-0.003" wide, UT down to the size of very small inclusions.

Ultrasonic should be able to detect any crack size.

Varies with used method.

Any existing crack can be detected.

Microscopic.

Hairline.

Less than hairline.

Any width with dye penetrant.

0.3-0.5 cm.

Hairline.

Unknown.

Too many variables to give definite answer.

UT detects extremely narrow cracks as well as slag and imperfections in weld. Normally hairline cracks are detected.

If exists, NDT will find it.

Question 17 :

What criteria are used to evaluate the need for repair of the fatigue cracks which are detected?

Member function (main or secondary), redundancy (fracture critical), crack growth evidence, crack size.

Member type and location, crack size, approximate age of crack, and crack propagation.

If crack is detected, it is generally drilled to stop it.

Any crack, after detection, is scheduled for repair.

Stress range.

Potential for crack growth and effect of fracture.

A consultant firm is responsible to evaluate fatigue cracks.

Crack location (primary or secondary), material, design, stress range, redundancy, amount of additional crack growth anticipated, remaining life of the structure, cost, replacement schedule, effects on traffic. All cracks in main load carrying members are arrested or the member is retrofitted in some manner.

All cracks are repaired as soon as possible. Cracks in non-redundant members are repaired immediately or traffic is routed.

Structures having significant traffic volumes are scheduled for rehabitation. Weld peening will be performed along with normal surfacing and safety upgrading practices.

Crack position (tension or compression), whether crack is active or dormant, redundancy of the structure, primary or secondary member.

Rate of propagation, tensile fracture critical.

Crack width, length, and location, and the visual progress of the crack.

No standard criteria, all cracks are repaired by drilling holes at crack tip, removing crack and rewelding, or replacing the member.

Consultant was retained to determine need and type of repair.

Presence of out of plane bending, tension zone, redundancy.

Mark the crack and monitor for a year or so, no set rules on repair, based on engineer's judgement.

As in bridge welding code, for fracture critical a flaw of any size should be repaired or defective part replaced.

Type of detail where crack exists.

In general all cracks should be repaired, when and how is the question.

Location is most important, if member failure would result in failure of the structure this would set priority treatment.

Own judgement, some type of work is done on all cracks.

All verified cracks are repaired.

Case by case basis, no specific criteria as fatigue cracking has been extremely limited.

Are they occurring in a tension zone, if the crack grows will it cause member failure.

Member function and load carrying capacity, estimated number of loading cycles and crack growth.

Location, criticality of the crack. Measures are usually taken once the crack is detected.

Location, structure type, ADT.

Structure type, crack location, ADTT, measured or calculated stress range.

Location (main or secondary member).

Crack ends determined by NDT. All cracking is to be arrested. 1" diameter holes are drilled at crack tip.

Crack size and growth.

Location, stress range, redundancy, and material toughness.

Type of member, size and location of crack, structure type.

Location, direction of travel and likely terminus, critical nature of member affected or likely to be affected.

Question 18 :

Which of the following repair techniques have been utilized to eliminate or minimize fatigue crack growth (please identify detail type):

No repair have been made to cracks at ends of cover plates.

- *Use of splice plates in cracked region*

Bolted plates or angles.

Once on a riveted girder built in 1963.

For cover plates.

Bolted splices.

- *Use of large diameter cores to remove cracks*

For cracks from coped corners.

At crack end to prevent further cracking.

- *Use of peening*

Not alone, only as added measure with other repairs.

For cover plate weld cracks.

- *Use of gas-tungsten arc remelting*

- *Removal and replacement of cracked members*

With improved details.

For cover plate weld cracks.

For clip angles.

- *Other (Specify)*

Grinding off cracked welds and re-weld.

Stop drilling at the end of crack.

Correction of poor detail to eliminate distortion induced cracking.

Post-tensioning & stiffening, removal of portions of members, especially at frozen bearings and "defective" pin-link joints, gouging & welding to eliminate crack, "rigidize" or "flexurize" joint details.

Large diameter holes to increase crack tip radius at the end, grinding.

Drill holes at the ends of the cracks.

Drill a 1/2" hole at the end of the crack.

Beams shipped to fabricator, old cover plates were removed and longer plates installed. Bolted cover plate extensions.

Use of holes at end of crack to stop the propagation.

Grinding out the weld defects and shallow cracks.

Make positive connection to the flange.

Drill ends of cracks.

Drill the crack tip, change the connection detail.

Cracks are removed by gouging and/or grinding and rewelding with an approved process. The back of the cover plate is often cut by 6".

Use of small diameter cores at crack end, removal and replacement of the region around the crack.

Placement of temporary members such as bearing chairs below some stringers to help support a cracked stringer floor beam connection.

Cracked weld removal by burrs, grindstones and flapper wheels. Drill hole (1" diameter) at crack tip.

Rigid attachments of cross frame plate (diaphragm stiffener) to flange.

Stiffen out of plane bending problem. Drill holes at crack tip and deburr edges of hole. Drill a hole at the end of the crack weld and test it using ultrasonic.

Question 19 :

Provide specific details, procedures, or comments that you believe should be noted for the repair techniques that you have used. Feel free to attach any sketches or specifications used for detail repair if you believe that these would be useful.

Cracks developed only in the weld. Grind out the cracks, check for cracks in bare metal, and re-weld. (no crack was found in the metal). Numerous cracks were found in girder webs due to out of plane bending at floor beam and diaphragm connections. For this type, drill out end of crack and monitor, and bolt angles or bent plates to give positive connection to flange.

Grinding should not be done perpendicular to the line of stress.

Drill a hole at the end of the crack is most often used for web cracks, splice plates are used to bridge cracks in flanges.

Drill a hole and provide a H.S. bolt.

Should try to eliminate all sharp corners, gouges, nicks, etc. Crack stopper holes should be rechecked after drilling with dye penetrant to insure that crack end was removed, if not redrill or grind out.

Some splice plate repairs can cover up and hide cracks making it very difficult to inspect and monitor any further crack growth.

More displacement induced cracking than load induced cracking.

Holes at ends of cracks (web damage). Cover plates (bolted) for flange splices.

All cracks occurred in floor system members and is due to out of plane bending.

Location of the crack end is very critical when using holes.

Question 20 :

How effective was the repair technique?

not yet done.

- *Very effective (crack stopped)*

Oldest is 2 years.

Where grinding can remove the entire crack, sometimes the holes at the crack tip are not large enough to arrest crack.

Crack arresting holes if crack end is eliminated.

In most cases.

Majority of repairs have been performed within the last 3-4 years.

90%.

- *Not effective*

Repairs tend to move cracks to other locations, splice plates with hole coring.

10%.

- *Not in service long enough to judge*

Seems to be working well.

For change in connection detail.

Cracks were later discovered in a different part of the bridge.

Moderately effective except when crack bifurcates.

<u>Question 21 :</u>

Since the repair, have any new cracks been detected?

- *Yes*

In one case.

Out of plane bending, crack jumps arrest holes.

Load induced cracking.

- *No*

Not yet done.

Load induced cracking has been generally retrofitted.

<u>Question 22 :</u>

Indicate the size and location of cracks detected after repair.

Crack propagated past relief hole.

Additional & new cracks at cross frame stiffener locations.

Small crack beginning at the opposite face of the end hole.

Sometimes the cracks extend through the hole 1/2"-1".

1" max, at the top of stiffeners, horizontal cracks at the toe of the weld between the web and the top flange.

Similar crack size and location.

The crack propagated through the hole.

<u>Question 23 :</u>

How was the additional cracking detected?

Visual.

Visual.

Visual.

Ultrasonic.

Routine inspection.

Visual.

Inspection.

Visual.

Visual.

<u>Question 24 :</u>

What did you do?

Plan to drill again.

Retrofit most by "flexurizing", unstiffened the stiffener to flange details.

Redrill crack end with a larger diameter core drill.

Drilled additional holes at the ends of cracks.

Redrill cracked-stop holes.

Continue repairs, get the structure on replacement list, replace cracked member.

At some locations just drill holes and monitor. At critical locations, conduct computer modeling research and develop simulated and filed applied retrofit.

Redrill crack tip and attempt to correct out of plane bending.

Repeated procedure. Drilled another 1" diameter hole at the new crack tip.

APPENDIX B
MATERIAL PROPERTIES

B.1. General

ASTM A36 mild steel was used for both the test beams and cover plates. Thirty specimens were fabricated from the same heat of steel, while the remaining three specimens were fabricated from a different heat of steel. The narrow cover plates were all fabricated from the same heat of steel; the wide cover plates were also fabricated from the same heat of steel. The mechanical and chemical properties of these different components, obtained both from the manufacturer and the investigators in this study, are presented in the following sections.

B.2. Mechanical Properties

The mechanical properties of the A36 steel used in this study were supplied by the manufacturer for the different heats of steel used. To check the supplied values, tension coupon tests conforming with the ASTM standards were cut from the remaining steel pieces. Four coupon tests were obtained from each of the different steel components (flange of the 30-specimen heat, web of the 30-specimen heat, flange of the 3-specimen heat, web of the three specimen heat, narrow cover plate, and wide cover plate).

These coupons were tested on a 200-kip MTS servo-hydraulic test machine to obtain the yield stress, ultimate strength, percent elongation, and modulus of elasticity. The results are listed, along with the manufacturer values, in Table B.1.

B.3. Chemical Composition

Four cubes 2-in × 2-in in cross-section were cut from the remaining pieces of steel. A complete chemical analysis was conducted. The composition obtained by chemical analysis, along with the manufacturer supplied values, are listed in Table B.2.

Table B.1. Mechanical Properties.

a- Flange of W 14 × 30 Heat (30 Specimens)

	Test Coupons					Manufacturer Values
	1	2	3	4	Average	
% Elongation*	26.56	28.13	28.13	25.78	27.15	29.00
Young's Modulus	**	29,250	29,290	28,640	29,060	---
Yield Stress	40.0	42.3	42.5	45.0	42.45	41.9
Ultimate Stress	63.6	62.0	62.3	62.3	62.55	67.5

b- Web of W 14 × 30 Heat (30 Specimens)

	Test Coupons					Manufacturer Values
	1	2	3	4	Average	
% Elongation*	26.56	21.88	32.81	32.03	28.32	29.00
Young's Modulus	30,440	30,270	30,870	32,540	31,030	---
Yield Stress	41.4	50.3	48.0	47.3	46.75	41.9
Ultimate Stress	63.9	66.0	64.8	65.0	64.93	67.5

c- Flange of W 14 × 30 Heat (3 Specimens)

	Test Coupons					Manufacturer Values
	1	2	3	4	Average	
% Elongation*	28.91	25.78	17.97	26.56	25.00	30.00
Young's Modulus	29,340	30,350	30,050	28,650	29,600	---
Yield Stress	42.4	41.1	42.5	42.6	42.15	39.9
Ultimate Stress	60.9	60.1	61.8	61.1	60.98	62.5

Values of stresses and Young's modulus are in ksi

* Based on 8" gage length

** No Gages were used

Table B.1. Mechanical Properties. (cont.)

d- Web of W 14 × 30 Heat (3 Specimens)

	Test Coupons					Manufacturer Values
	1	2	3	4	Average	
% Elongation*	24.22	25.78	35.16	30.47	28.91	30.00
Young's Modulus	31,140	28,840	27,890	32,090	29,990	---
Yield Stress	48.8	43.8	43.1	42.8	44.63	39.9
Ultimate Stress	63.2	58.9	58.3	60.1	60.13	62.5

e- Narrow Cover Plate (5.5-in wide)

	Test Coupons					Manufacturer Values
	1	2	3	4	Average	
% Elongation*	26.56	31.25	28.91	29.69	29.10	26.6
Young's Modulus	30,210	29,930	29,670	34,230	31,010	---
Yield Stress	46.6	47.5	46.8	47.5	47.1	44.4
Ultimate Stress	67.3	68.3	68.2	67.9	67.93	66.6

f- Wide Cover Plate (8.0-in wide)

	Test Coupons					Manufacturer Values
	1	2	3	4	Average	
% Elongation*	28.91	23.44	30.47	29.69	28.13	22.0
Young's Modulus	29,030	29,380	30,270	29,960	29,660	---
Yield Stress	48.4	48.2	48.3	48.6	48.38	46.5
Ultimate Stress	72.3	72.0	72.4	72.2	72.23	68.2

Values of stresses and Young's modulus are in ksi

* Based on 8" gage length

Table B.2. Chemical Composition.

a- W 14 × 30 Heat (30 Specimens)

Material	Chemical Composition %		
	Manufacturer	This Study	ASTM A36 Specifications
C	0.16	0.14	0.26 max
Mn	0.90	0.79	---
Si	0.03	< 0.05	---
P	0.015	0.015	0.04 max
S	0.022	0.016	0.05 max
Cu	---	0.06	0.20 min[1]
Ni	---	< 0.05	---
Cr	---	< 0.05	---
Mo	---	< 0.05	---
Al	---	< 0.008	---

b- W 14 × 30 Heat (3 Specimens)

Material	Chemical Composition %		
	Manufacturer	This Study	ASTM A36 Specifications
C	0.15	0.13	0.26 max
Mn	0.94	0.81	---
Si	0.04	< 0.05	---
P	0.01	0.009	0.04 max
S	0.026	0.017	0.05 max
Cu	0.03	< 0.05	20 min[1]
Ni	---	< 0.05	---
Cr	---	< 0.05	---
Mo	---	< 0.05	---
Al	---	< 0.008	---

[1] When copper steel is specified

Table B.2. Chemical Composition. (Cont.)

c- narrow cover plate

Material	Chemical Composition %		
	Manufacturer	This Study	ASTM A36 Specifications
C	0.13	0.13	0.25 max
Mn	0.76	0.69	---
Si	0.23	0.24	---
P	0.024	0.021	0.04 max
S	0.033	0.023	0.05 max
Cu	0.19	0.21	0.20 min[1]
Ni	0.11	0.09	---
Cr	0.11	0.08	---
Mo	0.023	< 0.05	---
Al	---	< 0.008	---

d- wide cover plate

Material	Chemical Composition %		
	Manufacturer	This Study	ASTM A36 Specifications
C	0.15	0.20	0.25 max
Mn	0.69	0.64	---
Si	0.21	0.14	---
P	0.006	0.01	0.04 max
S	0.027	0.02	0.05 max
Cu	0.13	0.38	0.20 min[1]
Ni	---	0.10	---
Cr	---	0.11	---
Mo	---	< 0.05	---
Al	---	< 0.008	---

[1] When copper steel is specified

APPENDIX C
COVER PLATE REPAIR PROCEDURES

The following sections describe the step-by-step procedures used for each cover plate repair method investigated.

C.1. Bolted Splice Repair

The bolted splice repair procedure is summarized by the following steps:

1- The beam is turned over (tension flange on top) to facilitate the drilling procedure.

2- Both sides of the tension flange and the connected plates are cleaned with the use of a degreaser to remove any oil that might decrease the friction between the flange and the plates.

3- The positions of the holes are marked with the use of a template with the same bolt pattern as the pre-drilled plates - see Fig. C.1.

4- A magnetic drill is used to drill 15/16-in diameter holes - see Fig. C.2.

5- The splice plates are connected to the beam flange with the use of the bolts. The bolt head is placed in the inside of the beam to facilitate the tightening of the nuts. Two ASTM F436 hardened washers were used, one between the bolt head and the splice plate and the other between the nut the splice plate.

6- The turn-of-nut tightening procedure described in the AASHTO specification is used for bolt installation . The bolts are placed in all holes of the connection and brought to a snug-tight condition. The snug-tight condition is attained when the plies of the joint are in firm contact, and can be accomplished by the full effort of a man using an ordinary wrench. The nuts are then tightened an additional one third of a turn with the use of an air pressure wrench - see Fig. C.3. An ordinary wrench is placed on the bolt head and held during the tightening procedure to make sure that all of the 1/3 turn is achieved through nut rotation.

7- Finally, the beam was turned over again to resume cycling.

C.2. Peening Repair

Based upon the findings by Hausammann et al. (1983), a peening procedure was selected for use in this study to repair fatigue cracks at the cover plate end welds. The following steps outline the procedure used to peen the tension side weld at the cover plate ends:

1- To facilitate the peening procedure, the beam is turned over so that the tension flange is facing upward. (Peening can also be performed from below the beam if the clearance is adequate.) The beam is peened from above because it is easier to control the peening tool in this position than when peening overhead.

2- The flange and the fillet weld are cleaned within the peening area with a wire brush.

3- Peening is performed using the hardened tool and a pneumatic hammer operated at 40 psi - see Fig. C.4. A total of six complete passes of the peening operation are performed around the weld, with each successive pass causing additional deformation of the base metal and the weld toe. The peening area includes about 2-in of the fillet welds parallel to the beam length along with all transverse welds at the end of the cover plate. The number of peening passes and the air hammer pressure were chosen after a review of the work conducted by Hausammann et al. (1983). Figure C.5 shows the surface deformation at the weld toe after one, four, and six passes of peening the tension flange at the cover plate ends. The weld toe surface is also shown in Fig. C.5.

4- The peened end is inspected using a 10X magnifying glass. When a crack located perpendicular to the direction of stress is visible after peening, then the peening is continued until all cracks disappear. (This condition did not happen during this study.)

5- The beam is then turned over to resume cycling.

To prevent the initiation of cracks in the compression flange, the cover plate ends welded to the compression flange were peened using a procedure similar to that used for the tension side welds. In that case, however, only one pass of peening at 30 psi air pressure was used. Figure C.6 shows the surface deformations induced during peening of the compression flange at the cover plate ends. Peening of the cover plate ends welded to the compression flange was mainly intended to release the tensile residual stresses induced during the welding process, and to induce compressive residual stresses that would slow the initiation of fatigue cracks. On the other hand, peening of the cover plate ends welded to the tension flange was intended to remove any initiated flaws in addition to releasing the tensile residual stresses. Thus, it was felt that peening the compression cover plate end welds should be less severe than peening the tension side. Hence, a value of 30 psi was selected for the air pressure and only one pass was applied.

C.3. Partial Bolted Splice Repair

The following steps outline the procedure used to repair the tension side weld at the cover plate ends:

1- The beam is turned over (tension flange on top) to facilitate the peening and drilling procedures.

2- Both sides of the tension flange and the connecting plates are cleaned with a de-greaser to remove any oil that might decrease the friction between the flange and the plates.

3- The positions of the holes for the splice connection are marked with the use of a template with the same bolt pattern as the pre-drilled plates.

4- A magnetic drill is used to drill 15/16-in diameter holes for the 7/8-in diameter high strength bolts.

5- Both sides of the flange are cleaned again to remove any oil from the drilling operation.

6- The weld toe area is peened using the same procedure described earlier.

7- The splice plates are connected to the beam flange with 7/8-in diameter ASTM A325 high-strength bolts. The bolt head is placed facing the inside of the beam to facilitate the tightening of the nuts. Two ASTM F436 hardened washers were used, one between the bolt head and the splice plate, and the other between the nut and the beam flange.

8- The turn-of-nut procedure described in the AASHTO specification is used for bolt installation. The bolts are placed in all holes of the connection and brought to a snug-tight condition. The snug-tight condition is attained when the plies of the joint are in firm contact, and can be accomplished by the full effort of a man using an ordinary wrench. An ordinary wrench is placed on the bolt head and held during the tightening procedure to make sure that all of the required 1/3 turn is achieved through rotation of the nut.

9- The beam is then turned over to resume cycling.

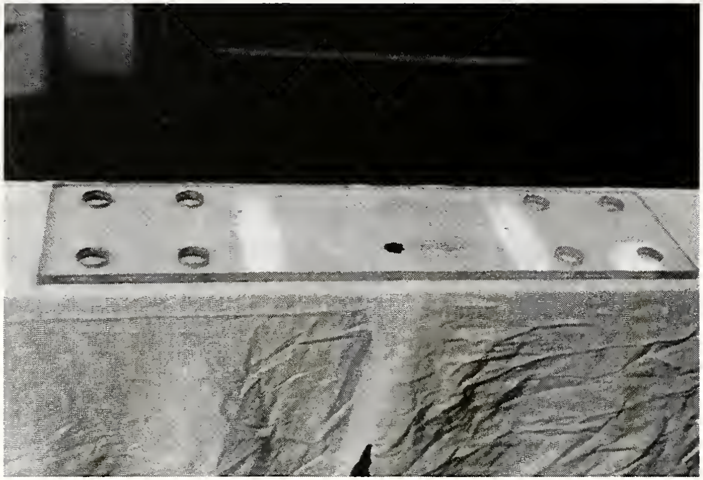

(a) Template

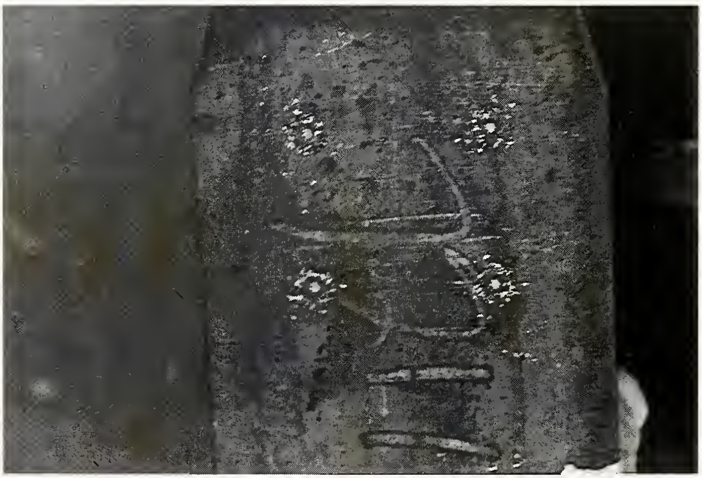

(b) Marked Holes

Fig. C.1. Hole Position Marking.

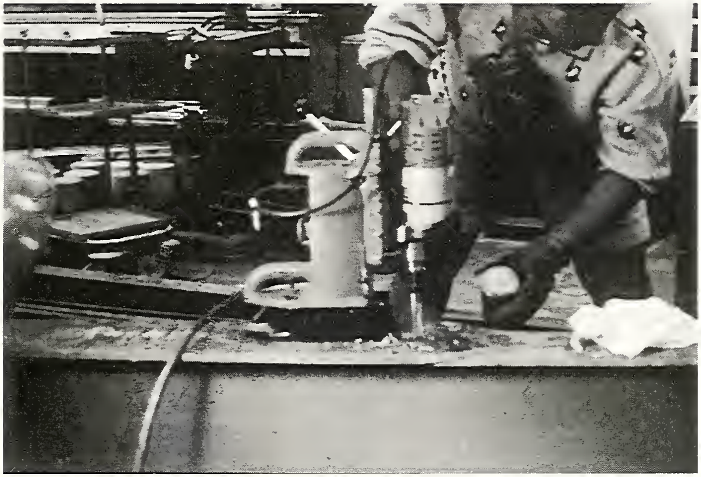

Fig. C.2. Hole Drilling.

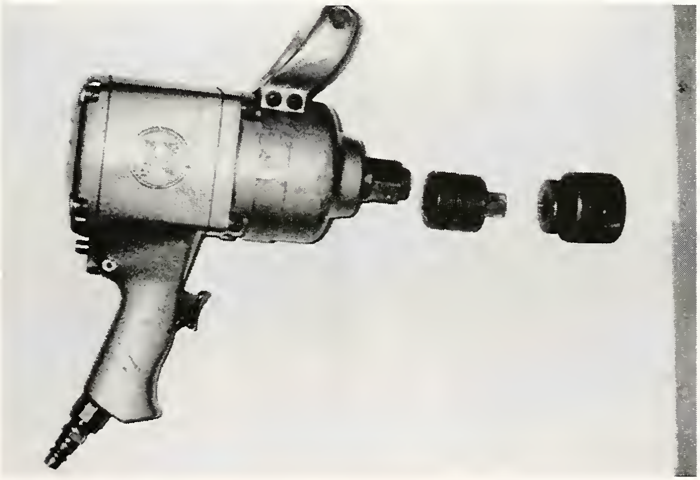

Fig. C.3. Air Pressure Wrench.

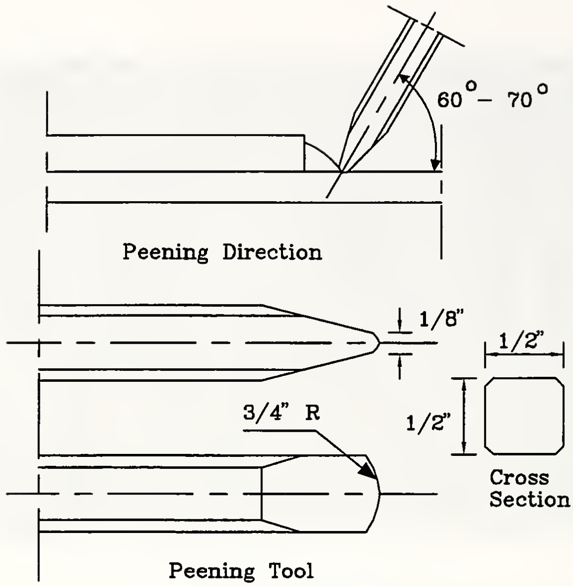

(a) Peening Tool

(b) Peening Operation

Fig. C.4. Air-Hammer Peening.

(a) Prior to Peening

(b) After One Pass of Peening

Fig. C.5. Surface Deformation at Cover Plate End Weld Toe Due to Peening.

(c) After Four Passes of Peening

(d) After Six Passes of Peening

Fig. C.5. Surface Deformation at Cover Plate End Weld Toe Due to Peening. (Cont.)

Fig. C.6. Surface Deformation Due to Air-Hammer Peening of Compression Flange.

APPENDIX D
CRACK SIZE AND NUMBER OF LOADING CYCLES
BEFORE AND AFTER REPAIR

D.1. General

This appendix presents a detailed discussion of the number of cycles applied and crack sizes measured during the experiments. This information was discussed in less detail in Chapters 5 to 8. The detail comments observed during each test are given in Table D.1 along with the crack sizes and number of loading cycles for each test specimen.

Table D.1. Crack Size and Loading Cycles Before and After Repair.

Specimen	End	Detectable Crack Size (in)		Final Crack Size (in)		Number of Loading Cycles (Thousands)		Notes
		W	E	W	E	Crack Detection	After Repair[6]	
DB1	N[1]	---	---	---	---	---	1,800	Beam thought to be cracked but no cracks were found at end of test. A 5 49/64" crack, 2" deep in the web, was found in the compression flange at 1,375,000 cycles. The beam was repaired with a 7/16" splice with drilling of the crack tip in the web.
	S[1]	---	---	---	---	---	1,800	Beam thought to be cracked but no cracks were found at end of test.
DB2	N[1]	3/16	---	15/32	1/2	200	1,800	A crack 1 19/64" found at 670,000 cycles in the compression flange which was peened. Compression side fractured at 951,000 cycles. Beam was then repaired with a 7/16" splice.
	S[1]	3/16	1/8	3 5/8		200	1,800	Cracks in the tension side at west and east side coalesced. A crack 39/64" found at 670,000 cycles in the compression flange which was peened. At 951,000 cycles, the beam was repaired with a 7/16" splice at the north side.
DB3	N[1]	7/32	---	1 25/64	1 3/32	200	1,800	
	S[1]	1/4	1/8	61/64	1 1/2	200	1,800	
NR1	N[1]	17/32	---	Fracture		240	2,000	Tension flange fractured at 1,564,000 cycles. A hole was drilled at the crack tip in the web.
	S[1]	5/16	3/8	Fracture		240	2,000	Crack was all the way through the flange east side at the end of test.

Table D.1. Crack Size and Loading Cycles Before and After Repair. (Cont.)

Specimen	End	Detectable Crack Size (in)		Final Crack Size (in)		Number of Loading Cycles (Thousands)		Notes
		W	E	W	E	Crack Detection	After Repair[6]	
NR2	N[2]	5/8	1/2	3 13/64		180	2,500	Weld at the compression west side fractured at 1,952,000 cycles. At 2,000,000 cycles, the 1" temporary repair plates were used for the compression flange. Tension cracks coalesced.
	S[2]	3/8	3/8	3 7/32		180	2,500	Tension cracks coalesced.
NR3	N[2]	---	3/8	2 11/32	2	200	3,000	Cracks from west and east side passed each other on different planes without joining.
	S[2]	---	7/16	1 5/32	1 11/32	200	3,000	A crack 2 15/16" long was detected at the compression flange at 1,883,000 cycles. The 1" thick repair plates were used. Cracks from west and east side passed each other on different planes without joining.
NR4	N[2]	7/32	11/16	3		165	2,000	Cracks coalesced.
	S[2]	3/8	5/16	1 1/2	1 7/16	165	2,000	Cracks from east and west sides passed each other on different planes without joining. A third crack 11/32" long formed between the weld returns starting from the west side.

Table D.1. Crack Size and Loading Cycles Before and After Repair. (Cont.)

Specimen	End	Detectable Crack Size (in)		Final Crack Size (in)		Number of Loading Cycles (Thousands)		Notes
		W	E	W	E	Crack Detection	After Repair[6]	
NR5	N[3]	---	---	5 3/8		75	1,511	At 1,509,000 cycles, a crack 5" long was observed. Only 1 3/4" of the east side of the flange remained un-cracked. This crack passed through the weld root at both the east and west sides. At 1,511,000 cycles, the crack propagated 1 1/2" into the web; only 1 3/8" of the east side flange remained un-cracked.
NR5	S[3]	---	---	5		75	1,186	At 1,186,000 cycles two cracks 2 22/32" and 3 4/32" long were observed at the east and west sides, respectively. The west side crack grew into the weld root, while the east side crack propagated at the weld toe. The 1" plates were used.
NR6	N[3]	---	---	6 1/2		75	1,006	At 881,000 cycles, two cracks 1 7/16" and 1 3/32" long were observed at the east and west sides of the weld root, respectively. At 1,006,000 cycles, the flange completely fractured. Only 1/4" was un-cracked at the west side of the flange. The crack propagated 3 3/4" into the web. A hole was drilled at the crack tip, and a bolt was placed in the hole. The 1" thick plates were used, and the test was resumed.
NR6	S[3]	---	---	5 1/8		75	1,773	At 1,508,000 cycles, a crack 3/4" long was observed at the west weld root. This crack propagated to 1 1/4" in length at 1,1702,000 cycles. At 1,755,000 cycles, the crack propagated to 4 5/32" long passing through the root of the east side weld. At 1,773,000 cycles, the flange completely fractured, only 1 20/32" remained un-cracked at the east side of the flange. The crack propagated 24/32" into the web.

Table D.1. Crack Size and Loading Cycles Before and After Repair. (Cont.)

Specimen	End	Detectable Crack Size (in)		Final Crack Size (in)		Number of Loading Cycles (Thousands)		Notes
		W	E	W	E	Crack Detection	After Repair[6]	
NR7[5]	N[4]	---	1/16	1/2	45/64	130	8,340	At 8340,000 cycles after repair, the compression flange fractured. The test was stopped.
	S[4]	5/32	---	31/32	29/64	130	8,340	At 5,446,000 cycles after repair, a 3" long crack was found in the compression flange west side. The crack propagated 1/2" into the web. The compression flange was ground and then joined with a full penetration weld. At 5,750,000 cycles, the flange fractured again at the same location. The same repair was repeated. At 6,540,000 cycles, the flange fractured one more time; a 5/16" splice connection was then used.
NR8[5]	N[2]	1/8	3/32	7/8	13/16	130	10,782	At 10,096,000 cycles, a 1 3/4" long root crack developed at the east return end weld of the compression flange. At 10,782,000 the compression flange fractured.
	S[2]	5/32	3/32	27/32	3/4	130	10,782	At 7,143,000 cycles a 3 1/2" long crack developed at the compression flange, east side. The 5/16" splice plate connection was used and the test was resumed. At 8,352,000 cycles a hole was drilled at the crack tip, a bolt placed in the hole, and the test was resumed.

Table D.1. Crack Size and Loading Cycles Before and After Repair. (Cont.)

Specimen	End	Detectable Crack Size (in)		Final Crack Size (in)		Number of Loading Cycles (Thousands)		Notes
		W	E	W	E	Crack Detection	After Repair[6]	
NR9	N[3]	1/4	3/16	5 1/2		120	265	At 264,000 cycles, a crack 3 15/32" long was found in the flange. The 1" thick plates were used and the test was resumed. At 275,000 cycles the total length was 4 5/32". At 400,000 cycles the 1" thick plates were removed and the test was continued for another 1,000 cycles after which the flange was completely fractured. At that time, the crack length was 5 1/2" long and it propagated about 1" into the web.
	S[3]	3/32	1/8	5 5/8		120	401	At 400,000 cycles a crack 4 7/32" long was found in the flange. The flange completely fractured at 401,250 cycles. At that time the total crack length was 5 5/8" long, this crack propagated 1 13/32" into the web.
NR10	N[3]	1/4	5/16	5 3/4		160	506	The east side crack was composed of two 1/8" long cracks. The flange completely fractured at 506,000 cycles. A crack 5.75" long was found in the flange; this crack propagated about 1 1/8" into the web.
	S[3]	---	1/8	6 1/8		160	436	At 432,000 cycles, a crack 4 7/8" long was found in the flange; this crack propagated about 11/16" into the web. At 436,000 cycles the flange fractured. At that time, the crack length was 6 1/8" while it propagated about 1 7/8" into the web. The 1" thick repair plates were used, and the test was resumed.

Table D.1. Crack Size and Loading Cycles Before and After Repair. (Cont.)

Specimen	End	Detectable Crack Size (in)		Final Crack Size (in)		Number of Loading Cycles (Thousands)		Notes
		W	E	W	E	Crack Detection	After Repair[6]	
NR11	N[4]	5/32	---	19/32	1 7/16	120	1,898	After the end of the test, the splice plates were removed. Two cracks 19/32" and 1 7/16" long were found at the west and east sides of the flange, respectively.
	S[4]	3/8	---	Fractured		120	1,898	The crack was composed of two cracks 1/4" and 1/8" long. At 1,410,000 cycles after repair, the crack was 4 19/32" long and propagated about 1 1/16" into the web. At 1,480,000 cycles, the flange fractured while the crack propagated about 2 3/4" into the web. A hole was drilled in the web at the crack tip, a bolt was placed in the hole. At 1,660,000 cycles after repair, the crack passed through the hole to about 6 1/4" into the web. A second hole was drilled, a bolt was placed in the hole, and the test was resumed. At 1,851,000 cycles after repair, the crack passed through the second hole to about 7 5/8" into the web. At 1,898,000 cycles after repair, the crack was about 8" into the web. The splice plates were then removed, and the 1" plates were clamped to the tension flange. The flange collapsed with the first cycle, and the 1" thick plates slipped. The test was stopped.

Table D.1. Crack Size and Loading Cycles Before and After Repair. (Cont.)

Specimen	End	Detectable Crack Size (in)		Final Crack Size (in)		Number of Loading Cycles (Thousands)		Notes
		W	E	W	E	Crack Detection	After Repair[6]	
NR12	N[4]	5/16	1/8	Fractured		140	1,800	The west side crack was composed of two cracks 1/4" and 1/16" long. At 1,185,000 cycles after repair, the crack was 1 5/8" long. At 1,347,000 cycles, the flange fractured, and the crack propagated about 4" into the web. A hole was drilled at the crack tip, a bolt was placed in the hole, and the test was resumed. At 1,610,000 cycles, the crack passed through the first hole to about 6" into the web. A second hole was then drilled, a bolt was placed in the hole, and the test was resumed.
	S[4]	3/8	---	Fractured		140	1,800	At 927,000 cycles after repair, the crack was 1 3/8" long. At 1,234,000 cycles, the flange fractured and the crack propagated about 3 1/4" into the web. A hole was drilled at the crack tip, a bolt was placed in the hole, and the test was resumed. At 1,430,000 cycles, the crack passed through the hole to about 6" into the web. A second hole was drilled, a bolt was placed in the hole, and the test was resumed. At 1,736,000 cycles, the crack passed through the second hole to about 7" into the web.
NN1	N[1]	3/16	---	1 1/8	1 13/32	160	1,800	
	S[1]	1/4	---	1 1/2	---	199	1,800	At 1,333,000 cycles a 1" long crack was observed at the compression flange - east side. The 1" thick plates were used. Two additional cracks 1 1/16 and 7/8" long were found under the cover plate.

Table D.1. Crack Size and Loading Cycles Before and After Repair. (Cont.)

Specimen	End	Detectable Crack Size (in)		Final Crack Size (in)		Number of Loading Cycles (Thousands)		Notes
		W	E	W	E	Crack Detection	After Repair[6]	
NN2	N[1]	---	3/16	1 19/32	2 22/32	140	1,800	
	S[2]	---	5/16	5/8	13/32	167	1,800	A compression crack 1 19/32" long formed at the east side of the top flange at 995,000 cycles. The beam was repaired using the 1" thick repair plates.
NN3	N[3]	---	---	5		75	308	At 304,000 cycles, a 4 1/2" long crack was observed. The crack was in the web fillet. At 308,000 cycles the crack grew to 5" in length. The 1" plates were used and the test was resumed.
	S[3]	---	---	5 1/16		75	413	At 413,000 cycles, a crack 5 2/32" long was observed. The test was then stopped.
NF1	N[1]	1/2	3/8	Fractured		200	1,800	Total crack size prior to repair was 1 3/8", as a third crack 1/2" long formed in the middle of the full end weld detail. Crack propagated into the fillet at 476,000 cycles. A hole was drilled at the crack tip in the web at 883,000 cycles. Tension flange fractured at 1,049,000 cycles. Crack was found to have passed through the drilled hole in the web at 1,340,000 cycles; a second hole was then redrilled.
	S[1]	9/16	1/4	Fractured		200	1,800	Crack propagated into the fillet at 650,000 cycles. A hole was drilled at the crack tip in the web at 883,000 cycles. Tension flange fractured at 1,179,000 cycles. Crack was found to have passed through the drilled hole in the web at 1,340,000 cycles; a second hole was then drilled.

Table D.1. Crack Size and Loading Cycles Before and After Repair. (Cont.)

Specimen	End	Detectable Crack Size (in)		Final Crack Size (in)		Number of Loading Cycles (Thousands)		Notes
		W	E	W	E	Crack Detection	After Repair[6]	
NF2	N[1]	1/8	1/4	Fractured		180	1,800	Total crack size prior to repair was 7/8" as a 1/2" long crack formed at the middle of the full end weld detail. Crack propagated into the web fillet at 810,000 cycles. Flange fractured at 1,095,000 cycles. A hole was drilled at the crack tip in the web and a bolt was put in the hole.
	S[2]	3/8	5/8	3 11/32		180	1,800	Total crack size prior to repair was 1 3/8" long as a 3/8" long crack formed at the middle of the full end weld detail. Crack propagated into the web fillet at 1,306,000 cycles. A 1 1/8" long compression crack at the west side was found at 1,457,000 cycles. The 1" thick plates were used and the test was resumed.
NF3	N[1]	9/32		Fractured		180	1,800	Crack propagated into the web fillet at 1,346,000 cycles. Tension flange fractured at 1,680,000 cycles.
	S[2]	1/2	3/8	2 31/32		200	1,800	Total crack length was 1 1/8" as a third crack 1/4" long formed in the middle of the full end weld detail. Crack propagated into web fillet at 1,680,000 cycles.

Table D.1. Crack Size and Loading Cycles Before and After Repair. (Cont.)

Specimen	End	Detectable Crack Size (in)		Final Crack Size (in)		Number of Loading Cycles (Thousands)		Notes
		W	E	W	E	Crack Detection	After Repair[6]	
NF4	N[3]	---	5/32	5 1/4		140	590	At 584,000 cycles a crack 3 7/8" long was found in the flange; that crack propagated about 11/16" into the web. At 590,000 cycles, the flange fractured. The crack was 5 1/4" long while it propagated about 1 1/8" into the web.
	S[3]	1/8	---	5 11/16		140	369	At 352,000 cycles a crack was detected in the southeast side fillet. No cracks could be seen from the bottom of the flange; while it could be seen from the top of the tension flange, only about 1 15/16" of the east side was not cracked. At 369,000 cycles the flange fractured. At that time the total crack was 5 11/16" long and propagated about 1 7/16" into the web. The 1" plates were used and the test was resumed.
NF5	N[4]	1/2		Fractured		200	1,152	At 955,000 cycles after repair, the crack was 3 1/2" long and propagated about 1/2" into the web. At 1,111,000 cycles, the flange fractured and the crack was 4 3/16" into the web. A hole was drilled, a bolt was placed in the hole, and the test resumed.
	S[4]	1/2	3/4	Fractured		200	1,152	A third crack 1/2" was found at the middle of the full end weld. At 800,000 cycles after repair, the flange fractured and the crack was 3 1/4" into the web. A hole was drilled at the crack tip, a bolt was placed in the hole. At 955,000 cycles, the crack passed through the hole to about 5 15/32" into the web. A second hole was drilled, and a bolt was placed in the hole. At 1,111,000 cycles, the crack passed through the second hole and was 6 3/4" into the web. At 1,152,000 cycles, the crack was 7 1/4" into the web.

Table D.1. Crack Size and Loading Cycles Before and After Repair. (Cont.)

Specimen	End	Detectable Crack Size (in)		Final Crack Size (in)		Number of Loading Cycles (Thousands)		Notes
		W	E	W	E	Crack Detection	After Repair[6]	
WF1	N[2]	1/8	1/2	Fractured		145	1,800	Total crack size prior to repair was 1 1/8" as a 1/2" long crack was found at the middle of the full end weld detail. Crack propagated into web fillet at 690,000 cycles. The crack propagated 1", 1 7/16", and 1 7/8" into the web at 1,025,000, 1,200,000, and 1,377,000 cycles, respectively. At 1,377,000 cycles a hole was drilled at the crack tip and a bolt was placed in the hole. At 1,744,000 cycles the flange fractured.
	S[1]	5/32	1/2	Fractured		180	1,800	At 515,000 cycles the crack propagated in the web fillet. At 900,000 cycles, the crack propagated 2 13/32" into the web while the flange completely fractured. A hole was then drilled at the tip of the web crack and a bolt was placed in the hole. At 1,377,000 cycles a second hole was drilled as the crack passed the first hole.
WF2	N[1]	5/32	---	Fractured		134	1,800	At 1,002,000 cycles the crack propagated in the web fillet. At 1,315,000 cycles a hole was drilled at the tip of the web crack and a bolt was placed in the hole. At 1,485,000 cycles the flange completely fractured.
	S[1]	3/16	3/32	Fractured		134	1,800	At 1,002,000 cycles the crack propagated into the web. At 1,315,000 cycles the flange was found to be completely fractured. A hole was then drilled at the crack tip and a bolt was placed in the hole.

Table D.1. Crack Size and Loading Cycles Before and After Repair. (Cont.)

Specimen	End	Detectable Crack Size (in)		Final Crack Size (in)		Number of Loading Cycles (Thousands)		Notes
		W	E	W	E	Crack Detection	After Repair[6]	
WF3	N[1]	7/32		Fractured		140	1,800	At 967,000 cycles the crack propagated 1" in the web. At 1,324,000 cycles the flange was completely fractured and the crack was 3" in the web. A hole was drilled at the crack tip, a bolt was placed in the hole, and the test was resumed.
	S[2]	7/16		4		140	1,800	At 1,473,000 cycles the crack propagated in the web fillet.
WR1	N[1]	5/32	3/16	Fractured		143	1,800	At 820,000 cycles the crack propagated in the web fillet. At 1,174,000 cycles the flange was completely severed and the crack was 2 3/4" in the web. A hole was drilled at the crack tip, a bolt was placed in the hole, and the test was resumed.
	S[1]	3/16	3/8	Fractured		143	1,800	At 1,174,000 cycles the crack propagated in the web fillet. At 1,495,000 cycles the flange was completely fractured and the crack was 3 1/4" in the web. A hole was drilled at the crack tip, a bolt was placed in the hole, and the test was resumed.
WR2	N[1]	1/4	3/32	Fractured		140	1,800	At 1,350,000 cycles the crack propagated into the web fillet. At 1,520,000 cycles the north west side of the tension flange fractured while the crack grew 1 7/8" into the web. At 1,561,000 cycles the flange fractured while the crack grew 2 1/4" into the web. A hole was then drilled at the crack tip, a bolt was placed in the hole, and the test was resumed.
	S[2]	13/32	1/4	1 5/8	1 1/32	140	1,800	

Table D.1. Crack Size and Loading Cycles Before and After Repair. (Cont.)

Specimen	End	Detectable Crack Size (in)		Final Crack Size (in)		Number of Loading Cycles (Thousands)		Notes
		W	E	W	E	Crack Detection	After Repair[6]	
WR3	N[2]	3/16	15/32	3 11/32		140	1,800	The compression flange was found completely severed at the end of the test and the crack was 4" into the web.
WR3	S[1]	1/4	3/16	Fractured		140	1,800	The crack grew into the web fillet at 1,000,000 cycles. At 1,170,000 cycles the east side of the tension flange fractured while the crack grew 1 7/8" into the web. At 1,211,000 cycles the tension flange completely fractured and the crack grew 2 3/8" into the web. A hole was then drilled at the crack tip, a bolt was placed in the hole, and the test was resumed.
WR4	N[3]	3/8	---	6 1/4		140	300	At 145,000 cycles, a crack 1/2" long was detected at the north east weld root. At 257,000 cycles, a crack was observed emerging from the northwest side of the web fillet. The crack was only observed from the top of the tension flange. At 297,000 cycles, the northwest side of the flange fractured and the crack propagated in the web. At 300,000 cycles, the crack propagated to a 6 1/4" long crack and grew 2 24/32" into the web.
WR4	S[3]	5/16	1/4	6 1/16		140	216	At 216,000 cycles, the south end cracks coalesced into a 6 1/16" long crack; only 22/32" of the flange was not cracked. This crack propagated 2 28/32" into the web. A hole was drilled at the crack tip, and a bolt was placed in the hole. The 1" thick repair plates were used and the test was resumed.

Table D.1. Crack Size and Loading Cycles Before and After Repair. (Cont.)

Specimen	End	Detectable Crack Size (in)		Final Crack Size (in)		Number of Loading Cycles (Thousands)		Notes
		W	E	W	E	Crack Detection	After Repair[6]	
WR5	N[3]	3/8	3/16	5 1/16		120	223	At 222,000 cycles, a crack 5 3/8" long was observed. Only 1 3/8" of the east side of the flange remained un-cracked. The crack propagated at the weld toe of the west side weld and the weld root of the east side weld.
	S[3]	1/2	1/4	5 1/16		120	160	At 160,000 cycles, a crack 5 1/16" long was observed. Only 1 11/16" of the east side of the flange remained un-cracked. In 500 cycles the crack grew 1" into the web. The 1" thick temporary repair plates were used and the test was resumed.
WR6	N[4]	1/4	3/8	1	31/32	150	2,200	At 1,326,000 cycles after repair, the compression flange fractured. The crack passed through the west side return weld and was at the east side weld toe.
	S[4]	---	1/4	Fractured		150	2,200	At 1,157,000 cycles after repair, the crack propagated to about 3 7/16" passing through the west side return of the cover plate weld. The crack propagated about 3/4" into the web. At 1,326,000 cycles, the flange fractured and the crack was 5 1/4" into the web. A hole was drilled at the crack tip, a bolt was placed in the hole. At 1,494,000 cycles, the crack passed through the hole. A second hole was drilled. At 2,100,000 cycles, the crack passed through the second hole.

Table D.1. Crack Size and Loading Cycles Before and After Repair. (Cont.)

Specimen	End	Detectable Crack Size (in)		Final Crack Size (in)		Number of Loading Cycles (Thousands)		Notes
		W	E	W	E	Crack Detection	After Repair[6]	
WR7	N[4]	3/16	5/16	Fractured		140	1,313	At 604,000 cycles after repair, the crack was 3 31/32" long and propagated about 1 1/8" into the web. At 631,000 cycles, the flange fractured. At 686,000 cycles, the crack propagated about 4 1/8" into the web. A hole was drilled at the crack tip, a bolt was placed in the hole. At 929,000 cycles, the crack passed through the hole. A second hole was drilled, a bolt was placed in the hole, and the test was resumed. At 1,313,000 cycles, the crack passed the second hole to about 7" into the web.
	S[4]	13/32	1/4	Fractured		140	1,313	At 604,000 cycles after repair, the flange fractured while the crack propagated about 4 5/8" into the web. A hole was drilled at the crack tip, a bolt was placed in the hole. At 847,000 cycles, the crack passed through the hole to about 7 5/8" into the web. A second hole was drilled, a bolt was placed in the hole, and the test was resumed. At 1,313,000 cycles, the crack passed the second hole and was about 8" into the web.

[1] End repaired with 5/16-in bolted splice plate connection.

[2] End repaired with 7/16-in bolted splice plate connection.

[3] End repaired with peening.

[4] End repaired with partial bolted splice plate connection.

[5] Specimen subjected to 15.0-ksi stress range.

[6] Total number of cycles applied after repair until end of test.

APPENDIX E
SAMPLE SPECIFICATION RECOMMENDATIONS

E.1. Retrofit Type-1 (Bolted Splice Plate at End of Tapered Cover Plates)

E.1.1. Description

This work shall consist of pencil sandblasting; visual inspection of the girder flange and web adjacent to the tapered, partial-length cover plate ends for fatigue cracks; non-destructive testing of the cover plate ends; drilling holes in the girder flange and cover plate on each side of the cover plate ends; spot painting the sandblasted and drilled portions of the girder; and installation of splice and filler plates with high-strength structural bolts.

E.1.2. General Procedure

1) Clean the retrofit area near the cover plate end by pencil sandblasting the paint and/or rust from the surface of the flange, welds, and cover plate. Clean an area at least 2 inches on each side of the cover plate ends, or as shown on the plans. For cover plate wider than the flange, the cleaned area shall include the weld ends at the intersection of the cover plate with the beam flange.
2) The contractor, accompanied by the engineer, shall visually inspect the cleaned area using a 10X magnifying glass and a 12V spot/flood lighting. At the direction of the engineer, grinding shall be performed to enhance investigation for crack presence. All grinding and grinding marks shall be parallel to the girder length.
3) The contractor shall non-destructively test (NDT) for cracks at the toe of the cover plate welds along the entire end of the plate and 2 inches along the tapered side of the cover plate. For cover plates wider than the flange, inspection should also be conducted near the weld ends at the intersection of the cover plate with the beam flange. The NDT inspection shall be conducted using magnetic particle (MT) and/or dye penetrant (PT) inspection.
4) If cracks are detected in steps 2 or 3, then the engineer should be consulted to evaluate the structural integrity of the beam and to design the bolted splice connection (proceed to step 5). If no cracks are detected, then a degreaser should be used to remove any oil or foreign material from the cleaned area. A primer and a top coat

should be applied to completely seal the entire cleaned area.

5) The engineer must provide the number of high-strength bolts and the splice plate thickness needed for the bolted splice connection. Mark the position of the holes on the girder flange and cover plate. The inside holes through the cover plate shall be located on each side of the web at 1/2 inch from the end of the taper (see Fig. E.1 for a four-bolt layout). The holes near the cover plate end shall be located such that a minimum distance of 1/2 inch is provided between the filler plate end and the cover plate end weld. The holes at each end of the splice shall be spaced at a 3 inch pitch center to center between holes.
6) A degreaser should be used to remove any residual oil or foreign materials from the entire area being retrofitted. A primer and a top coat shall be applied to seal the retrofit area for a distance 3 inches beyond the drilled holes.
7) High-strength structural bolts shall be used to connect the filler and splice plates to the girder flange. A filler plate, equal in thickness to the cover plate and equal in width to the splice plate, shall extend 1 1/4 inches beyond the center of the holes near the cover plate end. The splice plates on the inside of girder flanges shall have the holes placed at mid-width. Refer to Figs. E.1 and E.2. for specific details - a four bolt splice detail is shown for illustration purposes only.
8) A silicon caulk should be used to fill the gaps between the splice plates and the beam flange in order to prevent water, salt, dirt, and foreign materials from storing in the area between the splice plate and the flange.

E.1.3. Requirements

Pencil Sandblasting. The pencil sandblasting, grinding, and NDT shall be performed in accordance with requirements of special provision pencil sandblasting, grinding and NDT.

Drilling Holes. All holes shall be drilled 1/16 inch larger than the required size structural bolt. The use of a cutting torch is not permitted.

Bolting. ASTM 325 or A490 high-strength structural bolts shall be used to connect the splice plate to the girder flange. ASTM F436 hardened washers shall be placed beneath the bolt head or nut being turned in tightening. The bolts shall be tightened by the turn-of-the-nut method, or other appropriate methods, to produce a bolt tension equal to or greater than that required for a slip-critical fastener.

E.2. Retrofit Type-2 (Air-Hammer Peening at Ends of Tapered Cover Plates)

E.2.1. Description

This work shall consist of pencil sandblasting; visual inspection of the girder flange and web adjacent to the tapered, partial-length cover plate ends for fatigue cracks; non-destructive testing of the cover plate ends; peening of the weld toe at the cover plate ends; and spot painting.

E.2.2. General Procedure

1) Clean the retrofit area near the cover plate end by pencil sandblasting the paint and/or rust from the surface of the flange, welds, and cover plate. Clean an area at least 2 inches on each side of the cover plate ends, or as shown on the plans. For cover plate wider than the flange, the cleaned area should include the weld ends at the intersection of the cover plate with the beam flange.
2) The contractor, accompanied by the engineer, shall visually inspect the cleaned area using a 10X magnifying glass and a 12V spot/flood lighting. At the direction of the engineer, grinding shall be performed to enhance investigation for crack presence. All grinding and grinding marks shall be parallel to the girder length.
3) The contractor shall non-destructively test (NDT) for cracks at the toe of the cover plate welds along the entire end of the plate and 2 inches along the tapered side of the cover plate. For cover plates wider than the flange, inspection should also be conducted near the weld ends at the intersection of the cover plate with the beam flange. The NDT inspection shall be conducted using magnetic particle (MT) and/or dye penetrant (PT) inspection.
4) If cracks larger than 3/16 inch in length are detected, then the cover plate must be repaired with a splice plate retrofit. If no cracks are detected, or if the cracks are less than 3/16- inch in length, then proceed with step 5.
5) Use a pneumatic hammer operated at 40 psi with the peening tool, shown in Fig. E.3, to peen the weld toe. The peening area (Fig. E.4) includes all transverse welds at the end of the cover plate and 2 inches of the weld from the cover plate end. A total of

six (6) complete passes of the peening operation are to be conducted over the entire peening area.

6) Inspect the peened ends using a 10x magnifying glass and spot/flood lighting. When a crack located perpendicular to the girder length is visible after peening, the engineer shall be consulted. At the direction of the engineer, the peening may be continued until all cracks disappear. The engineer shall be consulted if the cracks do not disappear.
7) A degreaser should be used to remove any oil or foreign materials from the entire retrofit area. A primer and a top coat shall be applied to seal the retrofit area for a distance 3 inches beyond the cover plate ends.

E.2.3. Requirements

Pencil Sandblasting. The pencil sandblasting, grinding, and NdT shall be performed in accordance with requirements of special provision pencil sandblasting, grinding and NDT.

Peening Tool. The peening tool shall be made from a high grade carbon steel rod with the dimensions shown in the attached drawing.

Peening Operation. Peening should be performed with the peening tool placed at a 60 to 70 degree angle from girder flange. The operator, in as much as possible, should maintain a steady pressure on the pneumatic hammer so that the peening tool remains in continuous contact with the toe of the cover plate fillet weld.

E.3. Retrofit Type-3 (Partial Bolted Splice at End of Tapered Cover Plates)

E.3.1. Description

This work shall consist of pencil sandblasting; visual inspection of the girder flange and web adjacent to the tapered, partial-length cover plate ends for fatigue cracks; non-destructive testing of the cover plate ends; peening of the weld toe at the cover plate ends; drilling holes in the girder flange and cover plate on each side of the cover plate ends; spot painting the sandblasted and drilled portions of the girder; and installation of splice plates with high-strength structural bolts.

E.3.2. General Procedure

1) Clean the retrofit area near the cover plate end by pencil sandblasting the paint and/or rust from the surface of the flange, welds, and cover plate. Clean an area at least 2 inches on each side of the cover plate ends, or as shown on the plans. For cover plates wider than the flange, the cleaned area shall include the weld ends at the intersection of the cover plate with the beam flange.
2) The contractor, accompanied by the engineer, shall visually inspect the cleaned area using a 10X magnifying glass and a 12V spot/flood lighting. At the direction of the engineer, grinding shall be performed to enhance investigation for crack presence. All grinding and grinding marks shall be parallel to the girder length.
3) The contractor shall non-destructively test (NDT) for cracks at the toe of the cover plate welds along the entire end of the plate and 2 inches along the tapered side of the cover plate. For cover plates wider than the flange, inspection shall also be conducted near the weld ends at the intersection of the cover plate with the beam flange. The NDT inspection shall be conducted using magnetic particle (MT) and/or dye penetrant (PT) inspection.
4) If cracks are detected in steps 2 or 3, then the engineer should be consulted to evaluate the structural integrity of the beam and to design the partial bolted splice connection (proceed to step 5). If no cracks are detected, then a degreaser should be used to remove any oil or foreign material from the cleaned area. A primer and a top coat shall be applied to completely seal the entire cleaned area.
5) The engineer must provide the number of high-strength bolts and the splice plate thickness needed for the partial bolted splice condition. Mark the position of the holes on the girder flange and cover plate. The inside holes through the cover plate shall be located on each side of the web at 1/2 inch from the end of the taper. The holes near the cover plate end shall be located such that a minimum distance of 1/2 inch is provided between the filler plate end and the cover plate end weld. The holes at each end of the splice shall be spaced at a 3 inch pitch center to center between holes.
6) Use a pneumatic hammer operated at 40 psi with the peening tool, shown in Fig. E.3, to peen the weld toe. The peening area (Fig. E.4) includes all transverse welds at the

end of the cover plate and 2 inches of the weld from the cover plate end. A total of six (6) complete passes of the peening operation are to be continued over the entire peening area.

7) Inspect the peened ends using a 10x magnifying glass. When a crack located perpendicular to the girder length is visible after peening, the engineer shall be consulted. At the direction of the engineer, the peening may be continued until all cracks disappear. The engineer shall be consulted if the cracks do not disappear.
8) A degreaser should be used to remove any residual oil or foreign materials from the entire area being retrofitted. A primer and a top coat shall be applied to seal the retrofit area for a distance 3 inches beyond the drilled holes.
9) High-strength structural bolts shall be used to connect the splice plates to the girder flange. The two splice plates are positioned on the inside of the girder flanges with the holes placed at mid-width. Refer to Fig. E.5 for specific details - a four bolt splice detail is shown for illustration purposes only.

E.3.3 Requirements

Pencil Sandblasting. The pencil sandblasting, grinding, and NDT shall be performed in accordance with requirements of special provision pencil sandblasting, grinding and NDT.

Drilling Holes. All holes shall be drilled 1/16 inch larger than the required size structural bolt. The use of a cutting torch is not permitted.

Bolting. ASTM 325 or A490 high-strength structural bolts shall be used to connect the splice plate to the girder flange. ASTM F436 hardened washers shall be placed beneath the bolt head or nut being turned in tightening. The bolts shall be tightened by the turn-of-the-nut method, or other appropriate methods, to produce a bolt tension equal to or greater than that required for a slip-critical fastener.

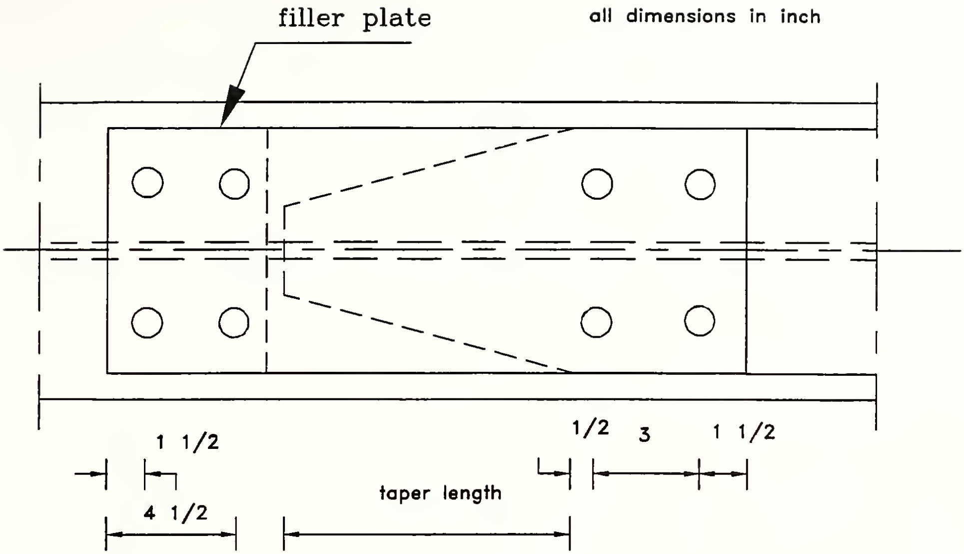

Narrow Cover Plate

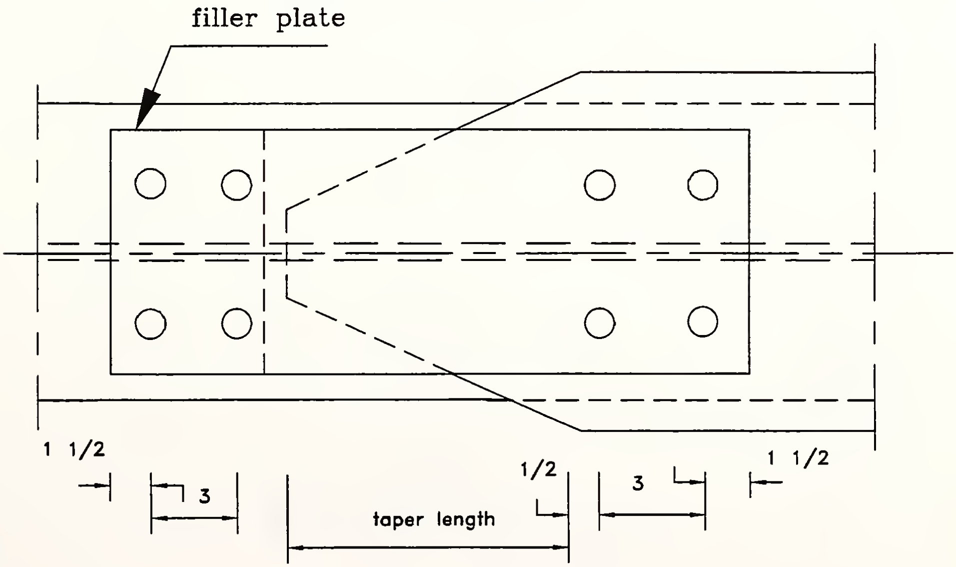

Wide Cover Plate

Fig. E.1. Bolts Lay-Out.

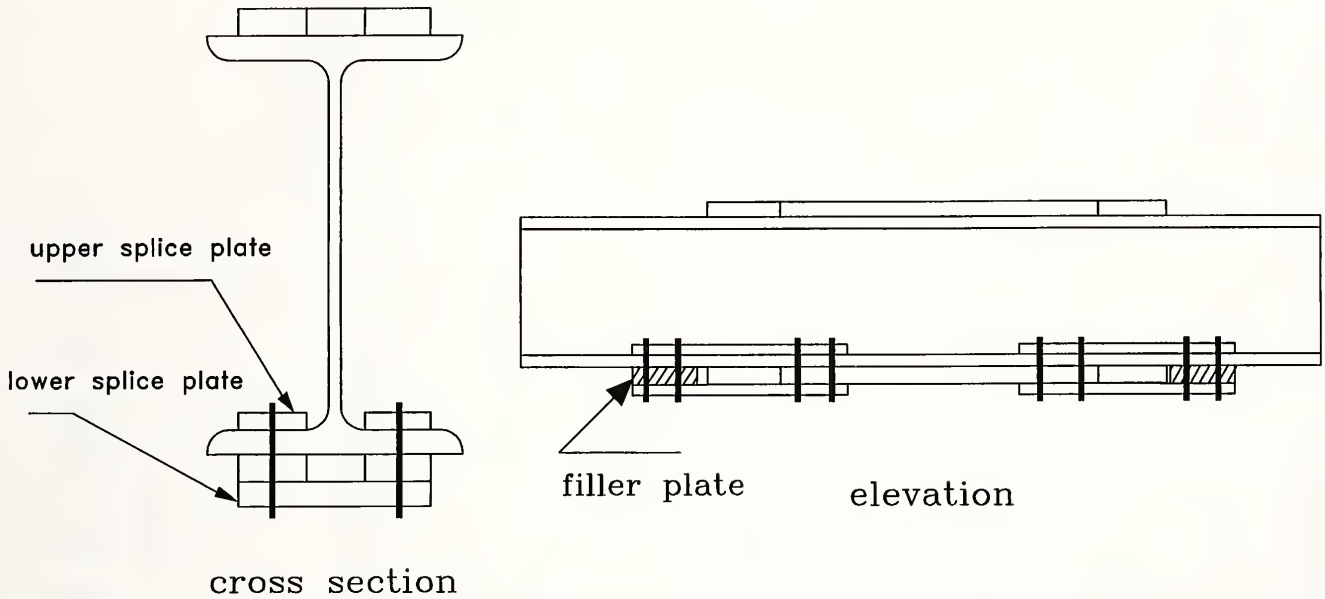

Fig. E.2. Bolted Splice Connection.
(Elevation and Cross–Section)

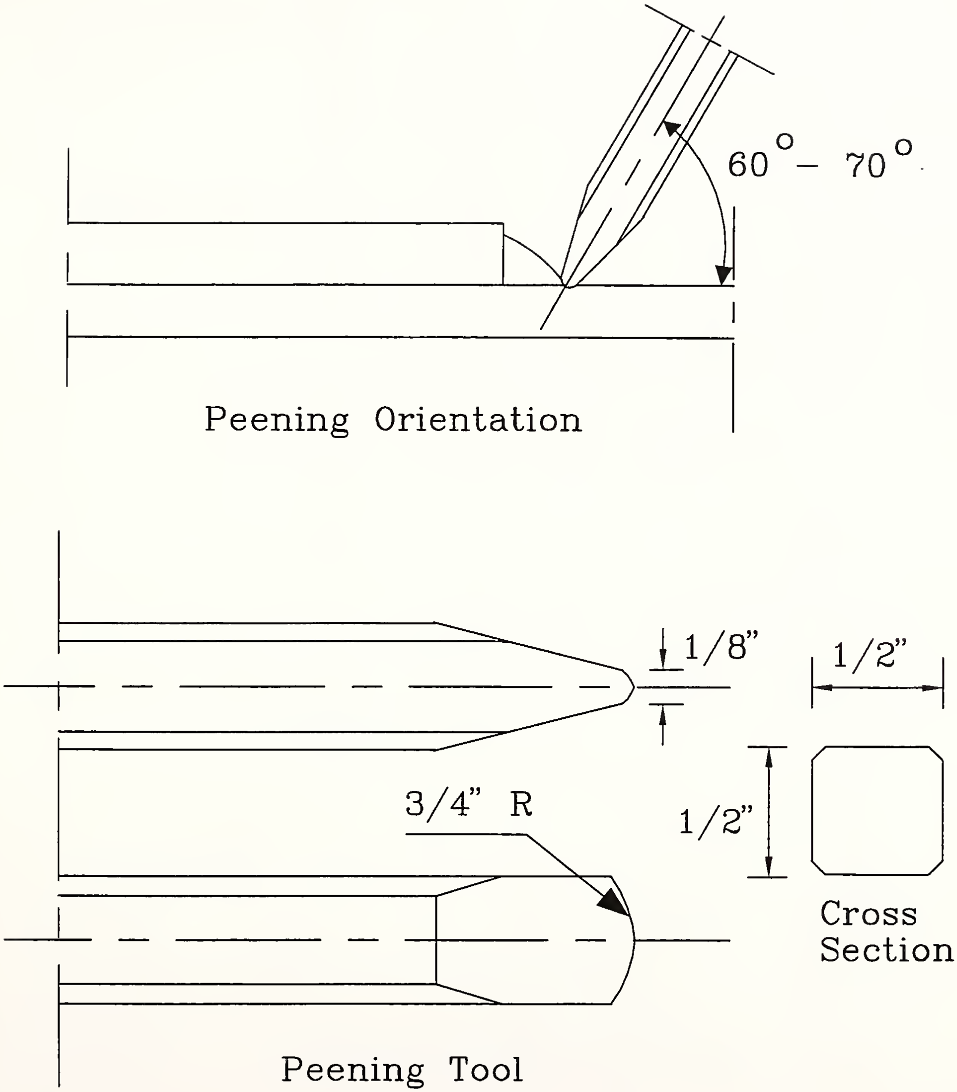

Fig. E.3. Air–Hammer Peening Tool.

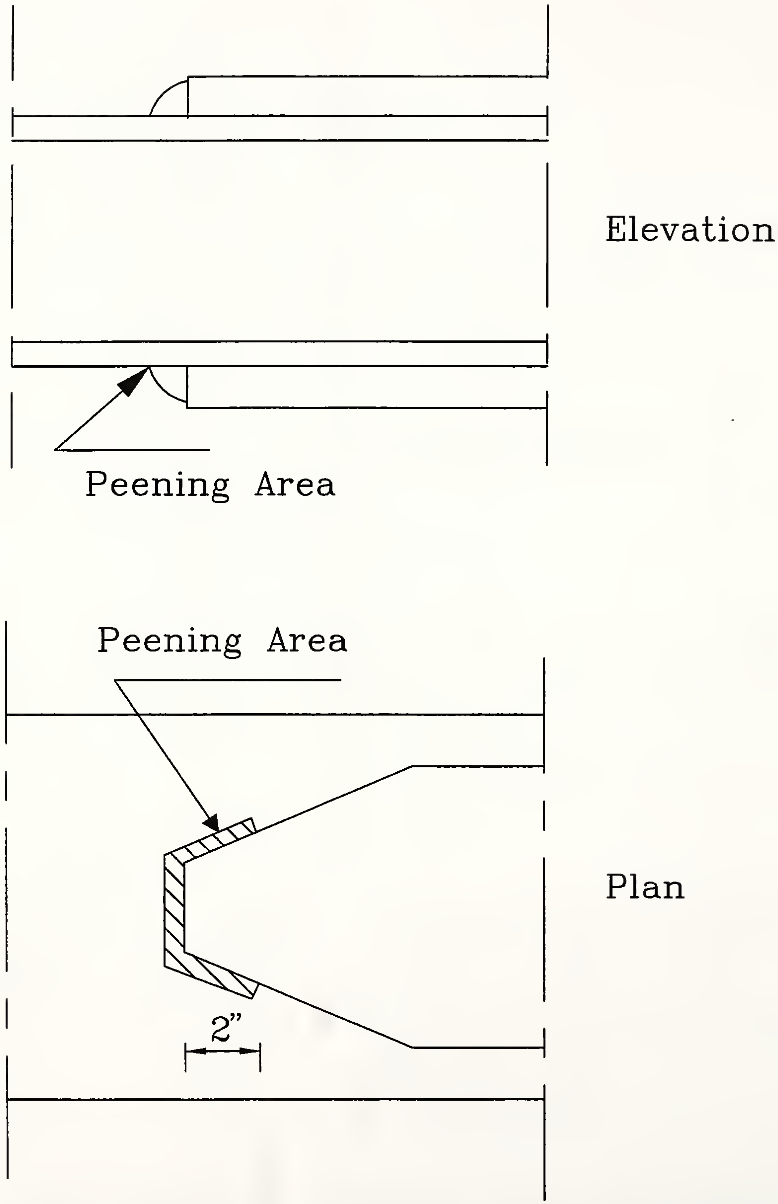

Fig. E.4. Peening Area.

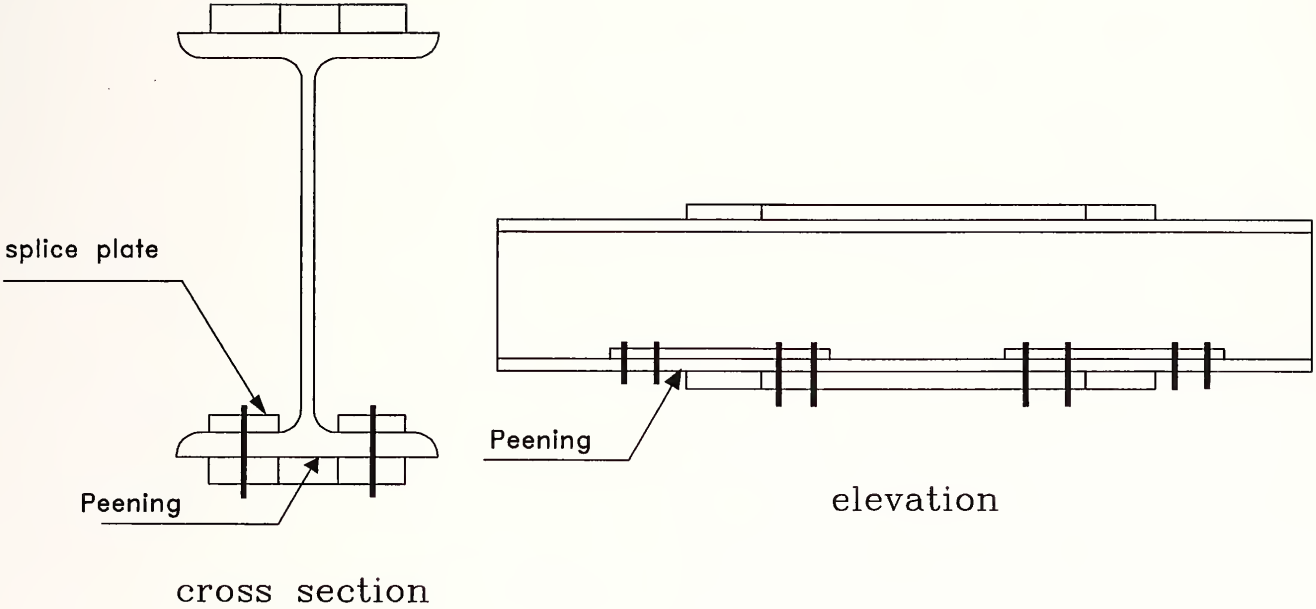

Fig. E.5. Partial Bolted Splice Connection.
(Elevation and Cross–Section)

APPENDIX F
STRESS INTENSITY FACTOR SOLUTION
NEWMAN AND RAJU (1981)

F.1. General

Surface cracks are common flaws in many structural components. Accurate stress analyses of these components is required for crack growth predictions. But, because of the complexity of such problems, exact solutions are often not available.

The finite element method is one of the tools used to obtain empirical solutions of stress intensity factors for complicated cases. Raju and Newman (1979) discussed the determination of stress intensity factor using the nodal force method. In this method, the nodal forces normal to the crack plane and ahead of the crack front are used to estimate the stress intensity factor.

F.2. Stress Intensity Factor Solution

Newman and Raju (1981) developed an empirical equation for the Mode I stress intensity factor of elliptical surface cracks in finite plates subjected to both tension and bending. The equation was based on a three-dimensional finite element analysis of semi-elliptical surface cracks in finite elastic plates subjected to tension or bending loads. The plate and crack dimensions and configurations are shown in Fig. F.1. The solution is expressed as follows:

$$K_I = (S_t + H\,S_b)\sqrt{\pi\,\frac{a}{Q}}\;F\left(\frac{a}{c},\frac{a}{t},\frac{c}{b},\phi\right) \qquad \text{(F.1)}$$

where

$$Q = 1 + 1.464\left(\frac{a}{c}\right)^{1.65} \qquad \text{(F.2)}$$

$$F = [\ M_1 + M_2 \left(\frac{a}{t}\right)^2 + M_3 \left(\frac{a}{t}\right)^4\ ]\ f_\phi\ g\ f_\omega \tag{F.3}$$

$$M_1 = 1.13 - 0.09 \left(\frac{a}{c}\right) \tag{F.4}$$

$$M_2 = -0.54 + \frac{0.89}{0.2 + \left(\frac{a}{c}\right)} \tag{F.5}$$

$$M_3 = 0.5 - \frac{1.0}{0.65 + \left(\frac{a}{c}\right)} + 14\ \left(1 - \frac{a}{c}\right)^{24} \tag{F.6}$$

$$g = 1 + [\ 0.1 + 0.35 \left(\frac{a}{t}\right)^2\ ]\ (\ 1 - \sin\phi\ )^2 \tag{F.7}$$

$$f_\phi = \left[\left(\frac{a}{c}\right)^2 \cos^2\phi + \sin^2\phi\right]^{\frac{1}{4}} \tag{F.8}$$

$$f_\omega = \left[\ \sec \left(\frac{2\ \pi\ c}{2\ b} \cdot \sqrt{\frac{a}{t}}\right)\ \right]^{\frac{1}{2}} \tag{F.9}$$

$$H = H_1 + (\ H_2 - H_1\ )\ .\ \sin^p\phi \tag{F.10}$$

$$p = 0.2 + \frac{a}{c} + 0.6\ \frac{a}{t} \tag{F.11}$$

$$H_1 = 1 - 0.34\ \frac{a}{t} - 0.11\ \frac{a}{c} \left(\frac{a}{t}\right) \tag{F.12}$$

$$H_2 = 1 + G_1 \left(\frac{a}{t}\right) + G_2 \left(\frac{a}{t}\right)^2 \tag{F.13}$$

$$G_1 = -1.22 - 0.12 \frac{a}{c} \tag{F.14}$$

$$G_2 = 0.55 - 1.05 \left(\frac{a}{c}\right)^{0.75} + 0.47 \left(\frac{a}{c}\right)^{1.5} \tag{F.15}$$

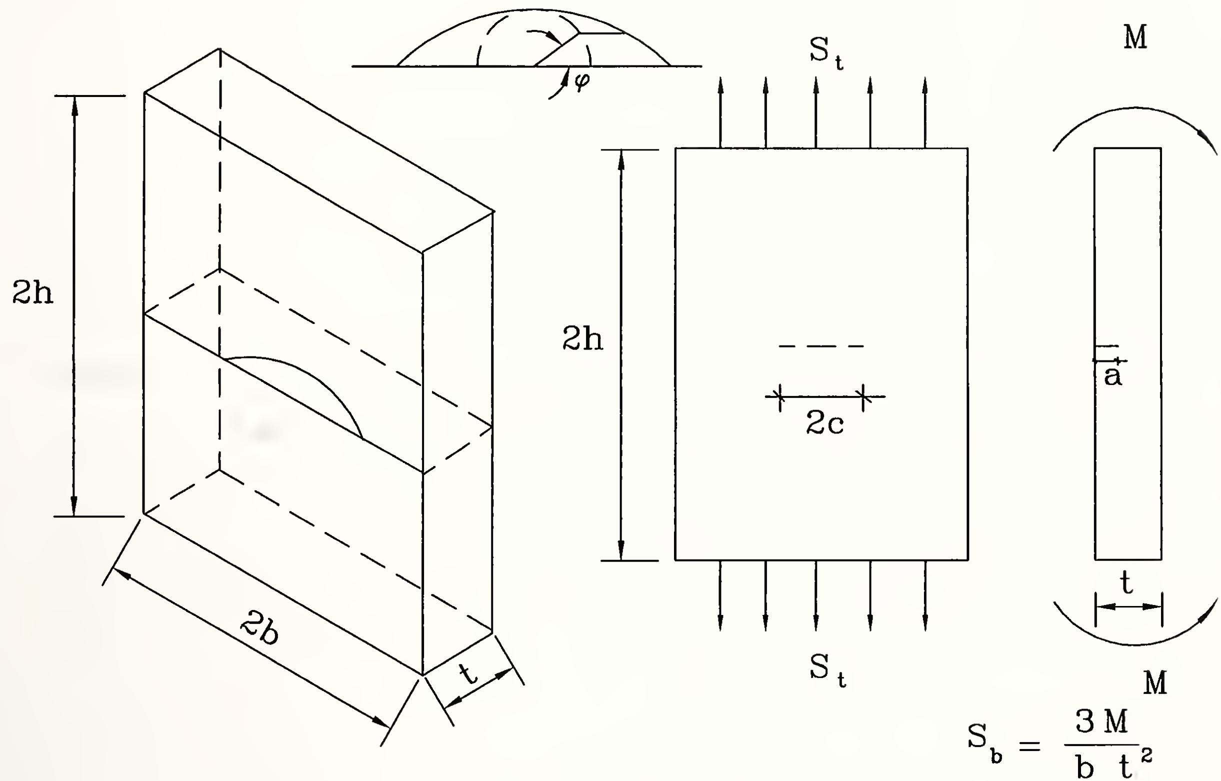

Fig. F.1. Surface Crack in Finite Plate Subjected to Tension or Bending Loads. (Newman and Raju (1981))

APPENDIX G
DETERMINATION OF THE STRESS GRADIENT DISTRIBUTION DUE TO THE WELDED COVER PLATE

G.1. General

The previously mentioned solution of stress intensity factor by Newman and Raju (1981) assumes a uniform opening stress. Due to the existence of a welded cover plate, the actual stress distribution in the flange at the cover plate end is non-uniform. The effect of the non-uniform opening stress could be included in the stress intensity factor solution through a geometric correction factor, F_G. To determine this geometric correction factor, the stress gradient distribution, K_t, has to be estimated for the non-cracked geometry along the expected crack growth trajectory.

G.2. Stress Gradient

Finite element analysis was carried out using an existing general purpose finite element computer package, ANSYS (1993), to determine the stress concentration distribution. To include the effects of the cover plate width, end weld condition, and weld shape, and to avoid using a complicated three dimensional analysis, the analysis was conducted in two phases.

In the first phase, the cover plate and the flange were analyzed to obtain the stress concentration factor due to the end weld condition and cover plate width. Fig. G.1 shows a plan view of the typical mesh used in the first phase of the finite element analysis. Six-node triangular plane stress elements were used to mesh the cover plate and the flange. The weld was represented by spring elements in both the X and Y directions. The stiffness of these spring elements was obtained from the load-deformation curve of welded joints outlined in the AISC Manual (1986), and can be expressed as:

$$k \approx 5940 * A_w \qquad \text{(G.1)}$$

where A_w is the weld area (in^2) associated with a specific node and equals the product of the weld size and the weld length attributed to that specific node, and k is the spring stiffness (kip/in). The weld stiffness was assumed to be the same in both the X and Y directions. The stress concentration factor, which is the ratio of the maximum stress at the cover plate end to the

nominal stress in the beam flange, was found to be 1.252, 1.214, 1.373, 1.235, and 1.197 for the NR, NF, NN, WR, and WF specimens, respectively. These stress concentration values represent the effect of the cover plate taper and end weld condition only. Figure G.2 illustrate the stress contour lines for the NR detail. For clarity, Figure G.3. shows the same contour lines without shading and without the finite element mesh. Figures G.4 to G.7. show the stress contour lines for the NF, NN, WR, and WF details without shading and without the finite element mesh.

In the second phase, the effect of weld geometry is considered, as shown in Fig. G.8. Both six-node triangular and eight-node rectangular plane strain elements were used to represent the cover plate, the flange, and the connecting welds. It was assumed that the weld material has the same properties as the flange and cover plate. The weld shape was obtained from measurements of fillet weld sizes conducted by Quinn (1991). One of the factors affecting the stress concentration at the weld toe is the weld radius at the toe (r). The smaller the radius the higher the stress concentration. To simulate the worse condition a weld toe radius of zero was used for the determination of the stress concentration factor. The stress concentration factor at the weld toe was found to be approximately 4.151. The stress distribution in the flange, $k_t(a)$, at a cross section passing through the weld toe was obtained from the finite element analysis. Regression analysis of the results yielded the following equation to represent the stress distribution in the flange at the weld end:

$$k_t(a) \approx 0.8 + 3.615 * e^{\left(-4.6 * \left(\frac{a}{t_f}\right)^{\frac{1}{3}}\right)} \qquad \text{(G.2)}$$

where a is the crack depth and t_f is the flange thickness.

Using superposition, the total stress concentration factor is obtained by multiplying the stress concentration factors from the two phases for each condition of cover plate width and end weld detail. The geometric correction factor is then computed using the stress gradient distribution, $k_t(a)$, and substituting it in Eq. 9.2.

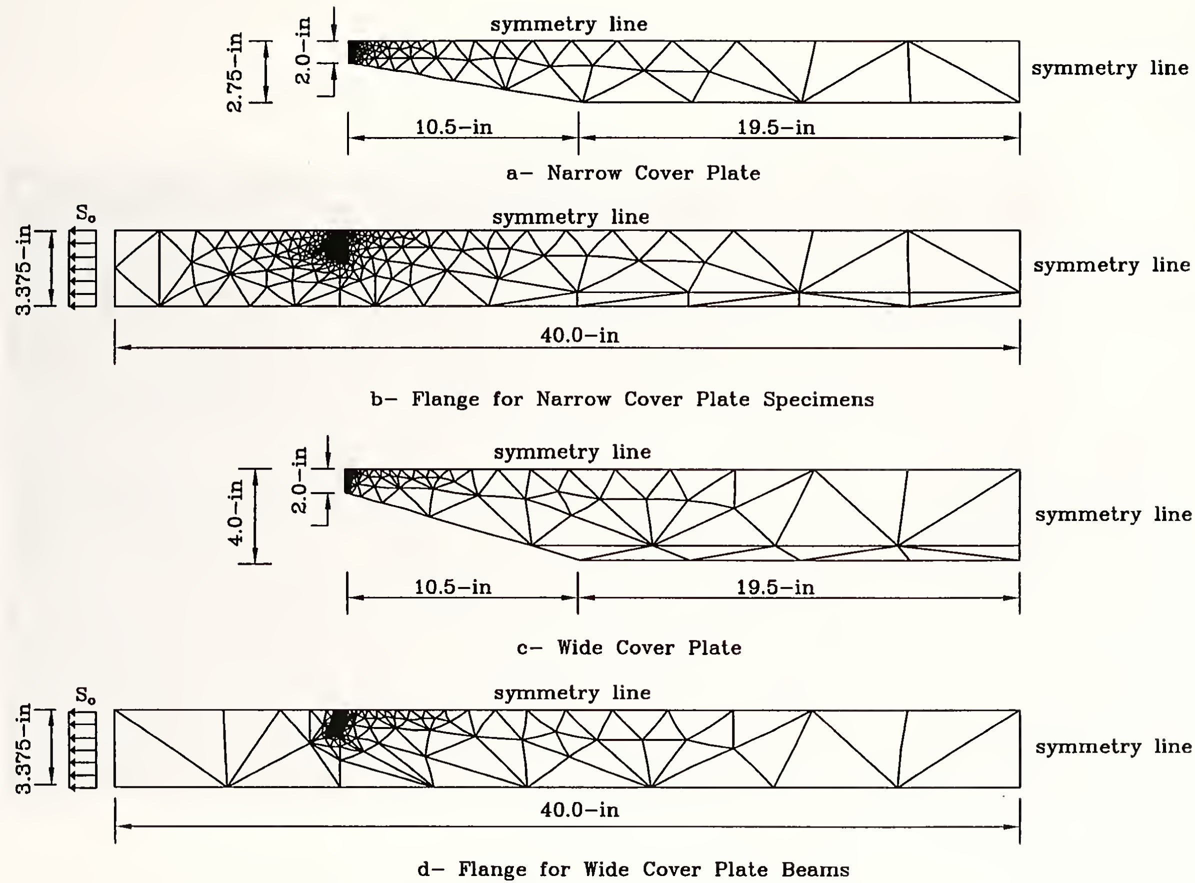

Fig. G.1. Finite Element Mesh.
(Effect of Cover Plate Width and End Weld Condition)

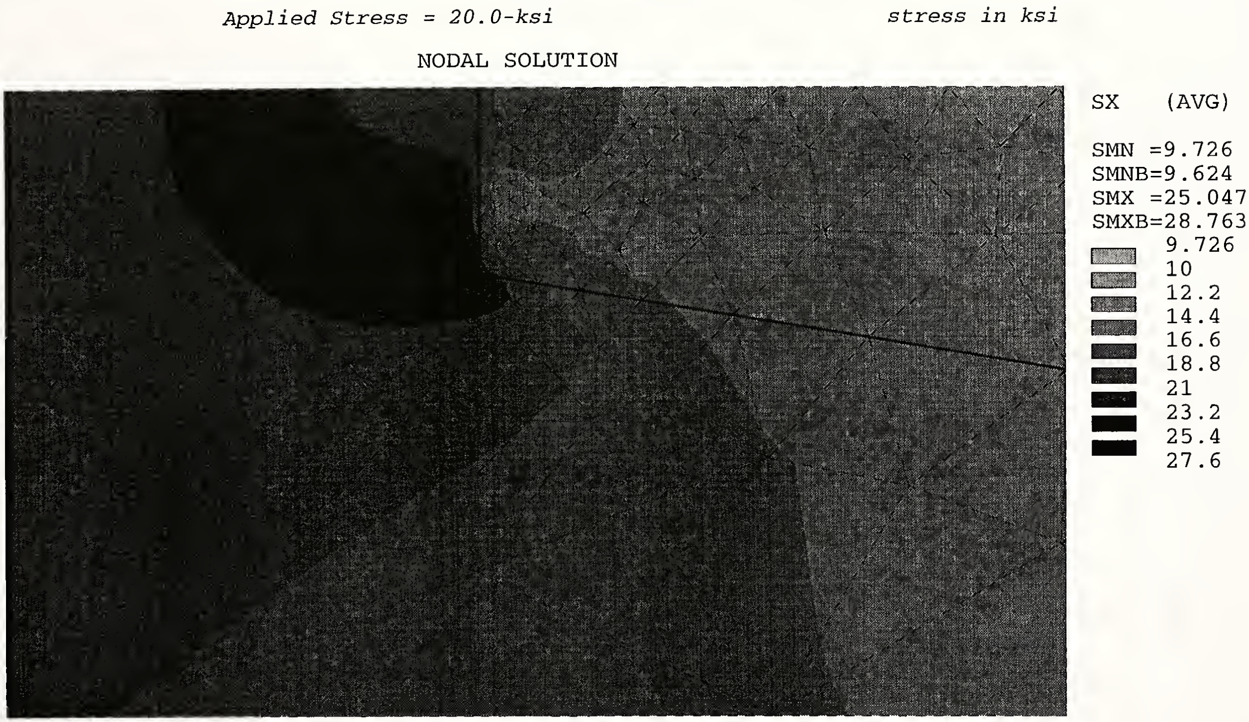

Fig. G.2. Stress Contours for NR Detail.

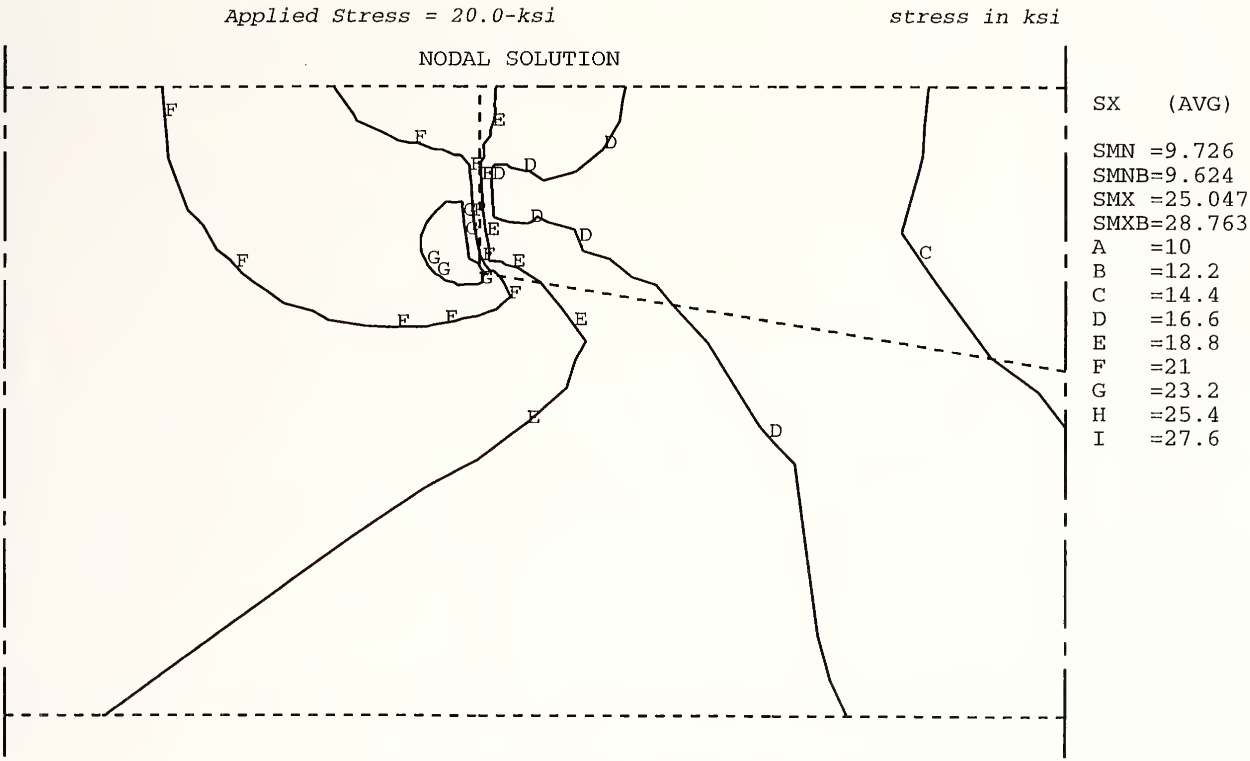

Fig. G.3. Stress Contour Lines for NR Detail.

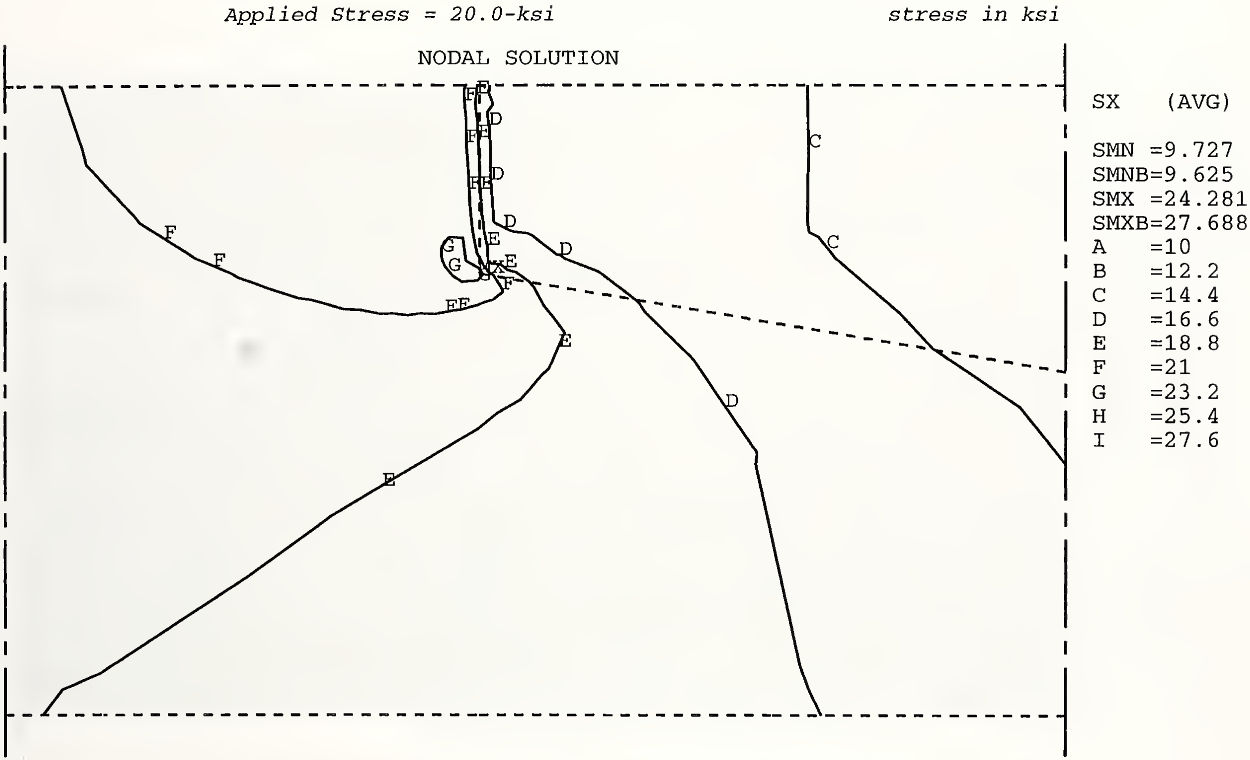

Fig. G.4. Stress Contour Lines for NF Detail.

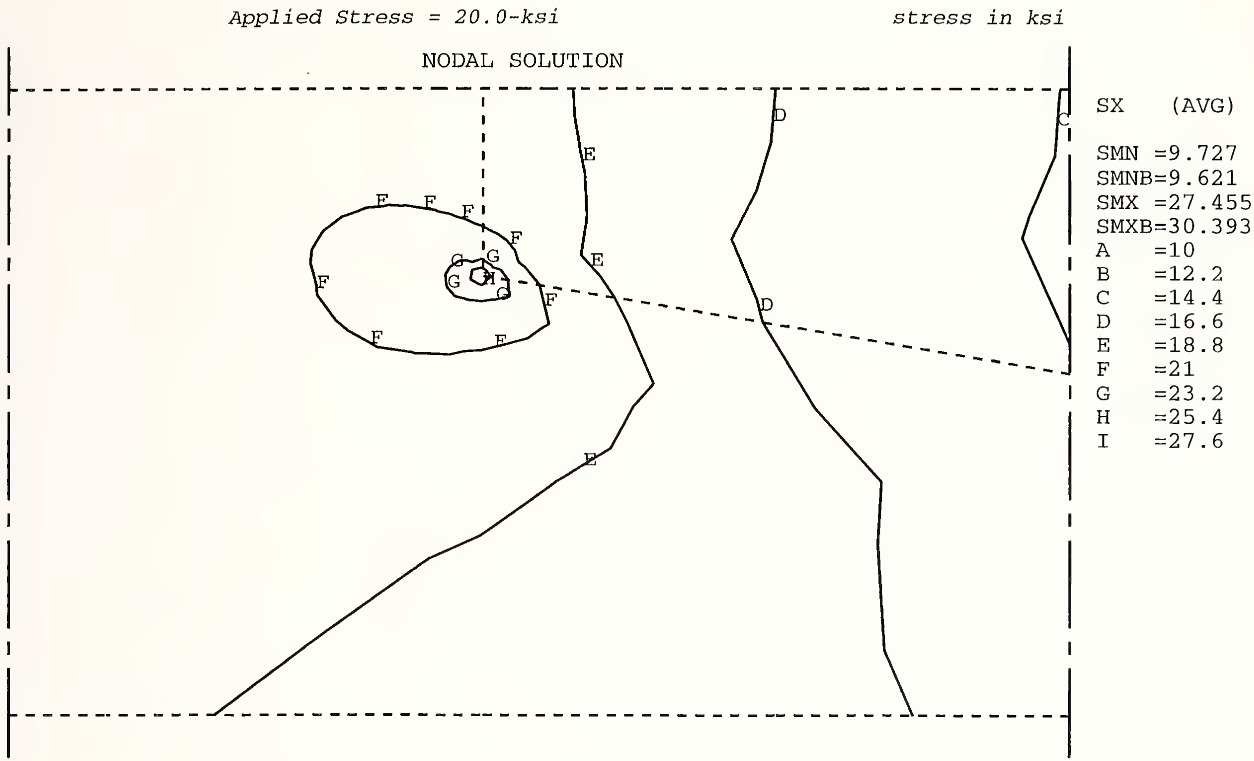

Fig. G.5. Stress Contour Lines for NN Detail.

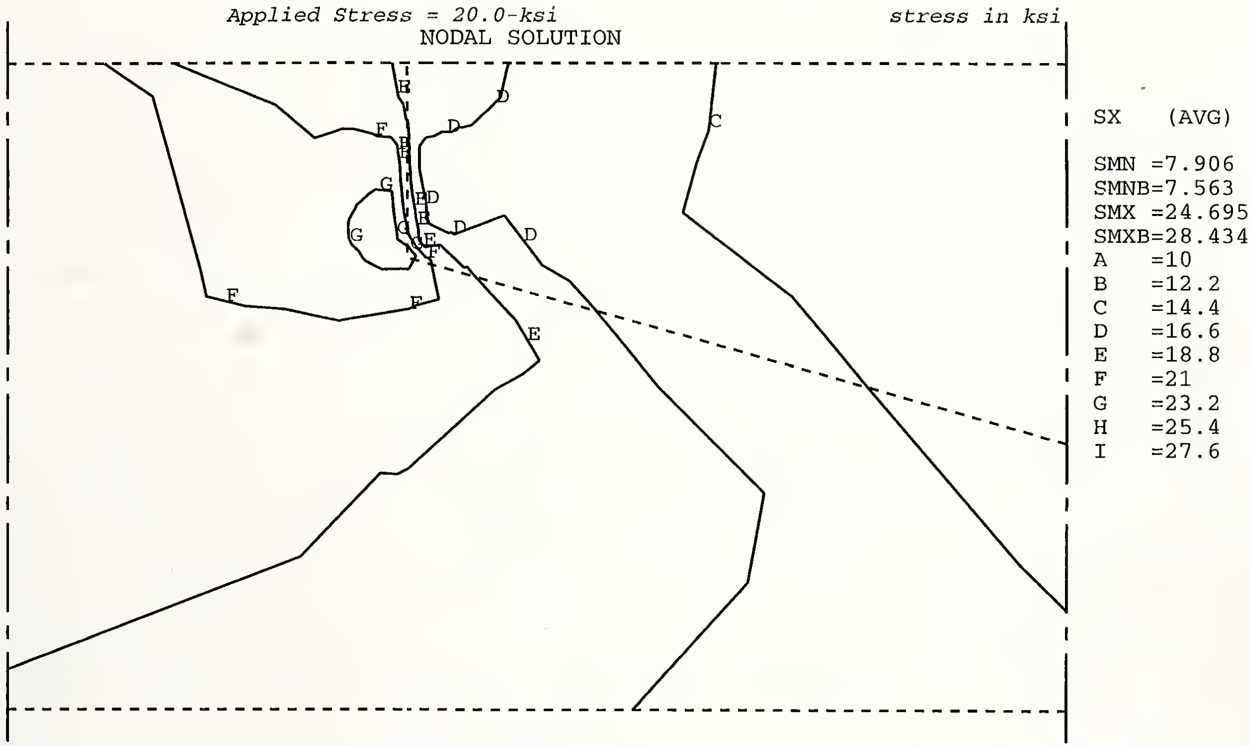

Fig. G.6. Stress Contour Lines for WR Detail.

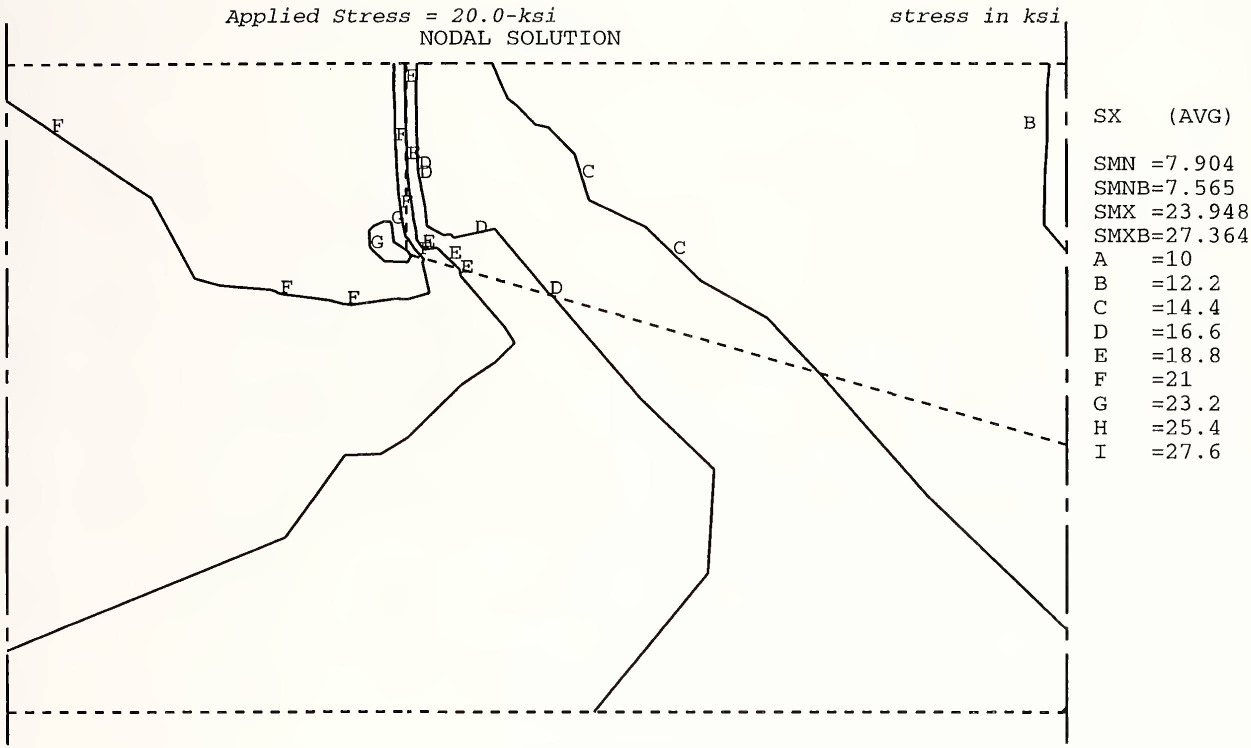

Fig. G.7. Stress Contour Lines for WF Detail.

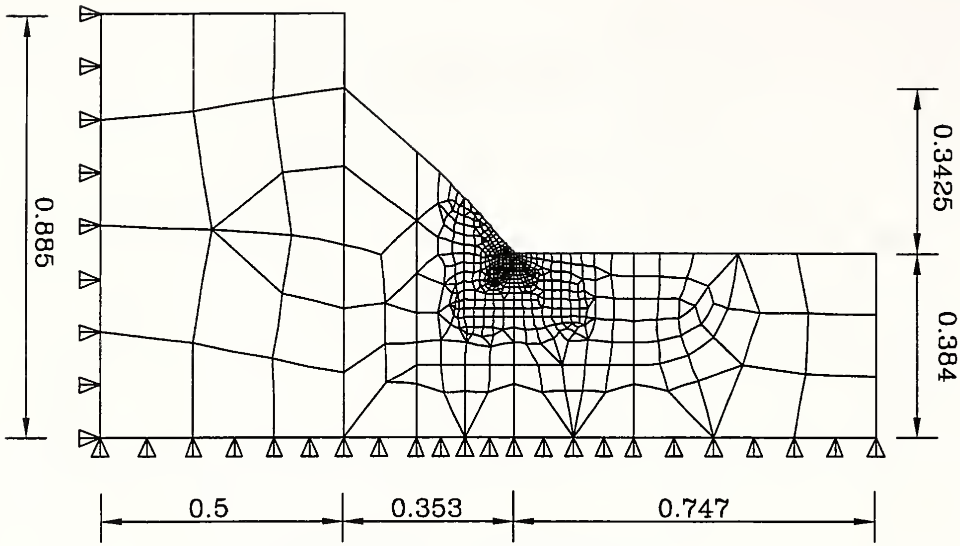

a– Complete Finite Element Mesh

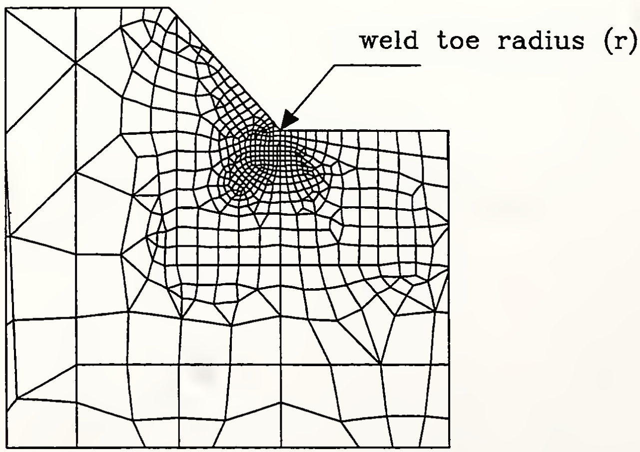

b– Close–Up of Weld Toe Area

Fig. G.8. Finite Element Mesh for Weld Toe Stress Concentration.

APPENDIX H
CRACK PROPAGATION PROGRAM

H.1. General

The FORTRAN computer program used to calculate the crack propagation life of steel beams with welded tapered cover plates is listed in the following section. A description of the input parameters is then provided. Sample input and corresponding output files are also listed.

H.2. Program List

```
c      **********************************************
c      *                                            *
c      *   PROGRAM  GROWTH ( 2-D Elliptical Flaw )  *
c      *                                            *
c      *  Crack in the flange at the cover plate end *
c      *                                            *
c      *                    by                      *
c      *                                            *
c      *              Ahmed  F.  Hassan             *
c      *                                            *
c      **********************************************

      program growth
      real n, m, mk, mkr, kc
      open (5,file='data.inp')
      open (4,file='input.out')
      open (7,file='life.out')
  700 format (a4)
 1000 format (/,/,5x,'Half the Flange Plate Width = ',f5.3,2x,'in.')
 1100 format (/,/,5x,'Flange Plate Thickness = ',f5.3,2x,'in.')
 1300 format (/,/,5x,'Initial Crack Depth = ',f5.3,2x,'in.')
 1400 format (/,/,5x,'Half the Initial Crack Width = ',f5.3,2x,'in.')
 1500 format (/,/,5x,'Extreme Fibers Nominal Stress Range ='
     ,,f6.3,2x,'ksi')
 1530 format (/,/,5x,'Nominal Stress Ratio =',f6.3)
 1600 format (/,/,5x,'Detail Type =',2x,a4)
 1700 format (/,/,5x,'Propagation Model No.',2x,i1)
 1800 format (/,/,5x,'Residual Stress Model No.',2x,i1)
 2000 format (//,7x,'step No.',6x,'No. of Cycles',5x,'Crack Depth "a"'
     ,,5x,'1/2 Crack Width "c"',//)
 2100 format (5x,i7,5x,f15.1,5x,f15.10,5x,f15.10,2x,f15.10)
 4000 format (//,5x,'Program Growth')
 4100 format (//,5x,'Ratio of Crack Depth to half Crack Width EXCEEDED'
     ,,/,5x,'a/c =',f6.3)
 4200 format (//,5x,'Ratio of Crack Depth to Flange Thickness EXCEEDED'
     ,,/,5x,'a/pt =',f6.3)
 4300 format (//,5x,'Ratio of Crack width to Flange Width EXCEEDED',/
     ,,5x,'c/pw =',f6.3)
 4400 format (//,5x,'Growth Rate TOO FAST - Rate =',f6.3)
 4500 format (//,5x,'Total Stress Intensity Factor is Larger than the
     , Fracture Toughness',/,5x,'Total Stress Intensity Factor =',f9.5)
 5500 format (//,1x,'Percentage of Force Transmitted through the flange'
     ,,f9.5)
```

```
c     pw = half of the flange plate width   (in)
c     pt = flange plate thickness           (in)
c     db = half of the beam depth           (in)
c     cpw = cover plate width at end of taper (in)
c     ai = initial crack depth       (in)
c     ci = half initial crack width  (in)
c     sef = extreme fibers stress range     (ksi)
c     rns = nominal stress ratio
c     st = nominal axial stress range       (ksi)
c     sb = nominal bending stress range     (ksi)
c     sro = residual stress at flange fibers (ksi)
c     cp = Paris Constant
c      m = Paris Exponent
c      a = Actual crack depth       (in)
c      c = actual crack width        (in)
c      l = flag    =  0    if  point a for an elliptical crack
c                  =  1    if  point c for an elliptical crack
c                  =  2    if through crack
c     dc = Step of increase in "c" direction
c     da = Corresponding increase in "a" direction
c     dn = Corresponding increase in Cycles
c     skr = stress intensity factor range
c     skm = minimum stress intensity factor
c     skh = Stress concentration in the horizontal direction due to taper in
c           the cover plate geometry and weld geometry
c     mkr = geometric correction factor for residual stress effect
c     mk = geometric correction factor for welded cover plate effect
c     kc = Fracture Toughness
c     sift = Total Stress Intensity Factor
c     ll = flag  for type of model used for propagation
c               =  0   User's defined, the program will expect values
c                      for Paris constants "m" and "c"
c               =  1   for Conservative estimates by Barsom and Rolf
c               =  2   for Average propagation of A36 steel (Barsom)
c               =  3   for Average propagation of ferrite-pearlite steels
c                      by Yamada
c               =  4   for average propagation of ferritic steels
c                      by EASON  with R-ratio effect
c     lll = flag for residual stress distribution and effect
c           refer to Fig. L.1 for details.
c               =  1   for residual stress from welding and rolling.
c                      The distribution is assumed to be linear from
c                      a certain amount (sro) at the bottom fibers of
c                      the flange (position of crack initiation) to
c                      zero at the end of the flange thickness.
c               =  2   for residual stress from peening.
c                      The distribution is assumed to be constant with
c                      a stress "sp1" for a distance "td" from the
c                      bottom fibers of the flange (peening position).
c                      Then the stress falls to a stress "sp2" after
c                      a distance "0.2t", and remains constant for an
c                      additional distance "0.8t". After that, the stress
c                      turns to a stress "sp3" and remains constant
c                      till the thickness of the flange. The section is
c                      not in equilibrium, but the equilibrium  may be
c                      satisfied through other sections in the flange width.
c               =  3   for residual stress due to peening. The
c                      distribution is assumed to have a constant
c                      stress of "sp1" for a thickness "t1" and then
c                      a constant stress "sp2" for the remaining
c                      thickness "t2". Stress "sp2" and thickness "t2" are
c                      calculated so that the section is in equilibrium.
c    lt = flag that determines type of repair
c                = 1   if the flange stress after repair is equal to the
```

```
c                         input value of nominal stress "sef"
c                         The nominal stress range "sef" is used for
c                         computations of crack growth life
c                         This case is used for peening or no repair.
c                   = 2   if the flange stress after repair is different
c                         from the input nominal stress value "sef"
c                         This case is used for bolted splice repair.
c                         The nominal stress value is reduced by a factor
c                         according to the parametric equation that
c                         computes the ratio of the flange to splice plate
c                         stresses.
c    rat1   =   sp2/sp1
c    rat2   =   sp3/sp1
c    ni = number of segments for integration to obtain the geometric
c         correction factor due to the detail geometry



c  READ INPUT DATA

      read (5,700) type
      read (5,*) pw,pt,bd,cpw
      read (5,*) ai,ci
      read (5,*) sef, rns, ni
      read (5,*) ll, lll, lt, kc
      if (ll.eq.0) then
           read (5,*) cp, m
      endif
      if (lll.eq.1) then
           read (5,*) sro
      else
        if (lll.eq.2) then
           read (5,*) sp1,sp2,sp3,td,t
        else
          if (lll.eq.3) then
             read (5,*) sp1,t1
          endif
        endif
      endif
      if (lt.eq.2) then
         read (5,*) asp, afl, acp, aw
         read (5,*) lsp, tsp, dw, tw
      endif
      if (type.eq.'NR') then
         skh = 1.25235
       else
          if (type.eq.'NF') then
              skh = 1.21405
           else
              if (type.eq.'NN') then
                 skh = 1.37275
               else
                  if (type.eq.'WR') then
                     skh = 1.23475
                   else
                      if (type.eq.'WF') then
                         skh = 1.1974
                       else
                          read (5,*) skh
                      endif
                  endif
              endif
          endif
      endif
```

```
c WRITING INPUT INFORMATION

      write (4,4000)
      write (7,4000)

      write (4,1600) type
      write (4,1000) pw
      write (4,1100) pt
      write (4,1300) ai
      write (4,1400) ci
      write (4,1530) rns
      write (4,1700) ll
      write (4,1800) lll
      write (7,2000)

c Initial Crack Conditions

      n = 0.
      i = 0
      a = ai
      c = ci
      j = 0
      write (7,2100) j,n,a,c

c Calculating Required Stress Values that are Independent from the crack size

c     COMPUTING THE PERCENTAGE OF FORCE TRANSMITTED THROUGH THE FLANGE
      if (lt.eq.1) then
         sf = 1.
      else
        if (lt.eq.2) then
           x1 = asp / afl
           x2 = acp / afl
           x3 = aw / afl
           x4 = dw / tw
           x5 = lsp / tsp
           sf = 0.28128573+.31143275*x1-.06566232*x2-.0011347*x5
           sf = sf-.03573589*x1*x1
           sf = 1. - sf
         endif
      endif
      st = sf*.5*(sef+sef*(bd-pt)/bd)
      sb = sf*(sef - st/sf)
      if (lll.eq.2) then
         rat1 = sp2/sp1
         rat2 = sp3/sp1
      endif

      write (4,1500) sef

c Start Cycle by Cycle Calculations

  100 continue
      l=1
      if (c.lt.cpw/2.) then
         mk = skh * 4.41539
         mkr = 1.
      else
         mk =1.
         mkr = 0.
      endif
      if (lll.eq.1) then
           s = sro
      else
```

```
      if (type.eq.'NN'.and.c.gt.0.125) then
             s = 0.0
   else
             s = spl
      endif
   endif
   call sif(a,c,pt,pw,l,st,skr,skm,sb,mk,mkr,s,sift,rns,j)
   call gro(skr,skm,R,l,gr,cp,m,a,c,j,sift,ll,i)
   if (i.eq.6) goto 500
   dc = c/1000.
   dn = dc/gr

   if (gr.ge.0.001) then
       i = 4
       goto 190
   endif

   l=0
   call conc(mk,skh,pt,a,ni)
   if (lll.eq.1) then
        call res (mkr,a,pt)
        s = sro
   else
       if (lll.eq.2) then
          call res1 (rat1,rat2,td,t,a,mkr)
          s = spl
       else
          if (lll.eq.3) then
             call res2 (a,pt,spl,t1,mkr)
          endif
       endif
   endif
   call sif(a,c,pt,pw,l,st,skr,skm,sb,mk,mkr,s,sift,rns,j)
   call gro(skr,skm,R,l,gr,cp,m,a,c,j,sift,ll,i)
   if (i.eq.6) goto 500
   da = dn*gr
   if (gr.ge.0.001) then
       i = 4
       goto 190
   endif

   j = j+1
   if (j/500*500.eq.j) goto 120
   goto 130

120 continue
   write (7,2100) j,n,a,c

130 continue
   call check(a,c,pt,pw,gr,i,sift,kc)
   if (i.ne.0) goto 190

   a = a + da
   c = c + dc
   n = n + dn

   goto 100

190 continue
   write (7,2100) j,n,a,c
   if (i.eq.1) goto 200
   if (i.eq.2) goto 210
   if (i.eq.3) goto 220
   if (i.eq.4) goto 230
   if (i.eq.5) goto 240
```

```
  200 write (7,4100) a/c
      goto 250
  210 write (7,4200) a/pt
      goto 250
  220 write (7,4300) c/pw
      goto 250
  230 write (7,4400) gr
      goto 250
  240 write (7,4500) sift

  250 continue
      if (i.ne.2) goto 500

c If the crack propagates through the whole flange thickness, it is
c assumed to be a through crack with a length equal to "2C"
c Neglect the effect of residual stress for the through crack

      l = 2
      skm = 0.
  300 continue
      call check1(c,pw,gr,i,sift,kc)
      if (i.ne.2) goto 190
      call sif1(c,st,pw,skr,sift,rns,skm)
      call gro(skr,skm,R,l,gr,cp,m,a,c,j,sift,ll,i)
      if (i.eq.6) goto 500
      dc = c/1000.
      dn = dc/gr
      c = c +dc
      n = n + dn
      if (j/500*500.eq.j) goto 400
      goto 450
  400 continue
      write (7,2100) j,n,a,c
  450 continue
      j = j+1
      goto 300

  500 continue
      write (7,5500) sf

      stop
      end


c     ********************Subroutines******************

c Calculates the stress intensity factors for elliptical Crack

      subroutine sif(a,c,pt,pw,l,st,skr,skm,sb,mk,mkr,s,sift,rns,j)

      real mk, mkr
      pi = 4. * atan(1.)
      if (l.eq.1) goto 200
      fi = pi/2
      goto 210
  200 fi = 0.
  210 continue
      q = 1. + 1.464*(a/c)**1.65
      sm1 = 1.13 - .09*(a/c)
      sm2 = -.54 + .89/(.2+(a/c))
      sm3 = .5 - 1/(.65+(a/c)) + 14*(1.-(a/c))**24
      g = 1. + (.1+.35*(a/pt)**2)*(1-sin(fi))**2
      ff = (((a/c)**2)*(cos(fi))**2 + (sin(fi))**2)**.25
      fw = (1/cos(pi*c/pw/2*(a/pt)**.5))**.5
```

```
      f = (sm1 + sm2*(a/pt)**2 + sm3*(a/pt)**4)*ff*g*fw
      p = 0.2 + (a/c) + 0.6 * (a/pt)
      h1 = 1- 0.34 *(a/pt) - 0.11 * (a/c) * (a/pt)
      g1 = -1.22 - 0.12 *(a/c)
      g2 = 0.55 - 1.05 * (a/c)**0.75 + 0.47 * (a/c) **1.5
      h2 = 1 + g1 * (a/pt) + g2 * (a/pt)**2
      h = h1 + (h2-h1) * (sin(fi))**p

      skr = mk * (st+ h * sb)*f*(pi*a/q)**.5
      skm = s * f * mkr * (pi*a/q)**.5 + skr * rns/ (1.-rns)
      sift = skm + skr

      return
      end

c Calculates the stress intensity factors for through crack

      subroutine sif1(c,st,pw,skr,sift,rns,skm)

      pi = 4. * atan(1.)
      fw = (1/cos(pi*c/2/pw))**.5
      skr = st * fw * (pi*c)**.5
      skm = skr * rns / (1.-rns)
      sift = skr + skm

      return
      end

c Calculate the Geometric Correction Factor for Welded Cover Plate Effect
c Using Albrecht and Yamada's technique

      subroutine conc(mk,skh,pt,a,ni)

      real mk
      dimension y(100)
      val = 0.
      do 100 k=1,ni
      bi = (k-1)*10./ni/10.
      bi1 = k *10./ni/10.
      f1 = asin(bi1) - asin(bi)
      f2 = 0.8 + 3.61539*exp(-4.6262*(a/pt/ni*(k-1))**(1./3))
      y(k) = f1 * f2 *skh
      val = val + y(k)
  100 continue
      pi = 4. * atan(1.)
      mk = val *2/pi

      return
      end

c Calculates the growth rate

      subroutine gro(skr,skm,R,l,gr,cp,m,a,c,j,sift,l1,i)

 3350 format (1x, 'Stress Intensity Factor Range Smaller than Zero',
     ,/,'Non-Propagating Crack!!!!',/,'Stress Intensity Range=',f9.5)
      real m
      R = skm / sift
      if (skm.lt.0.) then
          sk = sift
      else
          sk = skr
      endif
      if (sk.lt.0.) then
```

```
          write (7,3350) sk
          i = 6
          goto 300
      endif

      if (ll.eq.1) then
          cp = 3.6e-10
          m  = 3.
          gr = cp * (sk)**m
      else
        if (ll.eq.2) then
             cp = 1.0e-10
             m = 3.3
             gr = cp  * (sk)**m
        else
          if (ll.eq.3) then
               cp = 2.507e-10
               m = 3.
               gr = cp * (sk)**m
          else
            if (ll.eq.4) then
                 cp = 4.16e-9
                 m = 3.07
                 gr = cp*((sk/(2.88-R))**m)
            endif
          endif
        endif
      endif

  300 continue

      return
      end

c Calculates the Geometric Correction Factor for Residual Stress Effect
c due to welding and rolling

      subroutine res (mkr,a,pt)

      real mkr
      pi = 4. * atan(1.)
      mkr = 1. - 2 * a /pi/pt
      return
      end

c Calculating the Geometric Correction Factor for Residual Stress Effect
c due to Peening using the model proposed by Hausammann, Fisher, and Yen

      subroutine res1 (rat1,rat2,td,t,a,mkr)

      real mkr
      pi = 4. * atan(1.)
      fg1 = 2./pi*asin(td/a)
      fg2 = (rat1+(1-rat1)*(0.2*t+td)/0.2/t)*(1-2./pi*asin(td/a))
      fg3 = 2./pi*(1-rat1)/.2/t*(a*a-td*td)**.5
      fg4 = 2./pi*(rat1+(1-rat1)*(.2*t+td)/.2/t)*(asin((td+.2*t)/a)
     ,-asin(td/a))
      fg5 = 2./pi*(1-rat1)/.2/t*((a*a-(td+.2*t)**2)**.5-(a*a-td**2)
     ,**.5)
      fg6 = rat1*(1-2./pi*asin((td+.2*t)/a))
      fg7 = 2./pi*rat1*(asin((td+t)/a)-asin((td+.2*t)/a))
      fg8 = rat2*(1-2./pi*asin((td+t)/a))
      if (a.le.td) then
         mkr = 1.
```

```
      else
         if (a.gt.td.and.a.le.(td+0.2*t)) then
            mkr = fg1 + fg2 -fg3
         else
            if (a.gt.(td+0.2*t).and.a.le.(td+t)) then
               mkr = fg1 + fg4 + fg5 + fg6
            else
               if (a.gt.(td+t)) then
                  mkr = fg1 + fg4 + fg5 + fg7 +fg8
               endif
            endif
         endif
      endif
      return
      end

c Calculates the geometric correction factor for the effect of peening
c using the simplified model

      subroutine res2 (a,pt,sp1,t1,mkr)

      real mkr
      pi = 4. * atan(1.)
      t2 = pt - t1
      sp2 = -1*sp1*t1/t2
      if (a.le.t1) then
         mkr = 1.
      else
         if (a.gt.t1.and.a.le.pt) then
           mkr=2./pi*asin(t1/a)+sp2/sp1*(1.-2./pi*asin(t1/a))
         endif
      endif
      return
      end


c Checks for Fracture Criteria for eliprical crack

      subroutine check(a,c,pt,pw,gr,i,sift,kc)

      real kc
      if (a/c.gt.1.0) goto 400
      if (a/pt.ge.1.0) goto 410
      if (c/pw.ge.0.5) goto 420
      if (gr.ge.0.001) goto 430
      if (sift.ge.kc) goto 440
      goto 450
  400 i = 1
      goto 450
  410 i = 2
      goto 450
  420 i = 3
      goto 450
  430 i = 4
      goto 450
  440 i = 5

  450 continue

      return
      end


c Checks for fracture criteria for through cracks
```

```
      subroutine check1(c,pw,gr,i,sift,kc)
      real kc
      if (c/pw.ge.1.0) goto 420
      if (gr.ge.0.001) goto 430
      if (sift.ge.kc) goto 440
      goto 450
  420 i = 3
      goto 450
  430 i = 4
      goto 450
  440 i = 5
  450 continue
      return
      end
```

H.3. Input Parameter Description

The program listed earlier requires an input file named *"data.inp"* to compute the propagation life of a welded tapered cover plate detail. The following sections describe the input parameters and their location in the input file. The propagation life is found in the output file *"life.out"*.

<u>LINE 1</u> ***type***

type ⇒ type of detail analyzed

NR for narrow cover plate, return end-weld details

NF for narrow cover plate, full end-weld details

NN for narrow cover plate, no end-weld details

WR for wide cover plate, return end-weld details

WF for wide cover plate, full end-weld details

if the detail type is different from the five types listed, the user will need to input a value for the stress concentration due to the cover plate geometry and the end-weld condition (refer to line 10).

<u>LINE 2</u> ***pw, pt, bd, cpw***

pw ⇒ half the flange plate width (in)

pt ⇒ flange plate thickness (in)

bd ⇒ half of the beam depth (in)

cpw ⇒ cover plate width at the end of taper (in)

LINE 3 *ai, ci*

ai ⇒ equivalent initial crack depth (in)

ci ⇒ equivalent half initial crack length (in)

LINE 4 *sef, rns, ni*

sef ⇒ nominal stress range at the cover plate end for the bare cross section (ksi)

rns ⇒ nominal stress ratio

ni ⇒ number of segments for integration to obtain the geometric correction factor due to the detail geometry. (suggested number = 50)

LINE 5 *ll, lll, lt, kc*

ll ⇒ flag for type of propagation model used

0 for user's defined C and m values, where

$$\frac{da}{dN} = C\,(\Delta K)^m$$

1 for conservative propagation estimates of ferrite-pearlite steels (Barsom and Rolfe, 1987)

2 for average propagation estimates of ASTM A36 steel (Barsom and Rolfe, 1987)

3 for average propagation estimates of ferrite-pearlite steels (Yamada and Hirt, 1982)

4 for average propagation estimates of ferritic steels (Eason et al., 1988)

$$\frac{da}{dN} = 4.16 \times 10^{-9} \left(\frac{\Delta K}{2.88 - R}\right)^{3.07}$$

where, ΔK is the stress intensity factor range in ksi $in^{1/2}$, da/dN is the growth rate in in/cycles, and R is the stress intensity factor ratio (K_{min}/ K_{max})

lll ⇒ flag for residual stress distribution (refer to Fig. H.1)

1 for residual stress distribution from fabrication

2 for residual stress distribution from peening (Hausammann et al., 1983)

3 for simplified residual stress distribution from peening

lt ⇒ flag for repair type that determines the percentage of stress transmitted through the flange, which helps propagate cracks

1 for 100% of the nominal stress transmitted through the flange (ex: no repair, or repair using air-hammer peening)

2 for only a percentage of the nominal stress transmitted through the flange (ex: bolted splice plate repair)

kc ⇒ fracture toughness (ksi in$^{1/2}$)

LINE 6 *cp, m* **"ONLY IF ll = 0"**

cp and m ⇒ propagation model constants (refer to input in line 5)

LINE 7 refer to fig. H.1 for illustration of variables

IF lll = 1 ***sro***

IF lll = 2 ***sp1, sp2, sp3, td, t***

IF lll = 3 ***sp1, t1***

LINE 8 ***asp, afl, acp, aw*** **"ONLY IF lt =2"**

asp ⇒ splice plate area (in^2)

afl ⇒ flange area (in^2)

acp ⇒ cover plate area (in^2)

aw ⇒ web area (in^2)

LINE 9 ***lsp, tsp, dw, tw*** **"ONLY IF lt = 2"**

lsp ⇒ unsupported length of the splice plate (i.e. distance between inner bolts for the splice plate connection) (in)

tsp ⇒ splice plates thickness (in)

dw ⇒ web depth (in)

tw ⇒ web thickness (in)

LINE 10 *skh* **"ONLY IF *type* is different"** (refer to line 1)

skh ⇒ stress concentration factor due to cover plate geometry and end-weld condition

H.4. Input File

An input file for the computation of the fatigue life of a cracked W 14 × 30 beam with a narrow cover plate, full end-weld detail is listed next. The equivalent initial crack was 1/8-in deep and 1 3/8-in long. The detail was subjected to a stress range of 8.67-ksi and a stress ratio of 0.05. The detail is not repaired and the crack propagates to fracture of the flange. The residual stresses from fabrication were assumed to have a maximum value of 42.0-ksi.

```
NF
3.375 .384 6.92 2.
.125 .6875
8.67 .05 50
2 1 1 150.
42.
```

H.5. Output File

The output file that corresponds to the input file listed earlier is given next. It can be seen that 1,050,000 cycles of loading are required to propagate the initial cracks to full fracture of the flange.

```
Program Growth

    step No.      No. of Cycles     Crack Depth "a"     1/2 Crack Width "c"
        0                0.0         0.1250000000         0.6875000000
      411           507496.7         0.3846752346         1.0357249975
  Ratio of Crack Depth to Flange Thickness EXCEEDED
  a/pt = 1.002
      500           598958.7         0.3846752346         1.1332132816
     1000           946188.4         0.3846752346         1.8678864241
     1500          1048827.4         0.3846752346         3.0788509846
     1567          1049654.9         0.3846752346         3.2888016701
  Growth Rate TOO FAST - Rate = 0.001
Percentage of Force Transmitted through the flange  1.00000
```

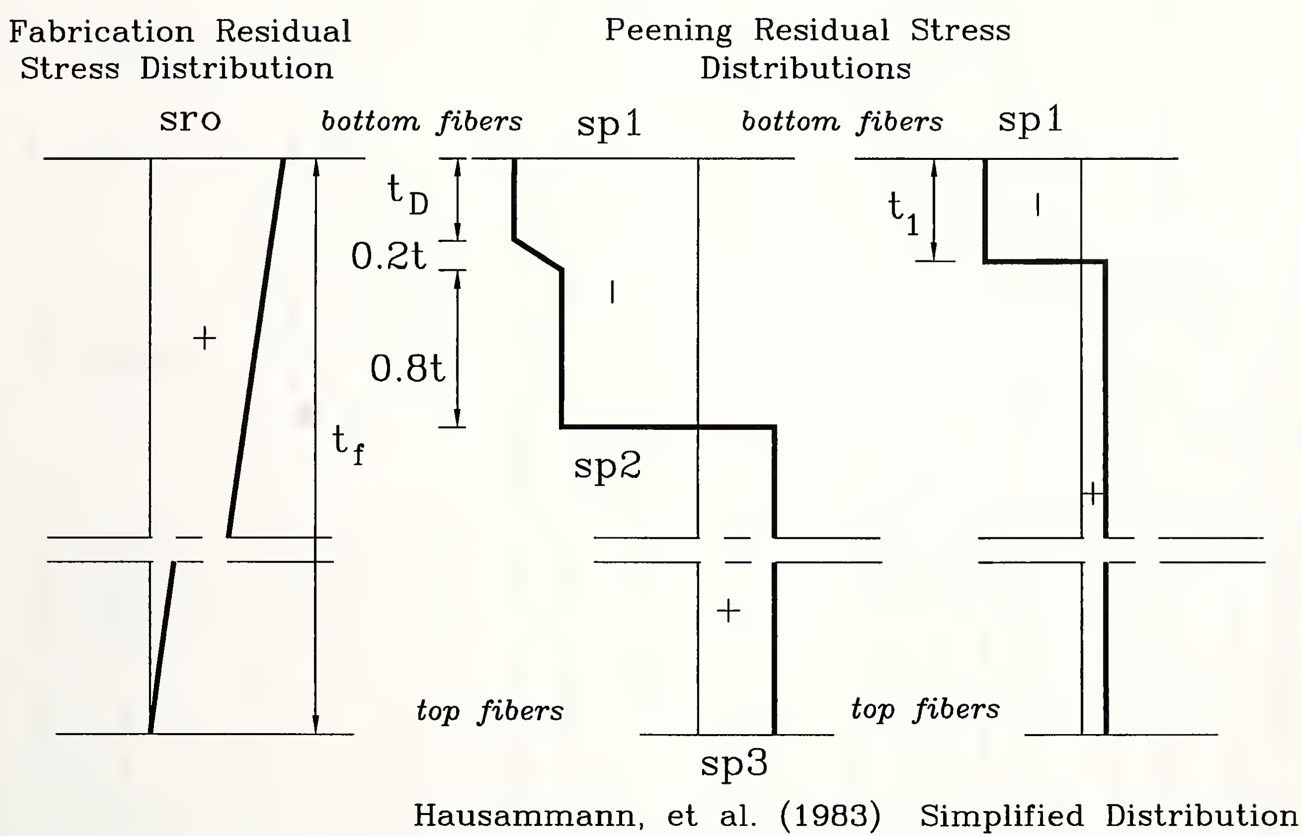

Fig. H.1. Residual Stress istribution.

APPENDIX I
SPLICE PLATE FORCE COMPUTATION

I.1. General

The nominal flange stress is responsible for the propagation of existing cracks and must be accurately evaluated to obtain a good estimation of the propagation life. When a splice plate connection is used to repair a cover plate end, a portion of the total flange force prior to applying the splice repair will be carried by the splice plates. The remaining force will be carried by the flange and will propagate existing cracks.

This appendix presents the finite element analysis involved in determining the splice plate force - that portion of the force which does not affect the crack propagation. The results are used both for program verification with existing test results and for predictions of the fatigue life of typical bridge girders.

I.2. Program Verification

Two dimensional finite element analysis was carried out using ANSYS (1993). Six-node triangular and eight-node rectangular plane stress elements were used to represent the beam flanges, web, cover plates, and splice plates. Due to symmetry of loading, only 1/4 of the beam was modeled. First, the bare beam was modeled and the results were compared to the strain gage measurements obtained during the experimental part of the study (Specimen DB1). The cover plate taper was modeled by dividing the taper length into five portions each with a constant width equal to the width of the middle section of the portion. The cover plate was assumed to be fully connected to the flange surface; the cover plate and flange surfaces were modeled with the same nodes.

The beam behavior was accurately modeled using the 2-D analysis. The maximum deflection measured during the tests at the middle of the beam was about 0.33", while the maximum deflection obtained from the finite element analysis was about 0.337". The maximum flange stresses at about 6" from the cover plate ends was about 19.20 ksi and 19.468 ksi for the experimental and analytical analyses, respectively. The maximum cover plate stress in the constant moment region was about 14.11 ksi and 14.88 ksi for the experimental and analytical analyses, respectively.

The next step involved modeling the splice plates. The same element type and material properties were used for the splice plates as for the beam. Several trials were made to represent the friction behavior between the splice plate and beam surfaces. Unfortunately, the finite element method does not have an accurate representation of Coulomb friction. Modeling of friction requires the knowledge of stiffness values for the interface elements that represent friction. These values must be obtained from a trial and error procedure to yield the observed behavior during the tests. Because the connection was designed as a friction type and no slippage between the splice plate and beam surfaces was observed during the tests, the splice plate was restricted from horizontal movement at the bolt center-line locations. To represent the effects of clamping forces induced during bolt tightening, all coincident nodes on any interface surface that lie within the bolt diameter were linked together in the vertical direction (i.e., these nodes will have the same vertical displacement value).

The finite element mesh used to model the test beams is shown in Fig. I.1. The stresses developed in the upper and lower splice plates are compared in Table I.1 for the values predicted analytically and measured experimentally. It can be seen that the finite element analysis yields results in good agreement with the strain gage measurements.

The force carried by the splice plate is obtained from the finite element analysis and subtracted from the total flange force. Then, the stresses in the flange, after repair, are calculated assuming a uniform distribution through the flange thickness. Table I.2 shows the splice plate force and the nominal flange stress after repair.

A similar finite element analysis was conducted to determine the flange stress for the partial bolted splice repair technique. The same finite element mesh was used, with the omission of the bottom splice plate and filler plate. The upper fiber stresses at the middle of the splice plates were 8.7 ksi and 9.1 ksi for strain gage measurements and finite element analysis, respectively. The splice plates were found to carry about 21.0 kips of the total 51.8 kips flange force. Therefore, the nominal flange stress was found to be about 11.9 ksi.

I.3. Life Prediction for Typical Bridge Girders

Finite element analysis was conducted also to determine a general equation which could be used to calculate the splice plate force. The same assumptions previously mentioned were used also for this analysis.

Discussion with Indiana Department of Transportation engineers showed that the following range of beam sizes represents nearly all of the bridge girders containing the tapered cover plate detail in Indiana: W36 × 136 to W36 × 194; W33 × 118 to W 33 × 152; W30 × 99 to W30 × 132; W27 × 84 to W27 × 114. Also, the cover plate thickness ranged from 3/8-in to 15/16-in. The taper length ranged from 1-ft to 2-ft (1 1/2-ft was the usual taper length), and the cover plate width at the end of taper ranged from 2-in to 4-in (3-in was the usual width).

To simulate AASHTO loading, the girders were assumed to be loaded with equal two-point loads 14-ft apart, with each load located 7-ft from the center of the girder. The total cover plate length was assumed to be 24-ft (21-ft of straight cover plate and two 1 1/2-ft of taper length). The beam length and the applied force were adjusted such that the maximum stress calculated for the bare beam cross section, at the cover plate ends equals 20.0 ksi (allowable stress for ASTM A36 steel). The adjustment was done in the following steps:

1. The applied loads were set to 30.0 kips each and the stress at the cover plate end of the middle beam size for each depth was set to 20.0 ksi. The distance between the cover plate ends and the support was therefore set.

2. A round number was selected for that distance and kept constant for each beam depth. The applied forces were then adjusted accordingly to maintain the 20.0 ksi stress value at the cover plate ends.

As previously mentioned, three beam sizes were selected for each beam depth to represent the whole range of beams. Also three cover plate areas were selected to represent the range of cover plates. The middle size of each beam depth was selected to be the primary size. To model the lower and higher sizes, only the flanges were changed (i.e. the web thickness and depth were kept constant). In reality, the flange thickness changes considerably from one beam size to another (within the same beam depth), while the flange width remains relatively constant. Thus, exact modeling would require generation of the finite element mesh for each beam size. Trial runs, however, demonstrated that changing the flange width or thickness, while keeping the area constant, has only a small effect on the obtained splice plate force. A difference of about 0.7% was observed for the maximum change in flange width considered in this study. Thus, only the primary beam size (middle size) was modeled by its exact dimensions. The other beam sizes were simply modeled by changing the flange width of the primary size to achieve the required flange area.

For each beam analyzed, three cover plate areas were considered as follows:

(a) A middle value of cover plate area (5/8-in thick) with a narrow cover plate detail (about 1-in narrower than the flange width).

(b) A lower value of cover plate area (3/8-in thick) with a narrow cover plate detail.

(c) An upper value of cover plate area (15/16-in thick) with a wide cover plate detail (about 1-in wider than the flange width).

The last variable considered in the analysis is the splice plates area. For each beam depth, the splice plate widths were selected as follows:

(a) the width of the lower splice plate was selected to be equal to the narrow cover plate width.

(b) the upper splice plates width was chosen such that they fit on both sides of the web and such that their edges match the edges of the lower splice plate.

For each beam depth, a splice plate connection was designed for the primary size such that the stresses in the lower fibers of the bottom splice plate and the upper fibers of the compression flange do not exceed the allowable stress (e.g., 20.0 ksi for ASTM A36 steel). The design was conducted assuming that the tension flange was completely severed and does not contribute in carrying the applied bending moment. The splice plate thickness obtained using this procedure is referred to as the design thickness. The design thickness, along with higher of 1.25, 1.50, and 2.0 times the design value, were used to represent the range in splice plates area.

The same finite elements and assumption used for the program verification were used in these runs. Only one-quarter of the beam was modeled due to symmetry. Eight-node rectangular and six- node triangular plane stress elements were used to model the beam, cover plate and splice plates. The cover plate was assumed to be fully connected to the flange surface. As previously mentioned, the splice connection was modeled as a bearing connection.

Table I.1. Splice Plate Stresses (in ksi) by Finite Element and Experimental Measurements.

	5/16" Splice		7/16" Splice	
	Experiment	Finite Element	Experiment	Finite Element
Upper Splice Plate	7.5	7.8	6.0	6.9
Lower Splice Plate	9.8	9.6	7.3	7.8

Table I.2. Splice Plate Force and Nominal Flange Stress.

	5/16" Splice		7/16" Splice	
	Wide Cover Plate	Narrow Cover Plate	Wide Cover Plate	Narrow Cover Plate
Force in Top and Bottom Splice Plates (kips)	27.97	29.36	33.41	34.76
Total Flange Force (kips)	51.84	51.84	51.84	51.84
Net Flange Force (kips)	23.87	22.48	18.43	17.08
Flange Stress (ksi)	9.21	8.67	7.11	6.59

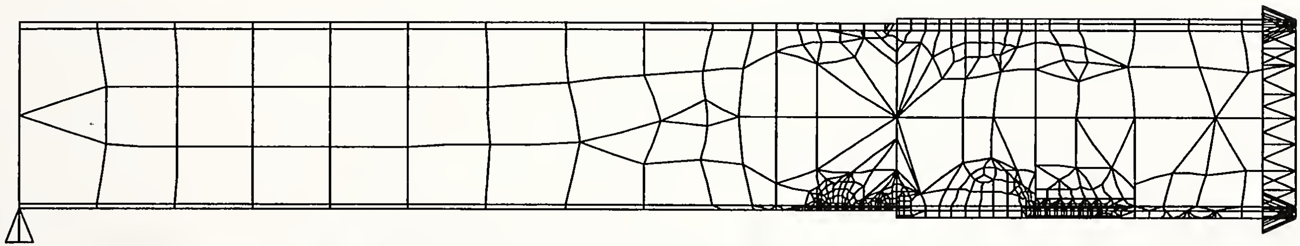

a– Two–Dimensional Test Beam
(Finite Element Mesh for Stress Calculations)

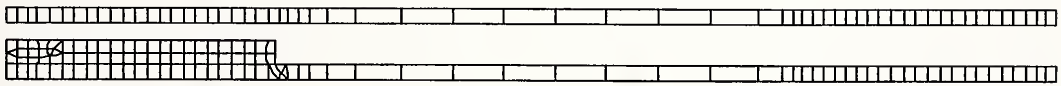

b– Finite Element Mesh of Splice Plates

Fig. I.1. Finite Element Mesh of Test Beams.

APPENDIX J
SPLICE PLATE FORCE
(FINITE ELEMENT ANALYSIS RESULTS)

J.1. General

This appendix presents the forces carried by the splice plates obtained from the finite element analysis. Results from the 144 finite element runs are listed hereafter. The estimated flange stresses after repair are also listed in the following tables. As previously mentioned, the splice plates were connected to the flange and cover plates by restricting the movement of nodes in the horizontal direction at the bolt center-line. This results in horizontal forces at these nodes. The splice plate force is calculated by adding the forces at the restricted nodes from the finite element analysis. The remaining flange force is then calculated by subtracting the splice plates force from the total flange force. Thus, the estimated flange stress is calculated by dividing the remaining flange force by the flange area. In other words, the flange stresses were assumed to be uniform after the splice plate connection has been used.

<u>W 36 X 135</u>
Flange Force = 20.0 * 0.79 * 11.95 = 188.81 kips
Flange Area = 0.79 * 11.95 = 9.4405 in^2
Taper Length = 18 in
Applied Force = 24.38888 kip

*<u>Cover Plate Area = 5/8 * 11 = 6.875 in^2</u>*

Splice Plates	Flange Stress (ksi)	Splice Plate Area (in^2)	Splice Plate Force (kip)
2# 5.0 * 5/8 & 1# 11.0 * 5/8	8.055	13.125	112.764
2# 6.25 * 5/8 & 1# 13.75 * 5/8	6.544	16.40625	127.030
2 # 7.5 * 5/8 & 1# 16.5 * 5/8	5.300	19.6875	138.766
2 # 10.0 * 5/8 & 1 # 22.0 * 5/8	3.373	26.25	156.966

<u>Cover Plate Area = 12.1875 in^2</u>

Splice Plates	Flange Stress (ksi)	Splice Plate Area (in^2)	Splice Plate Force (kip)
2# 5.0 * 5/8 & 1# 11.0 * 5/8	8.808	13.125	105.662
2# 6.25 * 5/8 & 1# 13.75 * 5/8	7.316	16.40625	119.744
2 # 7.5 * 5/8 & 1# 16.5 * 5/8	6.075	19.6875	131.458
2 # 10.0 * 5/8 & 1 # 22.0 * 5/8	4.127	26.25	149.848

<u>Cover Plate Area = 4.125 in^2</u>

Splice Plates	Flange Stress (ksi)	Splice Plate Area (in^2)	Splice Plate Force (kip)
2# 5.0 * 5/8 & 1# 11.0 * 5/8	7.575	13.125	117.294
2# 6.25 * 5/8 & 1# 13.75 * 5/8	6.065	16.40625	131.550
2 # 7.5 * 5/8 & 1# 16.5 * 5/8	4.833	19.6875	143.188
2 # 10.0 * 5/8 & 1 # 22.0 * 5/8	2.937	26.25	161.080

<u>W 36 X 160</u>
Flange Force = 20.0 * 1.02 * 12.0 = 244.8 kips
Flange Area = 1.02 * 12.0 = 12.24 in^2
Taper Length = 18 in
Applied Force = 30.11111 kip

*Cover Plate Area = 5/8 * 11 = 6.875 in^2*

Splice Plates	Flange Stress (ksi)	Splice Plate Area (in^2)	Splice Plate Force (kip)
2# 5.0 * 5/8 & 1# 11.0 * 5/8	9.690	13.125	126.196
2# 6.25 * 5/8 & 1# 13.75 * 5/8	8.286	16.40625	143.374
2 # 7.5 * 5/8 & 1# 16.5 * 5/8	7.114	19.6875	157.722
2 # 10.0 * 5/8 & 1 # 22.0 * 5/8	5.264	26.25	180.368

Cover Plate Area = 12.1875 in^2

Splice Plates	Flange Stress (ksi)	Splice Plate Area (in^2)	Splice Plate Force (kip)
2# 5.0 * 5/8 & 1# 11.0 * 5/8	10.309	13.125	118.618
2# 6.25 * 5/8 & 1# 13.75 * 5/8	8.930	16.40625	135.494
2 # 7.5 * 5/8 & 1# 16.5 * 5/8	7.767	19.6875	149.728
2 # 10.0 * 5/8 & 1 # 22.0 * 5/8	5.910	26.25	172.450

Cover Plate Area = 4.125 in^2

Splice Plates	Flange Stress (ksi)	Splice Plate Area (in^2)	Splice Plate Force (kip)
2# 5.0 * 5/8 & 1# 11.0 * 5/8	9.305	13.125	130.910
2# 6.25 * 5/8 & 1# 13.75 * 5/8	7.897	16.40625	148.144
2 # 7.5 * 5/8 & 1# 16.5 * 5/8	6.729	19.6875	162.440
2 # 10.0 * 5/8 & 1 # 22.0 * 5/8	4.900	26.25	184.824

W 36 X 194

Flange Force = 20.0 * 1.26 * 12.115 = 305.298 kips
Flange Area = 1.26 * 12.115 = 15.2649 in^2
Taper Length = 18 in
Applied Force = 36.88888 kip

*Cover Plate Area = 5/8 * 11 = 6.875 in^2*

Splice Plates	Flange Stress (ksi)	Splice Plate Area (in^2)	Splice Plate Force (kip)
2# 5.0 * 5/8 & 1# 11.0 * 5/8	10.793	13.125	140.544
2# 6.25 * 5/8 & 1# 13.75 * 5/8	9.460	16.40625	160.890
2 # 7.5 * 5/8 & 1# 16.5 * 5/8	8.331	19.6875	178.120
2 # 10.0 * 5/8 & 1 # 22.0 * 5/8	6.520	26.25	205.760

Cover Plate Area = 12.1875 in^2

Splice Plates	Flange Stress (ksi)	Splice Plate Area (in^2)	Splice Plate Force (kip)
2# 5.0 * 5/8 & 1# 11.0 * 5/8	11.314	13.125	132.592
2# 6.25 * 5/8 & 1# 13.75 * 5/8	10.008	16.40625	152.524
2 # 7.5 * 5/8 & 1# 16.5 * 5/8	8.893	19.6875	169.552
2 # 10.0 * 5/8 & 1 # 22.0 * 5/8	7.085	26.25	197.146

Cover Plate Area = 4.125 in^2

Splice Plates	Flange Stress (ksi)	Splice Plate Area (in^2)	Splice Plate Force (kip)
2# 5.0 * 5/8 & 1# 11.0 * 5/8	10.475	13.125	145.398
2# 6.25 * 5/8 & 1# 13.75 * 5/8	9.135	16.40625	165.858
2 # 7.5 * 5/8 & 1# 16.5 * 5/8	8.007	19.6875	183.078
2 # 10.0 * 5/8 & 1 # 22.0 * 5/8	6.210	26.25	210.500

<u>W 33 X 118</u>

Flange Force = 20.0 * 0.74 * 11.48 = 169.904 kips
Flange Area = 0.74 * 11.48 = 8.4952 in^2
Taper Length = 18 in
Applied Force = 24.9370555 kip

*<u>Cover Plate Area = 5/8 * 10.5 = 6.5625 in^2</u>*

Splice Plates	Flange Stress (ksi)	Splice Plate Area (in^2)	Splice Plate Force (kip)
2# 4.5 * 5/8 & 1# 10.5 * 5/8	9.084	12.1875	92.732
2# 5.625 * 5/8 & 1# 13.125 * 5/8	7.5869	15.234375	105.452
2 # 6.75 * 5/8 & 1# 15.75 * 5/8	6.33369	18.28125	116.098
2 # 9 * 5/8 & 1 # 21 * 5/8	4.35234	24.375	132.93

<u>Cover Plate Area = 3.9375 in^2</u>

Splice Plates	Flange Stress (ksi)	Splice Plate Area (in^2)	Splice Plate Force (kip)
2# 4.5 * 5/8 & 1# 10.5 * 5/8	8.698	12.1875	96.014
2# 5.625 * 5/8 & 1# 13.125 * 5/8	7.198	15.234375	108.752
2 # 6.75 * 5/8 & 1# 15.75 * 5/8	5.953	18.28125	119.334
2 # 9 * 5/8 & 1 # 21 * 5/8	4.000	24.375	135.924

<u>Cover Plate Area = 11.71875 in^2</u>

Splice Plates	Flange Stress (ksi)	Splice Plate Area (in^2)	Splice Plate Force (kip)
2# 4.5 * 5/8 & 1# 10.5 * 5/8	9.716	12.1875	87.368
2# 5.625 * 5/8 & 1# 13.125 * 5/8	8.241	15.234375	99.892
2 # 6.75 * 5/8 & 1# 15.75 * 5/8	6.995	18.28125	110.478
2 # 9 * 5/8 & 1 # 21 * 5/8	5.001	24.375	127.418

W 33 X 141
Flange Force = 20.0 * 0.96 * 11.535 = 221.472 kips
Flange Area = 0.96 * 11.535 = 11.0736 in^2
Taper Length = 18 in
Applied Force = 31.11111 kip

*Cover Plate Area = 5/8 * 10.5 = 6.5625 in^2*

Splice Plates	Flange Stress (ksi)	Splice Plate Area (in^2)	Splice Plate Force (kip)
2# 4.5 * 5/8 & 1# 10.5 * 5/8	10.443	12.1875	105.836
2# 5.625 * 5/8 & 1# 13.125 * 5/8	9.053	15.234375	121.224
2 # 6.75 * 5/8 & 1# 15.75 * 5/8	7.875	18.28125	134.272
2 # 9 * 5/8 & 1 # 21 * 5/8	5.983	24.375	155.222

Cover Plate Area = 3.9375 in^2

Splice Plates	Flange Stress (ksi)	Splice Plate Area (in^2)	Splice Plate Force (kip)
2# 4.5 * 5/8 & 1# 10.5 * 5/8	10.125	12.1875	109.354
2# 5.625 * 5/8 & 1# 13.125 * 5/8	8.729	15.234375	124.806
2 # 6.75 * 5/8 & 1# 15.75 * 5/8	7.554	18.28125	137.820
2 # 9 * 5/8 & 1 # 21 * 5/8	5.682	24.375	158.556

Cover Plate Area = 11.71875 in^2

Splice Plates	Flange Stress (ksi)	Splice Plate Area (in^2)	Splice Plate Force (kip)
2# 4.5 * 5/8 & 1# 10.5 * 5/8	10.970	12.1875	99.990
2# 5.625 * 5/8 & 1# 13.125 * 5/8	9.607	15.234375	115.092
2 # 6.75 * 5/8 & 1# 15.75 * 5/8	8.440	18.28125	128.014
2 # 9 * 5/8 & 1 # 21 * 5/8	6.545	24.375	148.992

W 33 X 152
Flange Force = 20.0 * 1.055 * 11.565 = 244.0215 kips
Flange Area = 1.055 * 11.565 = 12.201075 in^2
Taper Length = 18 in
Applied Force = 33.8194444 kip

*Cover Plate Area = 5/8 * 10.5 = 6.5625 in^2*

Splice Plates	Flange Stress (ksi)	Splice Plate Area (in^2)	Splice Plate Force (kip)
2# 4.5 * 5/8 & 1# 10.5 * 5/8	10.909	12.1875	110.918
2# 5.625 * 5/8 & 1# 13.125 * 5/8	9.559	15.234375	127.398
2 # 6.75 * 5/8 & 1# 15.75 * 5/8	8.408	18.28125	141.440
2 # 9 * 5/8 & 1 # 21 * 5/8	6.549	24.375	164.120

Cover Plate Area = 3.9375 in^2

Splice Plates	Flange Stress (ksi)	Splice Plate Area (in^2)	Splice Plate Force (kip)
2# 4.5 * 5/8 & 1# 10.5 * 5/8	10.615	12.1875	114.504
2# 5.625 * 5/8 & 1# 13.125 * 5/8	9.258	15.234375	131.064
2 # 6.75 * 5/8 & 1# 15.75 * 5/8	8.109	18.28125	145.086
2 # 9 * 5/8 & 1 # 21 * 5/8	6.266	24.375	167.566

Cover Plate Area = 11.71875 in^2

Splice Plates	Flange Stress (ksi)	Splice Plate Area (in^2)	Splice Plate Force (kip)
2# 4.5 * 5/8 & 1# 10.5 * 5/8	11.401	12.1875	104.916
2# 5.625 * 5/8 & 1# 13.125 * 5/8	10.077	15.234375	121.072
2 # 6.75 * 5/8 & 1# 15.75 * 5/8	8.939	18.28125	134.958
2 # 9 * 5/8 & 1 # 21 * 5/8	7.0806	24.375	157.630

W 30 X 99
Flange Force = 20.0 * 0.67 * 10.45 = 140.03 kips
Flange Area = 0.67 * 10.45 = 7.0015 in^2
Taper Length = 18 in
Applied Force = 24.9074074 kip

*Cover Plate Area = 5/8 * 9.5 = 5.9375 in^2*

Splice Plates	Flange Stress (ksi)	Splice Plate Area (in^2)	Splice Plate Force (kip)
2# 4 * 11/16 & 1# 9.5 * 11/16	7.814	12.03125	85.324
2# 5 * 11/16 & 1# 11.875 * 11/16	6.238	15.0390625	96.354
2 # 6 * 11/16 & 1# 14.25 * 11/16	4.936	18.046875	105.468
2 # 8 * 11/16 & 1 # 19 * 11/16	2.907	24.0625	119.678

Cover Plate Area = 3.5625 in^2

Splice Plates	Flange Stress (ksi)	Splice Plate Area (in^2)	Splice Plate Force (kip)
2# 4 * 11/16 & 1# 9.5 * 11/16	7.362	12.03125	88.488
2# 5 * 11/16 & 1# 11.875 * 11/16	5.788	15.0390625	99.504
2 # 6 * 11/16 & 1# 14.25 * 11/16	4.498	18.046875	108.540
2 # 8 * 11/16 & 1 # 19 * 11/16	2.502	24.0625	122.512

Cover Plate Area = 10.78125 in^2

Splice Plates	Flange Stress (ksi)	Splice Plate Area (in^2)	Splice Plate Force (kip)
2# 4 * 11/16 & 1# 9.5 * 11/16	8.566	12.03125	80.054
2# 5 * 11/16 & 1# 11.875 * 11/16	7.011	15.0390625	90.944
2 # 6 * 11/16 & 1# 14.25 * 11/16	5.711	18.046875	100.044
2 # 8 * 11/16 & 1 # 19 * 11/16	3.660	24.0625	114.404

<u>W 30 X 116</u>
Flange Force = 20.0 * 0.85 * 10.495 = 178.415 kips
Flange Area = 0.85 * 10.495 = 8.92075 in^2
Taper Length = 18 in
Applied Force = 30.462963 kip

*<u>Cover Plate Area = 5/8 * 9.5 = 5.9375 in^2</u>*

Splice Plates	Flange Stress (ksi)	Splice Plate Area (in^2)	Splice Plate Force (kip)
2# 4 * 11/16 & 1# 9.5 * 11/16	9.155	12.03125	96.746
2# 5 * 11/16 & 1# 11.875 * 11/16	7.674	15.0390625	109.958
2 # 6 * 11/16 & 1# 14.25 * 11/16	6.436	18.046875	121.004
2 # 8 * 11/16 & 1 # 19 * 11/16	4.480	24.0625	138.450

<u>Cover Plate Area = 3.5625 in^2</u>

Splice Plates	Flange Stress (ksi)	Splice Plate Area (in^2)	Splice Plate Force (kip)
2# 4 * 11/16 & 1# 9.5 * 11/16	8.774	12.03125	100.142
2# 5 * 11/16 & 1# 11.875 * 11/16	7.291	15.0390625	113.372
2 # 6 * 11/16 & 1# 14.25 * 11/16	6.060	18.046875	124.358
2 # 8 * 11/16 & 1 # 19 * 11/16	4.129	24.0625	141.580

<u>Cover Plate Area = 10.78125 in^2</u>

Splice Plates	Flange Stress (ksi)	Splice Plate Area (in^2)	Splice Plate Force (kip)
2# 4 * 11/16 & 1# 9.5 * 11/16	9.800	12.03125	90.992
2# 5 * 11/16 & 1# 11.875 * 11/16	8.342	15.0390625	103.996
2 # 6 * 11/16 & 1# 14.25 * 11/16	7.111	18.046875	114.978
2 # 8 * 11/16 & 1 # 19 * 11/16	5.144	24.0625	132.526

<u>**W 30 X 132**</u>
Flange Force = 20.0 * 1.0 * 10.545 = 210.9 kips
Flange Area = 1.0 * 10.545 = 10.545 in^2
Taper Length = 18 in
Applied Force = 35.185185 kip

*<u>Cover Plate Area = 5/8 * 9.5 = 5.9375 in^2</u>*

Splice Plates	Flange Stress (ksi)	Splice Plate Area (in^2)	Splice Plate Force (kip)
2# 4 * 11/16 & 1# 9.5 * 11/16	10.018	12.03125	105.258
2# 5 * 11/16 & 1# 11.875 * 11/16	8.601	15.0390625	120.200
2 # 6 * 11/16 & 1# 14.25 * 11/16	7.407	18.046875	132.798
2 # 8 * 11/16 & 1 # 19 * 11/16	5.500	24.0625	152.896

<u>Cover Plate Area = 3.5625 in^2</u>

Splice Plates	Flange Stress (ksi)	Splice Plate Area (in^2)	Splice Plate Force (kip)
2# 4 * 11/16 & 1# 9.5 * 11/16	9.684	12.03125	108.782
2# 5 * 11/16 & 1# 11.875 * 11/16	8.263	15.0390625	123.770
2 # 6 * 11/16 & 1# 14.25 * 11/16	7.072	18.046875	136.326
2 # 8 * 11/16 & 1 # 19 * 11/16	5.186	24.0625	156.212

<u>Cover Plate Area = 10.78125 in^2</u>

Splice Plates	Flange Stress (ksi)	Splice Plate Area (in^2)	Splice Plate Force (kip)
2# 4 * 11/16 & 1# 9.5 * 11/16	10.593	12.03125	99.202
2# 5 * 11/16 & 1# 11.875 * 11/16	9.201	15.0390625	113.878
2 # 6 * 11/16 & 1# 14.25 * 11/16	8.016	18.046875	126.370
2 # 8 * 11/16 & 1 # 19 * 11/16	6.105	24.0625	146.520

W 27 X 84
Flange Force = 20.0 * 0.64 * 9.96 = 127.488 kips
Flange Area = 0.64 * 9.96 = 6.3616 in^2
Taper Length = 18 in
Applied Force = 25.35714 kip

*Cover Plate Area = 5/8 * 9 = 5.625 in^2*

Splice Plates	Flange Stress (ksi)	Splice Plate Area (in^2)	Splice Plate Force (kip)
2# 4 * 9/16 & 1# 9 * 9/16	8.650	9.5625	72.418
2# 5 * 9/16 & 1# 11.25 * 9/16	7.109	11.953125	82.266
2 # 6 * 9/16 & 1# 13.5 * 9/16	5.817	14.34375	90.484
2 # 8 * 9/16 & 1 # 18 * 9/16	3.780	19.125	103.442

Cover Plate Area = 3.375 in^2

Splice Plates	Flange Stress (ksi)	Splice Plate Area (in^2)	Splice Plate Force (kip)
2# 4 * 9/16 & 1# 9 * 9/16	8.149	9.5625	75.650
2# 5 * 9/16 & 1# 11.25 * 9/16	6.591	11.953125	85.556
2 # 6 * 9/16 & 1# 13.5 * 9/16	5.302	14.34375	93.758
2 # 8 * 9/16 & 1 # 18 * 9/16	3.288	19.125	106.574

Cover Plate Area = 10.3125 in^2

Splice Plates	Flange Stress (ksi)	Splice Plate Area (in^2)	Splice Plate Force (kip)
2# 4 * 9/16 & 1# 9 * 9/16	9.477	9.5625	67.202
2# 5 * 9/16 & 1# 11.25 * 9/16	7.964	11.953125	76.822
2 # 6 * 9/16 & 1# 13.5 * 9/16	6.688	14.34375	84.942
2 # 8 * 9/16 & 1 # 18 * 9/16	4.648	19.125	97.918

W 27 X 102
Flange Force = 20.0 * 0.83 * 10.015 = 166.249 kips
Flange Area = 0.83 * 10.015 = 6.3616 in^2
Taper Length = 18 in
Applied Force = 31.7857 kip

*Cover Plate Area = 5/8 * 9 = 5.625 in^2*

Splice Plates	Flange Stress (ksi)	Splice Plate Area (in^2)	Splice Plate Force (kip)
2# 4 * 9/16 & 1# 9 * 9/16	13.096	9.5625	82.936
2# 5 * 9/16 & 1# 11.25 * 9/16	11.219	11.953125	94.878
2 # 6 * 9/16 & 1# 13.5 * 9/16	9.632	14.34375	104.976
2 # 8 * 9/16 & 1 # 18 * 9/16	7.092	19.125	121.132

Cover Plate Area = 3.375 in^2

Splice Plates	Flange Stress (ksi)	Splice Plate Area (in^2)	Splice Plate Force (kip)
2# 4 * 9/16 & 1# 9 * 9/16	12.551	9.5625	86.406
2# 5 * 9/16 & 1# 11.25 * 9/16	10.658	11.953125	98.450
2 # 6 * 9/16 & 1# 13.5 * 9/16	9.068	14.34375	108.560
2 # 8 * 9/16 & 1 # 18 * 9/16	6.546	19.125	124.604

Cover Plate Area = 10.3125 in^2

Splice Plates	Flange Stress (ksi)	Splice Plate Area (in^2)	Splice Plate Force (kip)
2# 4 * 9/16 & 1# 9 * 9/16	13.994	9.5625	77.224
2# 5 * 9/16 & 1# 11.25 * 9/16	12.166	11.953125	88.854
2 # 6 * 9/16 & 1# 13.5 * 9/16	10.604	14.34375	98.790
2 # 8 * 9/16 & 1 # 18 * 9/16	8.074	19.125	114.886

<u>**W 27 X 114**</u>
Flange Force = 20.0 * 0.93 * 10.07 = 187.302 kips
Flange Area = 0.64 * 9.96 = 9.3651 in^2
Taper Length = 18 in
Applied Force = 35.595238 kip

*Cover Plate Area = 5/8 * 9 = 5.625 in^2*

Splice Plates	Flange Stress (ksi)	Splice Plate Area (in^2)	Splice Plate Force (kip)
2# 4 * 9/16 & 1# 9 * 9/16	10.525	9.5625	88.730
2# 5 * 9/16 & 1# 11.25 * 9/16	9.125	11.953125	101.848
2 # 6 * 9/16 & 1# 13.5 * 9/16	7.933	14.34375	113.006
2 # 8 * 9/16 & 1 # 18 * 9/16	6.013	19.125	130.986

Cover Plate Area = 3.375 in^2

Splice Plates	Flange Stress (ksi)	Splice Plate Area (in^2)	Splice Plate Force (kip)
2# 4 * 9/16 & 1# 9 * 9/16	9.668	9.5625	96.760
2# 5 * 9/16 & 1# 11.25 * 9/16	8.228	11.953125	110.250
2 # 6 * 9/16 & 1# 13.5 * 9/16	7.019	14.34375	121.572
2 # 8 * 9/16 & 1 # 18 * 9/16	5.100	19.125	139.538

Cover Plate Area = 10.3125 in^2

Splice Plates	Flange Stress (ksi)	Splice Plate Area (in^2)	Splice Plate Force (kip)
2# 4 * 9/16 & 1# 9 * 9/16	10.766	9.5625	86.478
2# 5 * 9/16 & 1# 11.25 * 9/16	9.375	11.953125	99.502
2 # 6 * 9/16 & 1# 13.5 * 9/16	8.187	14.34375	110.630
2 # 8 * 9/16 & 1 # 18 * 9/16	6.262	19.125	128.656

APPENDIX K
PROPAGATION LIFE ESTIMATION EXAMPLES

K.1. General

This appendix presents several examples of estimating the fatigue life of cracked bridge girders repaired with either a friction-type bolted splice plate connection, air-hammer peening, or a partial bolted splice connection. The propagation program discussed in Appendix H is used for life predictions in the following examples. The assumptions mentioned during the model development are assumed to be valid and are used in the following calculations.

It should be noted that the propagation life obtained from the program correspond to the number of cycles required to fracture the flange. In all of the following examples, the total fatigue life of the detail is assumed equal to the number of cycles required to fracture the flange. This assumption may be true for air-hammer peening repair. However, if a splice plate is connected to the beam flange at the cover plate ends, a substantial number of loading cycles can still be sustained by the splice plates after flange fracture (as demonstrated by the tests).

K.2. Bolted Splice Repair Examples

It is assumed that an inspection of the cover plate ends of a full end-weld detail in a W33 × 130 girder reveals three cracks 1/2-in, 15/16-in, and 3/4-in in length. Moreover, assume that the following information is available for the girder:

- ☛ ASTM A709 Gr 36
- ☛ Allowable stress F_b = 20.0-ksi
- ☛ Cover plate thickness = 7/8-in
- ☛ Taper length = 18-in
- ☛ Cover plate width at the end of taper = 3.0-in
- ☛ Cover plate width of the straight portion = 12.5-in (wide cover plate)
- ☛ Flange plate = 0.885-in X 11.51-in
- ☛ Web plate = 0.58-in X 31.38-in

Using elastic beam theory, and assuming that the tension flange is completely severed, two upper splice plates 4.5-in × 5/8-in and one lower splice plate 10.5-in × 5/8-in are required to limit the stress in the bottom fibers of the lower splice plate and the upper fibers of the top

flange to 18.6-ksi and 19.4-ksi, respectively. The previous computation was conducted using elastic beam theory and assuming that the tension flange is completely severed. The following steps are required to estimate the remaining fatigue life of the specimen:

(1) First, the following parameters are computed:

$A_{sp} = (10.5 + 2 \times 4.5\ ) \times 5/8 = 12.1875\ in^2$

$A_{fl} = 0.855 \times 11.51 = 9.84105\ in^2$

$A_w = 31.38 \times 0.58 = 18.2004\ in^2$

$l_{sp} = 18.0 + 1.75 + 0.5 = 20.25\ in$

The unsupported length of the splice plates is assumed equal to the distance between the center of the inner bolt rows. To compute the unsupported splice plate length, the bolt lay-out of the splice connection has to be known. In this examples, it was assumed that the inner rows of bolts are at a distance of 1.75-in from the cover plate end and 0.5-in from the intersection of the tapered and straight portions of the cover plate.

(2) Assuming that the crack length to depth ratio of 4:1 is adequate, the three initial crack sizes are as follows:

Crack #	Length (in)	Depth (in)
1	1/2	1/8
2	15/16	15/64
3	3/4	3/16

Using the equivalent crack approach:

$2\ C_{equ.} = 1/2 + 15/16 + 3/4 = 2.1875\text{-in}$

$a_{equ.} = 15/64\text{-in}$

The following assumptions are made:

☞ Fracture toughness, $K_c = 150.0$ ksi $in^{1/2}$

☞ Yield stress, $F_Y = 36.0$ ksi

☞ The cover plate end is subjected to 20.0-ksi stress range with an R-ratio of 0.05

(3) Using the proposed program, a life of 642,000 cycles is expected for the cover plate end. As previously mentioned, this life corresponds only to flange fracture and does not account for any additional loading cycles that can be sustained by the splice plates. The category B and

C design life for a 20.0-ksi stress range is about 1,500,000 cycles and 486,000 cycles, respectively. Thus, the 5/8-in splice plate connection is adequate to achieve category C behavior. If category B behavior is required, a thicker splice plate connection is needed. Increasing the splice plates thickness of the previous connection to 7/8-in, a life of about 1,488,000 cycles is expected. This represents a 125% increase in the life with a 40% increase in the splice plate area. The 7/8-in splice plate connection satisfies category B design life for 20-ksi stress range loading. It should be noted, however, that the actual load fluctuations rarely produce such a high stress range. The input and output files for the two splice plate connections are listed next.

Input File *5/8-in splice connection*

```
WF
5.76 .86 16.55 3.
.23 1.09
20. .05 50
2 1 2 150.
36.
12.19 9.84 10.94 18.20
20.25 .63 31.38 .58
```

Output File *5/8-in splice connection*

```
Program Growth
    step No.       No. of Cycles      Crack Depth "a"  1/2 Crack Width "c"
        0                 0.0          0.2300000042        1.0900000334
      422            367795.3          0.8606402874        1.6602483988
  Ratio of Crack Depth to Flange Thickness EXCEEDED
  a/pt = 1.001
      500            406496.8          0.8606402874        1.7966567278
     1000            579813.9          0.8606402874        2.9614458084
     1500            639867.0          0.8606402874        4.8813805580
     1608            641542.0          0.8606402874        5.4323658943
  Growth Rate TOO FAST - Rate = 0.001
Percentage of Force Transmitted through the flange  0.49677
```

Input File *7/8-in splice connection*

```
WF
5.76 .86 16.55 3.
.23 1.09
20. .05 50
2 1 2 150.
36.
17.06 9.84 10.94 18.20
20.25 .88 31.38 .58
```

Output File *7/8-in splice connection*

```
Program Growth
    step No.       No. of Cycles      Crack Depth "a"   1/2 Crack Width "c"
        0                 0.0          0.2300000042         1.0900000334
      422            853069.8          0.8606403470         1.6602483988
  Ratio of Crack Depth to Flange Thickness EXCEEDED
  a/pt = 1.001
      500            942834.3          0.8606403470         1.7966567278
     1000           1344828.5          0.8606403470         2.9614458084
     1500           1484117.0          0.8606403470         4.8813805580
     1632           1488206.5          0.8606403470         5.5642523766
  Growth Rate TOO FAST - Rate = 0.001
Percentage of Force Transmitted through the flange  0.38498
```

K.3. Partial Bolted Splice Repair Examples

Assuming that clearance is a problem for the bridge site in the previous example, a partial bolted splice plate connection can be used to repair the cracked cover plate end. If only the two upper splice plates (4.5-in × 5/8-in) were used, the stress in the bottom fibers of the splice plates would be 27.7-ksi (for a bending moment that produces 20-ksi stress at the extreme fibers of the bare beam section). The previous computation was obtained using elastic beam theory and assuming that the tension flange is completely severed. The computed stress is higher than the allowable stress for ASTM A36 steel (20.0-ksi). However, as the tension flange is not completely severed, the actual stress is expected to be much smaller than the computed value. The same steps outlined in the bolted splice plate example are repeated:

$$A_{sp} = 2 \times 4.5 \times 5/8 = 5.625 \text{ in}^2$$

The remaining parameters did not change from the bolted splice plate example. However, it was assumed that the residual stress at the flange fibers due to peening is -42.0-ksi.

The expected propagation life of the detail repaired with a partial bolted splice connection (two plates 4.5-in × 5/8-in and air-hammer peening of the weld toes) is about 266,000 loading cycles under 20.0-ksi stress range. As expected the life of the detail repaired with the partial bolted splice connection is smaller than the same detail repaired with a full bolted splice plate connection. Thicker splice plates have to be used to increase the expected life. The propagation life of the detail for splice plate thickness of 7/8-in and 1-in is about 400,000 cycles, and 493,000 cycles, respectively. Thus, to achieve a Category C behavior a partial bolted splice connection with 1-in thick plates is required.

It should be noted that in the partial bolted splice connection examples, the percentage of flange stress was computed using the same regression equation developed for the bolted splice plate connection. The regression equation was developed for the range of parameters mentioned in Chapter 9, and should only be used within these ranges. The partial bolted splice connection has a much smaller splice plate area which would usually result in the violation of some of the parameter ranges. Thus, the previously mentioned propagation lives for the partial bolted splice plate connection involve some error in the computation of the nominal stress range transmitted through the flange after repair.

The input and output files for the 3 splice plate thicknesses are listed next.

Input File *5/8-in partial splice connection*

```
WF
5.76 .86 16.55 3.
.23 1.09
20. .05 50
2 3 2 150.
-42. .026
5.625 9.84 10.94 18.20
20.25 .63 31.38 .58
```

Output File *5/8-in partial splice connection*

```
Program Growth
    step No.       No. of Cycles      Crack Depth "a"  1/2 Crack Width "c"
       0                0.0          0.2300000042          1.0900000334
     414           157915.9          0.8610408306          1.6470260620
  Ratio of Crack Depth to Flange Thickness EXCEEDED
  a/pt = 1.001
     500           174559.7          0.8610408306          1.7966567278
    1000           241959.5          0.8610408306          2.9614458084
    1500           265313.1          0.8610408306          4.8813805580
    1564           265810.8          0.8610408306          5.1986389160
  Growth Rate TOO FAST - Rate = 0.001
Percentage of Force Transmitted through the flange  0.66139
```

Input File *7/8-in partial splice connection*

```
WF
5.76 .86 16.55 3.
.23 1.09
20. .05 50
2 3 2 150.
-42. .026
7.88 9.84 10.94 18.20
20.25 .88 31.38 .58
```

Output File *7/8-in partial splice connection*

```
Program Growth
    step No.       No. of Cycles      Crack Depth "a"  1/2 Crack Width "c"
       0                0.0          0.2300000042          1.0900000334
     407           241598.7          0.8620069623          1.6355428696
  Ratio of Crack Depth to Flange Thickness EXCEEDED
  a/pt = 1.002
     500           267759.9          0.8620069623          1.7966567278
    1000           365453.4          0.8620069623          2.9614458084
    1500           399303.6          0.8620069623          4.8813805580
    1584           400150.4          0.8620069623          5.3036050797
  Growth Rate TOO FAST - Rate = 0.001
Percentage of Force Transmitted through the flange  0.59102
```

Input File *1-in partial splice connection*

```
WF
5.76 .86 16.55 3.
.23 1.09
20. .05 50
2 3 2 150.
-42. .026
9. 9.84 10.94 18.20
20.25 1. 31.38 .58
```

Output File *1-in partial splice connection*

```
Program Growth
   step No.       No. of Cycles     Crack Depth "a"  1/2 Crack Width "c"
       0                0.0          0.2300000042        1.0900000334
     399           300333.2          0.8608956337        1.6225171089
 Ratio of Crack Depth to Flange Thickness EXCEEDED
 a/pt = 1.001
     500           334499.7          0.8608956337        1.7966567278
    1000           451591.8          0.8608956337        2.9614458084
    1500           492163.6          0.8608956337        4.8813805580
    1593           493229.9          0.8608956337        5.3515291214
 Growth Rate TOO FAST - Rate = 0.001
Percentage of Force Transmitted through the flange  0.55946
```

K.4. Air-Hammer Peening Examples

From the bolted splice and partial bolted splice examples, it could be speculated that air-hammer peening alone will not be effective in extending the life of the particular detail mentioned in the examples (because of the large initial cracks). However, for comparison purposes, the previously mentioned detail would have a life of about 64,000 cycles if repaired with air-hammer peening. The initial cracks were large, and peening is only effective for small cracks.

Assuming that a single crack 3/16-in long was detected in the same W33 × 130 detail, the expected life of the detail repaired with air-hammer peening is about 209,000 cycles. The Category E and D design life under 20.0-ksi stress range is about 117,000 cycles, and 287,000 cycles, respectively. If the detected crack was only 1/16-in long, the expected life would be about 351,000 cycles. Thus Category D behavior can only be attained for extremely small cracks. (It is unlikely that a 1/16-in long crack can be detected in a bridge girder.)

On the other hand, if the member is air-hammer peened prior to cracking, the expected life is about 3,038,000 cycles (assuming a 0.04-in long penny shape crack). It should be noted that the previously mentioned life corresponds to fracture of the weld toe detail. Experimental results demonstrated that in the case of weld toes peened prior to cracking, it is likely that the weld root fractures after a number of loading cycles smaller than that required to fracture the weld toe. In other words, the expected fatigue life of the cover plate end detail is smaller than 3,038,000 cycles.

The input and output files for the four peening examples are listed next.

Input File *air-hammer peening of multiple cracks*

```
WF
5.76 .86 16.55 3.
.23 1.09
20. .05 50
2 3 1 150.
-42. .026
```

Output File *air-hammer peening of multiple cracks*

```
 Program Growth
    step No.        No. of Cycles      Crack Depth "a"  1/2 Crack Width "c"
        0                  0.0          0.2300000042        1.0900000334
      420              37267.1          0.8601407409        1.6569329500
   Ratio of Crack Depth to Flange Thickness EXCEEDED
   a/pt = 1.000
      500              41215.0          0.8601407409        1.7966567278
     1000              58440.1          0.8601407409        2.9614458084
     1441              64188.8          0.8601407409        4.5972499847
   Growth Rate TOO FAST - Rate = 0.001
Percentage of Force Transmitted through the flange  1.00000
```

Input File *air-hammer peening of a single 3/16-in long crack*

```
WF
5.76 .86 16.55 3.
.05 .09
20. .05 50
2 3 1 150.
-42. .026
```

Output File *air-hammer peening of a single 3/16-in long crack*

```
 Program Growth
    step No.        No. of Cycles      Crack Depth "a"  1/2 Crack Width "c"
        0                  0.0          0.0500000007        0.0900000036
      500              31600.8          0.0594674759        0.1481997818
     1000              72018.0          0.0842147917        0.2442792356
     1500             108241.2          0.1308595985        0.4026478529
     2000             135671.5          0.2041700929        0.6636887789
     2500             154425.5          0.3114991188        1.0939645767
     2914             182012.1          0.8603252769        1.6546717882
   Ratio of Crack Depth to Flange Thickness EXCEEDED
   a/pt = 1.000
     3000             186245.2          0.8603252769        1.8049976826
     3500             203358.7          0.8603252769        2.9751930237
     3937             209006.2          0.8603252769        4.6001567841
   Growth Rate TOO FAST - Rate = 0.001
Percentage of Force Transmitted through the flange  1.00000
```

Input File *air-hammer peening of a single 1/16-in long crack*

```
WF
5.76 .86 16.55 3.
.03 .06
20. .05 50
2 3 1 150.
-42. .026
```

Output File *air-hammer peening of a single crack 1/16-in long*

```
Program Growth
    step No.       No. of Cycles      Crack Depth "a"  1/2 Crack Width "c"
        0                  0.0         0.0299999993        0.0599999987
      500              59401.5         0.0330451503        0.0987997428
     1000             148973.2         0.0474620499        0.1628526747
     1500             214865.1         0.0833324492        0.2684315443
     2000             254865.7         0.1392116547        0.4424583018
     2500             281634.7         0.2203549147        0.7293087840
     3000             299003.2         0.3352559805        1.2021254301
     3320             324000.9         0.8604749441        1.6552157402
  Ratio of Crack Depth to Flange Thickness EXCEEDED
  a/pt = 1.001
     3500             332376.2         0.8604749441        1.9834561348
     4000             347236.0         0.8604749441        3.2693510056
     4342             350974.9         0.8604749441        4.5970788002
  Growth Rate TOO FAST - Rate = 0.001
Percentage of Force Transmitted through the flange  1.00000
```

Input File *air-hammer peening prior to crack detection*

```
WF
5.76 .86 16.55 3.
.02 .02
20. .05 50
2 3 1 150.
-42. .026
```

Output File *air-hammer peening prior to crack detection*

```
Program Growth
    step No.       No. of Cycles      Crack Depth "a"  1/2 Crack Width "c"
        0                  0.0         0.0199999996        0.0199999996
      500              29607.8         0.0200296994        0.0329332501
     1000              89942.2         0.0201395284        0.0542841926
     1500             245430.9         0.0205275267        0.0894771591
     2000             679439.1         0.0217230078        0.1474859715
     2500            1788631.4         0.0244665537        0.2431027442
     3000            2918846.8         0.0964768752        0.4007087052
     3500            2961999.0         0.1921806335        0.6604914665
     4000            2982818.0         0.3063277602        1.0886949301
     4419            3010926.8         0.8602395058        1.6549500227
  Ratio of Crack Depth to Flange Thickness EXCEEDED
  a/pt = 1.000
     4500            3014926.2         0.8602395058        1.7963010073
     5000            3032155.5         0.8602395058        2.9608585835
     5441            3037907.5         0.8602395058        4.5963330269
  Growth Rate TOO FAST - Rate = 0.001
Percentage of Force Transmitted through the flange  1.00000
```

APPENDIX L
PROPAGATION LIFE RESULTS

L.1. General

Estimates of the fatigue crack propagation life of typical bridge members are presented in this section. The crack propagation program described in Appendix H was used to compute the crack propagation lives. Five variables were used to represent a range of possible critical factors: beam depth, crack size, stress range, cover plate detail type, and splice plate area. The combination of these variables provide 960 data to model crack propagation behavior that would be encountered in the repair of typical bridge girders.

Only the middle size of each beam depth was selected for propagation life estimates. The fatigue crack propagation life is calculated for four initial crack sizes: 1/2-in, 1.0-in, 1 1/2-in, and 2.0-in. Moreover, four nominal stress ranges are considered: 30.0 ksi, 20.0 ksi, 15.0 ksi, and 12.0 ksi. These stress ranges are computed for the bare cross section at the cover plate ends assuming a crack free section. Five specimen geometries are considered: NR, NF, NN, WR, and WF specimens. From the experimental phase of this study, it was observed that the NN specimens, NR and WR specimens, and NF and WF specimens generally initiated one, two, and three cracks per end, respectively. Thus, in the propagation life computations it was assumed that the NN specimens, NR and WR specimens, and NF and WF specimens had one, two, and three initial cracks, respectively. It should be noted that the crack lengths are total crack lengths per end. The final variable considered is the splice plate area. Three splice plate areas were considered: the design splice plate area, 1.25 times the design area, and 1.5 times the design area. The design splice plate area was obtained by determining the area needed to provide a moment capacity equal to that of the non-cracked girder if the tension flange is assumed to be completely severed.

The results obtained are presented both in a tabulated format and in a graphical representation (Figs. L.1-L.20). Each figure is an S-N curve for a specific beam size and specimen geometry.

W 36 X 160

Splice Plate as per usual Design

Splice Plate: 1 # 11" X 5/8" & 2 # 5" X 5/8"

$A_{sp} = 13.125$ in^2 $A_{fl} = 12.24$ in^2 $A_{cp} = 6.875$ in^2 $A_w = 22.0805$ in^2

$l_{sp} = 20.25$ in $t_{sp} = 5/8$ in $d_w = 33.97$ in $t_w = 0.65$ in

Specimen Life in Cycles

Stress Range (ksi)		Crack Length (in)			
		1/2	1	1 1/2	2
NR Specimens	30	289,000	225,100	189,700	166,300
	20	1,102,300	858,800	723,800	634,900
	15	2,848,700	2,219,400	1,870,700	1,640,800
	12	5,949,200	4,635,000	3,906,700	3,426,600
NF Specimens	30	344,300	274,400	234,700	208,000
	20	1,313,400	1,046,700	895,300	793,600
	15	3,394,000	2,705,000	2,313,800	2,050,800
	12	7,088,000	5,649,000	4,832,100	4,283,000
NN Specimens	30	195,200	149,100	126,100	112,300
	20	744,900	569,400	481,600	429,100
	15	1,925,000	1,471,500	1,244,800	1,109,000
	12	4,020,300	3,073,200	2,599,800	2,316,000
WR Specimens	30	298,400	231,400	194,300	169,900
	20	1,138,100	882,900	741,600	648,300
	15	2,941,100	2,281,800	1,916,500	1,675,600
	12	6,142,200	4,765,300	4,002,400	3,499,300
WF Specimens	30	356,100	282,800	241,200	213,300
	20	1,358,000	1,078,900	920,400	814,000
	15	3,509,400	2,788,200	2,378,600	2,103,100
	12	7,329,000	5,822,800	4,967,500	4,392,200

W 36 X 160

Splice Plate as per usual Design * 1.25

Splice Plate: 1 # 11" X 25/32" & 2 # 5" X 25/32"
Asp = 16.40625 in^2 Afl = 12.24 in^2 Acp = 6.875 in^2 Aw = 22.0805 in^2
lsp = 20.25 in tsp = 25/32 in dw = 33.97 in tw = 0.65 in

Specimen Life in Cycles

Stress Range (ksi)		Crack Length (in)			
		1/2	1	1 1/2	2
NR Specimens	30	467,600	364,300	307,000	269,200
	20	1,783,000	1,389,200	1,170,900	1,027,000
	15	4,607,600	3,589,800	3,025,700	2,653,900
	12	9,622,400	7,496,900	6,318,800	5,542,300
NF Specimens	30	557,200	444,000	379,800	336,600
	20	2,124,400	1,693,100	1,448,200	1,283,600
	15	5,489,600	4,375,100	3,742,500	3,317,100
	12	11,464,300	9,136,900	7,815,700	6,927,400
NN Specimens	30	315,900	241,500	204,200	181,900
	20	1,204,900	921,000	779,100	694,100
	15	3,113,700	2,380,200	2,013,500	1,793,700
	12	6,502,600	4,970,700	4,205,000	3,746,000
WR Specimens	30	482,800	374,500	314,500	275,000
	20	1,840,900	1,428,200	1,199,500	1,048,800
	15	4,757,100	3,690,700	3,099,900	2,710,200
	12	9,934,600	7,707,600	6,473,700	5,660,000
WF Specimens	30	576,100	457,700	390,400	345,200
	20	2,196,600	1,745,200	1,488,800	1,316,400
	15	5,676,300	4,509,800	3,847,300	3,401,700
	12	11,854,100	9418,000	8,034,600	7,104,100

W 36 X 160

Splice Plate as per usual Design * 1.5

Splice Plate: 1 # 11" X 15/16" & 2 # 5" X 15/16"
Asp = 19.6875 in^2 Afl = 12.24 in^2 Acp = 6.875 in^2 Aw = 22.0805 in^2
lsp = 20.25 in tsp = 15/16 in dw = 33.97 in tw = 0.65 in

Specimen Life in Cycles

Stress Range (ksi)		Crack Length (in)			
		1/2	1	1 1/2	2
NR Specimens	30	767,300	597,800	503,800	441,900
	20	2,925,100	2,278,900	1,920,800	1,684,800
	15	7,558,700	5,889,000	4,963,600	4,353,600
	12	15,785,300	12,298,300	10,365,800	9,091,900
NF Specimens	30	914,200	728,600	623,200	552,300
	20	3,485,000	2,777,500	2,375,900	2,105,800
	15	9,005,600	7,177,300	6,139,400	5,441,700
	12	18,806,800	14,988,800	12,821,300	11,364,200
NN Specimens	30	518,500	396,300	335,200	298,600
	20	1,976,700	1,511,000	1,278,200	1,138,700
	15	5,107,900	3,904,600	3,303,100	2,942,600
	12	10,667,200	8,154,200	6,898,100	6,145,300
WR Specimens	30	792,200	614,600	516,200	451,300
	20	3,020,000	2,343,000	1,967,900	1,720,500
	15	7,803,900	6,054,500	5,085,200	4,446,100
	12	16,297,300	12,644,000	10,619,800	9,285,000
WF Specimens	30	945,300	751,000	640,700	566,400
	20	3,603,500	2,863,000	2,442,400	2,159,500
	15	9,311,700	7,398,100	6,311,400	5,580,400
	12	19,446,200	15,450,000	13,180,500	11,654,000

W 33 X 141

Splice Plate as per usual Design

Splice Plate: 1 # 10.5" X 5/8" & 2 # 4.5" X 5/8"
Asp = 12.1875 in^2 Afl = 11.0736 in^2 Acp = 6.5625 in^2 Aw = 18.9849 in^2
lsp = 20.25 in tsp = 5/8 in dw = 31.38 in tw = 0.605 in

Specimen Life in Cycles

Stress Range (ksi)		Crack Length (in)			
		1/2	1	1 1/2	2
NR Specimens	30	293,300	225,000	187,500	163,100
	20	1,118,800	858,500	715,500	622,600
	15	2,891,100	2,218,700	1,849,200	1,608,900
	12	6,037,800	4,633,500	3,861,900	3,360,100
NF Specimens	30	351,800	276,900	234,400	206,100
	20	1,341,700	1,056,100	894,400	786,300
	15	3,467,200	2,729,300	2,311,300	2,032,200
	12	7,240,800	5,699,800	4,827,000	4,244,000
NN Specimens	30	195,200	146,700	123,100	109,300
	20	744,900	559,800	470,000	417,400
	15	1,925,200	1,446,900	1,214,600	1,078,900
	12	4,020,500	3,021,700	2,536,700	2,253,300
WR Specimens	30	302,900	231,400	192,100	166,600
	20	1,155,400	882,700	733,000	635,700
	15	2,985,700	2,281,200	1,894,200	1,642,800
	12	6,235,300	4,764,000	3,955,900	3,430,900
WF Specimens	30	363,900	285,400	241,000	211,300
	20	1,387,700	1,088,800	919,500	806,300
	15	3,586,100	2,813,700	2,376,100	2,083,700
	12	7,489,100	5,876,200	4,962,300	4,351,600

W 33 X 141

Splice Plate as per usual Design * 1.25

Splice Plate: 1 # 10.5" X 25/32" & 2 # 4.5" X 25/32"
Asp = 15.234375 in^2 Afl = 11.0736 in^2 Acp = 6.5625 in^2 Aw = 18.9849 in^2
lsp = 20.25 in tsp = 25/32 in dw = 31.38 in tw = 0.605 in

Specimen Life in Cycles

Stress Range (ksi)		Crack Length (in)			
		1/2	1	1 1/2	2
NR Specimens	30	480,500	368,700	307,300	267,300
	20	1,831,900	1,405,900	1,171,700	1,019,500
	15	4,734,000	3,633,000	3,028,000	2,634,500
	12	9,886,300	7,587,000	6,323,600	5,501,900
NF Specimens	30	576,200	453,600	384,100	337,700
	20	2,197,000	1,729,400	1,464,600	1,287,700
	15	5,677,200	4,468,900	3,784,600	3,327,500
	12	11,856,100	9,332,800	7,903,700	6,949,100
NN Specimens	30	319,900	240,400	201,800	179,200
	20	1,219,900	916,800	769,600	683,600
	15	3,152,300	2,369,200	1,988,900	1,766,700
	12	6,583,200	4,947,700	4,153,600	3,689,500
WR Specimens	30	496,200	379,100	314,700	272,900
	20	1,891,900	1,445,500	1,200,300	1,040,900
	15	4,888,900	3,735,300	3,101,700	2,690,000
	12	10,209,700	7,800,600	6,477,400	5,617,800
WF Specimens	30	596,000	467,600	394,900	346,200
	20	2,272,300	1,782,900	1,505,600	1,320,300
	15	5,871,900	4,607,300	3,890,800	3,411,900
	12	12,262,700	9,621,700	8,125,300	7,125,400

W 33 X 141

Splice Plate as per usual Design * 1.5

Splice Plate: 1 # 10.5" X 15/16" & 2 # 4.5" X 15/16"

Asp = 18.28125 in^2	Afl = 11.0736 in^2	Acp = 6.5625 in^2	Aw = 18.9849 in^2
lsp = 20.25 in	tsp = 15/16 in	dw = 31.38 in	tw = 0.605 in

Specimen Life in Cycles

Stress Range (ksi)		Crack Length (in)			
		1/2	1	1 1/2	2
NR Specimens	30	798,800	613,000	510,900	444,500
	20	3,045,300	2,337,000	1,947,800	1,694,700
	15	7,869,200	6,039,000	5,033,400	4,379,300
	12	16,433,700	12,611,600	10,511,500	9,145,600
NF Specimens	30	958,000	754,100	638,600	561,500
	20	3,652,000	2,874,800	2,434,600	2,140,500
	15	9,437,100	7,428,600	6,291,100	5,531,300
	12	19,707,900	15,513,600	13,138,000	11,551,300
NN Specimens	30	531,900	399,700	335,500	298,000
	20	2,027,800	1,524,000	1,279,400	1,136,400
	15	5,240,000	3,938,200	3,306,200	2,936,700
	12	10,943,100	8,224,400	6,904,400	6,133,000
WR Specimens	30	825,000	630,300	523,300	453,900
	20	3,144,900	2,402,800	1,995,200	1,730,400
	15	8,126,600	6,209,100	5,155,900	4,471,600
	12	16,971,300	12,966,800	10,767,200	9,338,200
WF Specimens	30	990,900	777,400	656,500	575,700
	20	3,777,300	2,963,700	2,502,800	2,194,800
	15	9,760,800	7,658,600	6,467,500	5,671,600
	12	20,383,900	15,993,800	13,506,500	11,844,300

W 30 X 116

Splice Plate as per usual Design

Splice Plate: 1 # 9.5" X 11/16" & 2 # 4" X 11/16"
A_{sp} = 12.03125 in^2 Afl = 8.92075 in^2 Acp = 5.9375 in^2 Aw = 15.42895 in^2
lsp = 20.25 in tsp = 11/16 in dw = 28.31 in tw = 0.545 in

Specimen Life in Cycles

Stress Range (ksi)		Crack Length (in)			
		1/2	1	1 1/2	2
NR Specimens	30	411,600	304,400	246,800	210,500
	20	1,569,400	1,160,700	941,200	802,800
	15	4,055,600	2,999,500	2,432,400	2,074,700
	12	8,469,600	6,264,000	5,079,700	4,332,800
NF Specimens	30	501,500	383,000	316,500	272,800
	20	1,911,900	1,460,500	1,206,800	1,040,200
	15	4,940,600	3,774,200	3,118,600	2,688,100
	12	10,317,800	7,881,800	6,512,900	5,613,700
NN Specimens	30	264,000	190,400	157,000	138,600
	20	1,007,000	726,200	598,900	528,800
	15	2,602,200	1,876,600	1,547,700	1,366,500
	12	5,434,200	3,919,100	3,232,200	2,853,800
WR Specimens	30	425,400	313,000	252,700	214,800
	20	1,621,900	1,193,600	963,800	819,400
	15	4,191,100	3,084,600	2,490,700	2,117,500
	12	8,752,500	6,441,700	5,201,400	4,422,100
WF Specimens	30	519,100	395,200	325,500	279,700
	20	1,979,300	1,506,800	1,241,200	1,066,600
	15	5,114,700	3,893,700	3,207,400	2,756,400
	12	10,681,200	8,131,500	6,698,200	5,756,400

W 30 X 116

Splice Plate as per usual Design * 1.25

Splice Plate: 1 # 9.5" X 55/64" & 2 # 4" X 55/64"

Asp = 15.039 in^2 Afl = 8.92075 in^2 Acp = 5.9375 in^2 Aw = 15.42895 in^2

lsp = 20.25 in tsp = 55/64 in dw = 28.31 in tw = 0.545 in

Specimen Life in Cycles

Stress Range (ksi)		Crack Length (in)			
		1/2	1	1 1/2	2
NR Specimens	30	762,700	564,100	457,400	390,100
	20	2,907,600	2,150,400	1,743,800	1,487,400
	15	7,513,400	5,556,900	4,506,200	3,843,700
	12	15,690,700	11,604,700	9,410,600	8,027,000
NF Specimens	30	929,200	709,800	586,500	505,500
	20	3,542,100	2,705,800	2,235,800	1,927,200
	15	9,153,000	6,992,000	5,777,600	4,980,000
	12	19,114,700	14,601,800	12,065,700	10,399,900
NN Specimens	30	489,300	352,900	291,000	256,900
	20	1,865,600	1,345,400	1,109,600	979,700
	15	4,820,800	3,476,600	2,867,300	2,531,600
	12	10,067,500	7,260,500	5,988,000	5,286,900
WR Specimens	30	788,200	580,100	468,400	398,200
	20	3,004,700	2,211,400	1,785,600	1,518,100
	15	7,764,400	5,714,500	4,614,200	3,922,900
	12	16,214,800	11,933,900	9,636,100	8,192,400
WF Specimens	30	961,900	732,300	603,200	518,400
	20	3,666,900	2,791,500	2,299,500	1,976,100
	15	9,475,400	7,213,500	5,942,000	5,106,500
	12	19,787,900	15,064,300	12,409,000	10,664,200

W 30 X 116

Splice Plate as per usual Design *1.5

Splice Plate: 1 # 9.5" X 1 1/32" & 2 # 4" X 1 1/32"
Asp = 18.046875 in^2 Afl = 8.92075 in^2 Acp = 5.9375 in^2 Aw = 15.42895 in^2
lsp = 20.25 in tsp = 1 1/32 in dw = 28.31 in tw = 0.545 in

Specimen Life in Cycles

Stress Range (ksi)		Crack Length (in)			
		1/2	1	1 1/2	2
NR Specimens	30	1,451,500	1,073,500	870,500	742,500
	20	5,532,700	4,092,000	3,318,300	2,830,400
	15	14,296,800	10,573,800	8,574,600	7,313,900
	12	29,856,900	22,081,900	17,906,800	15,274,100
NF Specimens	30	1,768,300	1,350,800	1,116,100	962,000
	20	6,740,100	5,148,800	4,254,500	3,667,100
	15	17,416,700	13,304,700	10,993,800	9,476,100
	12	36,372,100	27,784,800	22,959,000	19,789,400
NN Specimens	30	931,300	671,600	553,900	489,000
	20	3,549,900	2,560,100	2,111,400	1,864,200
	15	9,173,100	6,615,500	5,456,100	4,817,300
	12	19,156,700	13,815,400	11,394,200	10,060,200
WR Specimens	30	1,500,000	1,103,900	891,400	757,800
	20	5,717,500	4,208,000	3,397,800	2,888,700
	15	14,774,400	10,874,800	8,780,100	7,464,700
	12	30,854,100	22,708,300	18,336,000	15,588,900
WF Specimens	30	1,830,500	1,393,600	1,147,900	986,500
	20	6,977,500	5,311,900	4,375,600	3,760,300
	15	18,030,100	13,726,100	11,306,600	9,716,900
	12	37,653,100	28,665,000	23,612,300	20,292,300

W 27 X 102

Splice Plate as per usual Design

Splice Plate: 1 # 9.5" X 9/16" & 2 # 4" X 9/16"
Asp = 9.5625 in^2 Afl = 6.3616 in^2 Acp = 5.625 in^2 Aw = 13.09645 in^2
lsp = 20.25 in tsp = 9/16 in dw = 25.43 in tw = 0.515 in

Specimen Life in Cycles

Stress Range (ksi)		Crack Length (in)			
		1/2	1	1 1/2	2
NR Specimens	30	438,700	320,800	257,900	218,600
	20	1,672,500	1,223,400	983,500	833,700
	15	4,322,000	3,161,500	2,541,500	2,154,600
	12	9,026,000	6,602,300	5,307,600	4,499,500
NF Specimens	30	537,000	406,700	333,600	285,700
	20	2,047,400	1,550,700	1,272,000	1,089,600
	15	5,290,800	4,007,200	3,287,000	2,815,700
	12	11,049,100	8,368,400	6,864,400	5,880,300
NN Specimens	30	277,900	197,700	161,800	142,300
	20	1,059,800	754,000	617,100	542,900
	15	2,738,600	1,948,600	1,594,700	1,403,000
	12	5,719,300	4,069,400	3,330,400	2,930,000
WR Specimens	30	453,600	330,200	264,300	223,100
	20	1,729,600	1,259,000	1,007,800	850,800
	15	4,469,400	3,253,500	2,604,300	2,198,500
	12	9,333,700	6,794,500	5,438,700	4,591,400
WF Specimens	30	556,200	419,800	343,200	293,100
	20	2,120,400	1,600,500	1,308,700	1,117,700
	15	5,479,400	4,135,900	3,381,800	2,888,300
	12	11,443,000	8,637,200	7,062,500	6,031,800

<u>W 27 X 102</u>

<u>Splice Plate as per usual Design * 1.25</u>

Splice Plate: 1 # 9.5" X 45/64" & 2 # 4" X 45/64"
Asp = 11.953125 in^2 Afl = 6.3616 in^2 Acp = 5.625 in^2 Aw = 13.09645 in^2
lsp = 20.25 in tsp = 45/64 in dw = 25.43 in tw = 0.515 in

Specimen Life in Cycles

Stress Range (ksi)		Crack Length (in)			
		1/2	1	1 1/2	2
NR Specimens	30	863,400	631,500	507,700	430,400
	20	3,291,100	2,407,400	1,935,300	1,640,700
	15	8,504,500	6,220,900	5,001,000	4,239,600
	12	17,760,400	12,991,500	10,443,900	8,853,800
NF Specimens	30	1,056,900	800,500	656,600	562,400
	20	4,028,800	3,051,400	2,503,000	2,144,100
	15	10,410,800	7,884,900	6,467,800	5,540,600
	12	21,741,300	16,466,500	13,507,100	11,570,700
NN Specimens	30	547,000	389,200	318,500	280,200
	20	2,085,400	1,483,800	1,214,300	1,068,300
	15	5,388,800	3,834,300	3,138,000	2,760,700
	12	11,253,900	8,007,500	6,553,200	5,765, 300
WR Specimens	30	892,800	649,900	520,200	439,100
	20	3,403,400	2,477,500	1,983,100	1,674,100
	15	8,794,500	6,402,000	5,124,500	4,326,100
	12	18,366,000	13,369,600	10,701,700	9,034,500
WF Specimens	30	1,094,600	826,200	675,500	576,900
	20	4,172,500	3,149,400	2,575,200	2,199,400
	15	10,782,000	8,138,200	6,654,500	5,683,300
	12	22,516,500	16,995,500	13,896,900	11,868,800

W 27 X 102

Splice Plate as per usual Design * 1.5

Splice Plate: 1 # 9.5" X 27/32" & 2 # 4" X 27/32"

Asp = 14.34375 in^2 Afl = 6.3616 in^2 Acp = 5.625 in^2 Aw = 13.09645 in^2

lsp = 20.25 in tsp = 27/32 in dw = 25.43 in tw = 0.515 in

Specimen Life in Cycles

Stress Range (ksi)		Crack Length (in)			
		1/2	1	1 1/2	2
NR Specimens	30	1,738,500	1,271,600	1,022,300	866,600
	20	6,626,400	4,847,100	3,896,600	3,303,400
	15	17,123,000	12,525,200	10,069,000	8,536,100
	12	35,758,800	26,157,000	21,027,700	17,826,300
NF Specimens	30	2,128,100	1,611,800	1,322,100	1,132,600
	20	8,111,700	6,143,700	5,039,500	4,317,000
	15	20,961,100	15,875,600	13,022,300	11,155,400
	12	43,774,000	33,153,800	27,195,200	23,296,400
NN Specimens	30	1,101,600	783,800	641,400	564,300
	20	4,198,800	2,987,600	2,445,000	2,151,000
	15	10,850,000	7,720,100	6,318,000	5,558,400
	12	22,658,500	16,122,300	13,194,200	11,607,900
WR Specimens	30	1,797,700	1,308,700	1,047,500	884,300
	20	6,852,400	4,988,200	3,992,800	3,370,800
	15	17,706,900	12,889,800	10,317,600	8,710,200
	12	36,978,000	26,918,400	21,546,900	18,190,000
WF Specimens	30	2,204,000	1,663,600	1,360,300	1,161,700
	20	8,401,000	6,341,100	5,185,000	4,428,300
	15	21,708,400	16,385,600	13,398,200	11,442,800
	12	45,334,800	34,218,800	27,980,100	23,896,600

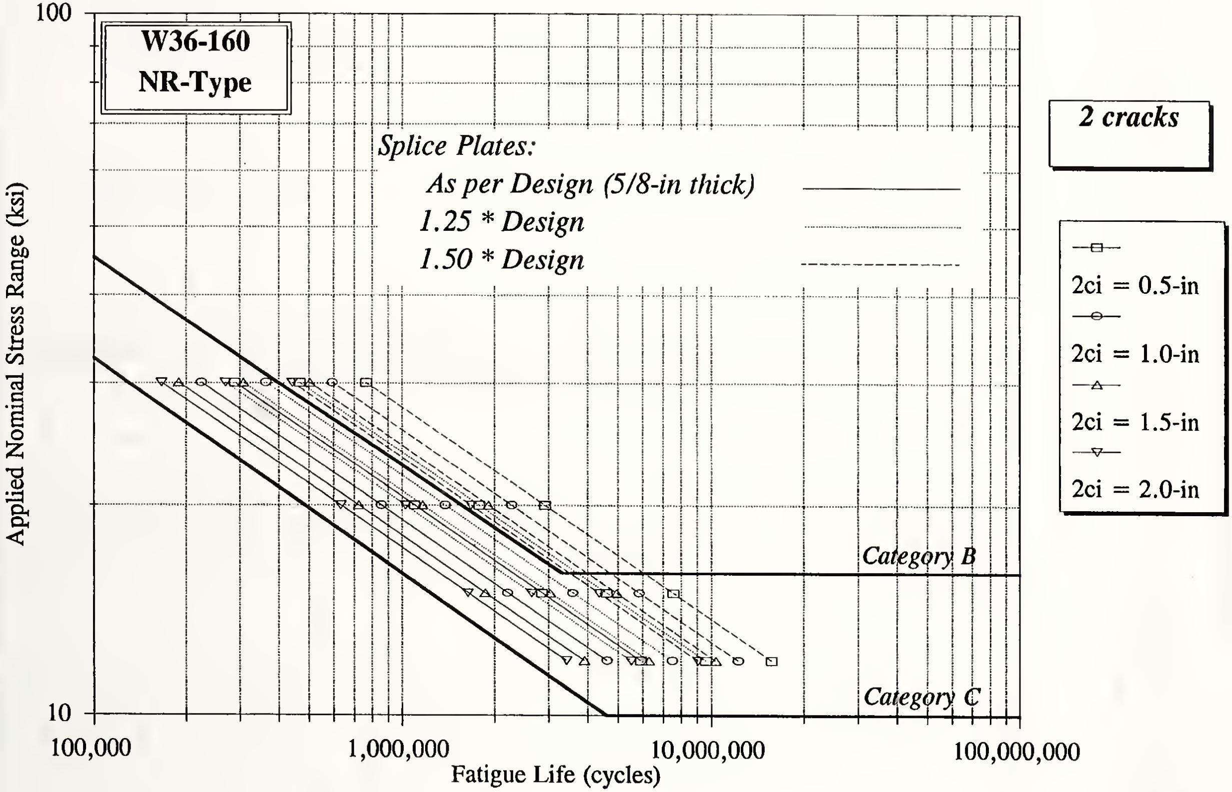

Fig. L.1. Fatigue Propagation Life of W 36 X 160 Girders Repaired with a Bolted Splice Plate Connection. (NR-Type)

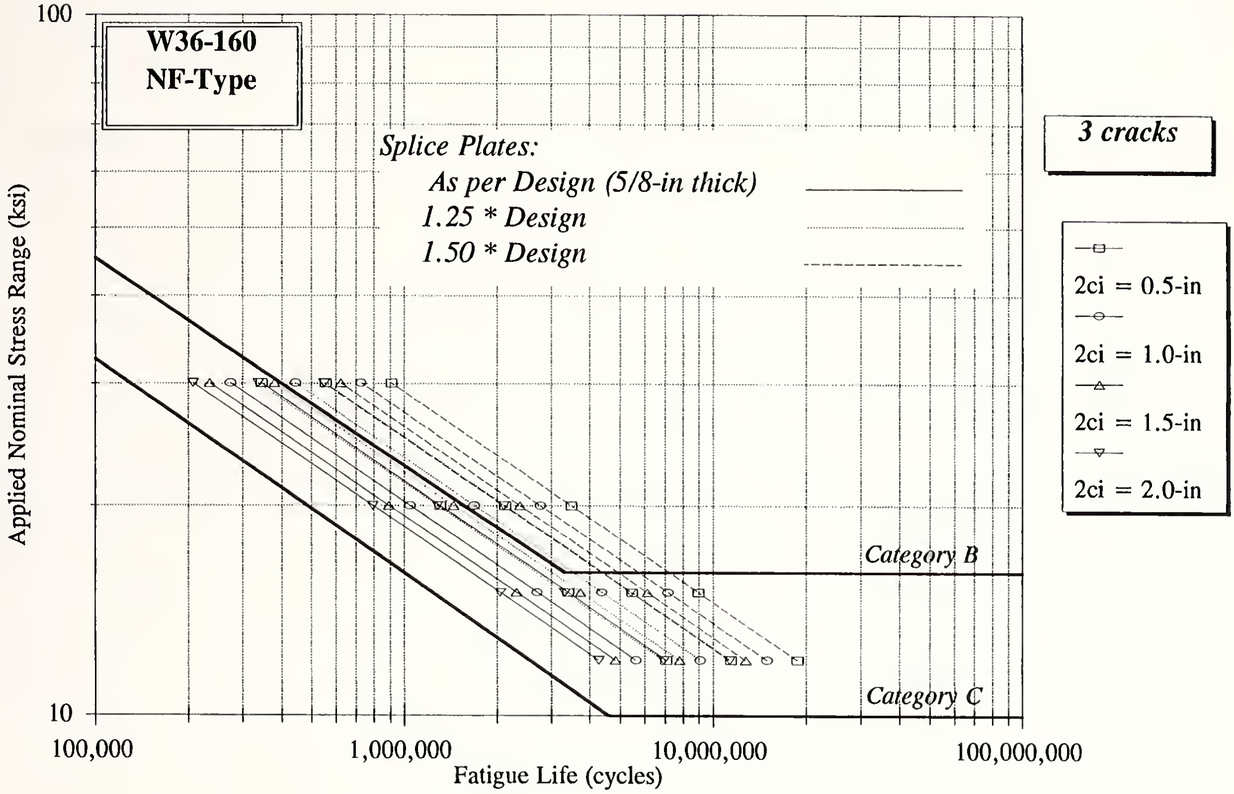

Fig. L.2. Fatigue Propagation Life of W 36 X 160 Girders Repaired with a Bolted Splice Plate Connection. (NF-Type)

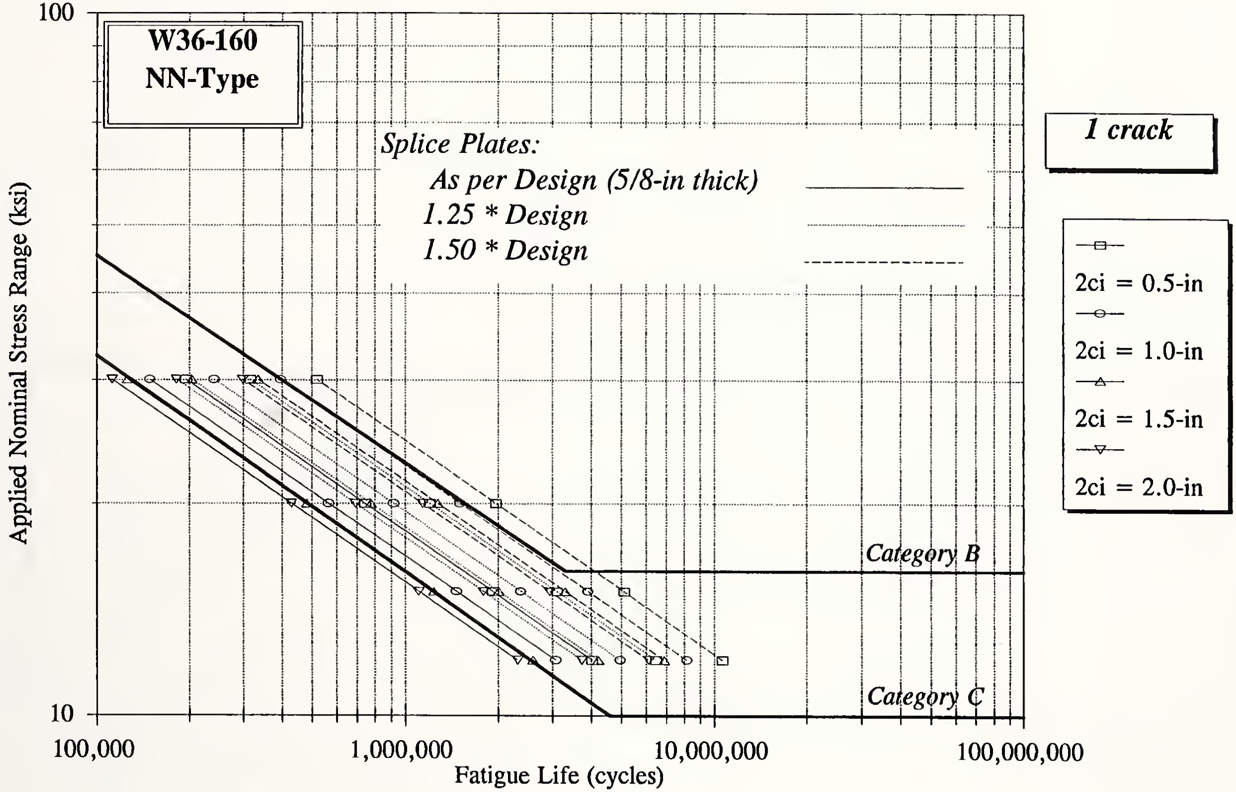

Fig. L.3. Fatigue Propagation Life of W 36 X 160 Girders Repaired with a Bolted Splice Plate Connection. (NN-Type)

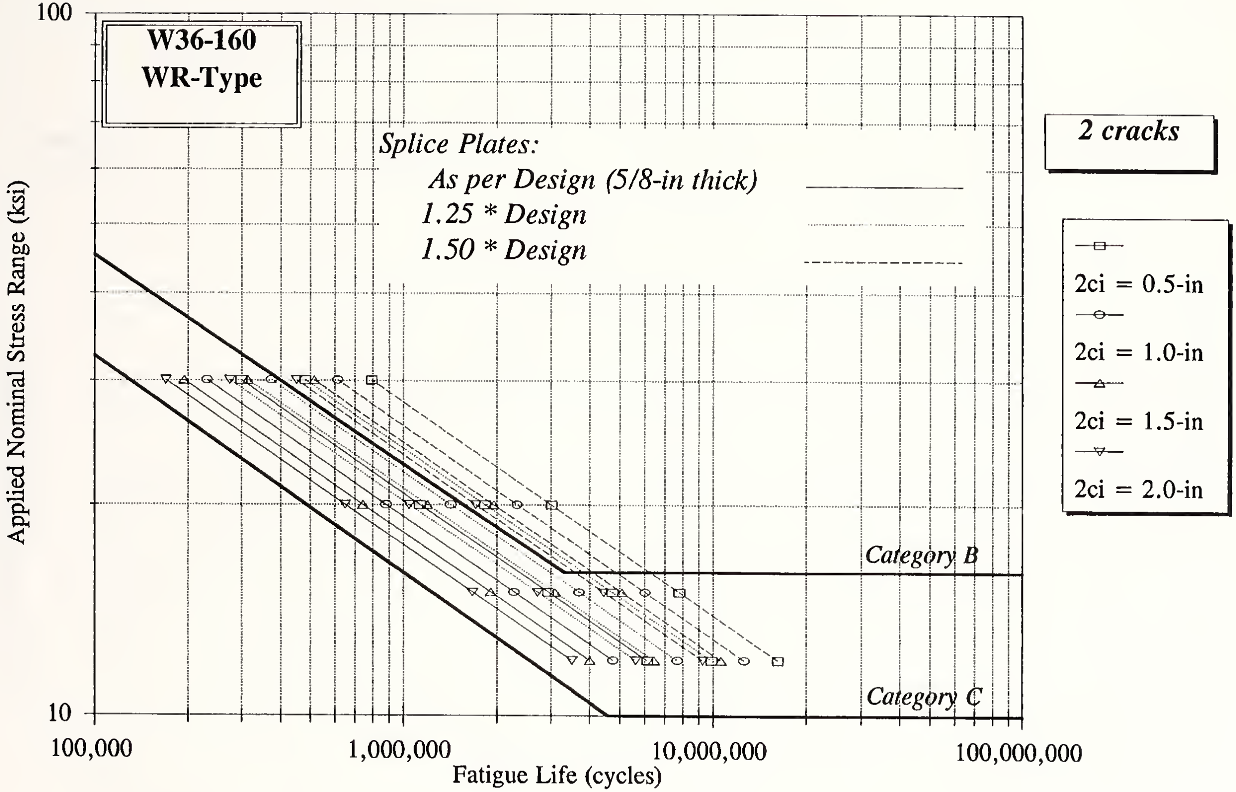

Fig. L.4. Fatigue Propagation Life of W 36 X 160 Girders Repaired with a Bolted Splice Plate Connection. (WR-Type)

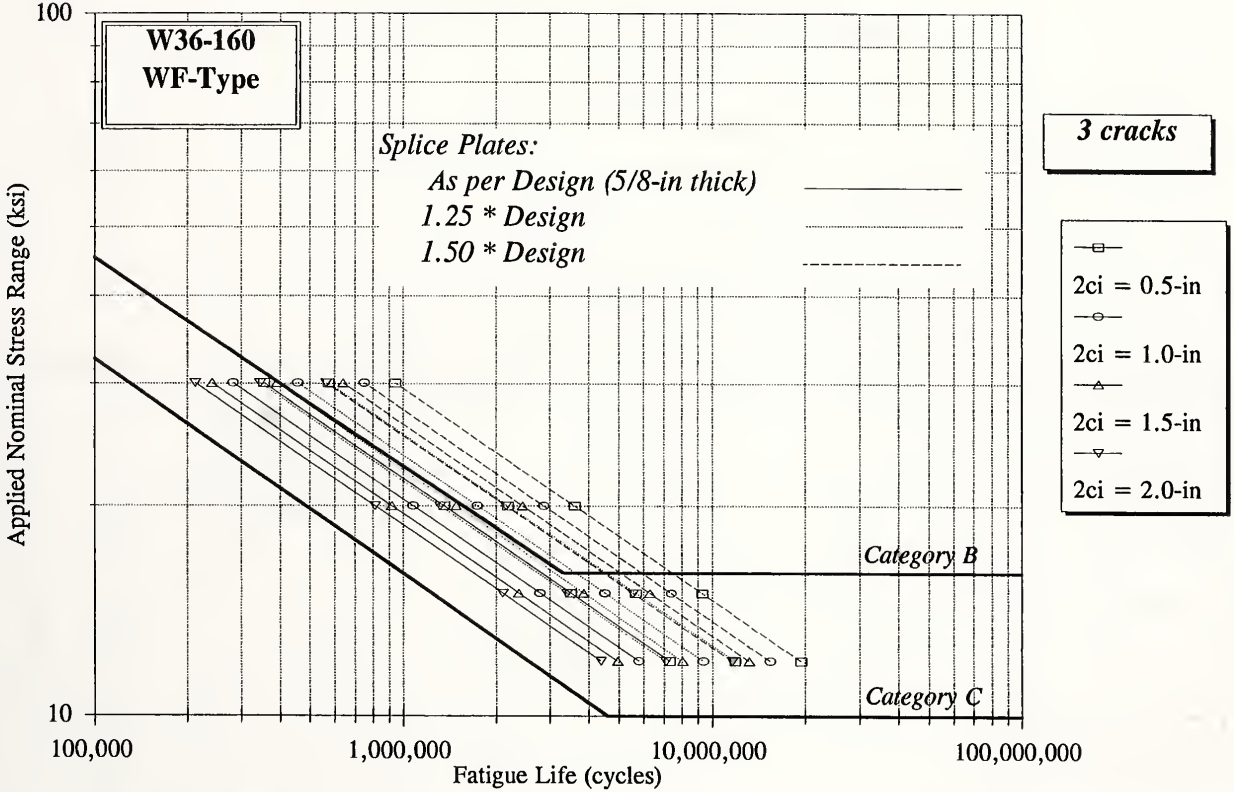

Fig. L.5. Fatigue Propagation Life of W 36 X 160 Girders Repaired with a Bolted Splice Plate Connection. (WF-Type)

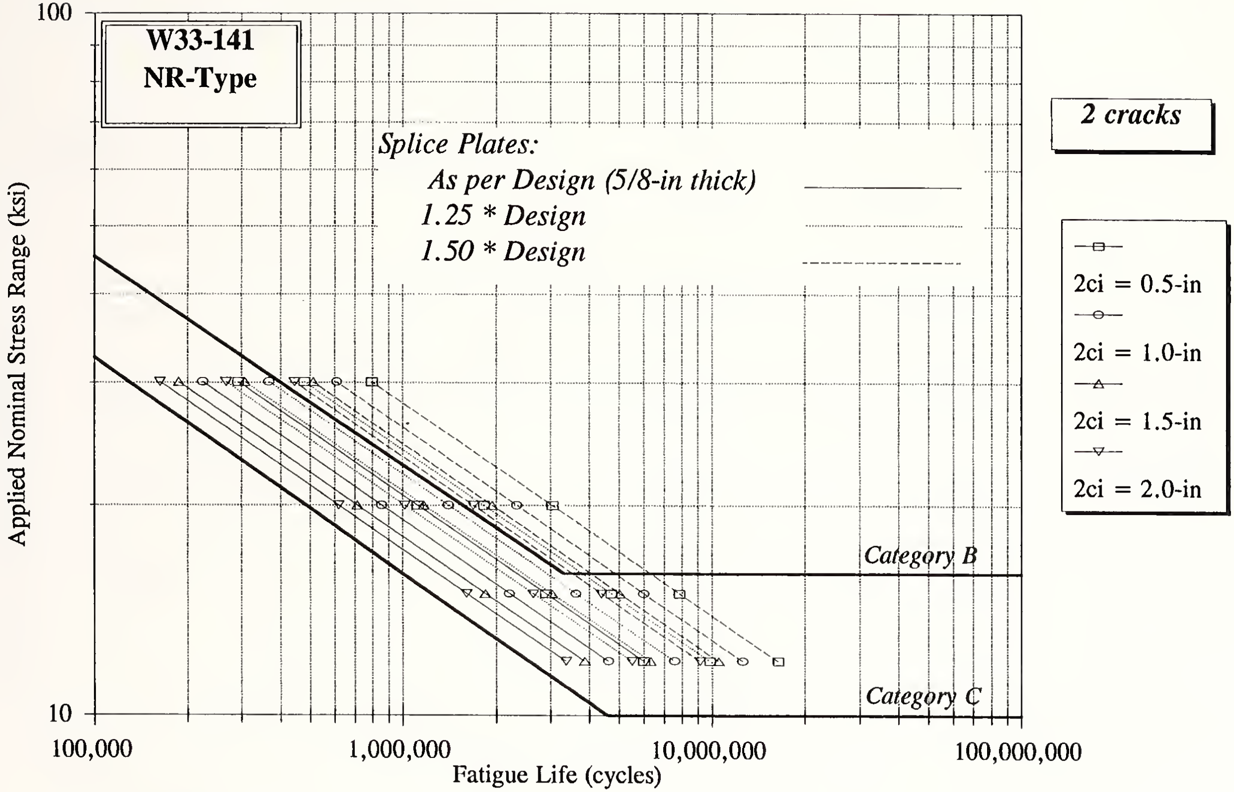

Fig. L.6. Fatigue Propagation Life of W 33 X 141 Girders Repaired with a Bolted Splice Plate Connection. (NR-Type)

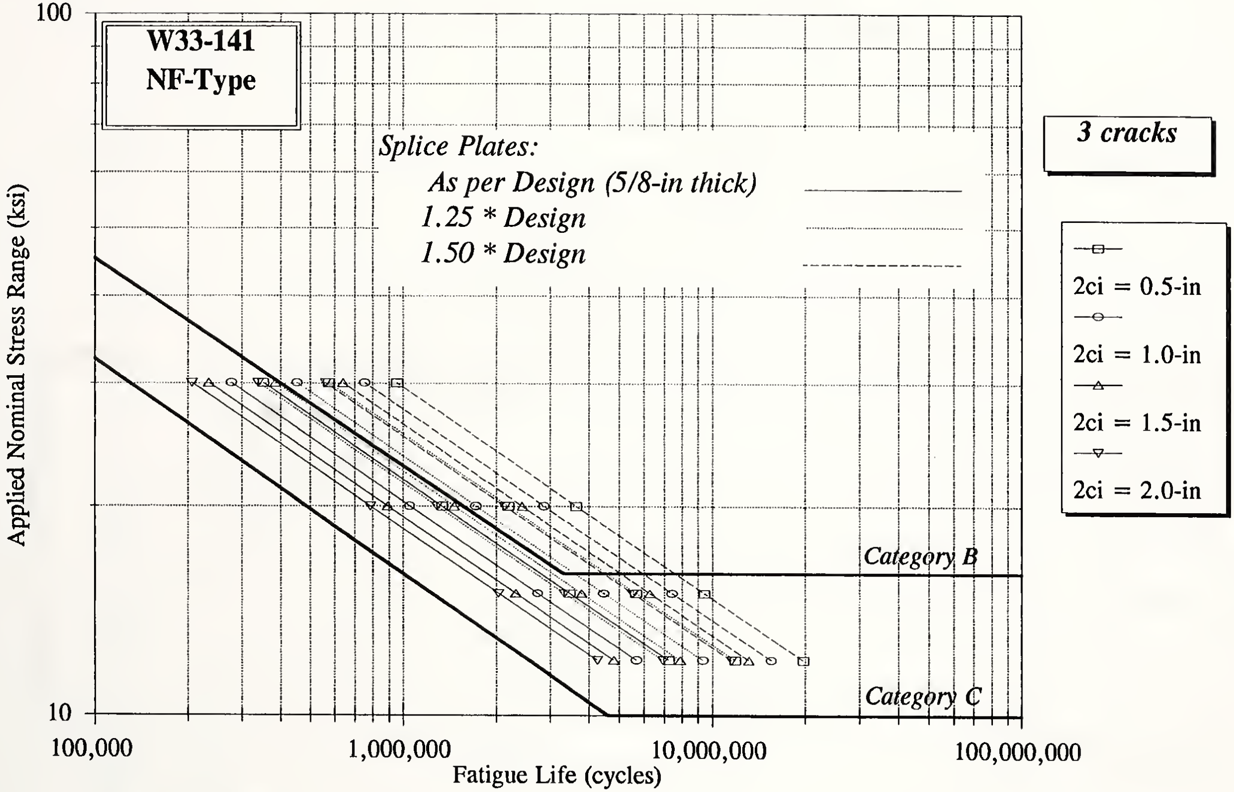

Fig. L.7. Fatigue Propagation Life of W 33 X 141 Girders Repaired with a Bolted Splice Plate Connection. (NF-Type)

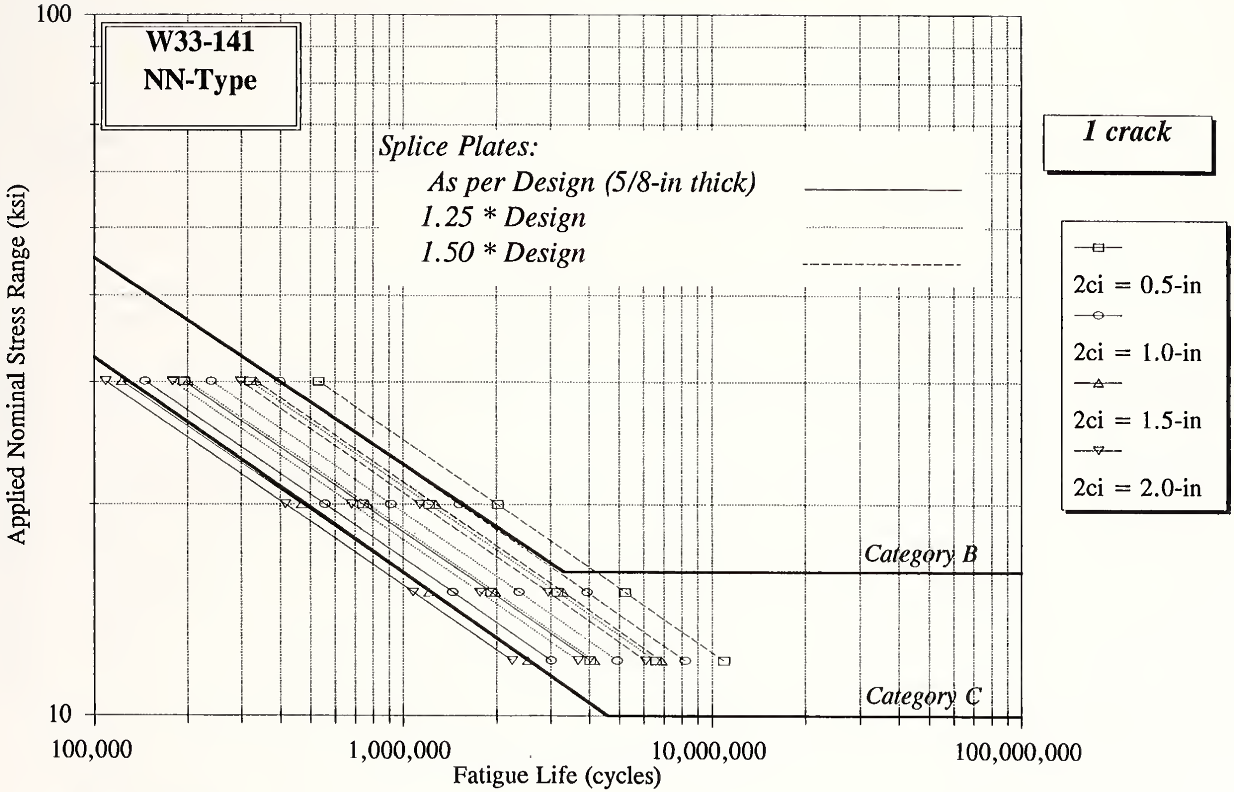

Fig. L.8. Fatigue Propagation Life of W 33 X 141 Girders Repaired with a Bolted Splice Plate Connection. (NN-Type)

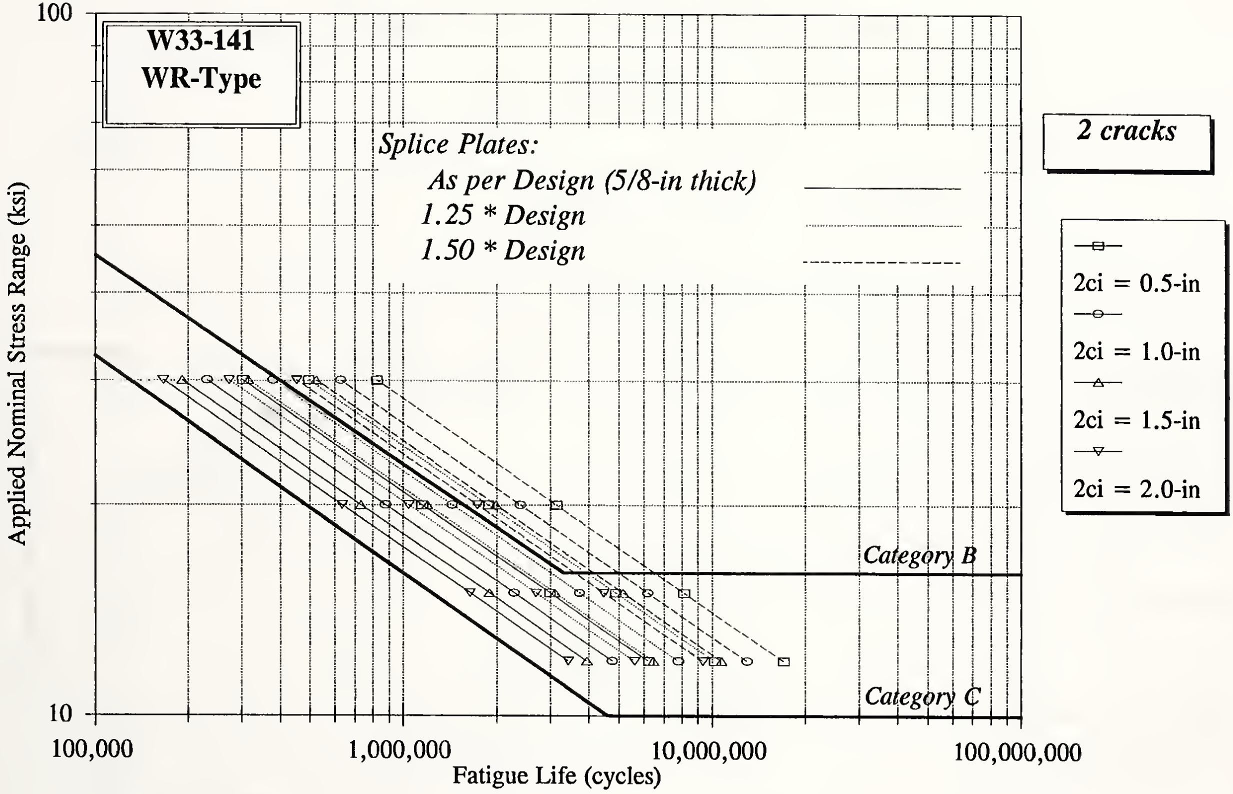

Fig. L.9. Fatigue Propagation Life of W 33 X 141 Girders Repaired with a Bolted Splice Plate Connection. (WR-Type)

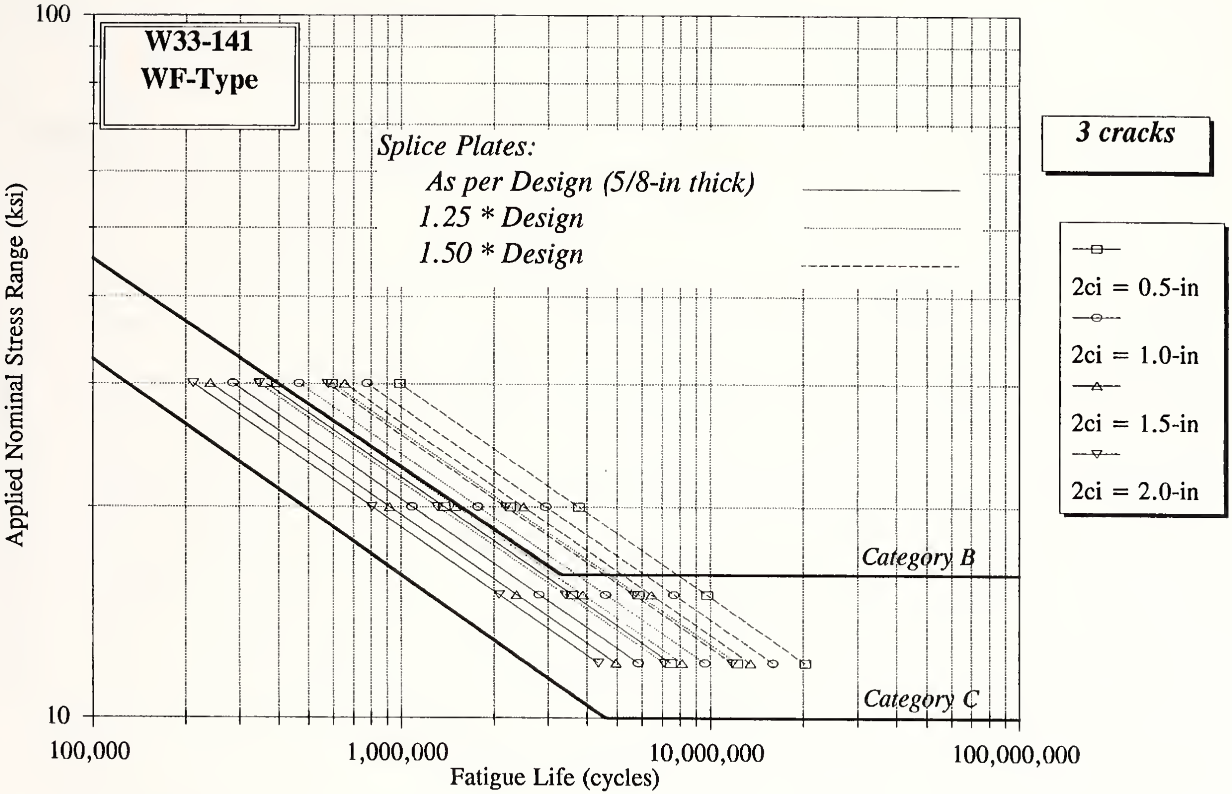

Fig. L.10. Fatigue Propagation Life of W 33 X 141 Girders Repaired with a Bolted Splice Plate Connection. (WF-Type)

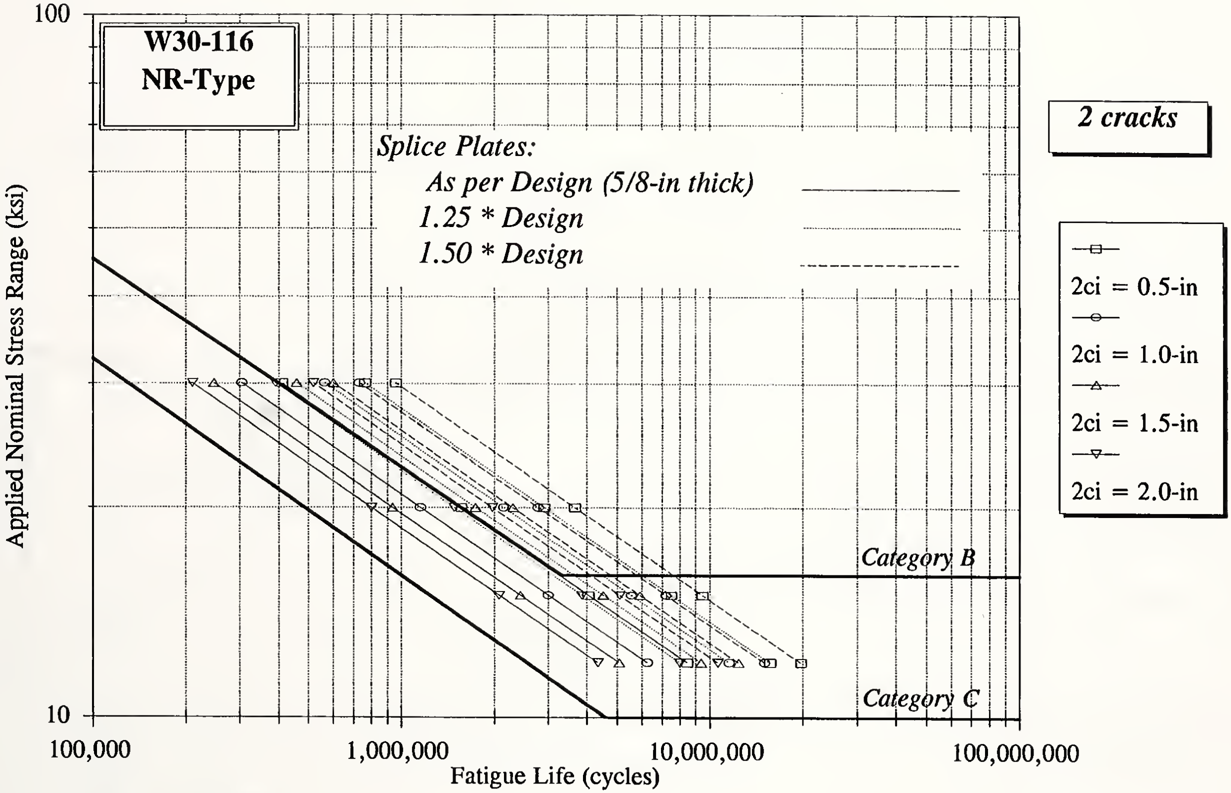

Fig. L.11. Fatigue Propagation Life of W 30 X 116 Girders Repaired with a Bolted Splice Plate Connection. (NR-Type)

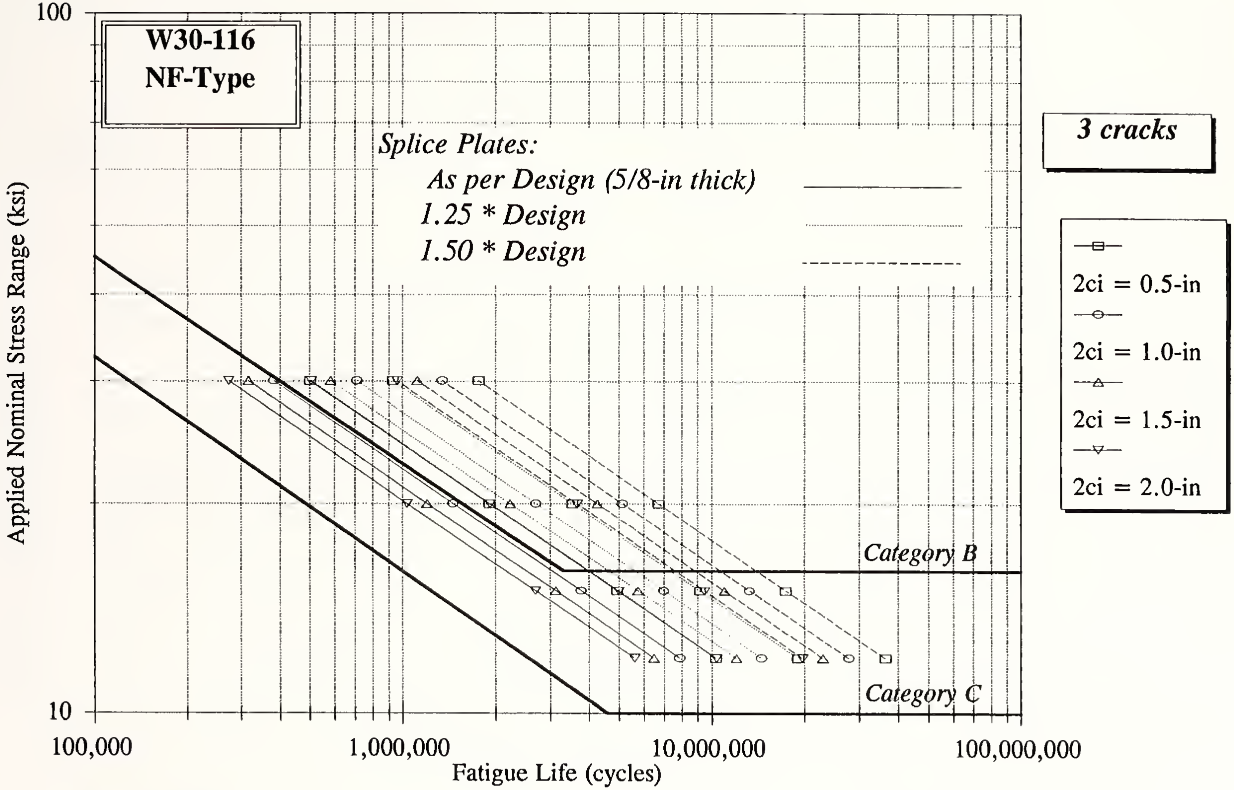

Fig. L.12. Fatigue Propagation Life of W 30 X 116 Girders Repaired with a Bolted Splice Plate Connection. (NF-Type)

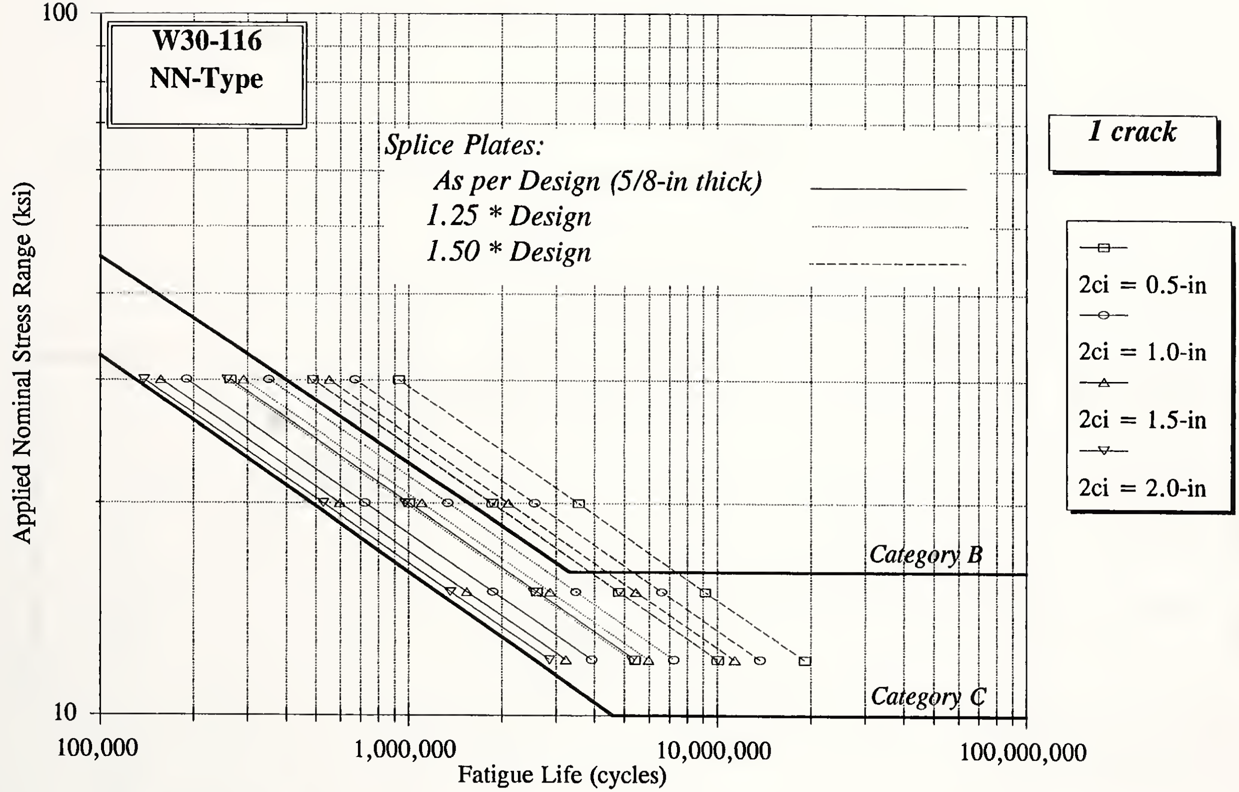

Fig. L.13. Fatigue Propagation Life of W 30 X 116 Girders Repaired with a Bolted Splice Plate Connection. (NN-Type)

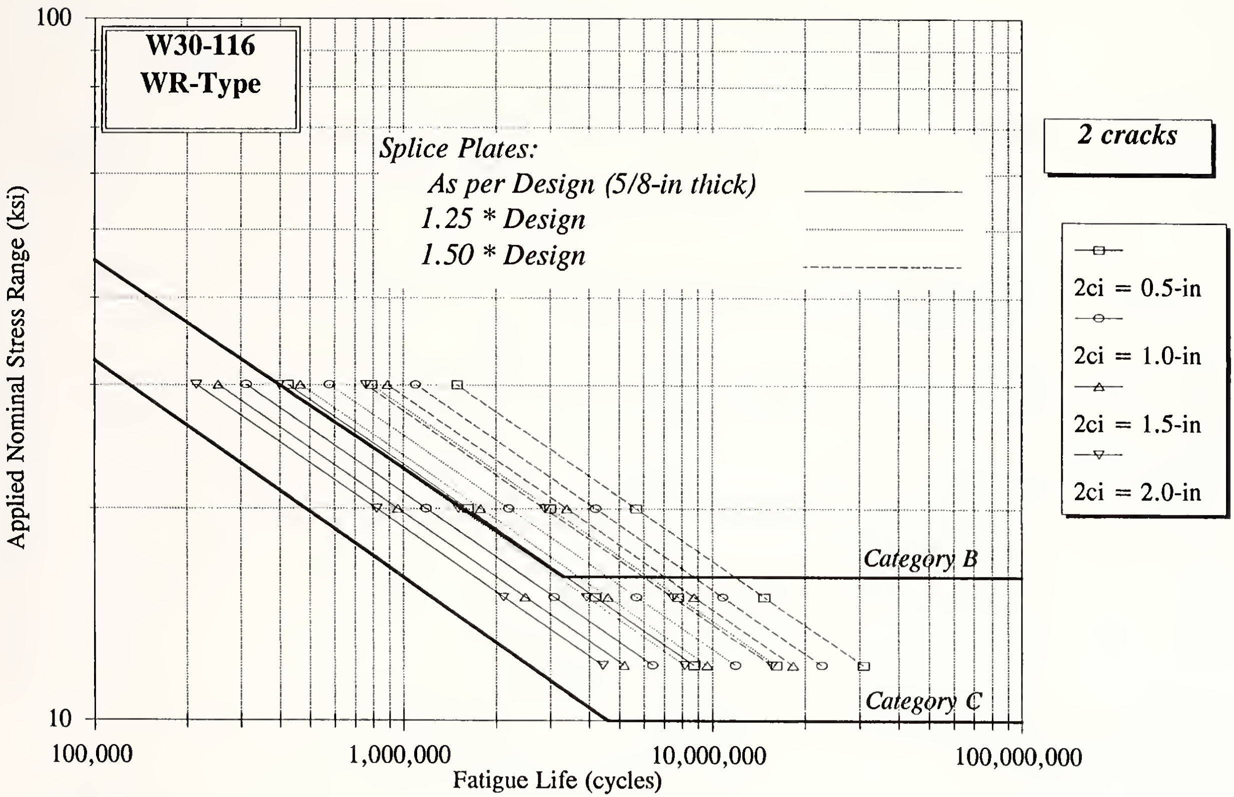

Fig. L.14. Fatigue Propagation Life of W 30 X 116 Girders Repaired with a Bolted Splice Plate Connection. (WR-Type)

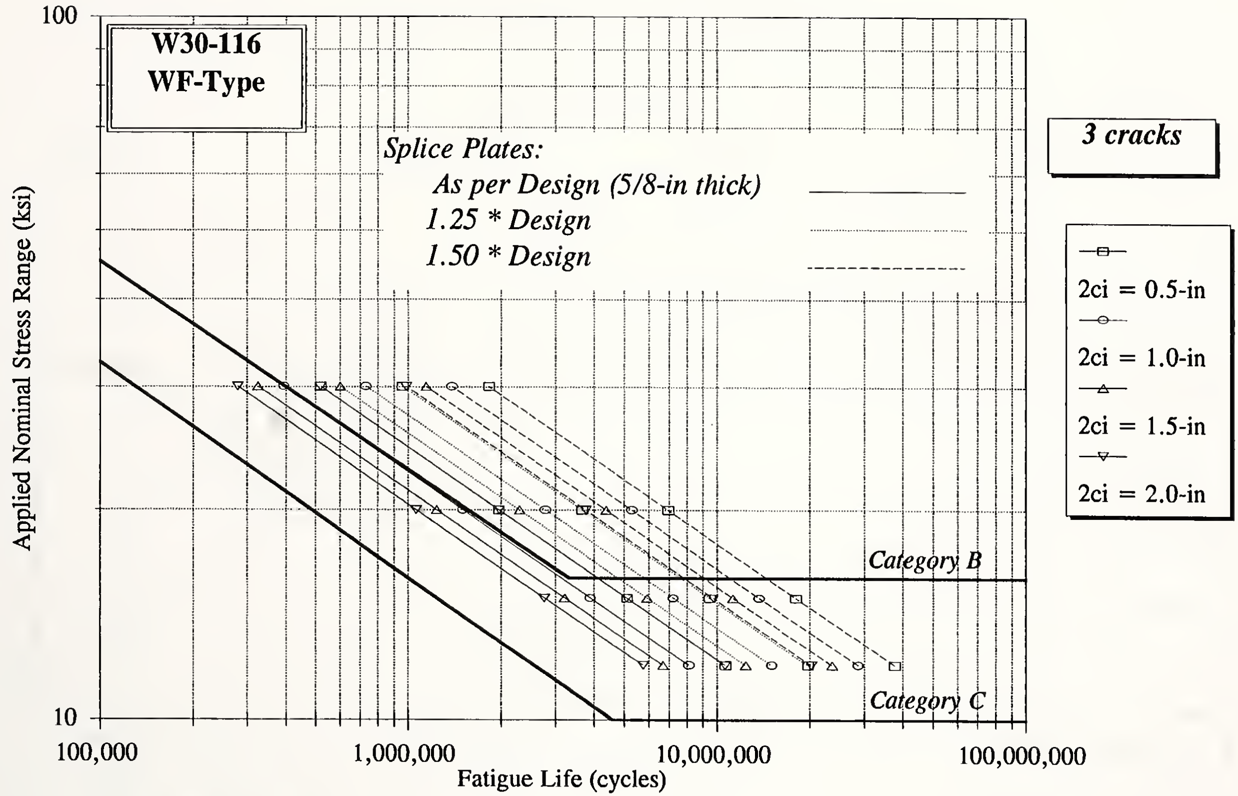

Fig. L.15. Fatigue Propagation Life of W 30 X 116 Girders Repaired with a Bolted Splice Plate Connection. (WF-Type)

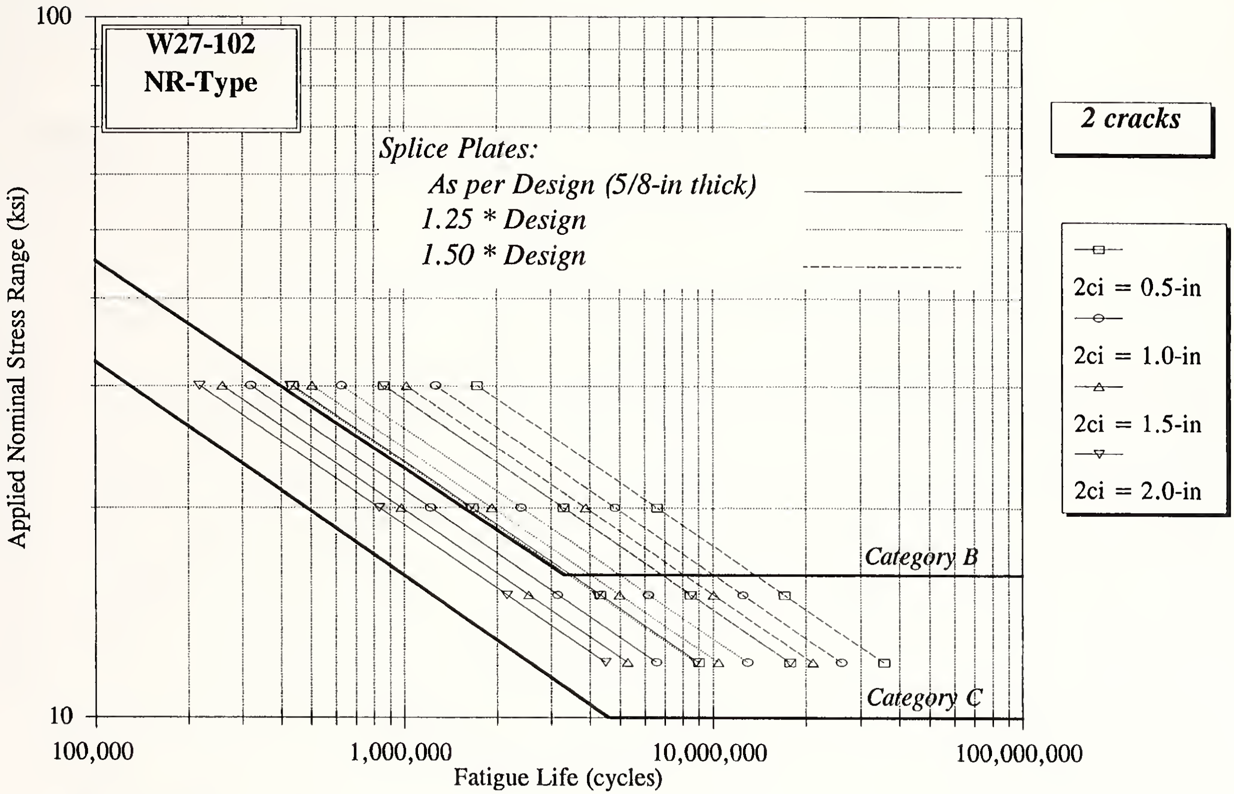

Fig. L.16. Fatigue Propagation Life of W 27 X 102 Girders Repaired with a Bolted Splice Plate Connection. (NR-Type)

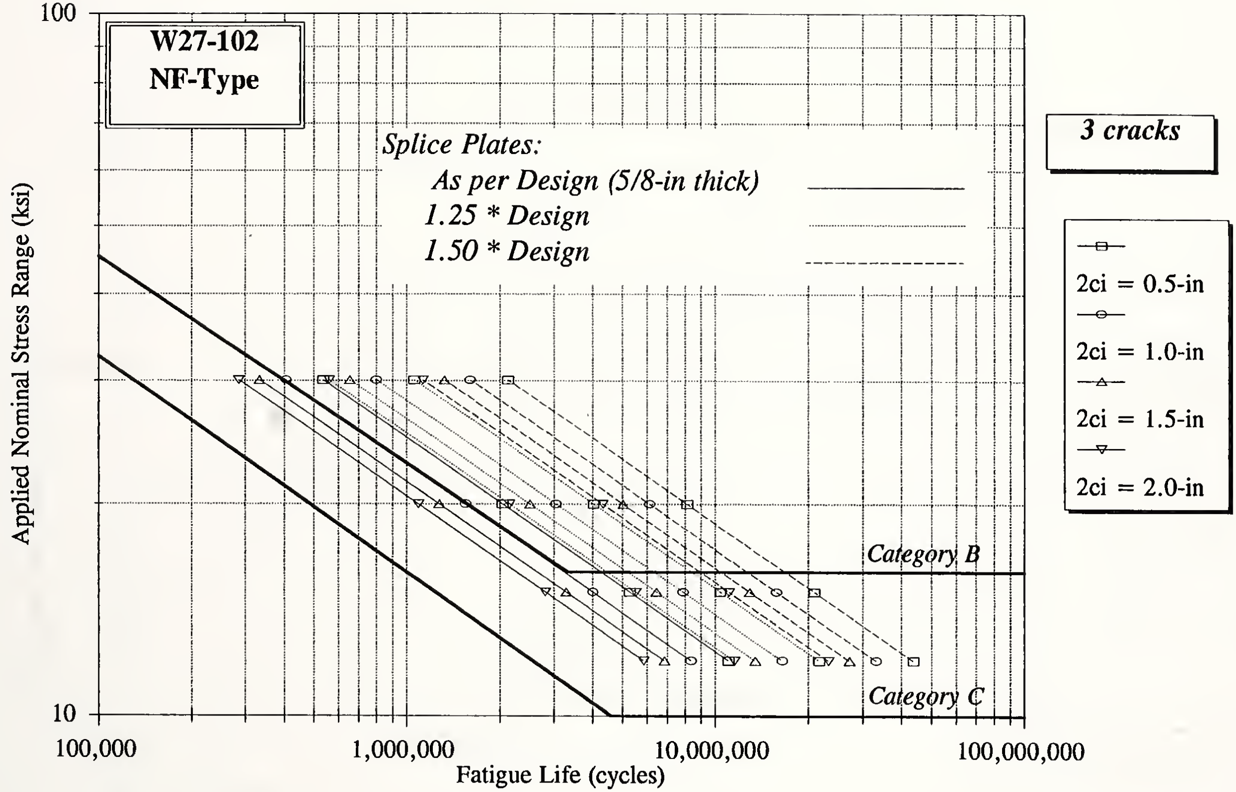

Fig. L.17. Fatigue Propagation Life of W 27 X 102 Girders Repaired with a Bolted Splice Plate Connection. (NF-Type)

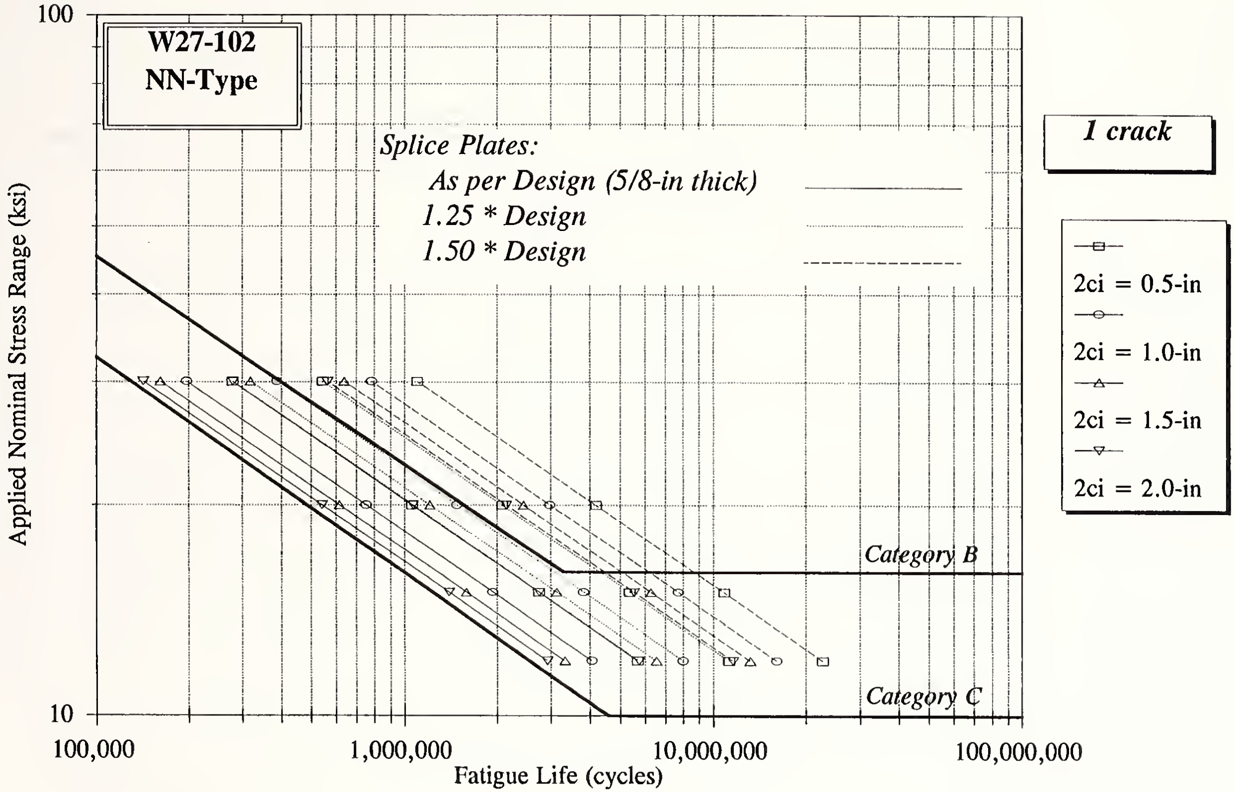

Fig. L.18. Fatigue Propagation Life of W 27 X 102 Girders Repaired with a Bolted Splice Plate Connection. (NN-Type)

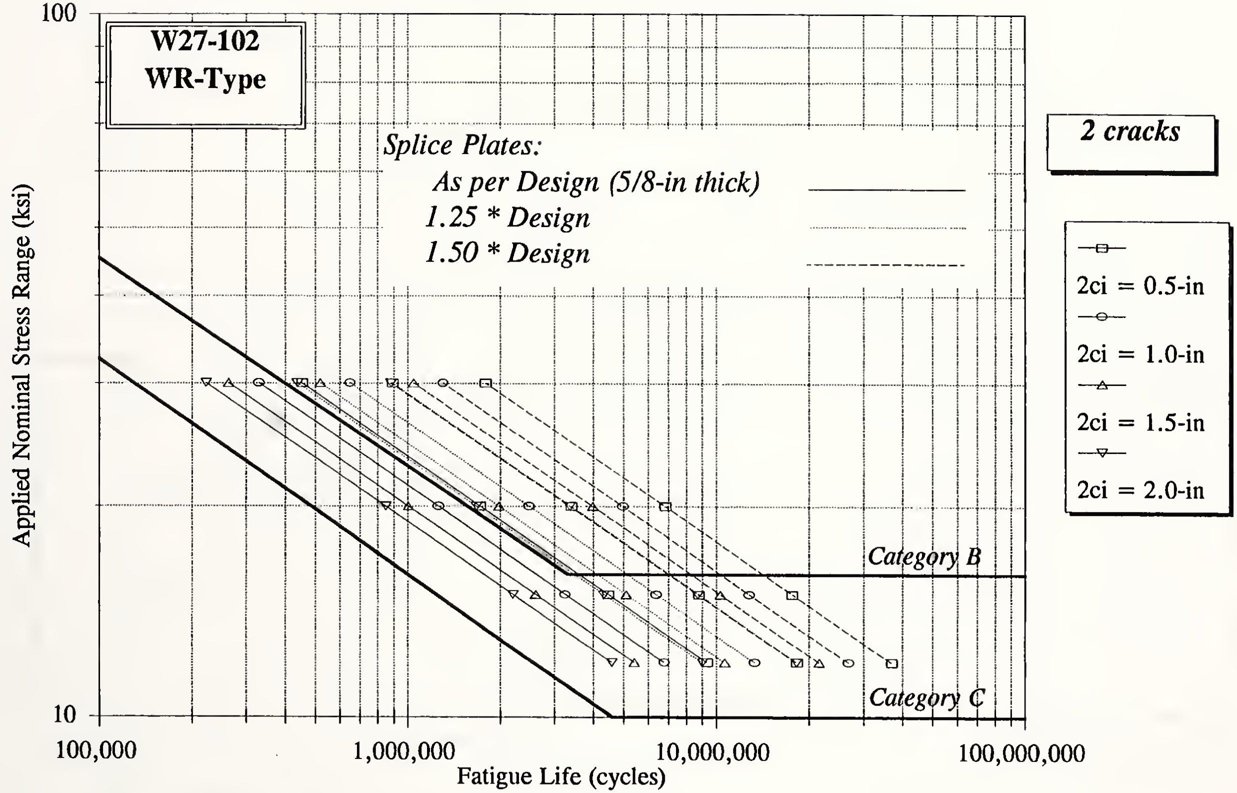

Fig. L.19. Fatigue Propagation Life of W 27 X 102 Girders Repaired with a Bolted Splice Plate Connection. (WR-Type)

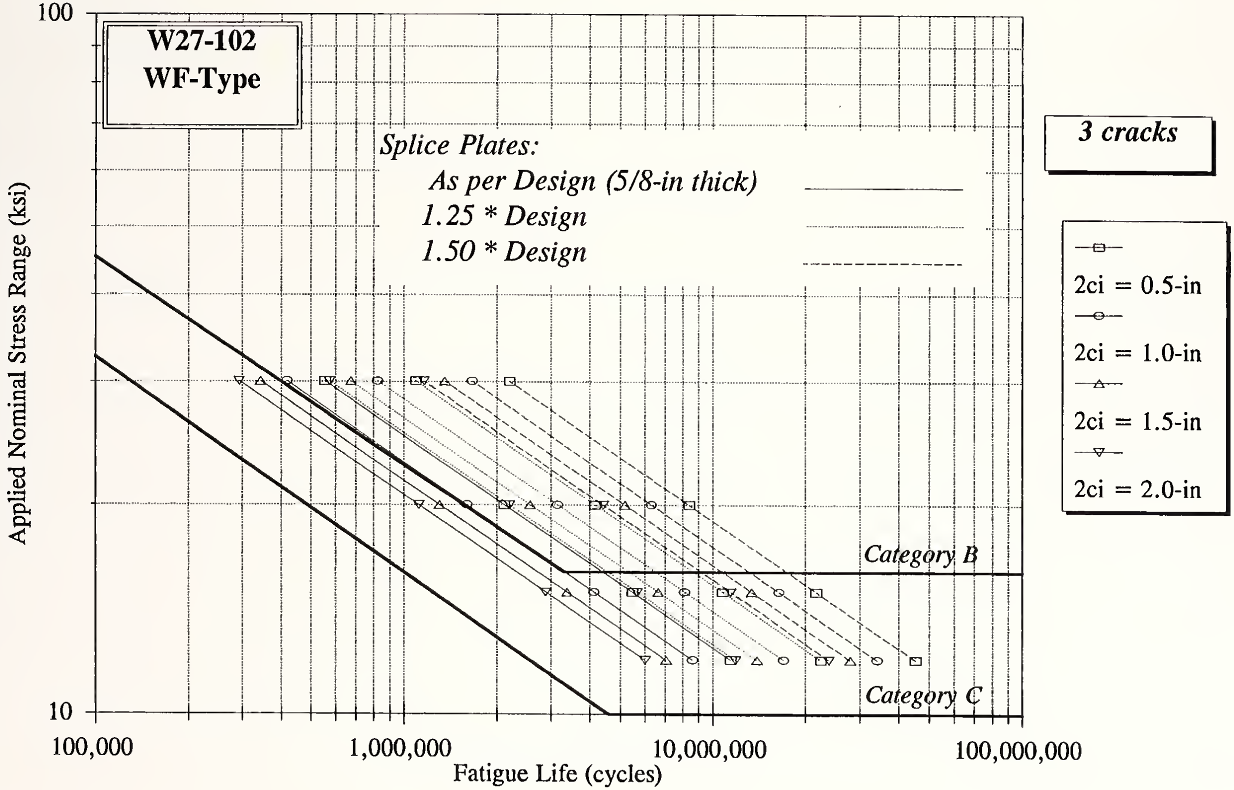

Fig. L.20. Fatigue Propagation Life of W 27 X 102 Girders Repaired with a Bolted Splice Plate Connection. (WF-Type)

COVER DESIGN BY ALDO GIORGINI